ACTIVE TECTONICS IN THE ZAGROS MOUNTAINS, IRAN

by

YOSEF SATTARZADEH-GADIM

Imperial College of Science, Technology and Medicine

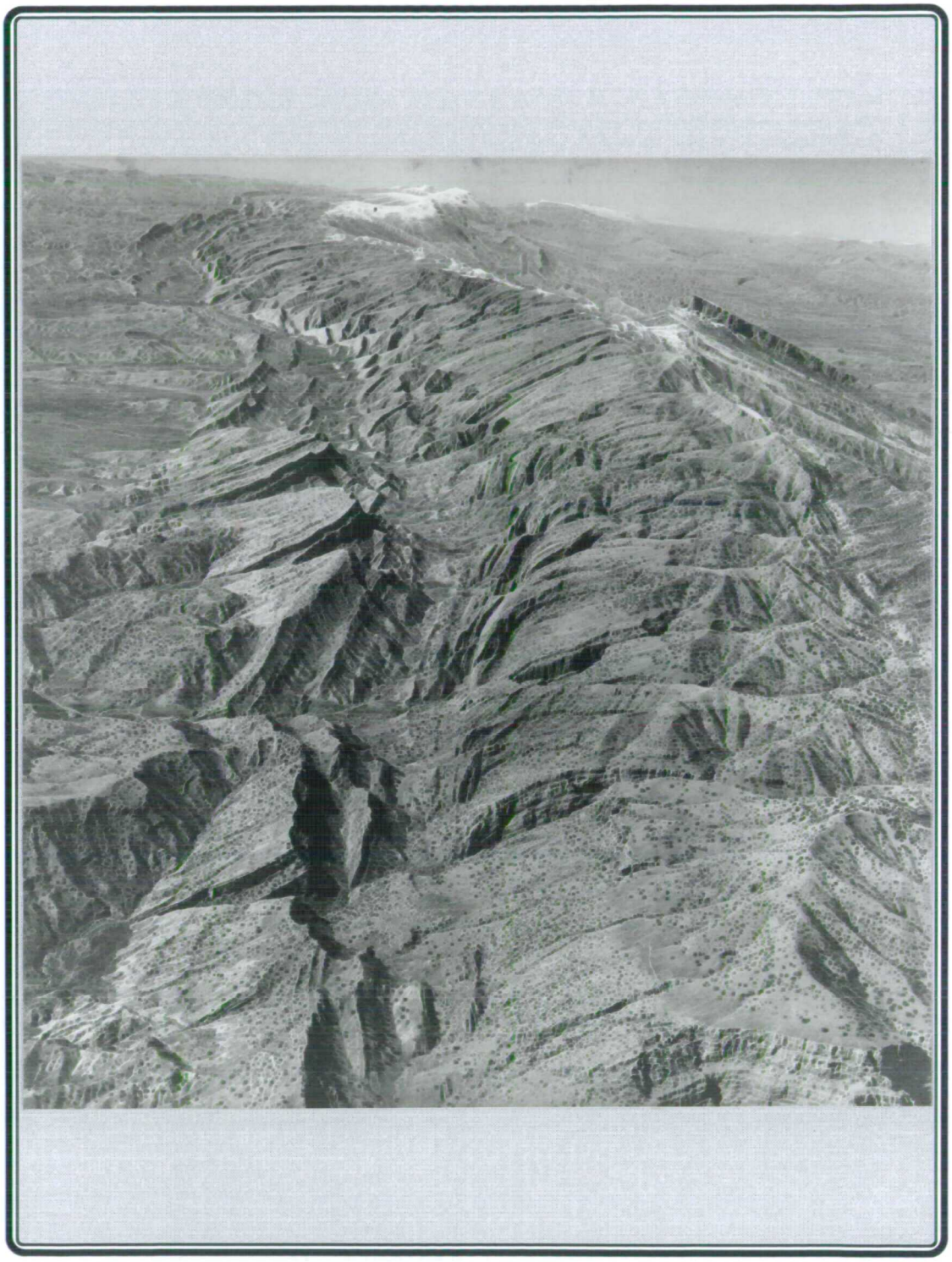
&

University College London

A thesis submitted for the degree of Doctor of Philosophy (PhD) of the University of London

July 1997

FRONTISPIECE



*An oblique air photograph of the '**Kabir Kuh**' anticline, the greatest mountain ridge in the 'Zagros Mountain Belt'. The entire length of the anticline is over 200 km, only about 80 km are visible in this photograph.*

ABSTRACT

ABSTRACT

The **Zagros Mountain Belt** along the NE margin of the Arabian plate represents one of the most spectacular exposed continent/continent collision zones, in the world, and displays unparalleled examples of major folds, faults and salt diapirs.

The study of the plate tectonic evolution of the Zagros mountain belt reveals that the belt is the product of complex deformation of the NE margin of the Arabian plate, initiated in Late Cretaceous times as a result of collision between the Arabian and Central Iranian plates and intensified in the Pliocene times. During the Pliocene a **deformation front migrated** from the collision zone towards the SW, into the almost undisturbed Zagros basin and led to the creation of the Zagros Mountain Belt.

The result of the studies described in this thesis show that the type and distribution of the deformation during the evolution of the Zagros deformation belt is controlled mainly by **plate velocity** (generated dominantly by the counterclockwise rotation of the Arabian plate around a pole in Syria) and the regional **stratigraphy** (composed of four mechanically contrasting litho-structural units over a rigid basement).

The sedimentary cover and the underlying metamorphic basement decouple along an important detachment horizon (the Hormuz Salt Formation) and they often deform independently. Uneven **distribution** and **thickness** of the Hormuz salt formation plays a **key role** in determining the rate of deformation and the geometry of the deformation belt.

The results of a **geometrical analysis** of the individual folds, their spatial distribution, and change in geometry across the deformation belt (deduced from the results of measurements of the half-wavelength/amplitude ratio of folds, the elevation and inclination of the median surface of the folds and variation of shortening of the sedimentary cover) provide strong evidence that the **south-westward migration** of the deformation front is achieved by the processes of **serial folding** and **footwall collapse**.

ABSTRACT

The results of above mentioned geometrical analysis, together with the results from other studies described in this thesis, reveal that there has been an important **interplay** between folds, faults and salt diapirs during the evolution of the Zagros deformation belt.

Analysis of earthquake data from the Zagros region also shows that the **coseismic brittle** deformation occurs predominantly in the upper parts of the basement and deformation above and below this level generally takes place dominantly in an **aseismic ductile** manner.

Studies of evidence for and effects of **neotectonic** movements including the present seismicity also show that the Zagros Mountain Belt along the NE margin of the Arabian plate **is still a tectonically active belt** and that the deformation processes, deduced from the different studies discussed in this thesis, **are still going on**.



ACKNOWLEDGEMENTS

ACKNOWLEDGMENTS

I am greatly indebted to a large number of people who made this study possible and who helped and encouraged me throughout the development of the thesis.

I would like to acknowledge and express my appreciation for the financial support provided by the Tabriz University in Iran. Also, I am most grateful to the staff of the Tabriz University and the Education Departments of the Ministry of Culture and Higher Education in Iran and the Embassy of the Islamic Republic of Iran in London for their constant support and encouragement throughout my study period at Imperial College.

I am also greatly indebted to my two supervisors, Dr John Cosgrove and Professor Claudio Vita-Finzi, for their constant help, friendship and encouragement. I was indeed most fortunate to have worked with both of them.

My thanks are also extended to Dr John McM Moore, the head of the Remote Sensing Section of the Geology department at Imperial College for his advice on the photogeological aspect of the study and for letting me use the facilities in his laboratory.

Many thanks also to Professor Douglas Shearman, the leader of the RGS/Imperial College Iranian Makran expeditions of 1974 and 1976, for his constant encouragement and help, especially in respect of my first seminar at Imperial College and when I was preparing my transfer report. I also would like to thank Dr Michael Ala and Dr Mokhles Rahman of the Petroleum Geology Section at IC, for their friendship, encouragement, and the scientific discussions with Dr Ala regarding the stratigraphy and salt diapirs of the study area.

Other members of the Geology department of Imperial College contributed in various ways to the eventual completion of this study, notably Alan Jones, Dick Campain, and Carol Kilby and their help is gratefully acknowledged.

Very special thanks are also due to Ella Ng Chieng Hin for her constant assistance with

computing, providing the computing facilities, and in particular, for the excellent rescuing some of my chapters from the damaged disks.

All my good friends in the Geology department of Imperial College (both past and present) have been great company, especially Dr Peter Connolly, Dr David Thomas, Matthew Brown, Barnaby Philps. At UCL, I would like to thank Professor Alan Lord (Dean of Faculty of Physical Sciences) for his friendship and encouragement and Celine Murphy of the administrative staff for her help in the early stages of this study.

At British Petroleum Exploration Operating Company Ltd. I owe thanks to all those who contributed to discussion of the Zagros region, especially Dr Robin Cleverly, who made it possible for me to visit BP and provided me with copies of geological maps and Landsat image of the Zagros folds which have been used in this thesis.

Most importantly, I like to express my profound gratitude to my dear and loving mother, wife and daughter to whom this thesis is dedicated, for all their encouragement, help, eternal support, and understanding.

Finally, I thank God for giving me good health and the ability to carry on with the work even in the face of immense difficulties.



TABLE OF CONTENTS

TABLE OF CONTENTS

Page

Frontispiece i
Abstract ii
Acknowledgements iv
Table of contents vi
List of figures x
List of tables xxii

Chapter (1) OBJECTIVES, METHODOLOGY, DATABASE AND THESIS OUTLINE

1. Introduction 1
2. Objectives 2
3. Methodology 4
4. Database 6
5. Thesis outline 9

Chapter (2) THE ZAGROS MOUNTAINS

1. Introduction 10
2. Geographical setting 10
   a) Location 10
   b) Settlements 11
   c) Climate 13
   d) Topography 14
3. Geological setting 28
   a) Major structural zones 28
   b) Stratigraphy 32
   c) Metamorphic rocks 38
   d) Ophiolitic and mélange rocks 40
   e) Volcanic rocks and associated intrusives 41
4. Previous work 43
   a) Geological mapping and structural studies 43
   b) Neotectonics and seismotectonic studies 46

TABLE OF CONTENTS

Chapter (3) LARGE-SCALE GEOLOGICAL STRUCTURES OF THE ZAGROS MOUNTAIN BELT

1. Introduction 47
2. The Zagros Folds 47
   a) Spatial distribution of the Zagros folds 48
   b) Geometry of the Zagros folds 53
   c) Mechanism of folding in the Zagros mountain belt 66
3. The Zagros Faults 87
   a) Spatial distribution of the Zagros faults 88
   b) Geometry of the Zagros faults 90
   c) Mechanism of faulting in the Zagros mountain belt 92
4. The Zagros salt diapirs 96
   a) Spatial distribution of the Zagros salt diapirs 96
   b) Geometry of the salt diapirs 100
   c) Mechanism of salt diapirism in the Zagros mountain belt 103

Chapter (4) GEOMETRICAL ANALYSIS OF THE ZAGROS FOLDS AND SEDIMENTARY COVER

1). Introduction 108
2). Half-wavelength/amplitude ratio of the folds 108
3). Elevation and inclination of median surface of the folds 120
4). Shortening of the sedimentary cover 130

Chapter (5) PLATE TECTONIC AND GEOMORPHOLOGICAL EVOLUTION OF THE ZAGROS MOUNTAIN BELT

1. Introduction 146
2. Plate tectonic models 146
3. Plate tectonic evolution 149
4. Geomorphological evolution 157

TABLE OF CONTENTS

Chapter (6) EVOLUTION OF THE ZAGROS DEFORMATION BELT

1). Introduction 161
2). Process of folding and evolution of the Zagros Fold Belt 161
3). Process of faulting and evolution of the Zagros Fault Belt 171
4). Process of salt diapirism and evolution of the Zagros diapir provinces 175

Chapter (7) NEOTECTONIC ACTIVITY IN THE ZAGROS MOUNTAIN BELT

1. Introduction 178
2. Origin of neotectonic activity 179
3. Effects of neotectonic activity 180
4. Evidence of neotectonic activity 180
a) Geological evidence 180
b) Geomorphological evidence 189
c) Archaeological evidence 195
d) Historical evidence 199

Chapter (8) SEISMOTECTONIC ACTIVITY IN THE ZAGROS MOUNTAIN BELT

1. Introduction 208
2. Quality of the Zagros earthquake data 208
3. Analysis of the Zagros earthquake data 212
a) Epicentres of the Zagros earthquakes 212
b) Magnitudes of the Zagros earthquakes 219
c) Focal depths of the Zagros earthquakes 227
d) Fault plane solutions of the Zagros earthquakes 231
4. Characteristics of the seismic activity in the Zagros mountain belt 237
5. Rates of neotectonic activity 238

Chapter (9) DISCUSSION AND CONCLUSIONS

1. Introduction 242
2. Discussion 244
3. Conclusions 255

References 258

LIST OF FIGURES

LIST OF FIGURES

Chapter (2) **(Page)**

Fig. 2.1 Plate tectonic map of the Middle East, showing the Zagros mountains along the northeastern margin of the Arabian plate (based on Berberian, 1981 and Nowroozi, 1987). ..... **(11)**

Fig. 2.2 Map of Iran, showing the provinces and the provincial capitals. ..... **(12)**

Fig. 2.3 Diagram of the Central Zagros showing the stepped southwestward dipping topography and the influence of the major structural grains and rock-type on the development of the contrasting morphological provinces (modified from Oberlander, 1965). ..... **(17)**

Fig. 2.4 A geomorphological map of the Zagros mountain belt, showing the stepped topography, different morphological provinces and major culminations and depressions along and across the belt (based on Oberlander 1965, the geological map of Iran (NIOC, 1975), and the geological map of Iraq and southwestern Iran (RRP, 1987)). ..... **(18)**

Fig. 2.5 Satellite image of the southern Zagros mountains, showing the intact, elongate and widely spaced anticlines in the south (near the Persian Gulf) and deeply dissected, tight, closely spaced folds to the north (near the Main Zagros Thrust). ..... **(19)**

Fig. 2.6 A dissected large-scale anticline in the Zagros Mountain, showing the effects of the these structures and the mechanically contrasting rock types in the creation of the present day topography. ..... **(20)**

Fig. 2.7 Drainage map of the Zagros Mountain Belt, showing the asymmetric southwestwards dipping topography and the influence of large-scale structural grains and major structural culminations and depressions in the creation of longitudinal and transverse drainage pattern. ..... **(21)**

Fig. 2.8 Development of transverse gorges in the Zagros Mountains. a) Drainage consequent on initial deformation of folds which are not exposed due to the presence of an overburden of erodible material, b) drainage discordance produced by renewed deformation or fault exposure of the fold structures (from Oberlander, 1965). ... **(22)**

LIST OF FIGURES

Fig. 2.9 Two views of the Tang-e Lailum, a transverse gorge through the Asmari limestone anticline of Kuh-e Kailan. The Kabir kuh anticline lies to the southwest (left) and the Milleh kuh anticline to the NE (right) (from Oberlander, 1965). ..... (**23**)

Fig. 2.10 The gorge of Zohreh River showing extreme constriction where it cuts solely in Asmari limestone (top) and abrupt expansion where underlying marls are exposed permitting spring-line sapping at the limestone marl contact (bottom) (from Oberlander, 1965). ..... (**24**)

Fig. 2.11 Vertical gorge of the Keshwar River, illustrating of the intense deformation of the Cenomanian limestone in the Bakhtiari Mountains (from Oberlander, 1965). (**25**)

Fig. 2.12 Aerial photograph of a portion of the 'Minab anticline' NE of the Strait of Hormuz transected by a transverse drainage system. ..... (**26**)

Fig. 2.13 Satellite image of the southeastern Zagros, showing the contrasting topography of the belt in the southwest and northeast and the Shiraz-Neyriz depression with the Bakhteghan, Maharlu and Tashk lakes. ..... (**27**)

Fig. 2.14 The major structural zones along the northeastern margin of the Arabian plate (the Zagros mountain belt) and southwestern margin of the Central Iranian plate (based on Stöcklin 1968 and Alavi 1980). ..... (**29**)

Fig. 2.15 Schematic cross-sectional view of the Zagros orogen (from Alavi, 1994).(**30**)

Fig. 2.16 Stratigraphical column and the lithological and structural divisions of the Zagros mountain belt (updated from Colman-Sadd, 1978). ..... (**33**)

Fig. 2.17 The location of outcrops of the Precambrian basement rocks, and ophiolitic and mélange rocks in the northeastern margin of the Arabian plate (the Zagros mountain belt) and southwestern margin of the Central Iranian plate (based on Stöcklin 1968).(**34**)

Fig. 2.18 Satellite image of the area NW of Neyriz, showing the outcrops of the ophiolitic mélange rocks, salt diapirs, and the Bakhteghan and Tashk lakes developed within the structural depression in the Imbricate Zone. ..... (**39**)

LIST OF FIGURES

Chapter (3)

Fig. 3.1 Distribution of the folds in the 'Simply Folded Belt' of the Zagros mountains, showing a wave-like (sinuous) geometry and the different distribution of the folds within the different fold zones (based on the Geological Map of Iran (NIOC, 1975) and the Geological Map of Iraq and Southwestern Iran (RRP, 1987)). ..... **(51)**

Fig. 3.2 The *en echelon* offset of the folds when viewed in plan. (a) Random offset, (b) and (c) consistent offset associated with sinistral and dextral strike-slip movement on basement faults, respectively. ..... **(52)**

Fig. 3.3 Satellite image of the southeastern end of the Zagros mountain belt, showing the Minab fold zone with folds of high aspect ratios and *en echelon* arrangement (see also Figs. 3.1 and 3.24). ..... **(57)**

Fig. 3.4 Satellite image of the Central Zagros, showing the Lorestan fold zone with the spectacular high aspect ratio '**Kabir Kuh**' anticline. The location of this anticline is shown in Figs 3.1 and 3.23). ..... **(58)**

Fig. 3.5 Six examples from 21 geological cross-sections taken from the British Petroleum Company Limited (1956), used by the present author for the geometrical analysis of the Zagros folds and for determining the variation in the percentage shortening of the sedimentary cover. The location of these sections is shown in Fig. 4.1. ..... **(59)**

Fig. 3.6 Development of asymmetric folds caused by shearing along the detachment horizon. Arrows show relative movement, and upward and downward displacement in anticlines. Potential faulting is omitted (from Colman-Sadd, 1978). ..... **(60)**

Fig. 3.7 Satellite image of part of the Fars fold zone, showing anticlines of different size and plan-shape separated by flat synclinal depressions. ..... **(61)**

Fig. 3.8 Satellite image of the area NW of the Strait of Hormuz, showing small-scale folds within larger fold structures. See also Fig. 3.11. ..... **(62)**

Fig. 3.9 Detail of Fig. 3.8 of the area NW of the Strait of Hormuz, showing smaller and almost intact folds encompressed by limbs of a deeply eroded, large folds. ..... **(63)**

Fig. 3.10 The close-up of the satellite image of the area NW of the Strait of Hormuz, showing disharmonic folding i.e. smaller folds enclosed within a large fold. Note also the salt diapirs forming a crater-like depression due to the exhausted or arrested of salt rise or undue erosion. See also Fig. 3.11. ..... (**64**)

Fig. 3.11 The development of disharmonic folds in the Competent Group. Relatively small-scale folds develop in a relatively thin competent unit beneath the thicker Asmari limestone which buckle with a larger wavelength. ..... (**65**)

Fig. 3.12 Buckling mechanism and examples of buckle folding. (a) Classical buckle fold. The stress distribution within a buckle depends on the mechanical properties of the layer. (b) Tengential longitudinal strain fold, typical of massive beds. (c) Flexural-slip fold, typical of well bedded units. ..... (**66**)

Fig. 3.13 Bending mechanism and different examples of folding by bending (b, c and d from Price & cosgrovr, 1990, and e from Heim, 1921/2). ..... (**67**)

Fig. 3.14 Step-like displacements of the basement of a model experiment produced curved reverse faults and forced folds in the sand representing the cover (from Sanford, 1959). ..... (**68**)

Fig. 3.15 Experiments showing the effects of (a) reverse and (b) normal faulting in a rigid basement on a layered, ductile cover (from Ameen 1988), and (c) and (d) the results of finite element analysis investigating the effect of faulting of a rigid basement on a viscous cover. Elements with black flags in the upper left hand corner show regions of yielding. The short lines in each element show the directions of least compressive stress (from Reddy *et al.*, 1982). ..... (**70**)

Fig. 3.16 Small-scale *en echelon* periclines in folded metasediments near Luarca. N. Spain (from Price & Cosgrove, 1990). ..... (**71**)

Fig. 3.17 Large-scale periclinal folds in the Jura Mountains (from Strahler, 1960). (**72**)

Fig. 3.18 (a) Shear in the basement induces compression in the cover rocks which produces *en echelon* folds such as are developed above (b) the Inglewood Fault (California) (c) the sinistral Dead Sea fault and (d) the San Andreas Fault (from Moody & Hill, 1956). ..... (**73**)

Fig. 3.19 (a) The amplification and coalescence of two periclines (shown in plan) separated by a distance X which is somewhat less than half the wavelength of the structure. (b) Two periclines separated by X' which is slightly greater than half the wavelength. The structures overlap and lock up, each preventing further propagation of the other. . . . . (**75**)

Fig. 3.20 A structural cross-section based on a seismic profile across 'Burujen' (51°.12′E-32°.59′N) (from Payne, 1990). The location of the profile is shown in the index map. . . . . (**78**)

Fig. 3.21 A portion of the geological map of Iran 1:1,000,000 (NIOC, 1975) showing en echelon alignment of buckle folds and thrust faults. These are used to detect the position and sense of shear on major basement strike-slip faults. The position, trend and sense of shear of these inferred faults is marked. The linear outcrop of the salt walls in the 'Thrust' zone are also shown (marked in red). . . . . (**81**)

Fig. 3.22 Fault map of the Zagros mountain belt, showing the spatial distribution, trend and sense of movements of mappable faults. . . . . (**82**)

Fig. 3.23 A portion of the geological map of Iran 1:1,000,000 (NIOC, 1975), showing the large-scale **Kabir kuh** anticline in the Lorestan fold zone, position of inferred basement strike-slip faults (the Bala Rud and Sumar lines) and the outcrop of the salt walls (marked in red) in the 'Zagros Thrust Zone'. . . . . (**83**)

Fig. 3.24 A portion of the geological map of Iran 1:1,000,000 (NIOC, 1975), showing the marked differences in geometry of the classical buckle folds and the forced folding associated with the Minab-Zendan fault zone, and the Hormuz salt diapirs (marked in red) which are approximately equant and aligned along inferred basement strike-slip faults. . . . . (**84**)

Fig. 3.25 Normal faults in the crest of the major anticlines (from McQuillan, 1974).(**89**)

Fig. 3.26 Faulting mechanism and the initial stress distribution causing (a) normal faulting, (b) reverse and (c) strike-slip faulting. σ_1, σ_2 and σ_3 are the maximum, intermediate and minimum principal stresses, respectively (from Hills, 1972). . . . . (**93**)

Fig. 3.27 The relationship between plate induced stresses (bold arrows) and the major known and inferred basement strike-slip faults. . . . . (**95**)

Fig. 3.28 Satellite image of the area NW of the Strait of Hormuz, showing equant salt diapirs. ..... (**98**)

Fig. 3.29 Aerial photograph of Hormuz Island. ..... (**99**)

Fig. 3.30 Cross-sectio through the Masjed-e Soleyman and Haft Kel areas, showing the Miocene Lower Fars salt rich evaporites (Gachsaran Formation) forming 'salt bulges' and'flow sheets' as a result of disharmonic folding (modified from O' Brien, 1957). (**100**)

Fig. 3.31 Two stages in the development of a dilational jog in a relay area between two overlapping strike-slip faults. These jogs provide ideal sites for the initiation and intrusion of salt diapirs. ..... (**103**)

Fig. 3.32 Boundary stresses and fluid (Newtonian) flow between parallel layers see text for details (from Price and Cosgrove, 1990). ..... (**105**)

Fig. 3.33 The initiation and evolution of the Lower Fars (Miocene) Gachsaran salt diapirs in the form of 'salt buldges' and 'flow-sheets' in the Haft Kel area (see Fig 3.21) as a result of disharmonic folding (see also Fig. 3.30) (from O'Brien, 1957). ... (**107**)

Chapter (4)

Fig. 4.1 The location of 21 geological sections (A-U) from British Petroleum Company Limited (1956) used by the present author for the geometrical analysis of the Zagros folds and for determining of the elevation and inclination of the median surface of the folds and variation in shortening of the sedimentary cover across the belt. ..... (**109**)

Fig. 4.2 The technique used for measuring the half-wavelength and amplitude of the Zagros folds. ..... (**110**)

Fig. 4.3 The morphologically and structurally contrasting fold zones and eleven, 20 km wide strips parallel to the northeastern margin of the 'Simply Folded Belt'. ..... (**113**)

Fig. 4.4 The half-wavelength/amplitude ratio of folds within the 20 km strips parallel to the northeastern margin of the 'Simply Folded Belt' in the **Lorestan** fold zone. . (**114**)

Fig. 4.5 The half-wavelength/amplitude ratio of folds within the 20 km strips parallel to the northeastern margin of the 'Simply Folded Belt' in the **Bakhtiari** fold zone. (**115**)

Fig. 4.6 The half-wavelength/amplitude ratio of folds within the 20 km strips parallel to the northeastern margin of the 'Simply Folded Belt' in the **Kohkiluyeh** fold zone. . . . . (**116**)

Fig. 4.7 The half-wavelength/amplitude ratio of folds within the 20 km strips parallel to the northeastern margin of the 'Simply Folded Belt' in the **Fars** fold zone. . . . (**117**)

Fig. 4.8 The average half-wavelength/amplitude ratio of folds within the 20 km strips parallel to the northeastern margin of the 'Simply Folded Belt' in **the whole belt**. . (**118**)

Fig. 4.9 The variation of the half-wavelength/amplitude ratio of the folds within the 20 km strips parallel to the northeastern margin of the 'Simply Folded Belt' in four of the morphologically and structurally distinct fold zones shown in Fig. 4.3. . . . . (**119**)

Fig. 4.10 The elevation and inclination of the median surface of the Zagros folds within the 20 km wide strips parallel to the northeastern margin of the 'Simply Folded Belt' in the **Lorestan** fold zone. . . . . (**123**)

Fig. 4.11 The elevation and inclination of the median surface of the Zagros folds within the 20 km wide strips parallel to the northeastern margin of the 'Simply Folded Belt' in the **Bakhtiari** fold zone. . . . . (**124**)

Fig. 4.12 The elevation and inclination of the median surface of the Zagros folds within the 20 km wide strips parallel to the northeastern margin of the 'Simply Folded Belt' in the **Kohkiluyeh** fold zone. . . . . (**125**)

Fig. 4.13 The elevation and inclination of the median surface of the Zagros folds within the 20 km wide strips parallel to the northeastern margin of the 'Simply Folded Belt' in the **Fars** fold zone. . . . . (**126**)

Fig. 4.14 The elevation and inclination of the median surface of the Zagros folds within the 20 km wide strips parallel to the northeastern margin of the 'Simply Folded Belt' in the **whole Zagros belt**. . . . . (**127**)

Fig. 4.15 Three dimensional plot of the position of the inflection points of the Zagros

folds along the Upper Cretaceous/Lower Cretaceous marker horizon showing 3-D geometry of the median surface of the folds. ..... (**128**)

Fig. 4.16 The contrasting southwestward inclination of the median surface of the folds within the four adjacent fold zone. ..... (**129**)

Fig. 4.17 Schematic progressive development of a fault-propagation fold at the tip of a thrust fault (from Suppe, 1983). ..... (**131**)

Fig. 4.18 Illustration of pin lines and the concept of constant bed length between pin lines. See text (from Dahlstrom, 1969). ..... (**132**)

Fig. 4.19 The percentage of shortening of three marker horizons within the 20 km wide strips parallel to the northeastern margin of the 'Simply Folded Belt' in the **Lorestan** fold zone. ..... (**136**)

Fig. 4.20 The percentage of shortening of three marker horizons within the 20 km wide strips parallel to the northeastern margin of the 'Simply Folded Belt' in the **Bakhtiari** fold zone. ..... (**137**)

Fig. 4.21 The percentage of shortening of three marker horizons within the 20 km wide strips parallel to the northeastern margin of the 'Simply Folded Belt' in the **Kohkiluyeh** fold zone. ..... (**138**)

Fig. 4.22 The percentage of shortening of three marker horizons within the 20 km wide strips parallel to the northeastern margin of the 'Simply Folded Belt' in the **Fars** fold zone. ..... (**139**)

Fig. 4.23 The average percentage of shortening of three marker horizons within the 20 km wide strips parallel to the northeastern margin of the 'Simply Folded Belt' in **the whole Zagros belt**. ..... (**140**)

Chapter (5)

Fig. 5.1 Palaeogeographic map showing the possible distribution of continental crust (stipple) and ocean crust thought to have existed in Early Mesozoic era. The position of the Tethys and Neo-Tethys sea between Laurasia and Gondwanalad are shown

(modified from Shearman, 1976). ..... (153)

Fig. 5.2 Plate tectonic evolution of the Zagros Mountain Belt (modified from Alavi, 1980). ..... (154 and 155)

Fig. 5.3 Plate tectonic map, showing the opening of the Arlantic Ocean and separation of the Arabian and Afrian plates by seafloor spreading in the Red Sea and the Gulf of Aden. ..... (156)

Chapter (6)

Fig. 6.1 The serial development of folds in a lubricated gelatine multilayer, as the result of the piston moving from right to left (from Blay *et al.*, 1977). ..... (162)

Fig. 6.2 (a), (b) and (c) Three types of apparatus used in experiments on folding. (d-g) A diagrammatic representation of the propagation of the stress front (s.f.) in the apparatus shown in (b) and (c) (from Blay, *et al.*, 1977). ..... (164)

Fig. 6.3 Eight stages in the deformation history of a model multilayer. To the right of the 'basement' uplift, folds develop synchronously as a wave-train in a pre-stressed region of the multilayer. To the left of the uplift, the folds are developed serially at the wave-front as it propagates by a stick-slip mechanism through the multilayer (from Blay *et al.*, 1977). ..... (165)

Fig. 6.4 The serial development of structures in the Jura Mountains deduced from field observations (from Buxtorf, 1916). ..... (167)

Fig. 6.5 (a) The stochastic development of isolated folds in a compressed gelatine multilayer, (from Blay *et al.*, 1977) and (b) a cross section through the Jura mountains between Blochmontkette and Delsberg, (from Buxtrof, 1916) which shows close similarity to the model structures. (c) Isolated, straight limbed conjugate folds in a wax multilayer (from Summers, 1979). ..... (169)

Fig. 6.6 Schematic progressive development of fault-bend folds as a thrust sheet rides over a step in décollement (from Suppe, 1983). ..... (172)

Fig. 6.7 The process of footwall collapse. ..... (173)

LIST OF FIGURES

Chapter (7)

Fig. 7.1 Chah Shirin fault, southern Iran, in Neogene beds and gravels laid down c. 30000-7000 years ago. As a second set of deposits dating from 1250-300 years ago is undisturbed, faulting dates from 7000-1250 years ago. Note the dip in the skyline where the fault outcrops (from Vita-Finzi, 1986). ..... **(183)**

Fig. 7.2 The aerial photograph of the area **NW** of the Strait of Hormuz, showing a recent fault affecting recent alluvial deposits, deflected the drainage system, and indicating **sinistral** strike-slip movement in NE-SW direction. ..... **(185)**

Fig. 7.3 The aerial photograph of the area **NE** of the Strait of Hormuz, showing a series of parallel recent fault affecting recent alluvial deposits, deflected the drainage system, and indicating **dextral** strike-slip movement in NW-SE direction. ..... **(186)**

Fig. 7.4 The aerial photograph of the area NW of the Strait of Hormuz, showing an example of a salt glacier around a Zagros salt diapir. ..... **(187)**

Fig 7.5 (a) Aerial photograph of the area along the eastern coast of the Strait of Hormuz, showing uplifted marine terraces along the coast. (b) Aerial photograph interpretation of a larger area of the eastern coast of the Strait of Hormuz, showing the influence of the Sukaron anticline on the development of the uplifted marine terraces. ..... **(193)**

Fig 7.6 The satellite image of the mouth of the 'Mehran River' northwest of the 'Qeshm Island' in the Strait of Hormuz, showing alluvial cones and river terraces along the shoreline of the Persian Gulf and the development of meanders in the NW side of an uplifted delta due to amplification of the Band-e Lengeh anticline. ..... **(194)**

Fig. 7.7 The Dez River canyon through the Upper Bakhtiari Conglomerate cuesta facing the mountain front. The gorge is some **1,500 feet** depth at this point. The Dez Dam is just out of sight behind the projecting wall on the right. The lower half of this canyon is occupied by the reservoir (from Oberlander, 1965). ..... **(195)**

Fig. 7.8 The aerial photographs of the area NW of the Strait of Hormuz showing the strings of well associated with qanats. ..... **(197)**

Fig. 7.9 The aerial photographs of the area NW of the Strait of Hormuz showing the strings of well associated with qanats. ..... **(198)**

Fig. 7.10 Seismicity map of the Zagros mountain belt, based on information from historical sources. Solid stars show the precise; open stars show imprecise locations. ..... **(207)**

Chapter (8)

Fig. 8.1 Epicentre distribution of the Zagros earthquakes of magnitude (3-7.1) for the period 1963-1988 (based on the NEIC data set). ..... **(215)**

Fig. 8.2 Epicentre distribution of the Zagros earthquakes of magnitude (3-7.3) for the period 1960-1988 (based on the ISC data set). ..... **(216)**

Fig. 8.3 Seismicity map of the Zagros mountain belt for the period from January 1961-April 1993 (from Ni & Barazangi, 1986). ..... **(217)**

Fig. 8.4 Epicentre distribution of **large earthquakes** within the Zagros belt for the periods, (a) 700-1900, (b) 1900-1950 and (c) 1950-1988 (based on Ambraseys & Melville 1982, Nowroozi 1976, and the NEIC data set). ..... **(218)**

Fig. 8.5 The latitude and longitude/magnitude plots for the entire data set shown in Fig.8.1. It should be noted that neither represents a normal profile across the deformation belt. ..... **(223)**

Fig. 8.6 The epicentre distribution/magnitude plots of the large magnitude earthquakes along the Zagros belt. (a) Historical earthquakes for the period 700-1900, and (b) modern events from 1963 to 1988 (based on a data set from Ambraseys & Melville 1982 and the NEIC data set. There is clear correlation between the location of the major earthquakes and the major strike-slip faults shown in Fig. 3.27). ..... **(224)**

Fig. 8.7 The time/magnitude plot of the Zagros historical earthquakes (based on a dataset from Ambraseys & Melville, 1982). ..... **(225)**

Fig. 8.8 The focal depth/magnitude plot of the Zagros modern earthquakes (based on the NEIC data set). ..... **(226)**

Fig. 8.9 The latitude and longitude/focal depth plots of the Zagros earthquakes (based on the NEIC data set). ..... (**230**)

Fig. 8.10 The focal sphere is shown surrounding the hypocentre (H). Note also the epicentre (E), the path of two earthquake waves (1 and 2), the epicentral distance (a) and the corresponding angle of emergence (b). The intersection of the seismic rays with the focal sphere permits the polarity observed at a station such as 2 in the figure to be plotted. It is usual to do so on either a stereographic or an equal-area projection of the lower hemisphere. Based on account in Kasahara (1981). The lower figures are idealized focal plane solutions. (i) Strike-slip; (ii) dip-slip reverse, (iii) dip-slip normal, (iv) normal with a small strike-slip component. Note that the data for (ii) are insufficient to constrain the solution unambiguously. The alternative (broken line) also indicates reverse faulting but on an ENE-WSW strike. At the nodal lines separating the compressive and dilational sectors the amplitude of the initial P-pulse tends towards zero. Open circles = dilational arrivals; solid circles and stipple = compression (from Vita-Finzi, 1986). ..... (**233**)

Fig. 8.11 Focal mechanism solutions for earthquakes in Iran. P-wave compression quadrants are shown by dark regions and the rarefraction quadrants by plane regions. The location of faults and other tectonic features are adapted from Berberian (1976) (from Chandra, 1984). ..... (**234**)

Fig. 8.12 Fault plane solutions in the Zagros (from Jackson & McKenzie, 1984).(**235**)

Fig. 8.13 Seismotectonic map of the Zagros showing epicentres of larger events and their fault plane solutions. Darkened regions in fault plane solutions indicate compression (from Ni & Barazangi, 1986). ..... (**236**)

Fig. 8.14 Direction and rates (in mm a^{-1}) of relative motion of the earth's major plates shown at selected points on their boundaries. Circled numbers represent absolute motions (in mm a^{-1}) of plates relative to the hotspot reference frame (from Chase, 1978). ..... (**238**)

LIST OF TABLES

LIST OF TABLES

Chapter (4) **(Page)**

Table 4.1 The results of measurements of the variation in percentage shortening of three marker horizons within the 20 km wide strips parallel to the northeastern margin of the 'Simply Folded Belt' in the **Lorestan** fold zone ..... **(141)**

Table 4.2 The results of measurements of the variation in percentage shortening of three marker horizons within the 20 km wide strips parallel to the northeastern margin of the 'Simply Folded Belt' in the **Bakhtiari** fold zone ..... **(142)**

Table 4.3 The results of measurements of the variation in percentage shortening of three marker horizons within the 20 km wide strips parallel to the northeastern margin of the 'Simply Folded Belt' in the **Kohkiluyeh** fold zone ..... **(143)**

Table 4.4 The results of measurements of the variation in percentage shortening of three marker horizons within the 20 km wide strips parallel to the northeastern margin of the 'Simply Folded Belt' in the **Fars** fold zone ..... **(144)**

Table 4.5 The results of measurements of the variation in percentage shortening of three marker horizons within the 20 km wide strips parallel to the northeastern margin of the 'Simply Folded Belt' in **the whole Zagros belt** ..... **(145)**

CHAPTER 1

Objectives, methodology, database, and thesis outline

1. INTRODUCTION

The '**Zagros Mountains**' form one of the world's best known mountain belts in part because it contains some of the most spectacular examples of large-scale geological structures such as folds, faults, and salt diapirs and in part because of the large oil and gas reserves found in this region. It has been produced as a result of collision between the Arabian and Central Iranian plates and has been a site of active tectonism from the Cretaceous to the present day.

Because of these various factors the Zagros mountain belt has attracted the attention of many geologists from all over the world. However, despite the considerable volume of work that has been carried out relating to its plate tectonic evolution and regional structures, many issues still remain controversial and many ambiguities and unsolved problems still remain.

The present study entitled '**Active Tectonics in the Zagros Mountains, Iran**' is an attempt to solve some of these problems.

2. OBJECTIVES

The main objectives of the present study can be summarised as follows:

i) To examine the spatial distribution, geometrical characteristics, and mechanism of formation of the large-scale geological structures (i.e. folds, faults, and salt diapirs) in order to determine their implications regarding the evolution of the *Zagros deformation belt*.

ii) To investigate the implications of the variations in the geometrical characteristics of the folds and sedimentary cover to the evolution of the *Zagros deformation belt* by a detailed analysis of the half-wavelength/amplitude ratio of the folds, elevation and inclination of the median surface of the folds and the variations in shortening of the sedimentary cover.

iii) To use the results of the above mentioned analyses for determining the characteristics of the governing processes of folding, faulting and salt diapirism, and thereby propose a new model for the evolution of the *Zagros deformation belt*, including the fold and fault belts and the salt diapir provinces.

iv) To study the origin, effects, and rates of the recent earth movements and evidence for the neotectonic activity in the Zagros Mountain belt in order to deduce the characteristics of the present active deformation in the Zagros region i.e. along the north-eastern margin of the Arabian plate.

v) To analyse earthquake data for the Zagros region in order to determine the origin and characteristics of the recent seismicity, the nature and spatial distribution of the active faults, the state of regional stress and the contribution of the seismic activity in the present active deformation in the Zagros Mountain Belt.

vi) To integrate these studies into a mechanically-sound model for the deformation processes controlling the evolution of the Zagros Mountain Belt.



3. METHODOLOGY

The present study was carried out in several stages, using different research methods as follows:

a) Almost all of the available geographical and geological maps, satellite images and relevant literature were reviewed in order to improve the understanding regarding the geographical and geological settings of the Zagros Mountains i.e. (**the study area**).

b) The spatial distribution and geometrical characteristics of the regional structures (folds, faults, and salt diapirs) were examined using aerial photographs, satellite images, geological maps, cross-sections, and published work.

c) Using the geological cross-sections the half-wavelength/amplitude ratio, the elevation and inclination of the median surface of the folds and the variation in percentage shortening of the Zagros sedimentary cover across different parts of the folded belt was determined.

d) The available previous work regarding the plate tectonic and geomorphological evolution of the Zagros mountain belt was carefully studied in order to understand different stages of its evolution and to distinguish the existing similarities and differences between the models proposed by different authors.

e) On the basis of the results of the above mentioned studies a new model was proposed for the evolution of the '**Zagros deformation belt**' which took into the processes responsible for folding, faulting, salt diapirism deduced from the studies described in this thesis.

f) The origin, effects and rates of recent movements and evidence for neotectonic activity in the whole Zagros belt were considered using mainly the available published

work. In addition, the evidence of neotectonic activity in the most active part of the belt (the Hormuzghan province on the Iranian side of the Strait of Hormuz) was considered by a careful examination of the aerial photographs of the region at the scale of 1:40,000, using a big mirror stereoscope.

g) Using various data sets the characteristics of the recent day seismic activity in the Zagros region, including the epicentral distribution, magnitude, focal depths, and focal mechanism solutions of the Zagros earthquakes were carefully analysed and several graphs showing the epicentral distribution, focal depths, magnitudes of earthquakes were plotted, using the 'Surfer program' of the 'Golden Software'. The sense of movement on active faults and the state of regional stress were also considered using the published fault plane solutions of the Zagros earthquakes.

h) Finally the result of all the different studies carried out during the present study were integrated and discussed in order to consider their compatibility with each other. On the basis of these studies a model was proposed for the plate tectonic and geomorphological evolution of the Zagros mountain belt which accounts for the existing structures and the characteristics of the present day deformation which is operating along the NE margin of the Arabian plate.

4. DATABASE

Geological maps and cross-sections on various scales, aerial photographs and satellite images, earthquake data, together with published books and papers were used as the data base for the present study.

a) GEOLOGICAL MAPS & CROSS-SECTIONS

A portfolio of geological maps, cross-sections and stratigraphical columns (BP, 1956), based on the work of the geological staff of the Anglo-Persian Oil Company (1909-1933), the Anglo-Iranian Oil Company (1933-1951), and the British Petroleum Company (from 1954 to the present) was used to carry out a geometrical analysis of fold structures, (in particular to evaluate the half-wavelength/amplitude ratio of folds and the general inclination of the folded sequence), and for determining the percentage shortening of the sedimentary cover across the Zagros belt in different places along the belt.

According to the introductory notes accompanying the portfolio the total geological and geophysical effort involved in its preparation was about 287 man years, including about 111 man-years on the field surveys. Although modern, computerized facilities were not used in the preparation of the maps and cross-sections, they are nevertheless well suited for the structural analysis required by the present study.

Other geological maps used for the analysis of large-scale geological structures and morphological features, as well as for the neotectonic and seismotectonic studies, were as follows:

i) *The Geological Map of Iran*, (1:2,500,000), published by the National Iranian Oil Company (NIOC) in 1957.

ii) *The Geological Map of Iran*, (1:2,500,000), published by the British Petroleum Company Limited in 1963.

iii) *The Tectonic Map of Iran*, (1:2,500,000) based on the geological map of Iran (1959), and later information up to 1972, compiled by J. Stöcklin and M. H. Nabavi, and published by the National Iranian Oil Company (NIOC) in 1973.

iv) *The Geological Map of Iran*, (1:1,000,000), sheets 3, 4, 5, and 6 (covering southwest Iran), published by (NIOC) in 1975.

v) *The Geological Map of Minab*, (1:100,000), published by the Geological Survey of Iran in 1980.

vi) *The Geological Map of Iraq and Southwestern Iran*, (1:1,000,000), Published by Robertson Research Publication (RRP) in 1987.

b) AERIAL PHOTOGRAPHS

A subset of glossy aerial photographs at a scale of 1:40,000, taken by Hunting Aerosurveys Ltd. in 1950, for British Petroleum Company Limited, housed in the Geological Sciences department of University College London, was used in the examination of regional structures and morphology as well as in the search for neotectonic movements.

c) LANDSAT IMAGES

A set of Landsat 1, infra-red, multi-spectral scanner satellite images at 1:1,000,000 scale together with a few other images from published work were also used for the structural and geomorphological studies.

d) EARTHQUAKE DATA

Several sets of earthquake data from different sources were used for the examination of the epicentral distribution, focal depth and magnitude of the Zagros earthquakes. A subset of a large earthquake data set provided by the National Earthquake Information Centre (NEIC), from the Global Hypocentre database CD-Rom, for the area between latitudes 20°- 40° N and longitudes 40°- 65° E was retrieved using the EPIC program software. The Zagros earthquakes, which were separated from the retrieved data set by the present author include 1075 earthquakes of magnitude 3 to 7.1 between 1960 to 1988.

A subset of earthquake data for the Zagros region provided by the International Seismological Centre (ISC), including 1560 earthquakes of magnitude 3.5 to 7.3, was also used for the examination of seismic activity in the Zagros active belt. A catalogue of over 600 relocated earthquakes prepared by Nowroozi (1976) was used for the examination of epicentre distribution during the first half of the twentieth century. An examination of historical earthquake data was also carried out using the catalogue of historical events prepared by Ambraseys and Melville (1982).

A study of focal mechanisms for the Zagros earthquakes was also carried out using a range of publications, including Nowroozi (1972), Jackson and Mckenzie (1984), Chandra (1984), and Ni and Barazangi (1986).

e) PUBLISHED WORK

A literature review of previous work on the Zagros Mountain belt has carried out and some of the publications studied such as those regarding the neotectonic activity and seismicity also provided the database for the further studies presented in this thesis.

5. THESIS OUTLINE

An introduction to the present study including the objectives, methodology, database, and the outline of the thesis are presented in Chapter 1. In Chapter 2 the most important aspects of the geographical and geological setting of the study area are described and relevant previous work is reviewed.

The spatial distribution, geometrical characteristics, and the mechanism of formation of the large-scale geological structures including folds, faults and salt diapirs are examined in Chapter 3, and a detailed analysis of the fold geometry and the variations in the elevation and inclination of the median surface of the folds and the variation in percentage shortening of the Zagros sedimentary cover across various parts of the belt is presented in Chapter 4.

The plate tectonic and geomorphological evolution of the Zagros Mountain Belt is considered in Chapter 5 and in Chapter 6 the evolution of the Zagros deformation belt including the fold and fault belts and diapir provinces and the processes of folding, faulting and salt diapirism are discussed.

Chapter 7 presents the results of an investigation of the origin and effects of recent earth movements and evidence for the neotectonic activity in the Zagros Mountains. Characteristics of the regional seismicity and the results of an analysis of the Zagros earthquake data are discussed in Chapter 8 and the general discussion and conclusions arising from this research project are presented in Chapter 9.



CHAPTER 2

The Zagros mountains

1. INTRODUCTION

This chapter summarises the most important aspects of the geographical and geological setting of the Zagros Mountains (**the study area**) and briefly reviews relevant published work.

2. GEOGRAPHICAL SETTING

Only a brief description of the location, settlements, climate and topography of the Zagros Mountains is given here.

a) LOCATION

As can be seen clearly from the plate tectonic map of the Middle East, drawn by the present author on the basis of the data from Berberian (1981) and Nowroozi (1987), the '**Zagros Mountains**' form a triangular '**Mountain Belt**' which extend over 1500 km along the northeastern margin of the Arabian plate from the Iraq-Turkey border to the Minab-Zendan fault zone east of the Strait of Hormuz in the Persian Gulf (Fig. 2.1).

The belt is bounded on the NE by the Main Zagros thrust line with its almost straight NW-SE trend, and a sinuous 'Mountain Front' on the southwest. The width of the 'Zagros Mountain Belt' is not constant and decreases when traced from SE to NW. The whole mountain belt covers an area of about 50,000 km^2.

The '**Zagros Mountains**' join the '**Taurus Mountains**' of southern Turkey at their northwestern end and are separated from the '**Makran Ranges**' by the north-south trending Minab-Zendan fault zone, west of the Strait of Hormuz (Fig. 2.1).

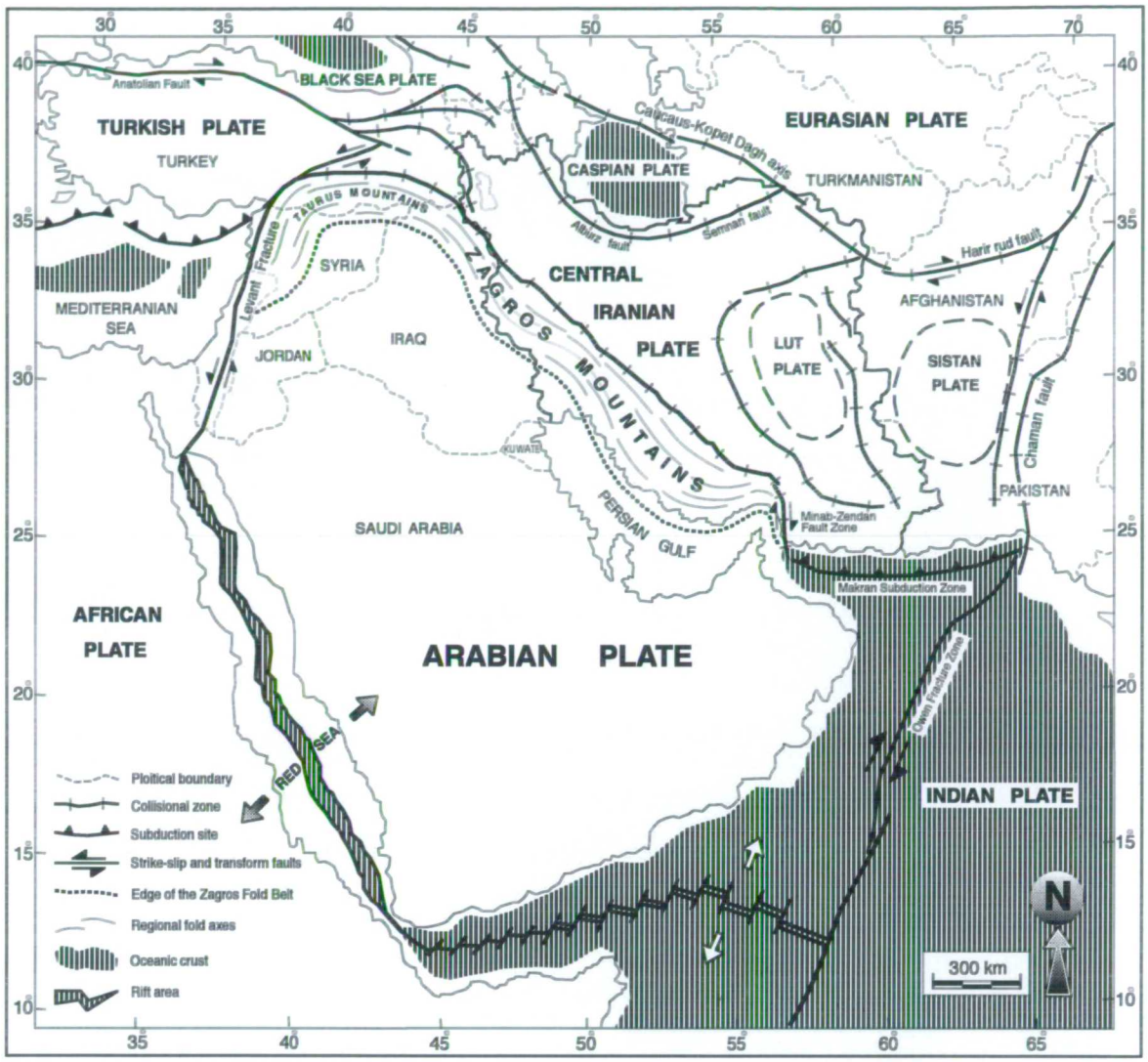


Fig. 2.1 Plate tectonic map of the Middle East, showing the Zagros mountains along the northeastern margin of the Arabian plate (based on Berberian, 1981 and Nowroozi, 1987).

b) SETTLEMENTS

The Iranian parts of the Zagros Mountains comprise nine of the southwestern provinces of Iran. These are Kermanshah, Lorestan, Ilam, Khuzestan, Boyerahmad va Kohkiluyeh, Chaharmahal Bakhtiari, Fars, Bushehr, and Hormuzghan. Kermanshah, Khorramabad, Ilam,

Ahwaz, Yasuj, Shahr-e Kord, Shiraz, Bushehr, and Bandar Abbas are the provincial centres, respectively (Fig. 2.2).

Most of these provinces are densely populated and contain numerous large cities, townships, and villages. Farsi is the common language but local native languages, including Turkish, Kordish, Lorish, and Arabic, are also widely used.



Fig. 2.2 Map of Iran, showing the provinces and the provincial capitals.

c) CLIMATE

The Zagros Mountains experience great extremes of climate in a very complex pattern characteristic of mountain climates (Oberlander, 1965). Temperatures in winter can be as low as -20°C and unpleasantly cold in the northern parts, while in summer temperatures as high as 50°C are nothing out of the ordinary in the southern parts. Seasonal temperatures, however, increase progressively in two perpendicular directions from NW to SE and NE to SW.

The northwestern parts are generally the coldest and the rainiest part of the Zagros Mountains. Snow frequently remains until early spring, or even later in the mountains. Summers are relatively mild, and spring and autumn are pleasant. Further south (in Khuzestan and Boyerahmad va Kohkiluyeh provinces) the winter is less severe, spring and autumn are pleasant, and summer is hot but rarely scorching.

In the provinces of Fars and Bushehr, summer is hot (regularly up to 45°C or even 50°C), with very oppressive humidity. Spring and autumn are warm and winter is pleasant. In the southeastern end of the Zagros Mountain, within about 200 km of the Persian Gulf and the Gulf of Oman, the climate is similar to that of the Fars and Bushehr provinces or even hotter, with strong winds during the summer.

The Zagros Mountains generally have a Humid Meso-thermal climate, with extreme seasonality in precipitation. The summer half of the year is totally rainless, but from November to April cyclonic depressions moving eastward from the Mediterranean and warm fronts associated with the Arabian anticyclone affect the Zagros, bringing cloudy weather and as much as 250 mm of precipitation in the northern section. Fifty to one hundred millimetres would be a figure more representative of precipitation in the mountain complex as a whole, north of latitude 30°N. Precipitation decreases progressively in a

southeastward direction, so that the uplands of Fars receive 25 mm of rain fall or less on average. Annual totals are everywhere quite variable (Oberlander, 1965).

South of latitude 34°N, agriculture dependent upon rainfall is almost everywhere marginal, and irrigation is practised in valleys throughout the highlands. Nevertheless, it must be emphasized that the Zagros Mountains rise from the surrounding deserts of Iraq and Iran as an island of moisture, the rainfall here being sufficient to support parklands and groves of both deciduous and evergreen hardwoods as far south as Boyerahmad va Kohkiluyeh province (Fig. 2.2).

High relief and the lack of vegetation in the surface sediments favour rapid runoff or flash floods in the southern parts of the belt. Strong winds, arid to semi-arid conditions, and seasonally high temperatures also promote high rates of evaporation and erosion throughout the southern Zagros.

d) TOPOGRAPHY

The **'Zagros Mountain Belt'** has an asymmetric topography and its elevation ascends northeastward by gradual steps from the Mesopotamian alluvial plains at around sea level to a crestline of imbricate slabs and permanent snowfields between 3350-4600 m above sea level (Fig. 2.3). The highest peaks immediately overlook the lesser mountains of the central Iranian plateau. Zard Kuh (Zardeh Kuh), at 4270 m is the culminating point of the mountain complex (Fig. 2.3).

However, as can be seen from a **new geomorphological map** drawn by the present author on the basis of data from Oberlander (1965), the 1:1,000,000 scale geological map of Iran (NIOC, 1975) and the 1:1,000,000 scale geological map of Iraq and southwestern Iran (Robertson Research Publication, 1987) (Fig. 2.4), the northeastward increase in elevation

of the Zagros mountains is not uniform everywhere across the belt. There are several major structural '**culminations**' and '**depressions**' along and across the belt which created a rather complex topography.

The topographic expression of the region is determined primarily by the '**rock type**' (which varies from very soft marls to extremely dense limestones), the '**large-scale structural grains**' (which is defined by spectacular, whaleback mountain ranges, each whaleback an elongate anticline) and '**major structural culminations and depressions**' along and across the belt (Figs. 2.3-2.6).

The external ranges which form the southwest margin of the belt are composed mainly of marl and sandy limestone and are essentially intact, isolated and gentle anticlines. The internal mountain ranges on the northeast margin are chiefly composed of dense limestone contain tight folds, imbricate fault slabs, and overthrust structures all intensively eroded. Deep dissection of the limestone beds of these tight, chevron folds, and intricate overturned structures has given a particularly wild aspect to the inner ranges. (Fig. 2.5).

The extensive development of conglomerate cuestas and mesas, fronting the range on the southwest of the Bakhtiari Mountains in the central Zagros, create a contrasting and rather gentle morphology in this part of the region (Fig. 2.3). Northwest and southeast of the Dezful Embayment the conglomerate cuesta and scarp are missing and the landscape is one of less conspicuous tablelands and mesas (Oberlander, 1965).

The development of alluvial deposits in the Mesopotamian plain in front of '**Mountain Front**' (Fig. 2.4) and coastal plain on the Iranian side of the Persian Gulf have also produced a contrasting, gentle topography.

As can be seen from **a new detailed drainage map** of the Zagros mountain belt, drawn by

the present author on the basis of data from 1:1,000,000 scale geological map of Iran (NIOC, 1975) (Fig. 2.7), north of latitude 30°N, the main drainage lines of the Zagros Highlands are transverse to its structure.

Major streams cross the orogenic system with little regard for geological barriers, and many of the drainage basins serving this half of the highland have their longer dimension across the structural grain. Some of the '**gorges**' created by these transverse streams are near-vertical slits hundreds of metres in depth (Figs. 2.8-2.11).

South latitude of 30°N, longitudinal drainage becomes characteristic of the mountain complex. Accordingly, the southern watersheds are elongated along strike. It might be supposed that greater aridity here might restrict the mechanism that drove the drainage of the north directly across the highland. However, even in the south anticlines have been transected by gorges although the numerous isolated domes provide easy consequent paths for surface water moving in any direction (Oberlander, 1965).

The aerial photograph of the '**Minab Anticline**', northeast of the Strait of Hormuz, provides an excellent example of such an anticlinal structure in the southern parts of the Zagros mountain belt which has been transected by the transverse drainage system (Fig. 2.12).

As can be seen from the drainage map of the Zagros mountain belt (Fig. 2.7), except for the area covering the major Shiraz-Neyriz structural depression (Fig. 2.4) where the rivers drain into the local '**Bakhteghan**', '**Maharlu**', and '**Tashk**' lakes (Fig. 2.13) all rivers drain into the Persian Gulf (Fig. 2.7).

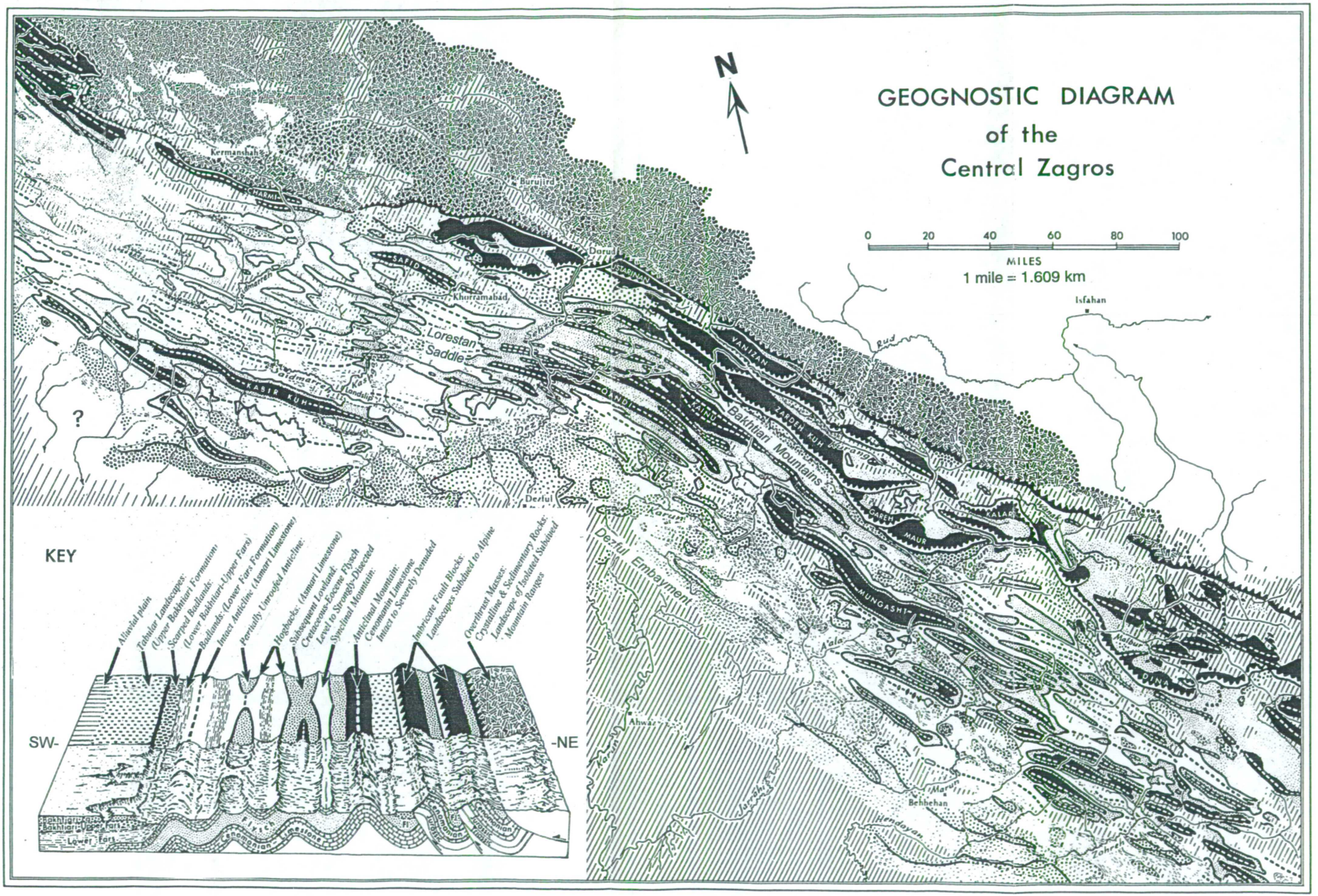


Fig. 2.3 Diagram of the Central Zagros showing the stepped southwestward dipping topography and the influence of the major structural grains and rock-type on the development of the contrasting morphological provinces (modified from Oberlander, 1965).

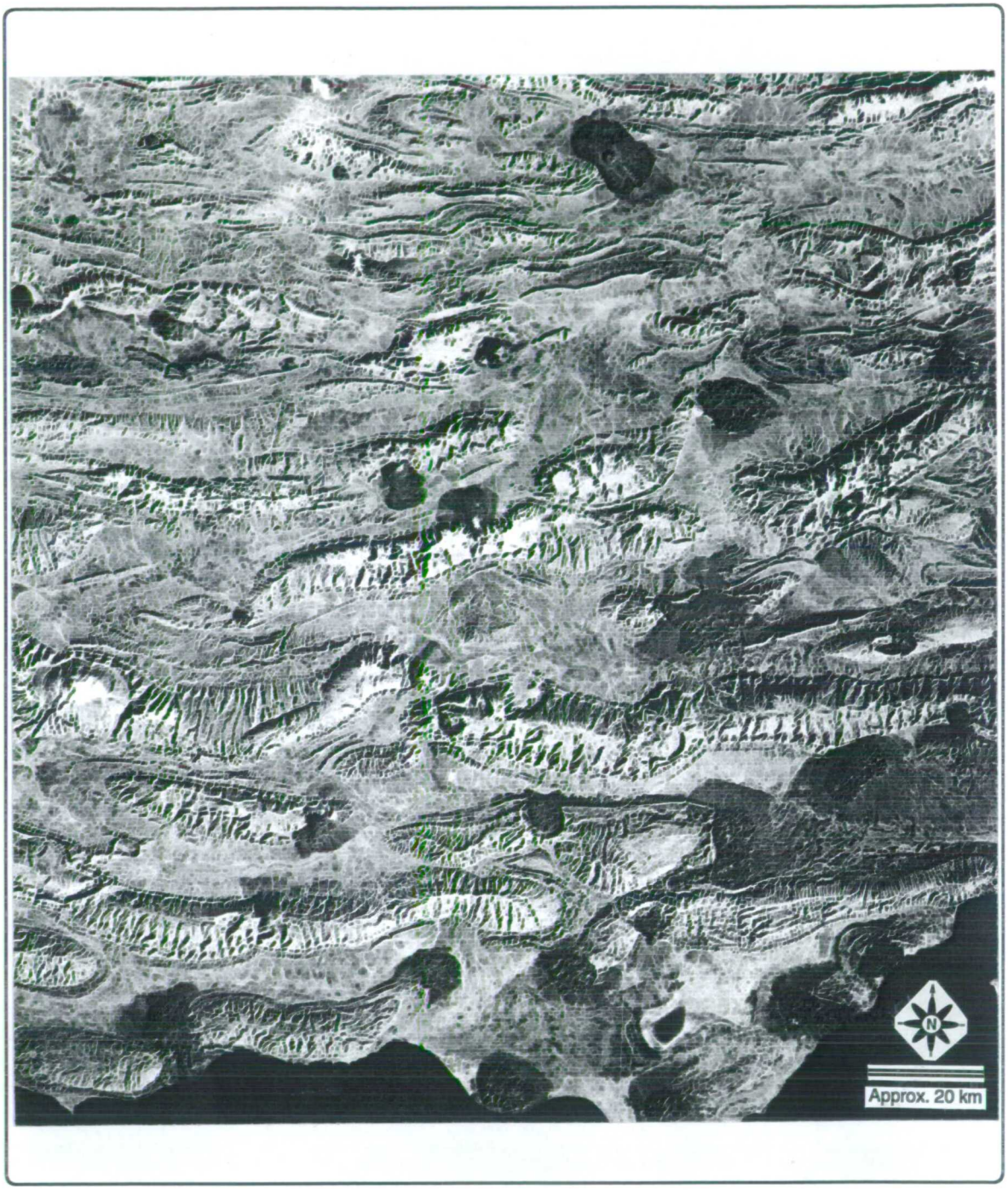


Fig. 2.5 Satellite image of the southern Zagros mountains, showing the intact, elongate and widely spaced anticlines in the south (near the Persian Gulf) and deeply dissected, tight, closely spaced folds to the north (near the Main Zagros Thrust).

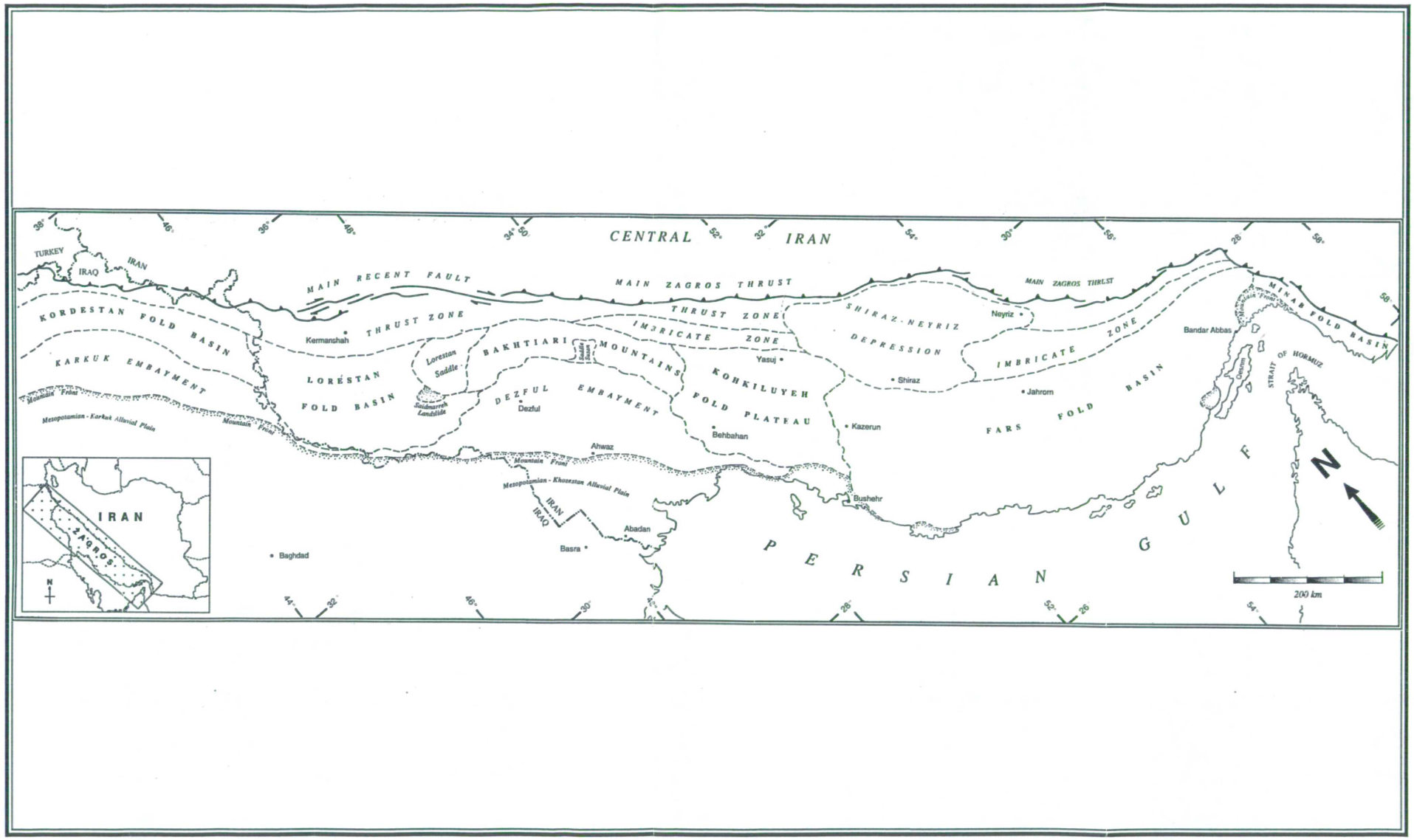


Fig. 2.4 A geomorphological map of the Zagros mountain belt, showing the stepped topography, different morphological provinces and major culminations and depressions along and across the belt, (based on Oberlander 1965, the geological map of Iran (NIOC, 1975), and the geological map of Iraq and southwestern Iran (RRP, 1987)).

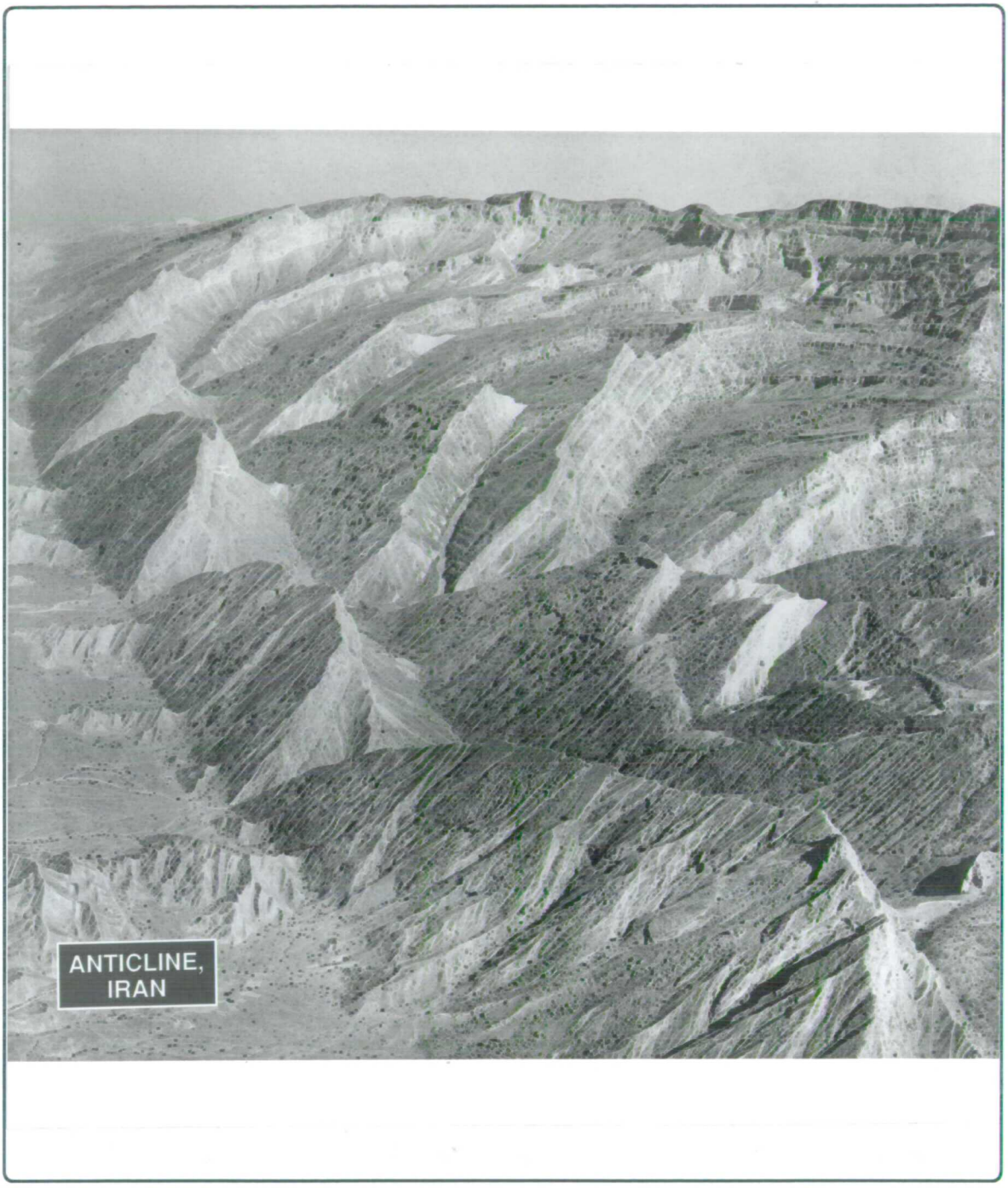


Fig. 2.6 A dissected large-scale anticline in the Zagros Mountain, showing the effects of the these structures and the mechanically contrasting rock types in the creation of the present day topography.

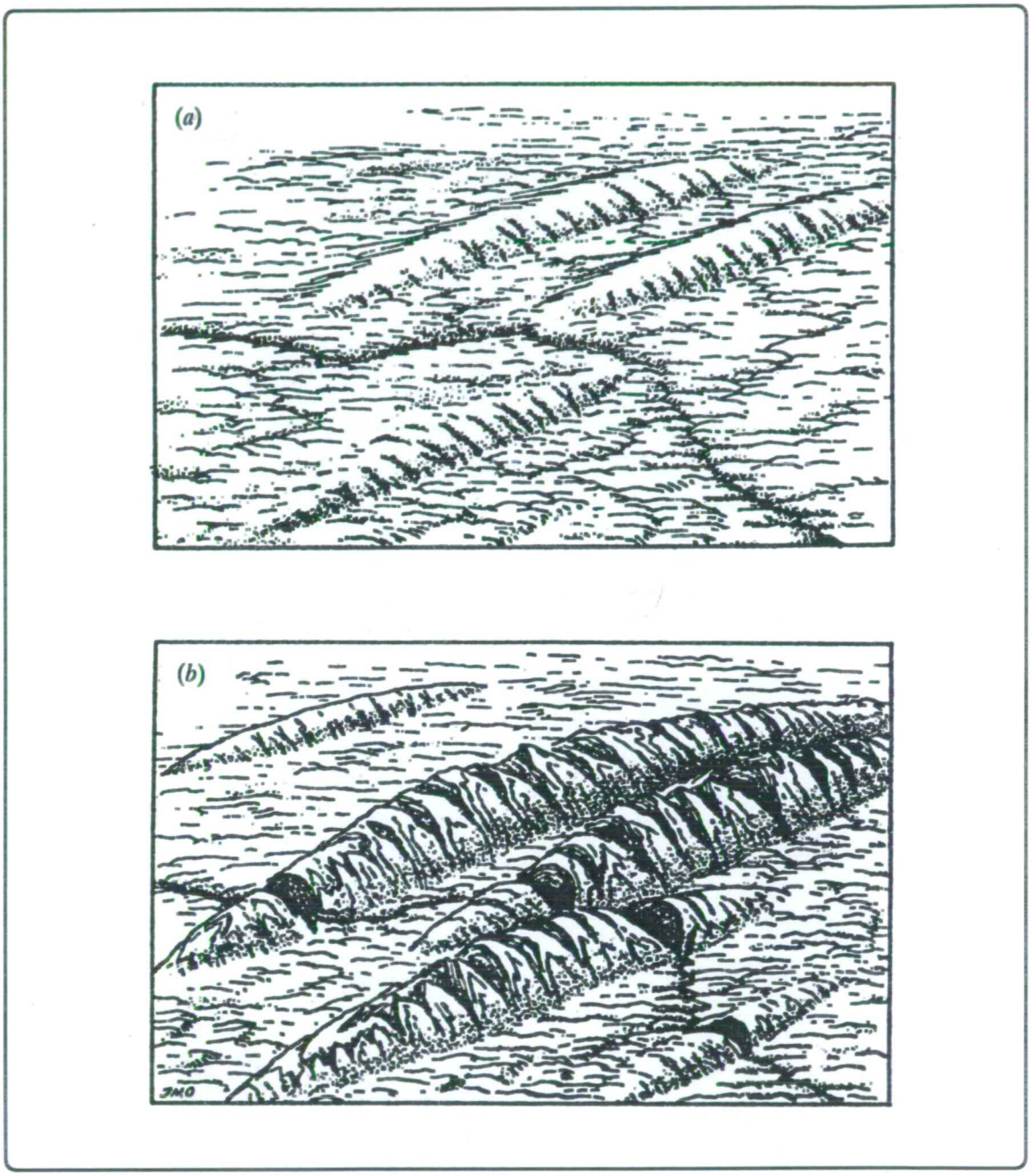


Fig. 2.8 Development of transverse gorges in the Zagros Mountains. a) Drainage consequent on initial deformation of folds which are not exposed due to the presence of an overburden of erodible material, b) drainage discordance produced by renewed deformation or fault exposure of the fold structures (from Oberlander, 1965).

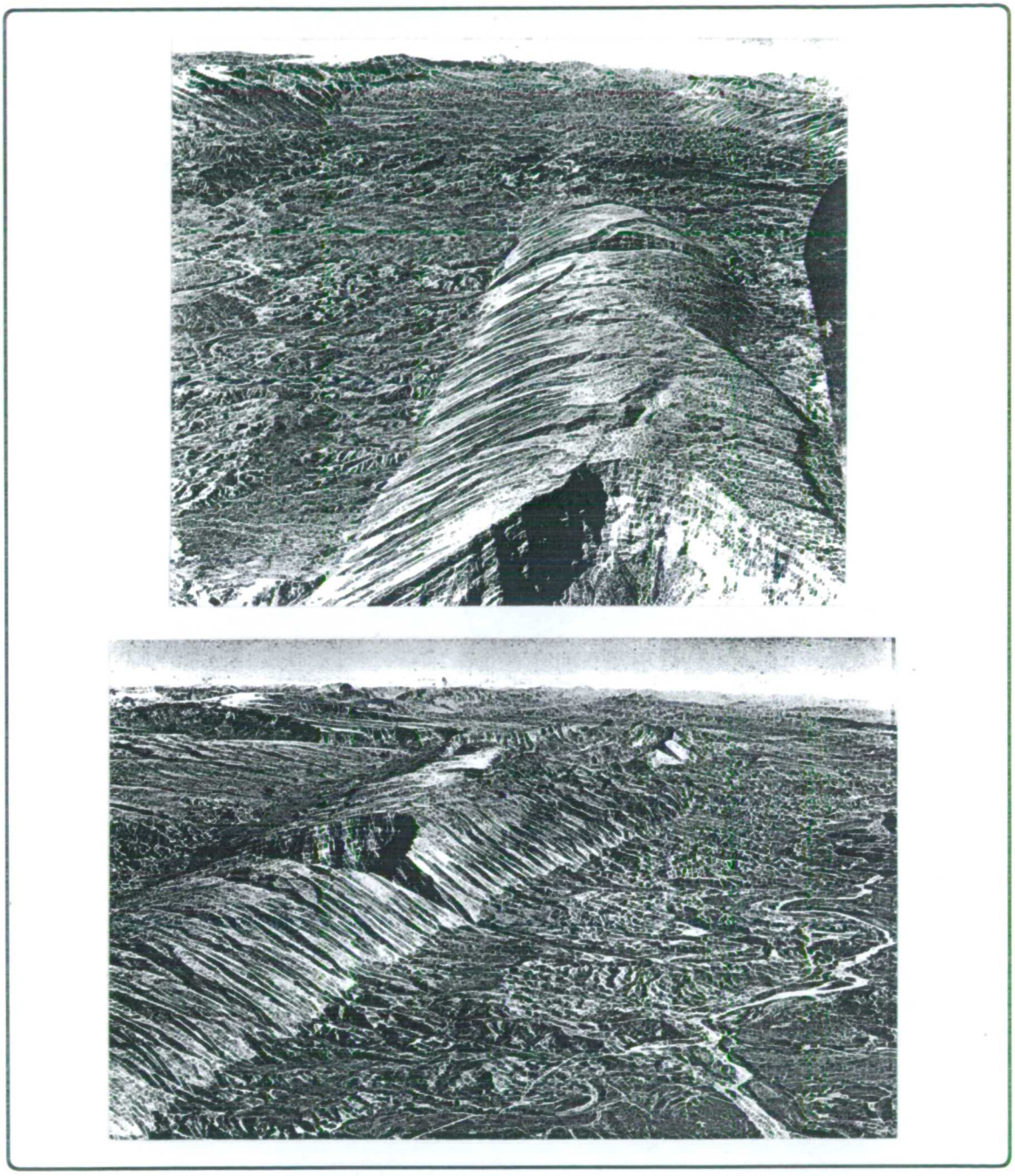


Fig. 2.9 Two views of the Tang-e Lailum, a transverse gorge through the Asmari limestone anticline of Kuh-e Kailan. The Kabir kuh anticline lies to the southwest (left) and the Milleh kuh anticline to the NE (right) (from Oberlander, 1965).

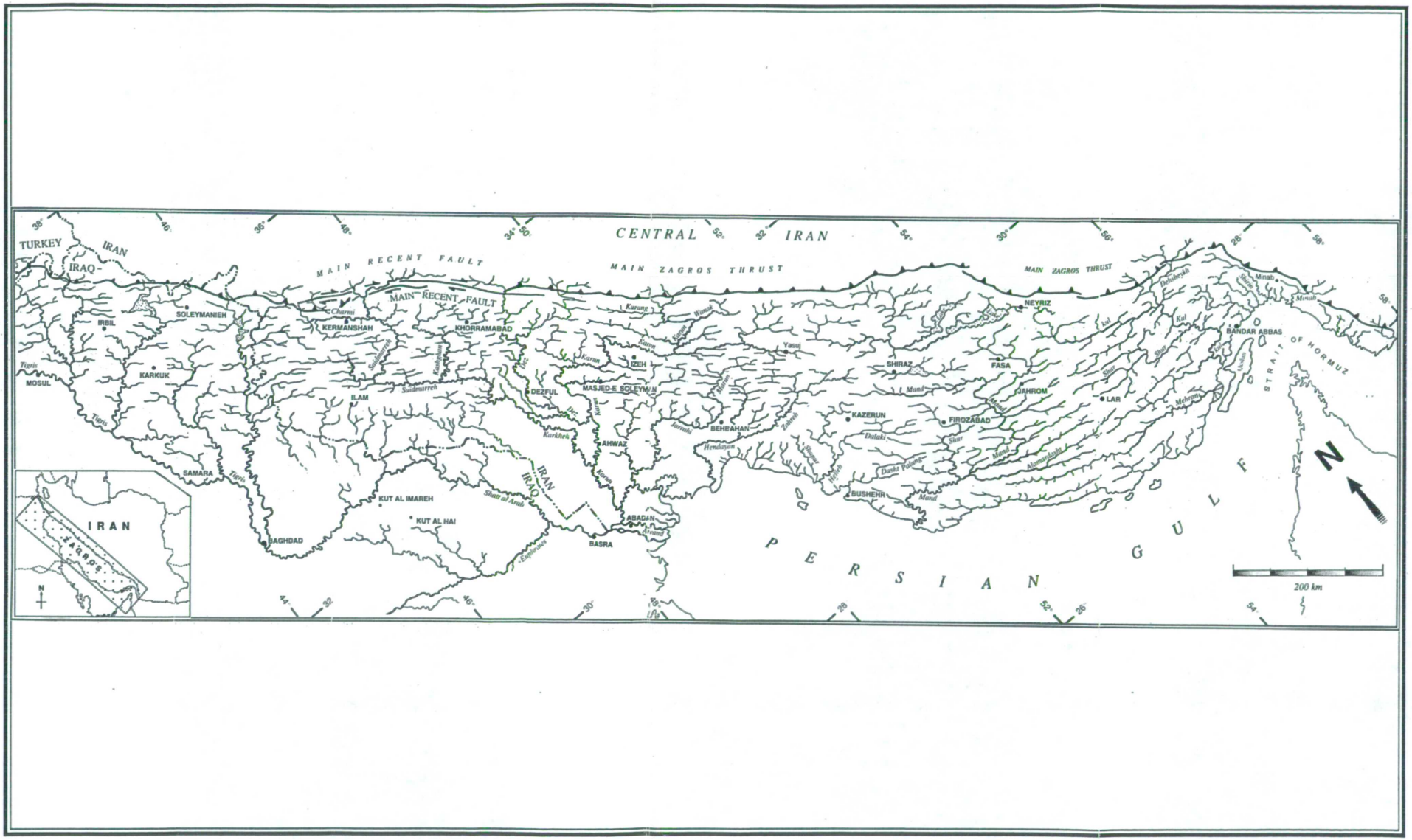


Fig. 2.7 Drainage map of the Zagros Mountain Belt, showing the asymmetric southwestwards dipping topography and the influence of large-scale structural grains and major structural culminations and depressions in the creation of longitudinal and transverse drainage pattern.

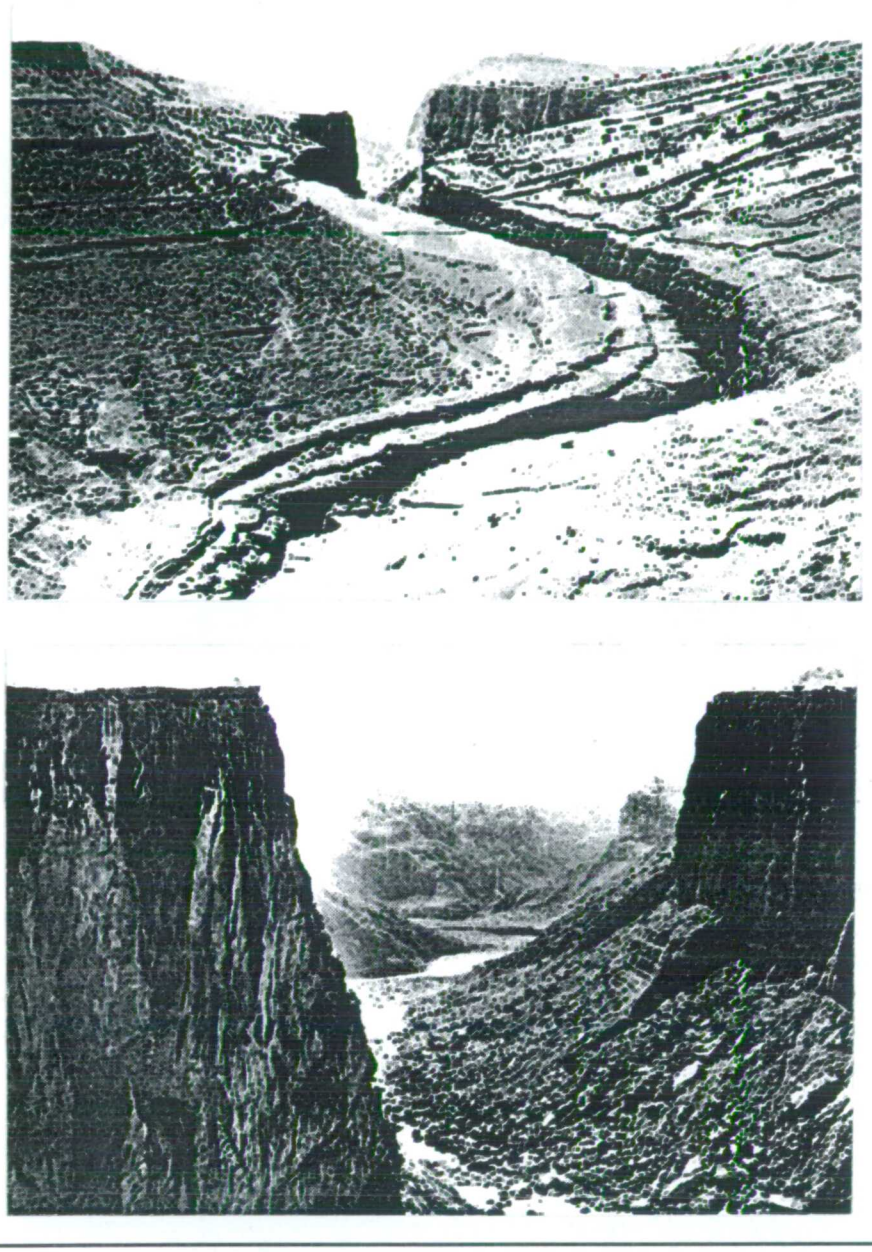


Fig. 2.10 The gorge of Zohreh River showing extreme constriction where it cuts solely in Asmari limestone (top) and abrupt expansion where underlying marls are exposed permitting spring-line sapping at the limestone marl contact (bottom) (from Oberlander, 1965).

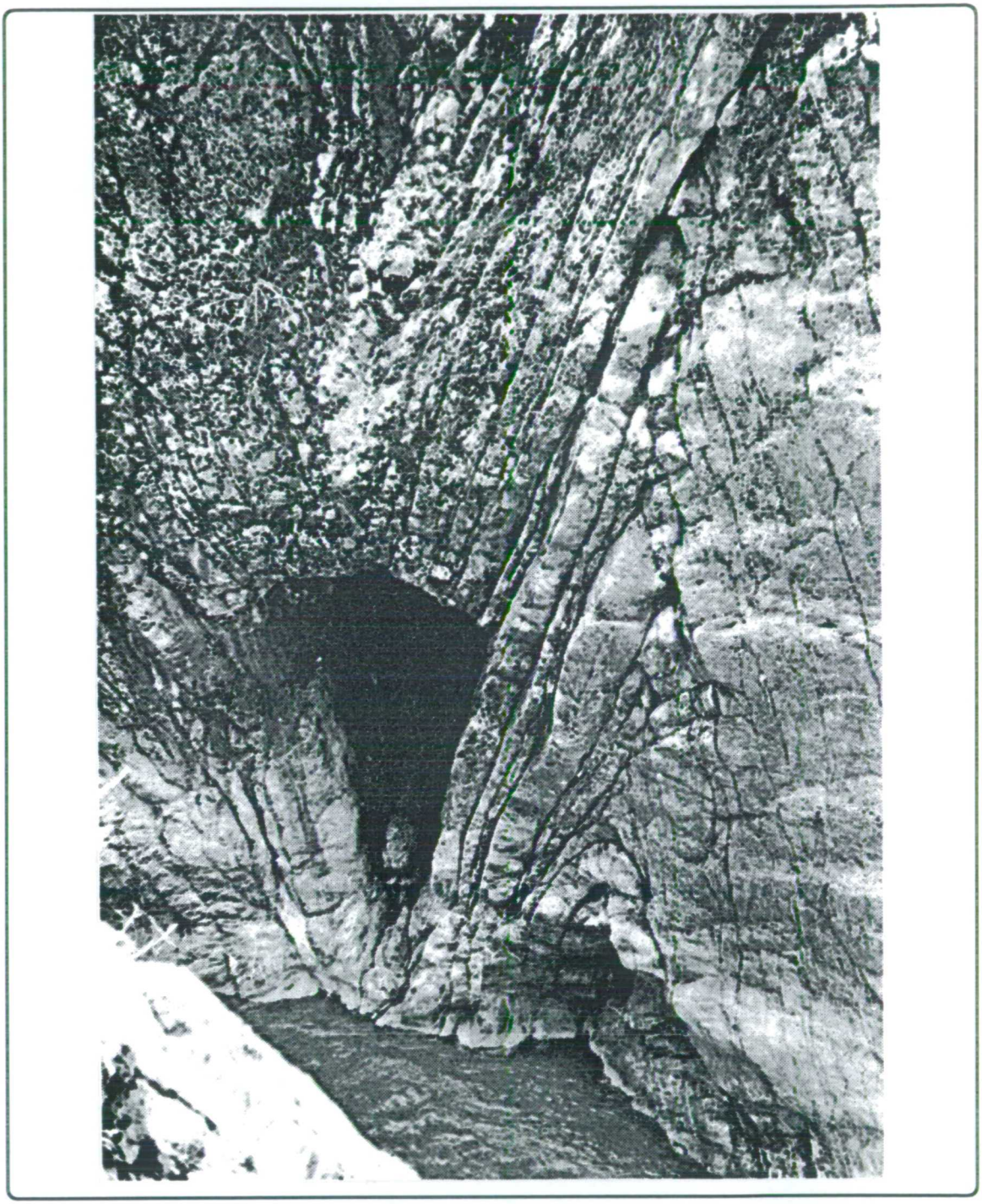


Fig. 2.11 Vertical gorge of the Keshwar River, illustrating of the intense deformation of the Cenomanian limestone in the Bakhtiari Mountains (from Oberlander, 1965).

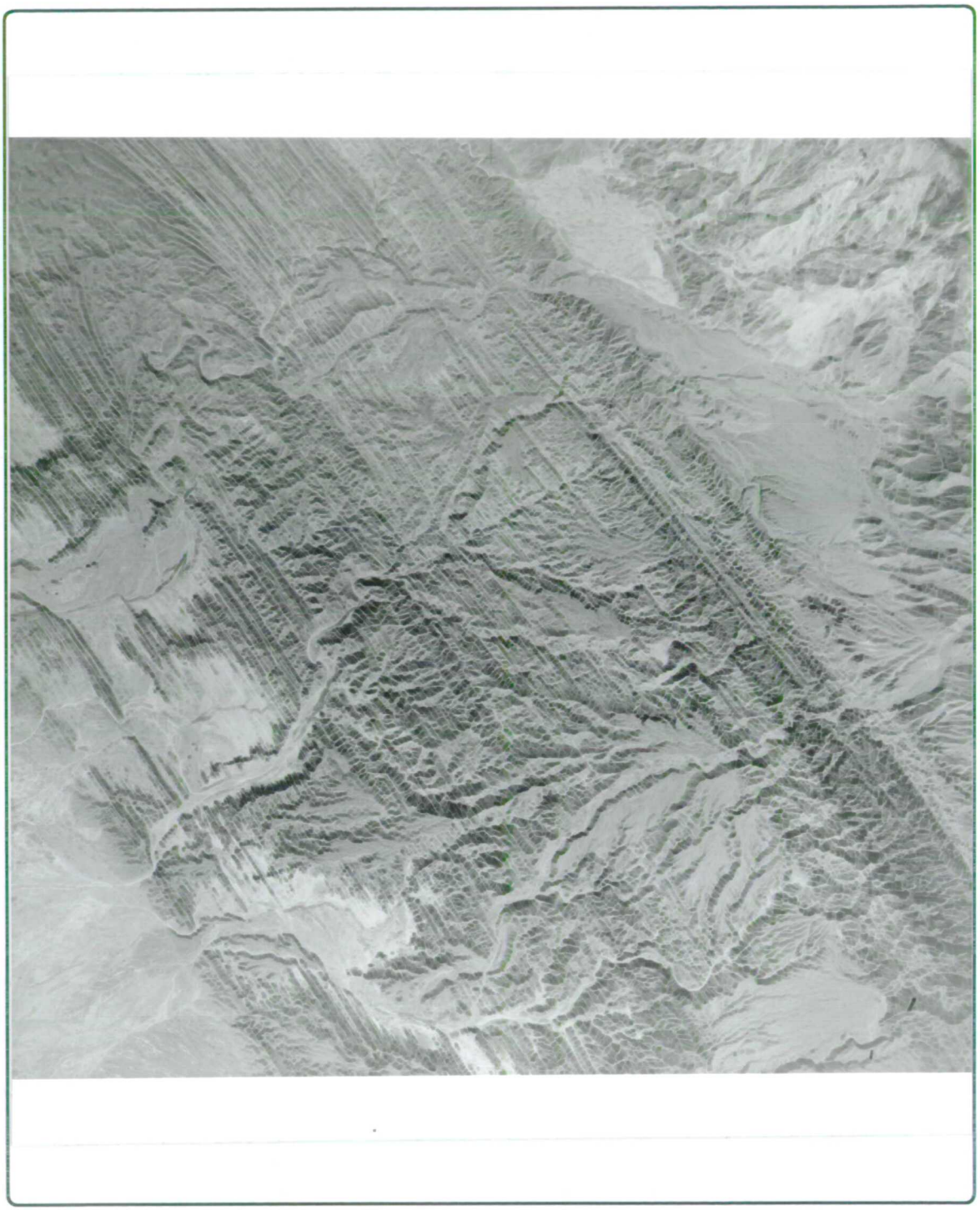


Fig. 2.12 Aerial photograph of a portion of the 'Minab anticline' NE of the Strait of Hormuz transected by a transverse drainage system (see also Figs. 3.1 and 3.24).



Fig. 2.13 Satellite image of the southeastern Zagros, showing the contrasting topography of the belt in the southwest and northeast and the Shiraz-Neyriz depression with the Bakhteghan, Maharlu and Tashk lakes.

3. GEOLOGICAL SETTING

Only brief descriptions of the major structural zones and a summary of regional stratigraphy, metamorphic rocks, ophiolitic and mélange rocks, and volcanic rocks are given here as an introduction to the geology of the study area. Details of the large-scale regional structures and the plate tectonic and geomorphological evolution of the region will be discussed in the later chapters.

a) MAJOR STRUCTURAL ZONES

The Zagros Mountain Belt has been divided into different structural zones by Oberlander (1965). As can be seen from **a new tectonic map** drawn by the present author on the basis of his division and on data from Stöcklin (1968) and (Alavi, 1980) (Fig. 2.14), the **Outer** (younger) Zagros, the southwestern half of the orogenic system, is a zone of strong folding produced for the most part by a late Pliocene orogeny, and is termed the '**Simply Folded Belt**'. This is composed of a thick sequence of late Precambrian to Pliocene shelf sediments without any visible angular unconformity.

The **Inner** (older) Zagros which makes up the northeastern parts of the highland and is essentially a zone of thrust faulting, is called the '**Thrust Zone**'. The structures of this zone have been developed by several periods of compression beginning with strong movements in the Late Cretaceous. The Thrust Zone is composed of a wide variety of lithologies including crushed limestones, radiolarites, ultrabasic rocks and metamorphic rocks all of which have been intensely faulted. The Thrust Zone of the Inner Zagros itself has been subdivided longitudinally by Oberlander into a zone of Horizontal Overthrusts referred to simply as the Thrust Zone and a zone of high-angle thrust faults which he termed the '**Imbricate Zone**' (Fig. 2.14).

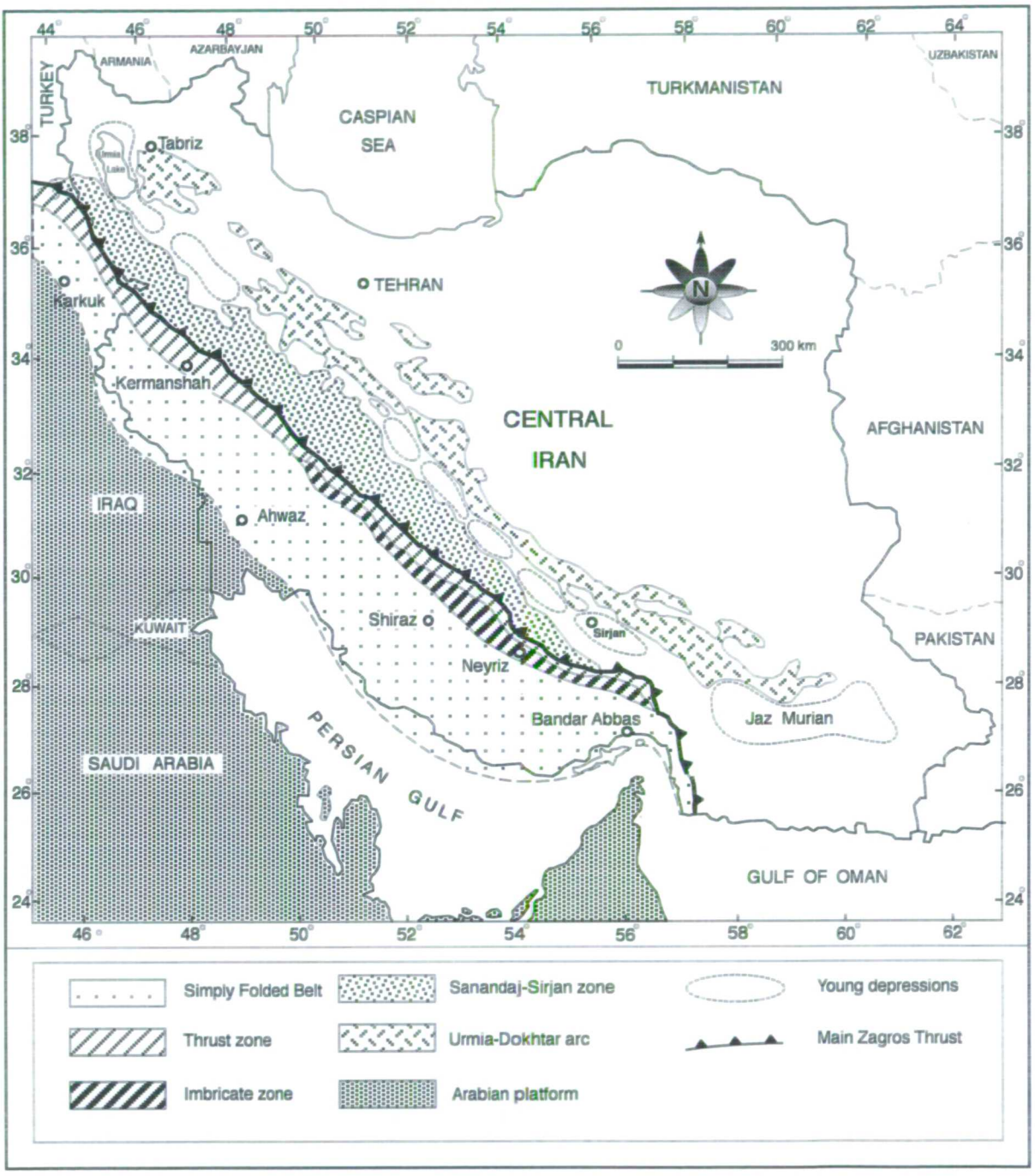


Fig. 2.14 The major structural zones along the northeastern margin of the Arabian plate (the Zagros mountain belt) and southwestern margin of the Central Iranian plate (based on Stöcklin 1968 and Alavi 1980).

Following this original division of Oberlander (1965), several other investigators have also divided the region into structural zones. Stöcklin (1968) and Kashfi (1976) divided it into two zones. Falcon (1967, 1974) and Alavi (1980) into three and Haynes & McQuillan (1974) and Jaros (1981) into four distinct structural zones.

Some of these authors, for example Alavi (1980, 1994) and Haynes and McQuillan (1974) believe that the '**Sanandaj-Sirjan Metamorphic Zone**' of Stöcklin (1968), and the '**Urmia-Dokhtar Magmatic Arc**' of Schröder (1944), both of which lie NE of the Main Zagros Thrust (Fig. 2.14), formed during and in association with the tectonic evolution of the Zagros fold-thrust belt, and should be considered as the structural zones of the Zagros region (Fig. 2.15).

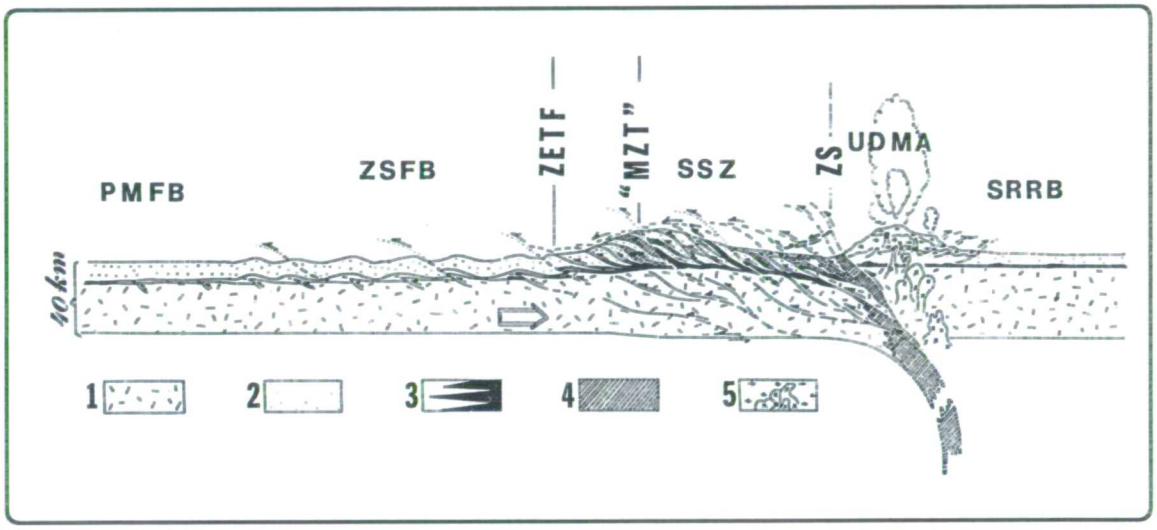


Fig. 2.15 Schematic cross-sectional view of the Zagros orogen. PMFB (Persian Gulf Mesopotamian Foreland Basin), ZSFB (Zagros Simply Folded Belt), SSZ (Sanandaj-Sirjan metamorphic Zone), ZS (Zagros Suture), UDMA (Urmia Dokhtar Magmatic Arc), and SRRB (Saveh-Rafsanjan Retroarc Basin), 1= continental crust, 2= Phanerozoic sedimentary cover, 3= evaporites (blank) and dolomites (black) at the sedimentary cover, 4= oceanic crust, 5= intrusive-extrusive rocks of the Urmia-Dokhtar magmatic assemblages (from Alavi, 1994).

The '**Sanandaj-Sirjan zone**', which was named later the 'Rezayeh-Esfandegheh belt' (Takin, 1972), the 'Stable Block' (Haynes & McQuillan, 1974), and the 'Metamorphic Zone' (Jaros, 1981) has a width of 150-250 km and its structural trends are parallel to the rest of the Zagros Mountain belt. It consists of intricately folded and strongly faulted rock assemblages ranging in age from Precambrian to Holocene. Parts of these have been affected by at least three phases of regional metamorphism; one in Precambrian times and the other two during late Mesozoic times (Alavi, 1980).

The '**Urmia-Dokhtar magmatic arc**' is a thick (more than 4 km) linear complex of Cretaceous to Holocene intrusive and extrusive igneous rocks, comprising andesitic, rhyolitic, and basaltic volcanic and volcaniclastic rocks that are associated with large dioritic and granodioritic plutons (Alavi, 1980, 1994). This structural unit extends along the entire length of the Zagros Mountains, parallel and roughly 150 km inland from the Main Zagros Thrust (Figs. 2.14, 2.15 and 2.17), and is generally considered to be the product of subduction and melting of the oceanic crust of the Neo-Tethys Sea under the southeastern margin of the Iranian continent (Takin 1972, Alavi 1980).

The boundary between the 'Sanandaj-Sirjan metamorphic belt' and the 'Urmia-Dokhtar magmatic arc' is marked by a series of '**elongate troughs**' which are generally considered to be the product of episodic subsidence during the intensive plutonic and volcanic activity in the Urmia-Dokhtar magmatic arc in Tertiary times (Tillman *et al.* 1981, Alavi 1980, 1994). Alavi (1980, 1994) believes that these elongated troughs mark the real suture between the two colliding plates (Figs. 2.14, 2.15 and 2.17).

b) STRATIGRAPHY

The stratigraphy of the Zagros sedimentary rocks (whose thickness ranges between 8-13 km) which cover the metamorphic basement complex has been described in detail in numerous publications by oil geologists working in the region (see for example, Lees & Richardson, 1940; Dunnington, 1958; James & Wynd, 1965).

A original generalized stratigraphic column published by the British Petroleum Company Ltd. (1956) was modified by Colman-Sadd (1978) on the basis of the five structural divisions of O'Brien, (1950). This amended column **has been updated** by the present author using new stratigraphic information (Fig. 2.16).

The **five structural divisions** of the stratigraphy proposed by O'Brien (1950) are crucial to an understanding of the Zagros folding. From bottom to top these are: **Basement Group**, **Lower Mobile Group**, **Competent Group**, **Upper Mobile Group**, and **Incompetent Group**.

The '**BASEMENT GROUP**' formed by the *Precambrian* rocks crops out within the Imbricate and Thrust zones in association with the major thrusts (Fig. 2.17). As can be seen from this figure, no outcrop of basement occurs within the Simply Fold Belt. The only evidence of these rocks in this region is provided by the igneous and metamorphic blocks carried up with the Hormuz salt plugs (Ala, 1982). The salt plug inclusions are mostly granitoids, basalt, and gabbro. The stratigraphy of these rocks is not well known.

The '**LOWER MOBILE GROUP**' consists of the 'Hormuz Series', which only outcrops as salt diapirs particularly in the Fars province. The series was named after an island in the Persian Gulf in the Straits of Hormuz. The series (about 1 km thick) begins with dark basal

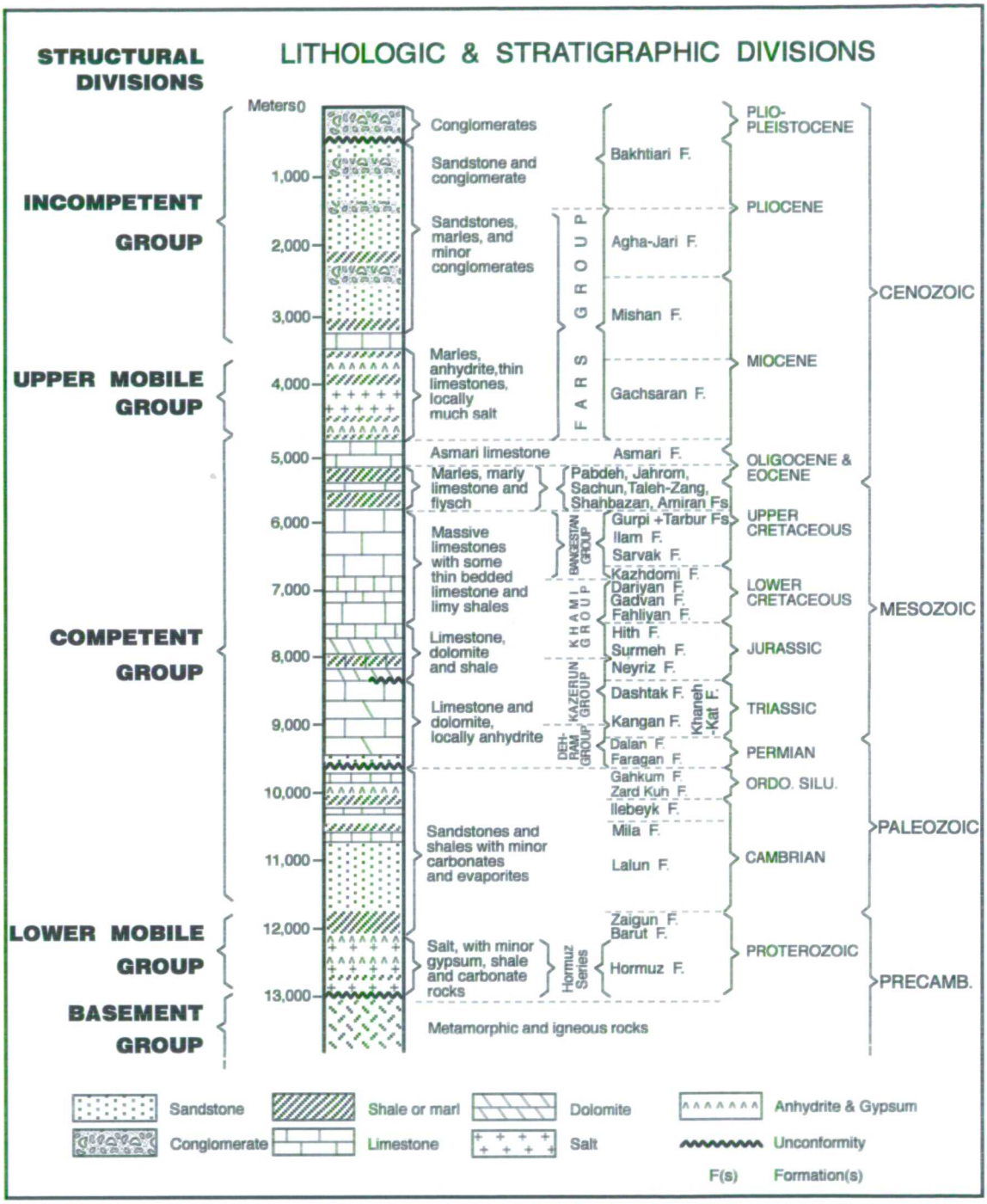


Fig. 2.16 Stratigraphical column and the lithological and structural divisions of the Zagros mountain belt (updated from Colman-Sadd, 1978).

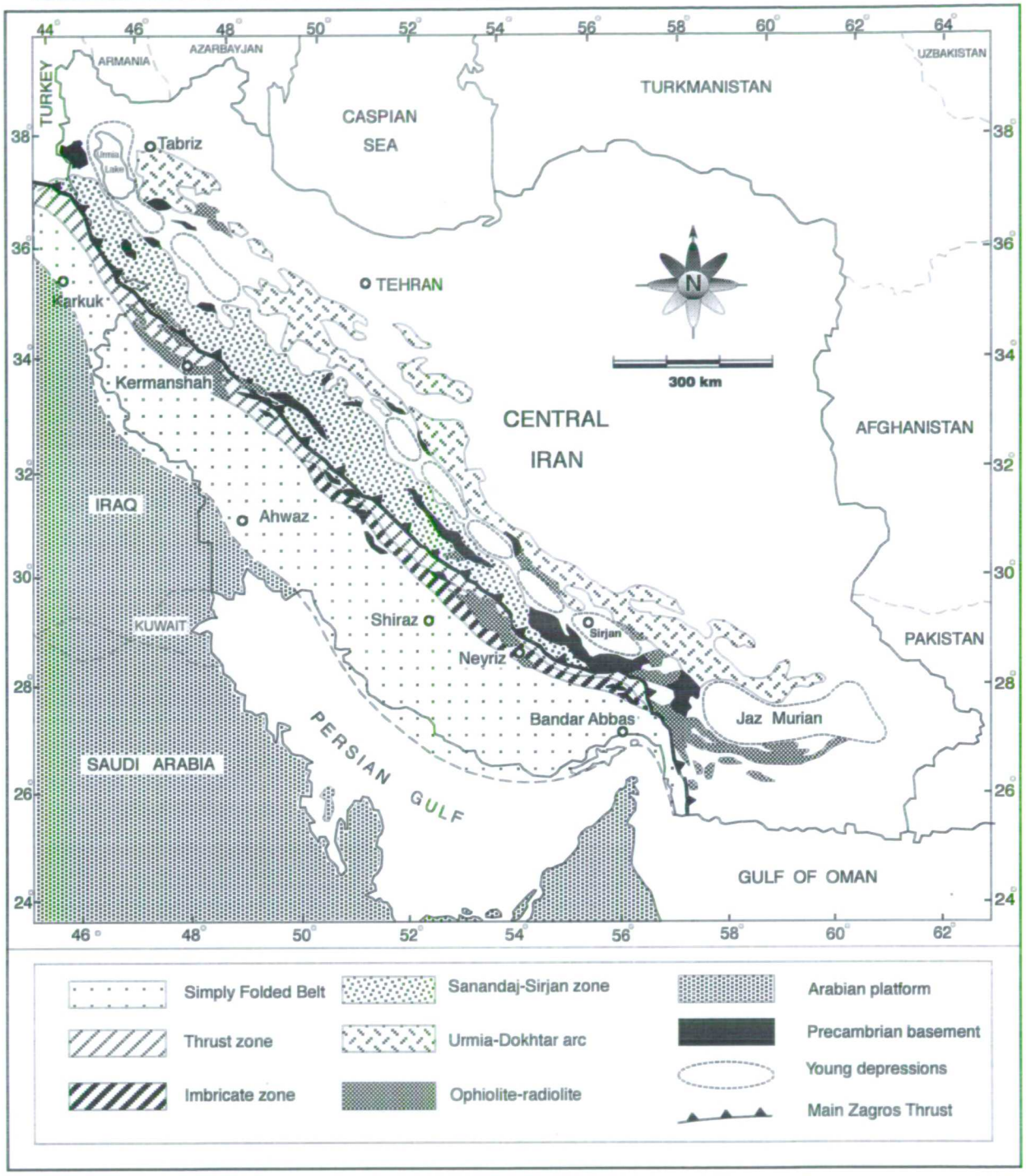


Fig. 2.17 The location of outcrops of the Precambrian basement rocks, and ophiolitic and mélange rocks in the northeastern margin of the Arabian plate (the Zagros mountain belt) and southwestern margin of the Central Iranian plate (based on Stöcklin 1968).

dolomites succeeded by gypsum and dull grey, coarsely crystalline halite beds which are in turn overlain by multicoloured shale units. The salt horizons in the succession contain many clasts of diverse sedimentary, igneous, and metamorphic rocks (Kent, 1958, 1979; Ala, 1974). The Hormuz Series was classified as *Infracambrian* by Stöcklin (1968). It is succeeded by the Barut and Zaigun Formations which are composed of mainly sandstones and micaceous shales.

The '**COMPETENT GROUP**' is the thickest group in the stratigraphic sequence and includes sediments ranging from *Cambrian* to *Miocene* in age. The group is made up predominantly of carbonate rocks with minor marls, shales, and evaporites. The total thickness of the Competent group is 6,000 to 7,000 m (BP, 1956, Colman-Sadd, 1978).

According to Ala (1979, 1982) terrestrial to shallow-marine clastic rocks with minor limestone beds make up the *Lower Paleozoic* succession (the Lalun, Mila, Ilebeyk, Zard Kuh, and Gahkum Formations), but the *Upper Paleozoic* is poorly represented by sediments. There is no paleontological evidence of the Devonian and Carboniferous. According to Ala (1982) the Hercynian or Variscan orogenic movements affected the Zagros region (as epirogenic movements) in Late Carboniferous time. They led to emergence and erosion, locally removing the sedimentary cover down to the Cambrian. Thus, the *Lower Paleozoic* succession is separated from the *Upper Paleozoic*, Deh-Ram Group of Permian (Faraghan and Dalan, Formations) by a regional unconformity (Fig. 2.16).

The *Mesozoic* succession begins with *Triassic* strata, which are scarce in the Zagros area as a result of strong pre-Jurassic erosion. Where found, the Triassic sequence is composed predominantly of anhydrite, dolomite, and limestone with minor intercalations of shallow-water shales and salt (the Kangan, Dashtak and Khaneh-Kat Formations). *Jurassic* beds typically, the 'Neyriz', 'Surmeh', and 'Hith' Formations are dominated by shallow-water

deposits, such as stromatolitic dolomites, shales, and evaporitic beds. These sedimentary rocks **unconformably** overlie the Triassic system in the greater part of the Persian Gulf area (Mina *et al.*, 1967). The Jurassic beds are overlain by the *Lower Cretaceous* succession, which consists of the 'Fahlian', 'Gadvan', 'Dariyan', and 'Kazhdomi' Formations dominated by shallow-water massive carbonate rocks and shales (Szabo & Kheradpir, 1978; Ala, 1979, 1982).

The *Middle and Upper Cretaceous* are characterized by facies which grade between continental and littoral in coastal Arabia to shallow marine-lagoonal-neritic towards the Iranian mainland. These facies are represented by the limestones of the 'Sarvak Formation' (Ala, 1982). The *Upper Cretaceous* is dominated by the shallow-water-marine and back-reefal limestones that form the 'Ilam', 'Gurpi', and 'Tarbur' Formations, which consist of massive limestones and shales with conglomeratic and cherty pebbles, reflecting a near-shore environment of deposition (Mina *et al.*, 1967).

The synchronous 'Pabdeh', 'Jahrom', 'Sachun', 'Taleh-Zang', 'Shahbazan', and 'Amiran' Formations represents the *Paleocene-Eocene* sequence in different parts of the belt. The 'Asmari Limestone' is the most oil-rich of the *Oligocene-Lower Miocene* carbonate formations. It attains an average thickness of around 300 m. The unit consists mainly of fractured, dolomitic, shallow-water limestone. The contacts with the underlying formations and the overlying 'Lower Fars' are transitional and conformable (Mina *et al.*, 1967).

'Fars' is a term applied by the British Petroleum Company in the 1950s to describe distinct lithological units that correspond to the arenaceous strata of the 'Upper Fars', marine limestones and marls in the 'Middle Fars', and evaporitic layers of the 'Lower Fars'. The 'Lower Fars Group' (the Gachsaran Formation), overlays the Asmari Limestone. It contains, 30-60 m thick anhydritic bed which is extremely important in providing the seal for the Asmari reservoirs.

The '**UPPER MOBILE GROUP**' consists of *Miocene* salt, gypsum, anhydrite, and marls of the central part of the 'Lower Fars' (the Gachsaran Formation). The dominant rocks of the Gachsaran Formation are multicoloured evaporites, marl, anhydrites with interbeded limestones, and thin salt beds; the total thickness varies from a few meters to more than 400 meters, due mostly to tectonic disturbance of the anhydritic and gypsum beds (Kashfi, 1980). The lagoonal phase of the 'Lower Fars' was followed by a marine transgression and the deposition of marls and reefal limestones of the 'Middle Fars' (the Mishan Formation). It contains a well-developed basal carbonate unit, referred to as the Gurpi Member, which consists of massive limestone (Mina *et al.*, 1967).

The remainder of the 'Mishan' section consists essentially of calcareous shales and limestone conglomerates, indicating the early stages of tectonic activity. These strata are conformably overlain by the estuarine deposits of the 'Upper Fars' (the Agha Jari Formation). This formation is made up of sandy shales grading up into sandstones which coarsen upward, and become conglomeratic toward the top (Mina, *et al.*, 1967; Szabo & Kheradpir, 1978).

The '**INCOMPETENT GROUP**' forms the remaining part of the stratigraphic sequence. It consists of a variety of thin-bedded marls, shales, sandstones, and conglomerates, with minor anhydrite (*Lower Miocene to Pliocene*), unconformably overlain by the Pliocene to Pleistocene syntectonic conglomerates of the 'Bakhtiari Formation'. The thickness of the incompetent group varies, reflecting unstable tectonic conditions during its deposition; an average figure is between 3,000 to 4,000 m. The Bakhtiari Formation, consists of a basal conglomerate with limestone boulders and grades upward to finer sandstones. The great variation in thickness (0-2000 m) was caused by the rapidly growing anticlines and consequent uplift.

c) METAMORPHIC ROCKS

The first metamorphic event in Central Iran and the northeastern margin of the Arabian plate occurred during the 'Assyntic Orogeny' in *Late Precambrian* times (Iranpanah & Esfandiari, 1979). It was followed by a phase of weak, high-pressure, low- temperature, regional metamorphism in *Early Cretaceous* times (or *Late Jurassic*, Iranpanah & Esfandiari, op. cit.) below the Zagros trench, as indicated by a glaucophane-jadeite mineral assemblage in the Zagros ophiolites (Alavi, 1980).

The first phase of high-temperature-high-pressure regional metamorphism (138 to 170 m.y. BP, Adib, 1978) affected the rocks along the edge of the Iranian continent during the emplacement of dioritic and granodioritic plutons and minor volcanic activity (the Sanandaj-Sirjan metamorphic belt) in *Middle Cretaceous* times (Alavi, 1980).

These events were followed by a second phase of high-pressure metamorphism (80 to 104 m.y. BP, Adib, 1978) associated with ophiolite emplacement in *Late Cretaceous* time, and by the formation of a range of greenschist, blueschist, and amphibolite grade metamorphic rocks throughout Cenozoic time along the Arabian and Iran suture zone (Adib, 1978; Delaloye & Desmons, 1980; Alavi, 1980, 1994).

Metamorphic rocks crop out in the 'Sanandaj-Sirjan metamorphic belt' and in some places along the Thrust zone of the Zagros Mountains, particularly in the Neyriz area, about 100 km southeast of Shiraz (Figs. 2.13 and 2.18), where there are metamorphic rocks of varied composition and grade. They are mainly schists and amphibolites which are cut or overthrust by slightly metamorphosed sedimentary rocks along NW-SE-trending thrust faults. The metamorphic rocks in this region are locally intruded by igneous rocks of granitic to gabbroic composition and by pegmatitic dykes and diabase sills (Adib, 1978;

d) OPHIOLITIC AND MÉLANGE ROCKS

Ophiolitic and mélange rocks crop out in several places along the strike of the Zagros Thrust and Imbricate Zones, as well as in the southeastern end of the Sanandaj-Sirjan metamorphic belt. Most of the ophiolites in the Zagros Thrust and Imbricate Zones are found near Kermanshah and in the area northwest of Neyriz (Figs. 2.13, 2.17 and 2.18). Gray (1950), Ricou (1968), and Hallam (1976) believe that these rocks occur in large overthrust sheets (nappes), Gansser (1955) and Wells (1969) believe that the ultramafic rocks are autochthonous and emplaced by igneous intrusion. Others Stöcklin (1968), Falcon (1969), Haynes & McQuillan (1974), Alavi (1980, 1994), De Jong (1982) suggest emplacement as a result of high-angle reverse faulting during the continent/continent collision of the Arabian and Central Iran crusts, in *Late Cretaceous* times.

According to Pamic *et al.* (1979) these rocks occur in two main forms: i) ultramafic mélanges, pelagic sediments, and radiolarites (predominantly thin cherts, intermingled with shales and mudstones), intensely deformed, faulted, and crushed (Delaloye & Desmons, 1980), and ii) thick sections of Alpine-type ultramafics which are mostly pridolites, gabbros, and ecologites as well as harzburgites and dunites.

The mélange rocks have been termed '**Coloured Mélange**' by oil company geologists (Gansser, 1960; Stöcklin, 1968). According to Shearman (1976) the diversity of rock types in even a small area is reflected in the patchwork of colours; white and pink limestones, red cherts and cherty shales, brown pillow lavas, green serpentities, dark grey turbidites and black ultramafics. The mélange rocks adjacent to the ultramafic bodies are intensely deformed (Haynes & McQuillan, 1974).

e) VOLCANIC ROCKS AND ASSOCIATED INTRUSIONS

Volcanic rocks are seen mainly in the 'Sanandaj-Sirjan metamorphic belt' and the 'Urmia-Dokhtar magmatic arc' northeast of the Main Zagros Thrust, in the active continental margin of Central Iran (Figs. 2.15 and 2.17) Stöcklin (1968), Alavi (1980, 1994), Kazmin *et al.* (1986), Tillman *et al.* (1981). The development of these two belts parallel to the strike of the Zagros Mountain belt has doubtless taken place during the evolution of the Zagros fold-thrust belt and they are generally considered to be part of the Zagros deformation belt (Haynes & McQuillan, 1974; Alavi, 1980; Tillman *et al.*, 1981).

Besides their occurrence in these two belts in Central Iran, small quantities of basic plutonic material are found in many places along the Main Zagros Thrust. According to Wells (1969) they have most commonly been intruded along more or less vertical bedding planes, and resemble irregular dykes, however the longer plutonic bodies from which they have come are also sometimes exposed. The great majority are of basic to ultrabasic composition. The longer intrusives, however, are often only slightly foliated, suggesting that intrusion and crushing were contemporaneous.

Kazmin *et al.* (1986) suggested an *Early Jurassic* age for the beginning of Calc-alkaline volcanism along the 'Sanandaj-Sirjan crustal block' probably related to subduction of the oceanic crust of the Neo-Tethys Sea, along a NW-SE-striking trench. According to these workers alkaline volcanism continued through Late Jurassic to Early Cretaceous times, prior to the collision of the Arabian and Iranian continents.

This was followed by widespread magmatism in the 'Urmia-Dokhtar magmatic arc' northeast of the 'Sanandaj-Sirjan zone', because of the intensive plutonic and volcanic activities along the edge of the Iranian continent, originating from the molten oceanic crust

during the 1950s. The more important results were summarized on the Geological Maps of Iran on the scales of 1:2,500,000 (NIOC, 1957) and 1:1000.000 (NIOC, 1975).

Since then the whole of Iran and the Zagros region in particular, have been studied in detail by the geologists of both the National Iranian Oil Company (NIOC) and the Geological Survey of Iran (GSI) and the results were published as maps on various scales, mainly 1:250,000 and 1:100,000.

Apart from some brief studies by oil company geologists (for example, Harrison & Falcon 1936, Falcon 1974) the geology of the southeastern end of the Zagros belt and the neighbouring Makran region was long neglected because of the lack of hydrocarbons. The earliest work was the geologic maps constructed by workers from the Imperial College expedition to the Makran (Shearman, 1976). Recent work has been based on mapping undertaken by Paragon-Conlech, an Iranian-Australian joint venture. Vita-Finzi (1979a, 1979b, 1982) also carried out a series of studies on different aspects of recent movements and depositions at this end of the Zagros.

Previous studies of the Zagros mountain belt relevant to the present work can be conveniently divided into two groups, namely those concerned with the evolution of the belt as a whole and those of concerned with the evolution of individual structures such as folds, faults and salt diapirs.

The important studies of regional evolution of the Zagros mountain belt have been carried out by workers such as Wells (1969), Falcon (1969, 1974), Takin (1972), Haynes & McQuillan (1974), Bird *et al.* (1975), Kashfi (1976), Alavi (1980, 1994) Jackson *et al.*, (1981) and Jaros (1981) who have studied geological and geophysical aspects of this orogenic belt and proposed various ideas or models concerning the tectonic evolution of the region. These various ideas and models are discussed in chapter 3 where a plate tectonic

model for the evolution of the Zagros Belt is considered.

More detailed studies of various structural elements and internal structures have been carried out by Richardson (1928), Lees (1928, 1931, 1933, 1952, 1955), Harrison (1930, 1931, 1952, 1956), Kent (1958, 1970, 1979), Gansser (1960), Oberlander (1965), Stöcklin (1968, 1974), Falcon (1947, 1961, 1967, 1969, 1974) and many others. Many of these studies were stimulated by the search for hydrocarbon and produced detailed information regarding the three dimensional geometry of a variety of structures mainly folds, faults and salt diapirs.

Salt diapirs of the Zagros and Persian Gulf regions attracted early attention for their remarkable admixture of rocks. Blanford (1872) was the first geologist to visit some of the Zagros salt plugs. He applied the term 'Hormuz Series' to the whole lithological section of the salt complex. Following Blanford, Pilgrim (1908, 1922) and many other workers such as Harrison (1930, 1931), O'Brien (1957), Kent (1958, 1970), Gansser (1960), Player (1965, 1969), Ala (1974), Talbot & Alavi (1996), Edgell (1996), and many others also investigated different aspects of salt diapirism in the Zagros. Koyi (1988) performed the only experimental work directly relevant to the Zagros belt and considered the role of gravity and lateral shortening in the structural evolution of the belt, with special reference to the intrusion of the Zagros salt plugs.

The ideas and observations contained in the references listed above, relating to the evolution of the major structures and structural elements within the mountain belt, especially folds, faults and salt diapirs are discussed in detail in chapter 3 where the spatial distribution, geometrical characteristics and mechanism of formation of these structures is considered.

The most comprehensive study on the morphological aspect and drainage system of the central Zagros was carried out by Oberlander (1965) and this work which has

already been mentioned earlier in this Chapter, is further considered in chapter 3.

b) NEOTECTONICS & SEISMOTECTONICS

Seismic activity in the Zagros region, which is the manifestation of its neotectonic activity, has been analyzed in recent years by many authors, either from the viewpoint of geophysics and seismology or that of neotectonics and seismotectonics.

Seismotectonic investigations have been carried out by workers such as Nowroozi (1971, 1972, 1976, 1985, and 1986), Tchalenko & Braud (1974), Berberian (1976, 1977, 1981), Jackson (1980a, 1980b, 1992), Jackson *et al.* (1981), Chandra (1981, 1984), Ambraseys & Melville (1982), Kadinsky-Cade & Barazangi (1982), Jackson & McKenzie (1983, 1984, 1988) and Ni & Barazangi (1986).

Other aspects of neotectonic activity in the Zagros region have been studied by Vita-Finzi (1969a, 1975, 1979a, 1979b, 1981, 1982, 1986, 1987) alone or with other authors (Mann & Vita-Finzi, 1989; Vita-Finzi & Ghorashi, 1978). During these investigations of the Quaternary deposition in Iran, the rate of Holocene serial folding in the Zagros, the recent coastal deformation near the Hormuz Strait and the Makran coast of Iran, and the recent faulting in Iranian Makran have been studied.

Kashfi (1984), Little (1970, 1972) and Falcon (1974), also investigated evidence of recent vertical movements by considering the raised beaches and terraces along the Persian Gulf and the Makran coast of Iran. The ideas encompassed in the reference listed above are discussed and considered in Chapter 7 and 8 on neotectonics and seismotectonics, respectively.

of the Neo-Tethys Sea subducted prior to the collision in *Late Cretaceous* (Alavi, 1980).

Takin (1972) believes that a pause in compression in *Eocene time*, due to slower seafloor spreading in the Indian Ocean or possibly the approach of India to the subduction zone in the old Tethys Sea at the end of Cretaceous time, facilitated the process of magmatism and the creation of the Urmia-Dokhtar magmatic arc in Early Tertiary time.

During the *Paleocene* and *Pliocene*, as more oceanic crust was lost beneath the magmatic arc much more volcanic activity occurred (Alavi, 1980). Quaternary volcanic activity along the Urmia-Dokhtar magmatic arc has also been reported by, for example, Stöcklin and Nabavi (1973) and Dimtrijevic (1973). According to Kazmin *et al.* (1986) the chemistry of volcanic rocks changed back to calc-alkaline during late Miocene-Quaternary times.

CHAPTER 3

Large-scale geological structures of the Zagros mountain belt

4. PREVIOUS WORK

As noted earlier the Zagros Mountain Range is one of the world's best known ranges, being part of Alpine-Himalayan mountain chain and the product of the collision between the Arabian and central Iranian plates. Considerably large oil and gas reserves are found in this area together with the most spectacular examples of large-scale geological structures such as folds, faults, and salt domes. As a result a considerable volume of work on this area exists.

a) GEOLOGICAL MAPPING & STRUCTURAL STUDIES

Prior to the geological mapping of the Zagros region by geologists of the Anglo-Persian Oil Company and later the British Petroleum Company, the Zagros Mountains had received very little attention from geologists. There were a few roadside observations to be found in earlier literature, but no comprehensive picture of any part of the region.

The earliest geologic and structural work in the Zagros Mountains was initiated in 1909 soon after the first commercial oil discovery was made at Masjed-e-Soleyman in Iran. This geologic work was supported by the Persian Bank Mining Rights Corporation (PBMRC), when it formed the Anglo-Persian Oil Company to develop and produce the Masjed-Soleyman oil field and to carry on the search for additional fields. All the geologic data and related discoveries at that time were based essentially on surface mapping guided by hydrocarbon seeps.

The geologic work done by Anglo-Persian Oil Company and BP concentrated on the Zagros range, and was published in 1963 as a series of maps and cross sections. These followed the systematic mapping of the whole of Iran by the National Iranian Oil Company (NIOC)

1. INTRODUCTION

Large-scale **folds**, **faults**, and **salt diapirs** are the dominating geological structures which have developed in the course of the structural evolution of the Zagros belt. This chapter focuses on the spatial distribution, geometry, and mechanism of formation of these regional structures in an attempt to improve our understanding of the processes responsible for their generation and their implications regarding the evolution of the '*Zagros deformation belt*'.

The stratigraphy of the Zagros region plays a critical role in controlling the deformation of the mountain belt and the evolution of all major structures. From a mechanical point of view, the stratigraphical column (Fig.2.16) can be considered to be made up of a rigid basement, under a sedimentary cover made up of four distinct units. These are in ascending order the 'Lower Mobile Group' made up predominantly of the thick Hormuz Salt Formation (about 1 km thick). This allows the complete decoupling of the basement and cover during deformation. Overlying the 'Lower Mobile Group' are, in ascending order, the 'Competent Group', the salt rich 'Upper Mobile Group' and the 'Incompetent Group'. Although the Competent and Incompetent groups often fold harmonically, in places where the 'Upper Mobile Group' is very thick and salt rich the two groups fold disharmonically and the deformation above and below this mobile group becomes completely decoupled.

2. THE ZAGROS FOLDS

'**Folds**' are perhaps the most common tectonic structures developed in deformed layered rocks under conditions conducive to ductile deformation. They form in rocks containing primary planar features such as sedimentary bedding or secondary planar anisotropic features, such as cleavage or schistosity, produced during an earlier deformation event.

Buckle folds are common because the growth rate of mechanical instabilities setting up

sideways deflections during the shortening along a planar feature is generally rapid. Not all folds, however, are formed by **buckling processes**. Folds can also be formed when non-uniform forces are applied across the layering. The formation of folds by this **bending process** can occur as the result of variable subsidence of crustal layers often related to basement faulting, differential shearing in shear zones or by the sliding of rock masses over underlying irregularities.

One of the most striking features of folds is their great variation in geometric type (generally termed fold style) and in their size. Variations in fold style are invariably linked with differences in the mechanical properties of the structures and especially with the rheological state of the rocks during the folding process.

The **Zagros Mountain Belt** of Iran is one of the best examples of a classical young orogenic belts in the world and shows a spectacular collection of folds with a large variety of fold styles. The spatial distribution, geometrical characteristics, and mechanisms of formation these folds is considered in the following sections.

a) SPATIAL DISTRIBUTION OF THE ZAGROS FOLDS

The Zagros folds are generally confined to what is referred to by Oberlander (1965) as the **'Simply Folded Belt'** (Figs. 2.14 and 3.1). Folds are also developed in the Imbricate Zone but they are commonly distorted and cut by the high-angle reverse faults and deeply dissected by a considerably long period of erosion (Figs. 2.3 and 2.5).

The 'Simply Folded Belt' of the Zagros mountains extends with a NW-SE trend along strike for about 1500 km from the Iraq-Turkey border to the Minab-Zendan fault zone east of the strait of Hormuz in the Persian Gulf. As can be seen from Figs. 2.14 and 3.1 although the belt runs approximately parallel to the Main Zagros Thrust, there are variation in its trend

which give it a wave-like (**sinuous**) geometry in plan.

The width of the 'Simply Folded Belt' is not constant everywhere along the Zagros Mountain Belt and as can be seen from Figs. 2.14 and 3.1 generally decreases from SE to NW. The northeastern margin of the 'Simply Folded Belt' is marked clearly by the sinuous boundary between the 'Simply Folded Belt' and the 'Imbricate Zone'. However, the southwestern margin is not well defined at the earth surface. Nevertheless, geological sections and seismic profiles indicate that the southwestern margin of the fold belt like its northeastern margin is a sinuous line (Fig. 3.1), and runs almost parallel to but about 50-100 km southwest of the sinuous '**Mountain Front**', under the Mesopotamian Alluvial Plain and offshore under the Persian Gulf (Figs. 2.4 and 2.14) .

The population and spatial distribution of the folds within the morphologically different zones along the 'Simply Folded Belt' are different and on the basis of these differences the 'Simply Folded Belt' can be divided into six contrasting fold zones. These are from northwest to southeast, the **Kordestan**, **Lorestan**, **Bakhtiari**, **Kohkiluyeh, Fars**, and **Minab** fold zones (Fig. 3.1).

Folds within these distinct fold zones are arranged in different ways, when they are viewed in plan. However, they are generally aligned with their hinges zones sub parallel to each other and are frequently offset from each other in an *en echelon* manner. The *en echelon* disposition of the folds may be either random or consistent. A random *en echelon* offset (Fig. 3.2 a) is a typical feature of classical buckle folding. A consistent *en echelon* offset of folds (Fig. 3.2 b and c) suggest the influence of the basement strike-slip faults. (see also Figs. 2.5 and 3.1).

It is clear from Fig. 3.1 that the Zagros folds form a '**sinuous fold belt**' which decreases in width when traced from SE to NW. This reduction in width is in part related to the

counterclockwise rotation of the Arabian plate (discussed briefly in Chapter 8) and the resultant decrease in convergence rate between the Arabian and Iranian plates from SE to NW. In addition the uneven thickness and distribution of the main detachment horizon (the Infra-Cambrian Hormuz salt Formation) also influence the width and trend of the 'Simply Folded Belt'.

The present writer also considers that the '**anomalous bending**' of the Simply Folded Belt around the Musandam Peninsula and the considerably narrower width of the belt in the 'Minab Fold Zone' east of the Strait of Hormuz are the result of the indentation of the Musandam peninsula into the Zagros basin during the *Pliocene* orogeny. The peninsula acted as a rigid body which acted as a barrier to the southwestward advancing fold front (Figs. 2.14 and 3.1).

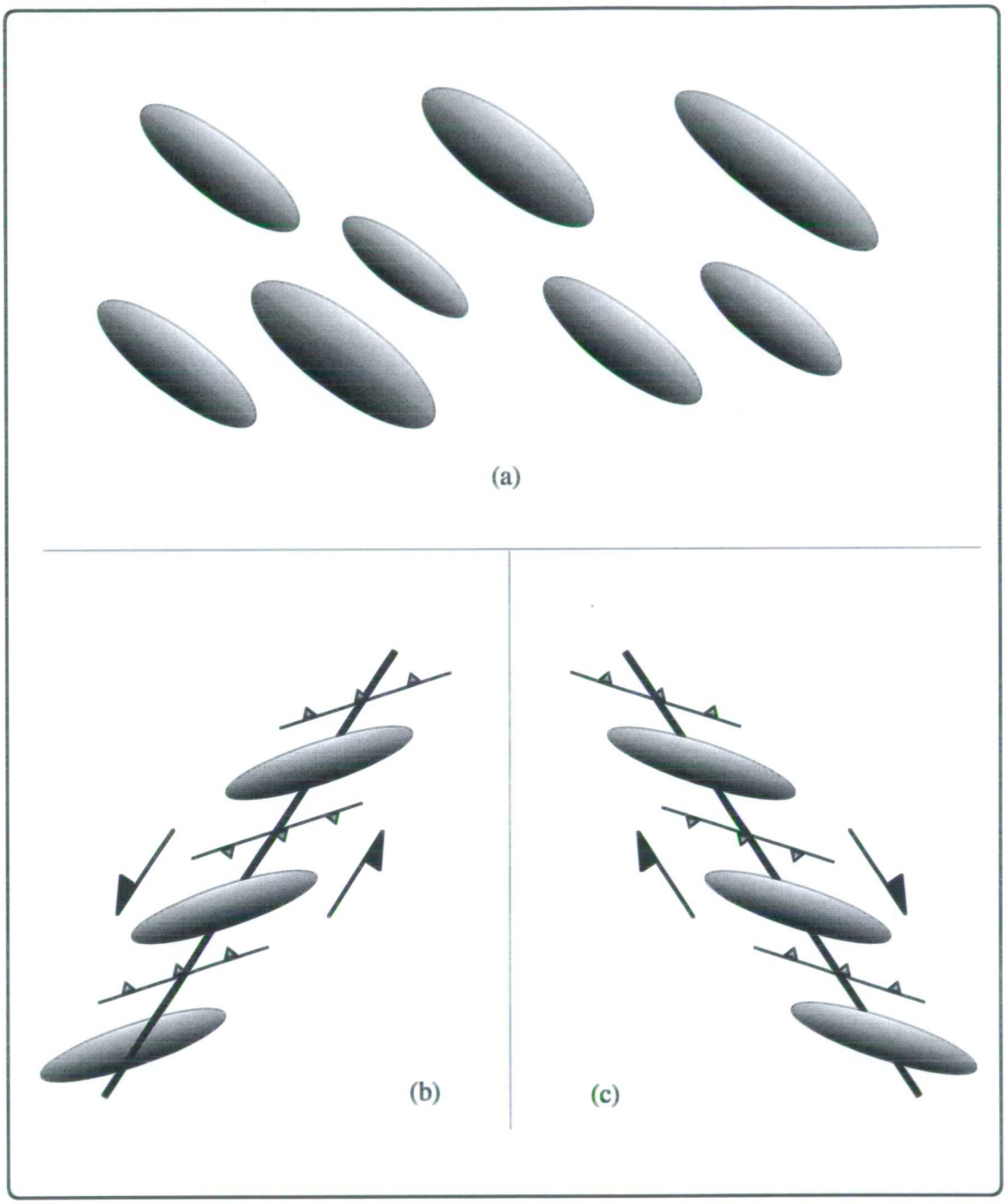


Fig. 3.2 The *en echelon* offset of the folds when viewed in plan. (a) Random offset, (b) and (c) consistent offset associated with sinistral and dextral strike-slip movement on basement faults, respectively.

b) GEOMETRY OF THE ZAGROS FOLDS

The Zagros folds are generally **large open folds** of the massive, predominantly carbonate rocks of the 'Competent Group', and **smaller folds** of the 'Incompetent Group', predominantly evaporitic in composition (Fig. 2.16). The plan shape and size of the Zagros folds are highly variable. They display oval, linear, triangular, arcuate or relatively irregular shapes of different sizes (Figs. 2.5 and 3.1).

The aspect ratio (Half-wavelength/hinge length ratio) of many of the Zagros folds is about 1:5 which is the typical aspect ratio of buckle folds. However, some of the Zagros folds such as the **Minab anticline** in the Minab fold zone and the **Kabir Kuh anticline** in Lorestan fold zone are characterized by high aspect ratios of the order of 1:20 to 1:30 (Figs. 3.3 and 3.4).

Most of the Zagros folds are '**asymmetric**' and with a few exceptions, the steepest limbs of the anticlines are on the southwest sides. The anticlinal limbs dip steeply (40°-60°), and their axial planes dip northeast at an angle of 60° or more (Figs. 3.5). The asymmetric geometry of the Zagros folds is considered to be the result of both gravity sliding and shearing in the detachment zone of the 'Lower Mobile Group'.

According to Colman-Sadd (1978) during the folding, the Competent Group moved southwestward relative to the basement complex, and imperfect detachment has caused drag one upon the other. The synclines in the Competent Group are separated from the basement by a thinner mobile layer than the anticlines. The more perfect detachment beneath the anticlines has caused them to override the synclines as both have moved southwest relative to the basement. (Fig. 3.6). An alternative explanation for this asymmetry has been given by Jackson *et al.*, (1980a) who suggested that some of the asymmetric folds in the sedimentary cover has been formed as a result of reactivation of basement normal faults as

high-angle reverse dip-slip faults.

The **'Kordestan Fold Zone'** in the northwestern parts of the Simply Fold Belt is dominated by short oval folds. At the northwestern end of this fold zone in southeast Turkey the fold axes trend E-W. When traced into northeastern Iraq they gradually turn to a NW-SE direction and extend with almost the same trend down to the vicinity of the Strait of Hormuz, where they are deflected around the Musandam Peninsula (Fig. 3.1).

Further southeast, in the **'Lorestan Fold Zone'** most of the anticlines also occur in an *en echelon* array, but their hinge lengths range from 2 or 3 km to over 200 km in the immense mountains ranges of 'Kabir Kuh' and 'Anaran' anticlines (Figs. 2.4, 3.1 and 3.4). Throughout the Lorestan fold zone, the density of folds is greater than in the Kordestan fold zone and the synclines are tighter. Southeast of the Kashghan River topographic hight of the Simply Folded Belt decreases forming the **'Lorestan saddle'** (Oberlander, 1965) (Figs. 2.3 and 2.4).

From the depression of the Lorestan Saddle the entire folded surface rises steeply to the southeast, to form a culmination which forms the **'Bakhtiari Mountains'** of the central Zagros. These mountains within the **'Bakhtiari Fold Zone'** are the surface expression of a great **'anticlinorium'** that rises steeply at the head of Dezful Embayment and represent the higher mountains of the Zagros range (Figs. 2.4 and 3.5).

One of the most noticeable features of this fold zone is that most of the folds here are concentrated in the northeastern part of the zone in the Bakhtiari mountains, where the folds have large amplitudes and are tight and closely spaced compared to the relatively low level foothills of the Dezful Embayment to the SW with rather gentle and sporadic folds, and the adjacent Lorestan and Kohkiluyeh fold zones (Figs. 3.1 and 3.5).

Inspection of Fig. 3.1 shows that the **'anticlinorium'** is composed of two sets of *en echelon*

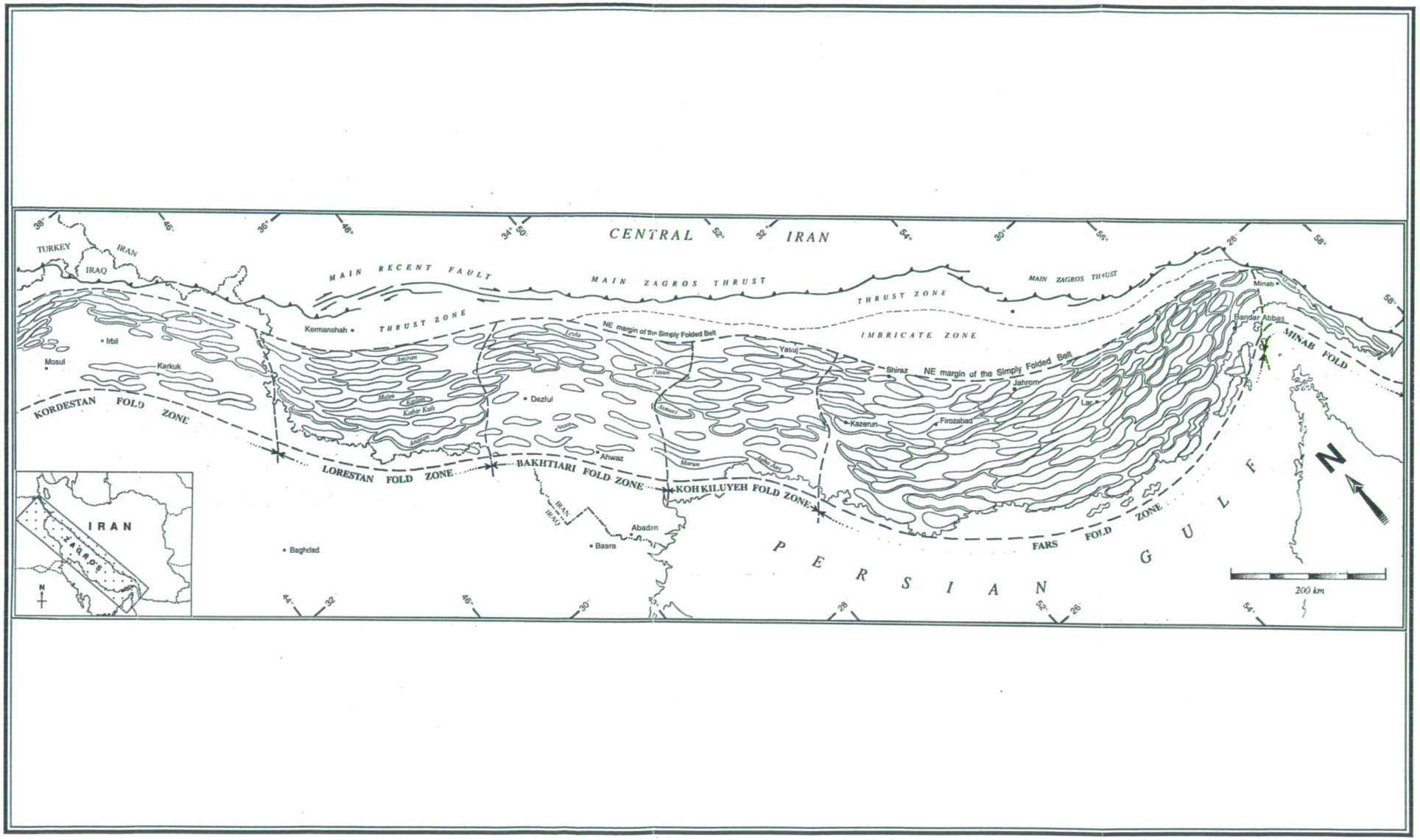


Fig. 3.1 Distribution of the folds in the 'Simply Folded Belt' of the Zagros mountains, showing a wave-like (sinuous) geometry of the belt and the difference in distribution of the folds within the different fold zones (based on the Geological Map of Iran (NIOC, 1975) and the Geological Map of Iraq and Southwestern Iran (RRP, 1987)).

fold groups bordering the Dezful Embayment and making up the topographic front in this area. The implication of these fold arrays is discussed later in this chapter. The anticlines in the Bakhtiari mountains are frequently of the chevron type, with occasional thrust-faulting at their crests (Figs. 2.11 and 3.5).

Falcon (1950, 1961, 1974) suggested that this major culmination (*anticlinorium*) in the central Zagros was formed during the latest phase of the Pliocene Orogeny with episodic warping occurring only after the development of the individual folds forming the Bakhtiari Mountains. These events however, were contemporary with the folding of the foothill belt.

Within the Dezful Embayment in front of the Bakhtiari Mountains the surface folds generally represent the '**dishamonic buckling**' of the 'Incompetent Group' due to the exceptional thickness of the 'Upper Mobile Group' (the Gachsaran Formation) in this area and the fact that it contains more salt (Fig. 3.5).

It was mentioned in the introduction to this chapter that where the 'Upper Mobile Group' is very thick and salt rich the underlying 'Competent Group' and overlying 'Incompetent Group' may fold '*disharmonically*'. The folds of the Bakhtiari Mountains (made up of rocks of the Competent Group) and those that occur in Dezful Embayment (made up of rocks of the Incompetent Group) are an excellent example of this phenomenon.

Southeast of the Bakhtiari Mountains in the '**Kohkiluyeh Fold Zone**' the folds become once more widely separated. They are greater in number and more even in distribution than in Lorestan and Bakhtiari fold zones (Fig. 3.1).

In the **'Fars Fold Zone'** the folds becomes even more widely separated than in the Kohkiluyeh Fold zone. Here folds are elliptical domes, short, broad, and often quite high, but widely separated by flat synclinal depressions (Figs. 2.5, 3.1 and 3.7). Most of the folds

within this zone, especially in the areas northwest of the Strait of Hormuz have developed '*disharmonically*'. For example, As can be seen from Figs. 2.5 and 3.8 in this part of the Fars fold zone, the smaller and almost intact folds whose wavelength is presumably governed by a very thin mechanically competent rock unit, often seen are encompassed by the limbs of a deeply eroded open and larger folds whose wavelength is controlled by a thicker competent unit (Figs. 3.8, 3.9, 3.10 and 3.11).

At the southeastern end of the Simply Folded Belt within the '**Minab Fold Zone**' the folds are once again closely spaced. The trend of fold axes is NNE-SSW, i.e. parallel to the Minab-Zendan fault zone. Nearly all of the folds within this zone are of high aspect ratios generally of the order of 20:1 to 30:1 (Figs. 2.12, 3.1 and 3.3).

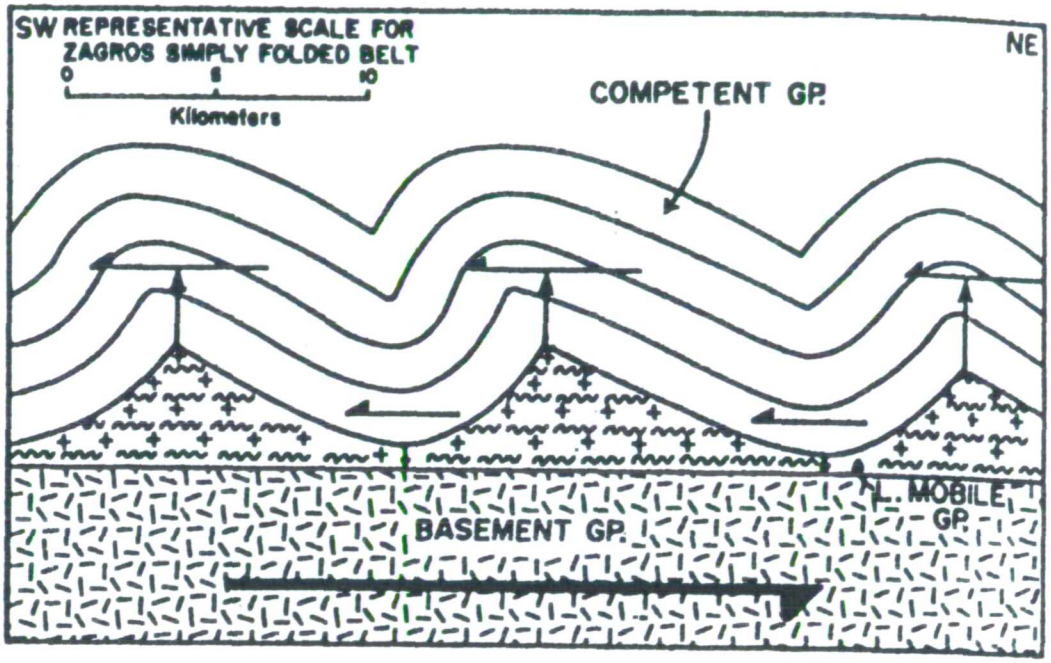


Fig. 3.6 Development of asymmetric folds caused by shearing along the detachment horizon. Arrows show relative movement, and upward and downward displacement in anticlines. Potential faulting is omitted (from Colman-Sadd, 1978).

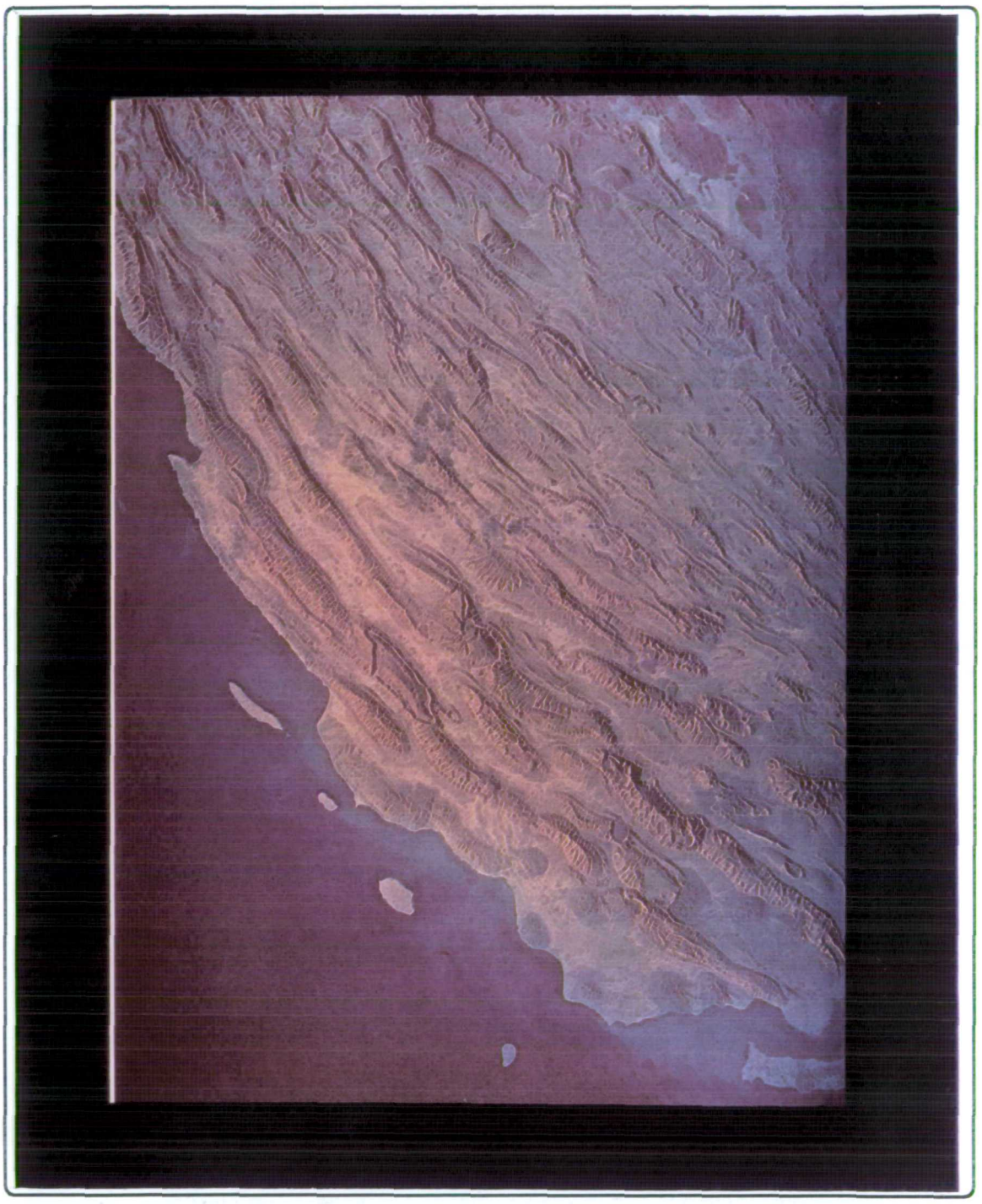


Fig. 3.7 Satellite image of part of the Fars fold zone, showing anticlines of different size and plan-shape separated by flat synclinal depressions.

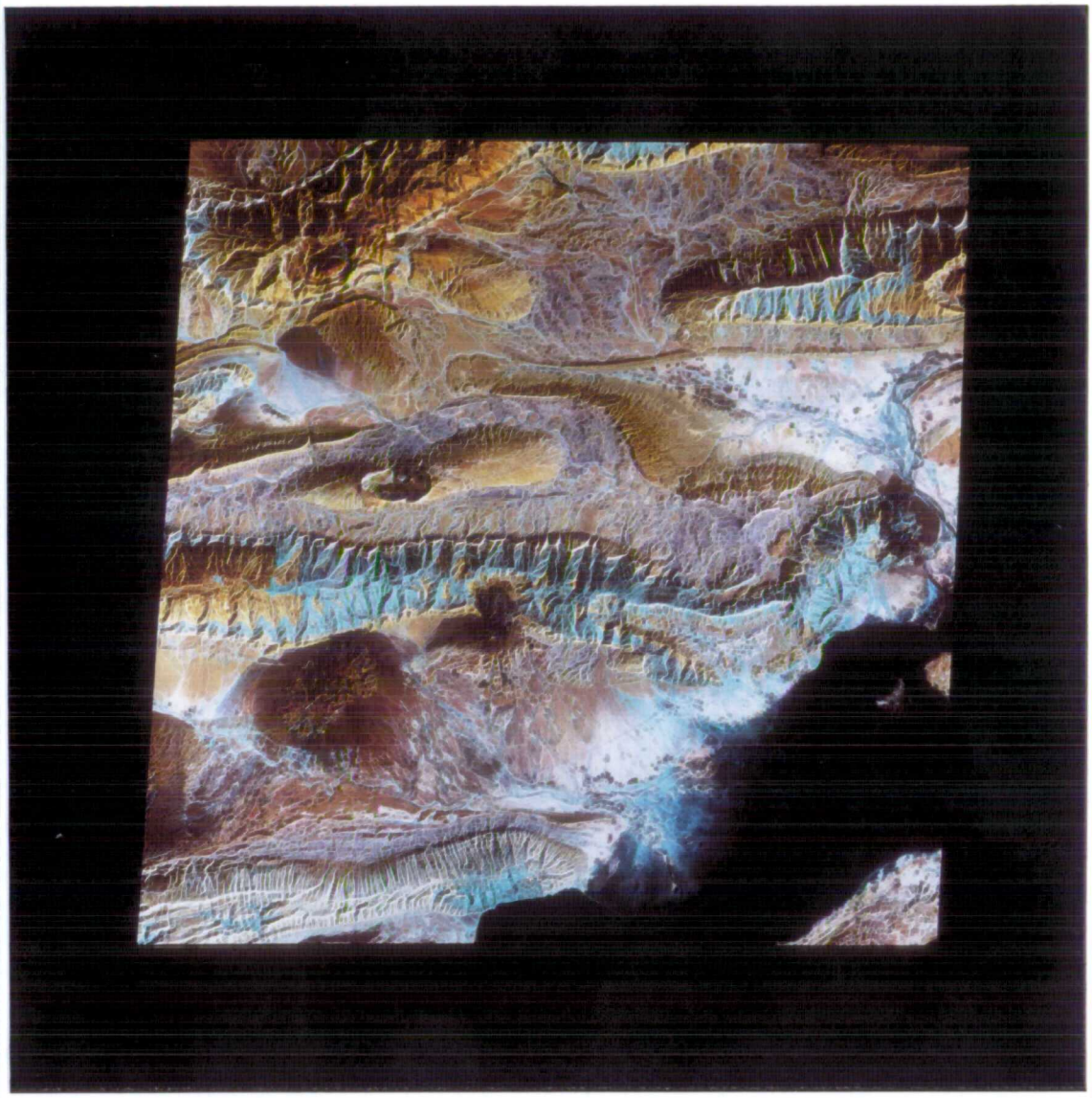


Fig. 3.9 Detail of Fig. 3.8 of the area NW of the Strait of Hormuz, showing smaller and almost intact folds encompressed by limbs of a deeply eroded, large folds. See also Fig. 3.11.



Fig. 3.10 The close-up of the satellite image of the area NW of the Strait of Hormuz, showing disharmonic folding i.e. smaller folds enclosed within a large fold. Note also the salt diapirs forming a crater-like depression due to the exhausted or arrested of salt rise or undue erosion. See also Fig. 3.11.

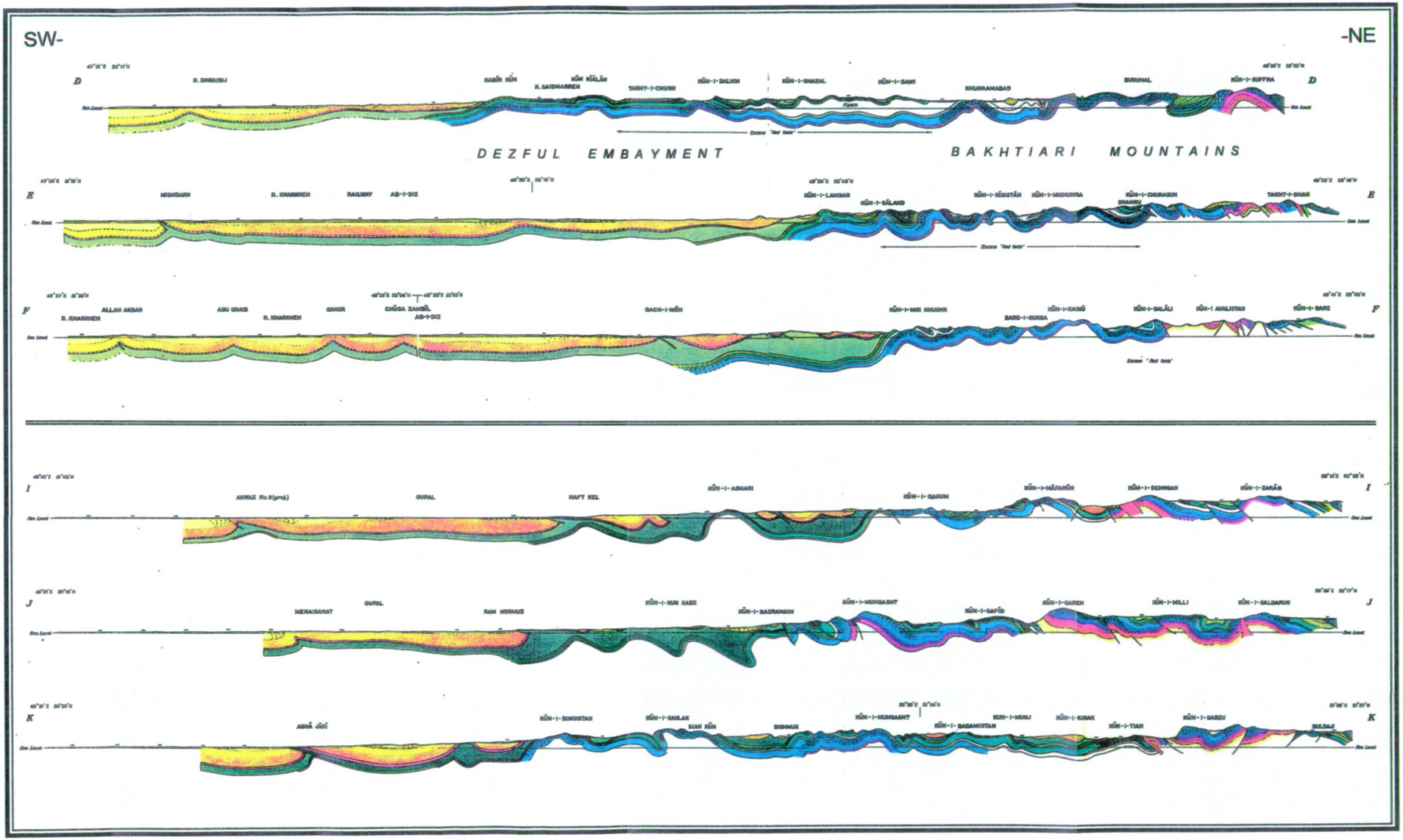


Fig. 3.5 Six examples from 21 geological cross-sections taken from the British Petroleum Company Limited (1956), used by the present author for the geometrical analysis of the Zagros folds and for determining the variation in the percentage shortening of the sedimentary cover. The location of these sections is shown in Fig. 4.1.

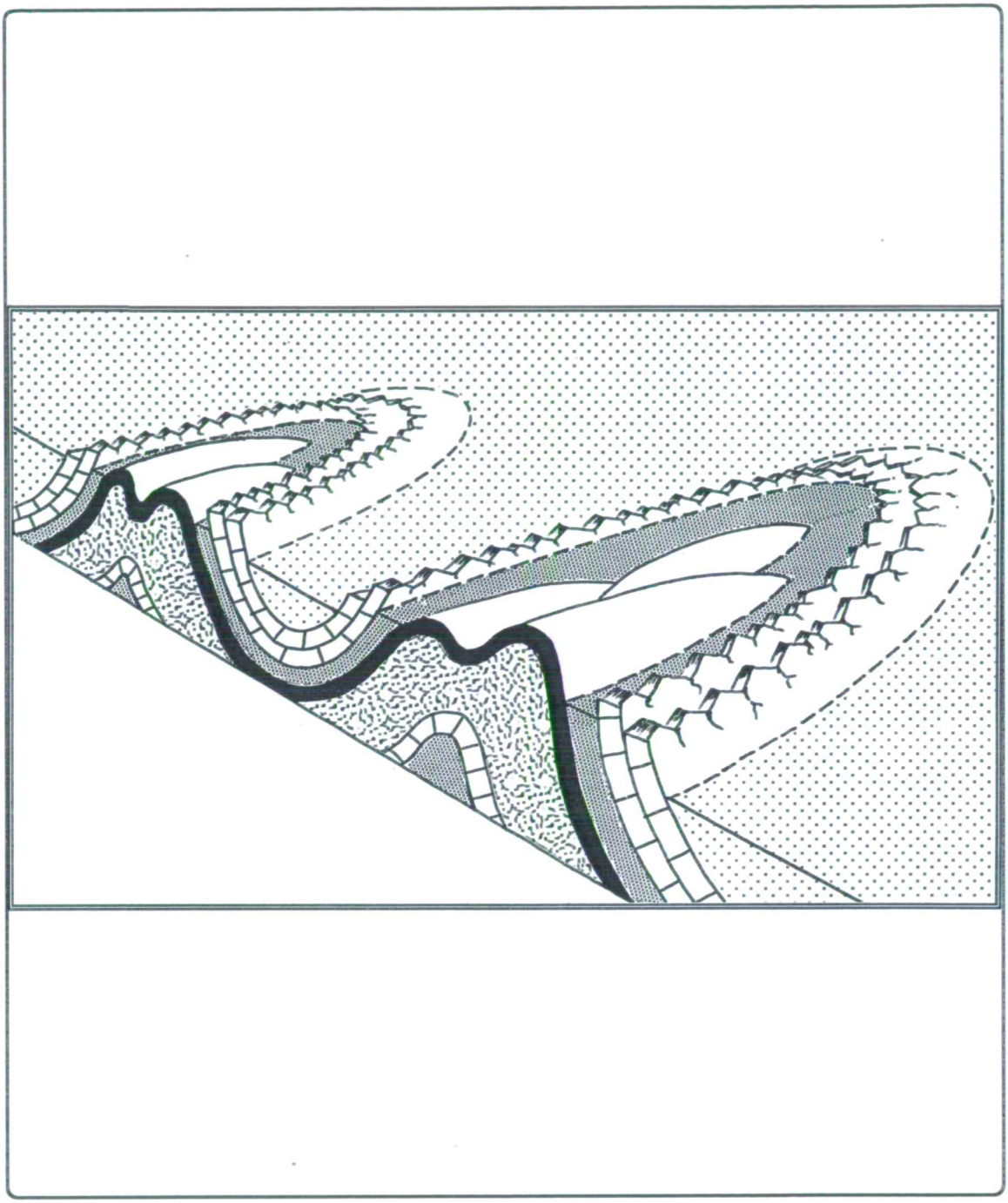


Fig. 3.11 The development of disharmonic folds in the Competent Group. Relatively small-scale folds develop in a relatively thin competent unit beneath the thicker Asmari limestone which buckle with a larger wavelength.

c) MECHANISMS OF FOLDING IN THE ZAGROS MOUNTAIN BELT

A variety of folding mechanisms have been proposed to account for the formation of natural folds. Three basic folding mechanisms are *classical buckling, bending, and passive folding.*

'Buckling' is the most commonly occurring fold mechanism in layered rocks. These folds are developed as a result of compression parallel or sub parallel to the bedding planes or layers (Fig. 3.12 a). *Flexure-slip folds* and *tangential longitudinal strain folds* are examples of typical types of buckle folding and which of them develops depends on the mechanical properties of the layered sequence (Fig. 3.12 b and c).

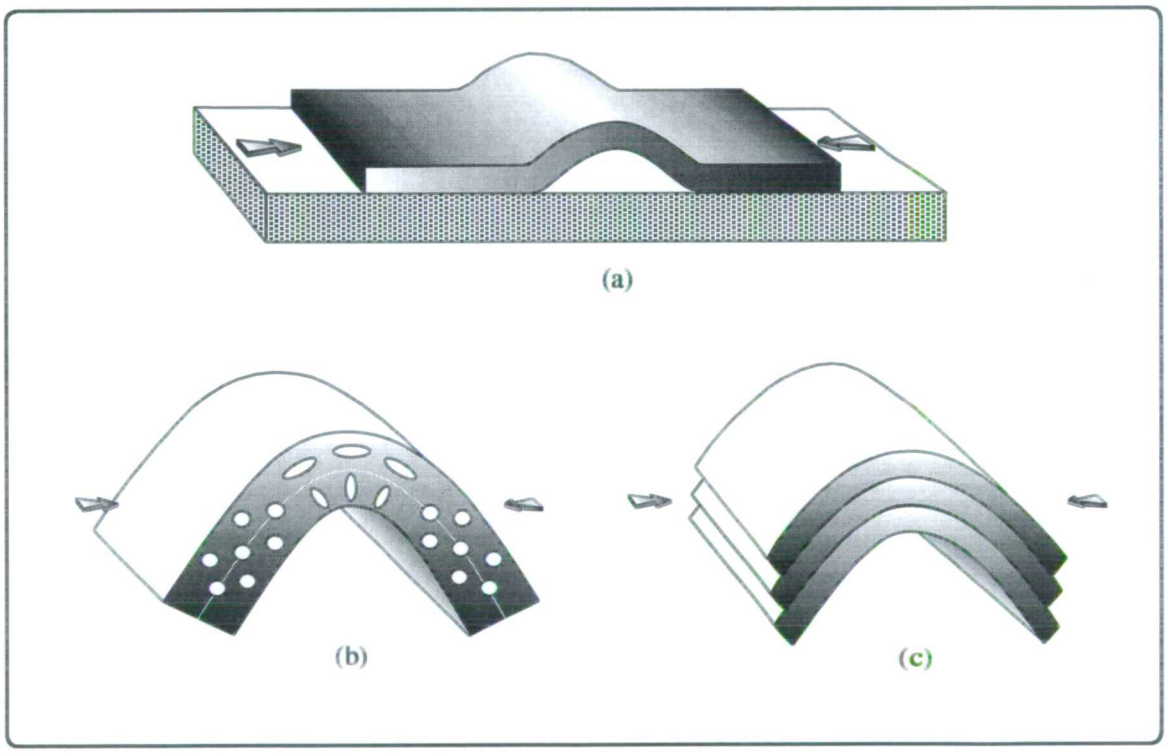


Fig. 3.12 Buckling mechanism and examples of buckle folding. (a) Classical buckle fold. The stress distribution within a buckle depends on the mechanical properties of the layer. (b) Tangential longitudinal strain fold, typical of massive beds. (c) Flexural-slip fold, typical of well bedded units.

'**Bending**' is the term used to describe the flexuring of a layer induced by a compression acting at high angle to the layering (Fig. 3.13 a). Geological flexures that are the result of bending are known as '**drape folds**' or '**forced folds**' and are frequently formed when sediments which cover a more rigid basement, flex in response to components of vertical movement along basement dip-slip and oblique-slip faults (Fig. 3.13 b-e).

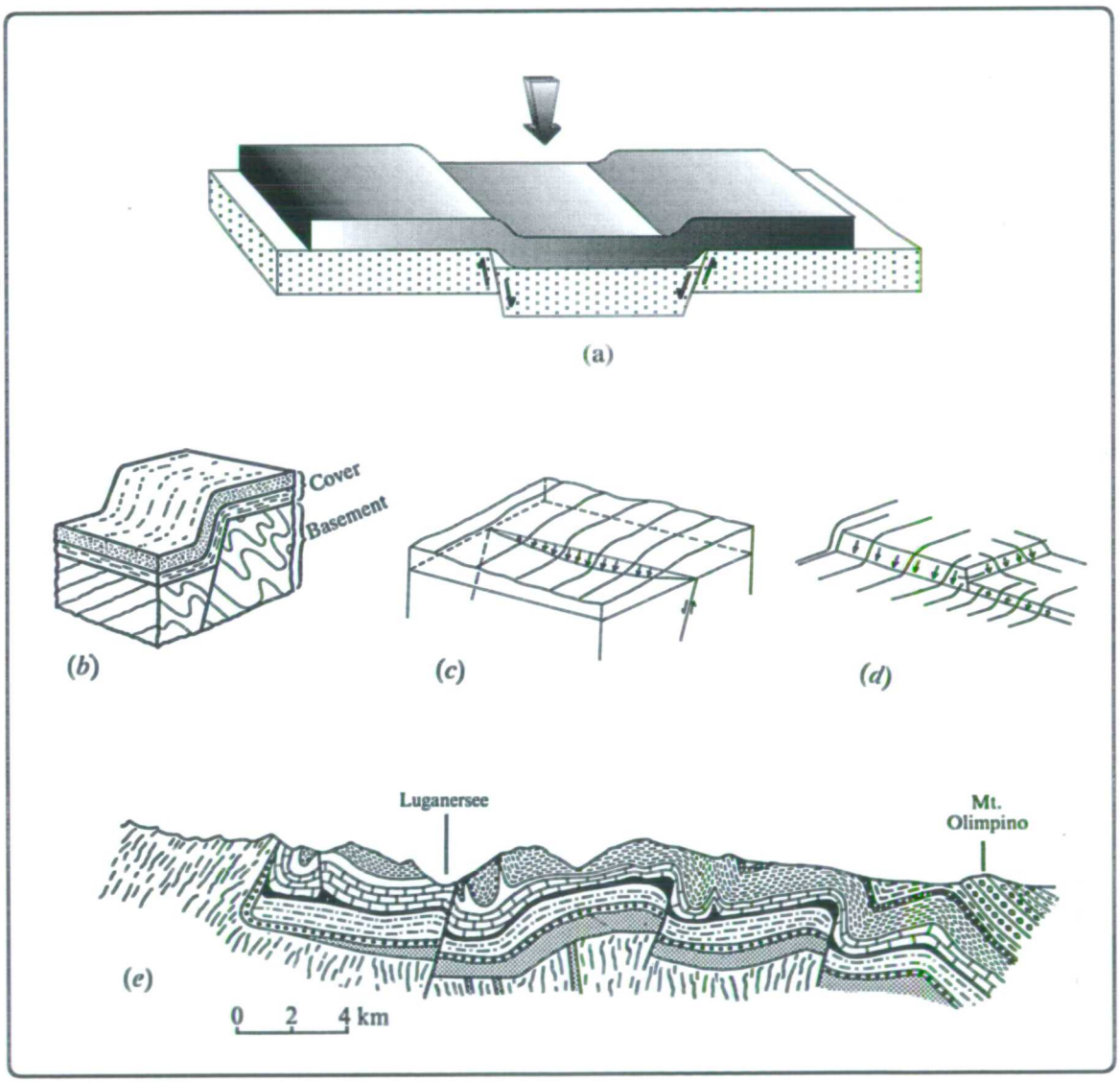


Fig. 3.13 Bending mechanism and different examples of folding by bending (b, c and d from Price & Cosgrove 1990, and e from Heim 1921/2).

(i) FOLDING OF SEDIMENTARY COVER IN ASSOCIATION WITH DIP-SLIP BASEMENT FAULTING

The folding of layered cover rocks as the result of dip-slip movement or a basement fault has been termed '**Forced Folding**' by Stearns (1978), who argues that the overall trend and shape of the fold is determined by the geometry of the forcing member(s) from below. Despite the relatively early use of model experiments in Geology, this approach was not used to study the effect of dip-slip movement of basement faults on cover rocks until 1959 when Sanford addressed this problem using both theoretical analysis and scale modelling. In his experiments the rigid basement was simulated by wooden blocks and the cover rocks by sand. The results of two of his experiments, which involved dip-slip movement on a vertical basement fault, are shown in Figs. 3.14.

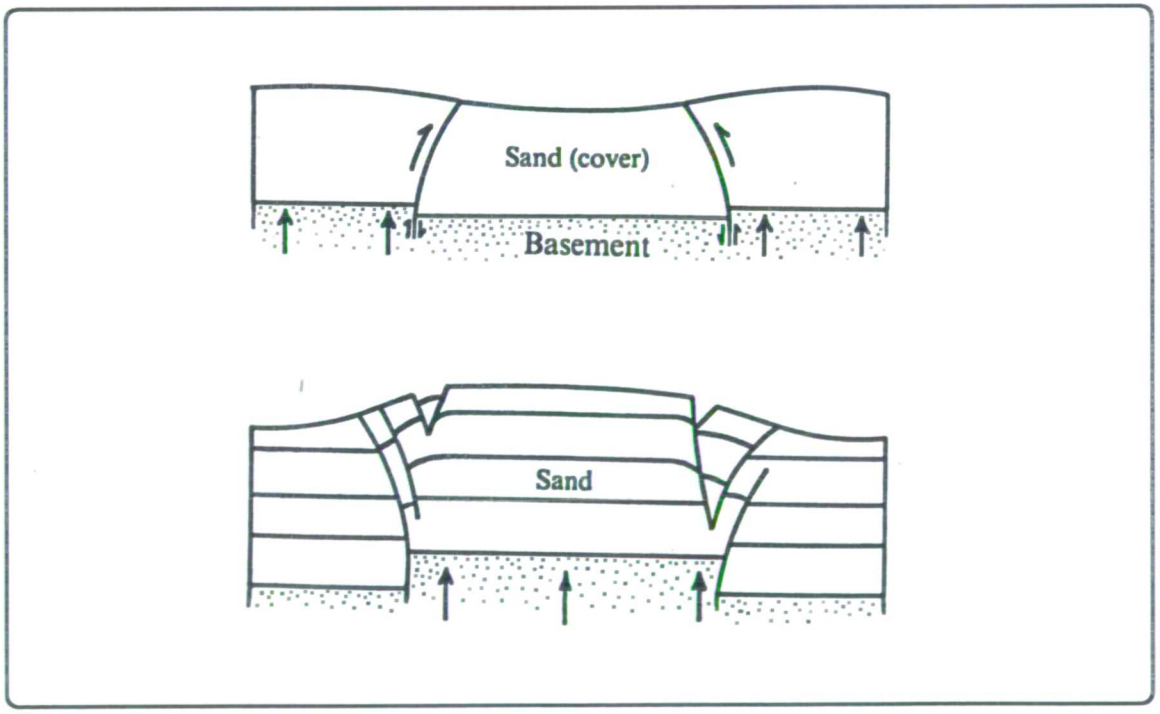


Fig. 3.14 Step-like displacements of the basement of a model experiment produced curved reverse faults and forced folds in the sand representing the cover (from Sanford, 1959).

The detailed geometry and character of the cover structures (faults and forced folds), are dependent on the mechanism by which the cover accommodates itself to the basement faulting. This in turn depends upon the rheology and physical environment of both basement and cover rocks during deformation and upon the geometry and sense of movement of the basement fault. The effect of normal and reverse movement on a basement fault on a layered cover has been studied experimentally by Ameen (1988).

During reverse faulting, horizontal shortening occurred along the cover in the direction normal to the strike of the basement fault and bedding plane slip developed in the vicinity of the fault and died off away from it. Although the strain distribution in the cover was complex, two of the axes of principal strain were always parallel to the layering with one parallel to the strike of the basement fault. The distribution of strain in the forced fold is shown in Fig. 3.15a.

Normal faulting in the basement caused horizontal extension of the cover in the direction normal to the strike of the basement fault and generated a relatively simple pattern of strain compared to reverse faulting (Fig. 3.15b). Again strain in the cover was concentrated in the vicinity of the basement fault. However, no significant bedding plane slip occurred. The cover accommodated itself to movement on the basement fault by thinning and thickening and the general strain pattern was dominated by bedding elongation perpendicular to the strike of the basement fault.

The effect of basement faulting on cover rocks has also been studied using the technique of finite element analysis by Reddy *et al.*, (1982). Their model consisted of a rigid 'basement' and a ductile cover. It was assumed that for stresses up to a particular yield point the material had one viscosity, and for stresses greater than the yield stress the viscosity decreased by a factor of 100 prior to further deformation. Using this model the response of the body to local yielding or fracturing can be modelled. The result of one such 'experiment'

in which normal faulting occurred in the basement, is shown in Fig. 3.15 c and d. It can be seen that a high angle reverse fault developed in the cover directly above the basement fault together with a near-surface region of normal faulting.

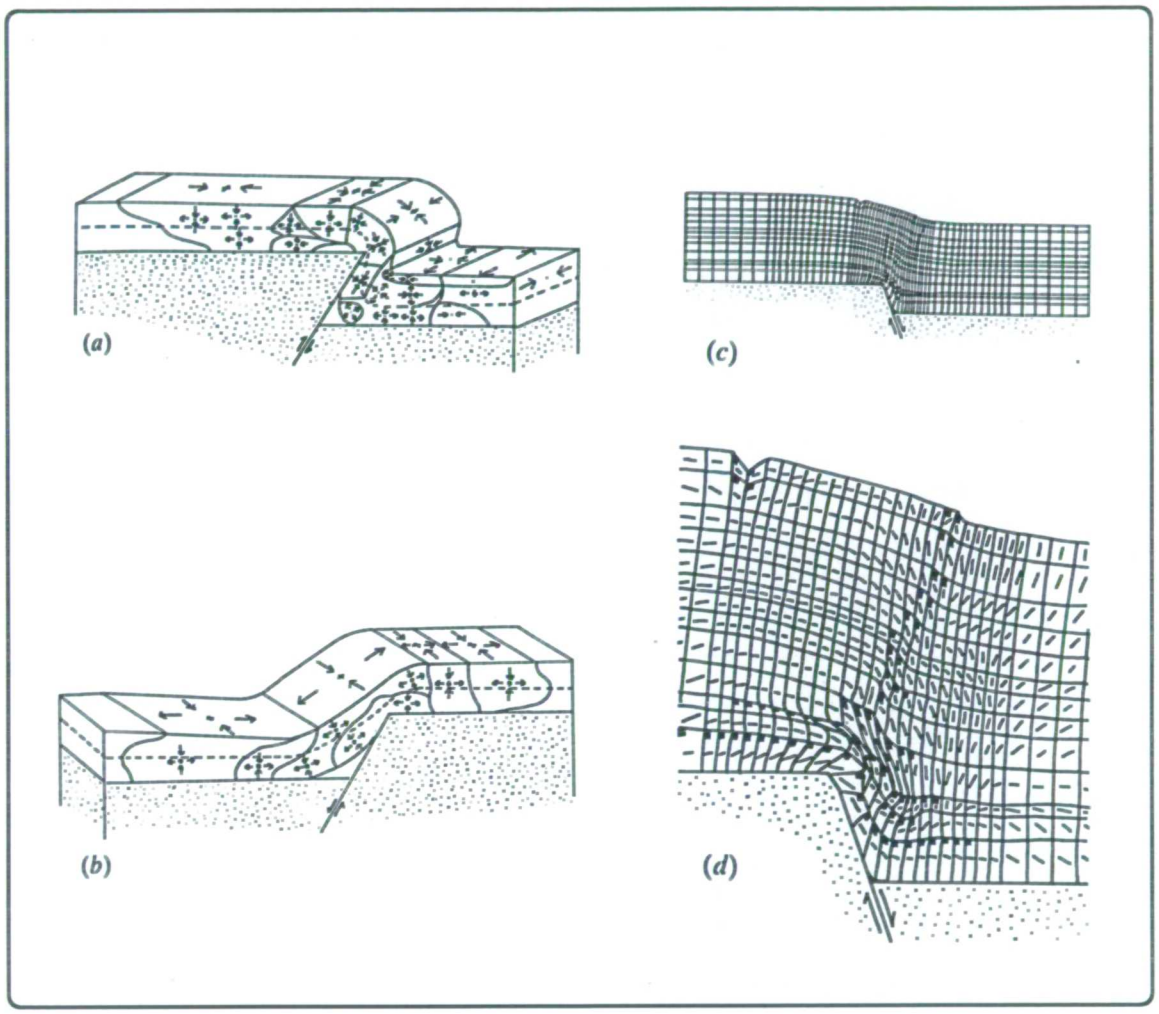


Fig. 3.15 Experiments showing the effects of (a) reverse and (b) normal faulting in a rigid basement on a layered, ductile cover (from Ameen 1988), and (c) and (d) the results of finite element analysis investigating the effect of faulting of a rigid basement on a viscous cover. Elements with black flags in the upper left hand corner show regions of yielding. The short lines in each element show the directions of least compressive stress (from Reddy *et al.*, 1982).

To summarise the geometry of forced folds will be determined by the geometry of the fault scarp in the basement and will therefore, tend to be a long, linear feature with a very large half-wavelength/hinge length ratio. In contrast experimental work and field observations on the three dimensional geometry of buckle folds show that these structures are generally not cylindrical and die out, often quite rapidly, when traced along the fold hinge. In addition they are frequently replaced by other folds offset from them in an *en echelon* manner (Fig. 3.16).

For buckle folds the ratio of the maximum profile wavelength to the length of the fold hinge is approximately 1:5. This geometry and spatial arrangement of folds can be found on a wide range of scales. For example minor folds with wavelengths of a few centimetres which exhibit an *en echelon* arrangement and which die out rapidly along the hinge line are shown in Fig. 3.16.



Fig. 3.16 Small-scale *en echelon* periclines in folded metasediments near Luarca. N. Spain, (from Price & Cosgrove, 1990).

The principal folds of the Jura Mountains (Fig. 3.17) have wavelengths which may attain 2 km or even more and display the same aspect ratio and *en echelon* arrangement. In passing, it can be seen that like the Zagros region this area provides an excellent example of concordant morphology (i.e. the mountains coincide with the anticlines and the valleys with synclines), characteristics of young (near surface) fold belts.

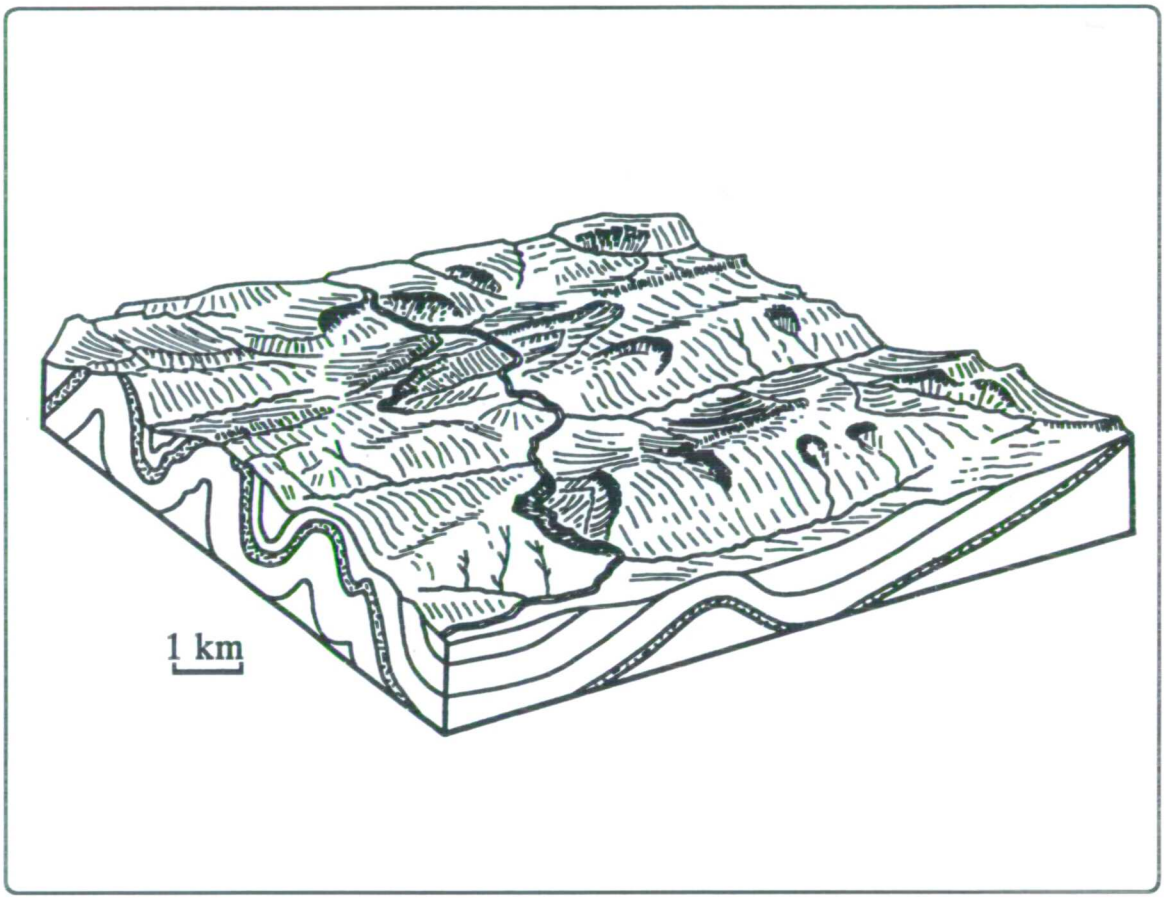


Fig. 3.17 Large-scale periclinal folds in the Jura Mountains (from Strahler, 1960).

The two types of folds discussed above, namely '**forced**' and '**buckle**' folds (one produced by dip-slip motion on basement faults and the other by layer parallel compression) can be treated as two end members and folds generated by a combination of layer parallel compression and movement on a basement fault are common.

(ii) FOLDING OF SEDIMENTARY COVER IN ASSOCIATION WITH STRIKE-SLIP BASEMENT FAULTING

A considerable amount of analogue modelling has been carried out on the effect of strike-slip motion of basement faults on the deformation of the overlying cover rocks (e.g., Oliver, 1987) .The result of such movement is the production of an *en echelon* array of pure buckle folds directly above the basement fault (Fig. 3.18). These folds are offset in a constant sense and can be used as a kinematic indicator to show the sense of movement on the underlying strike-slip fault.

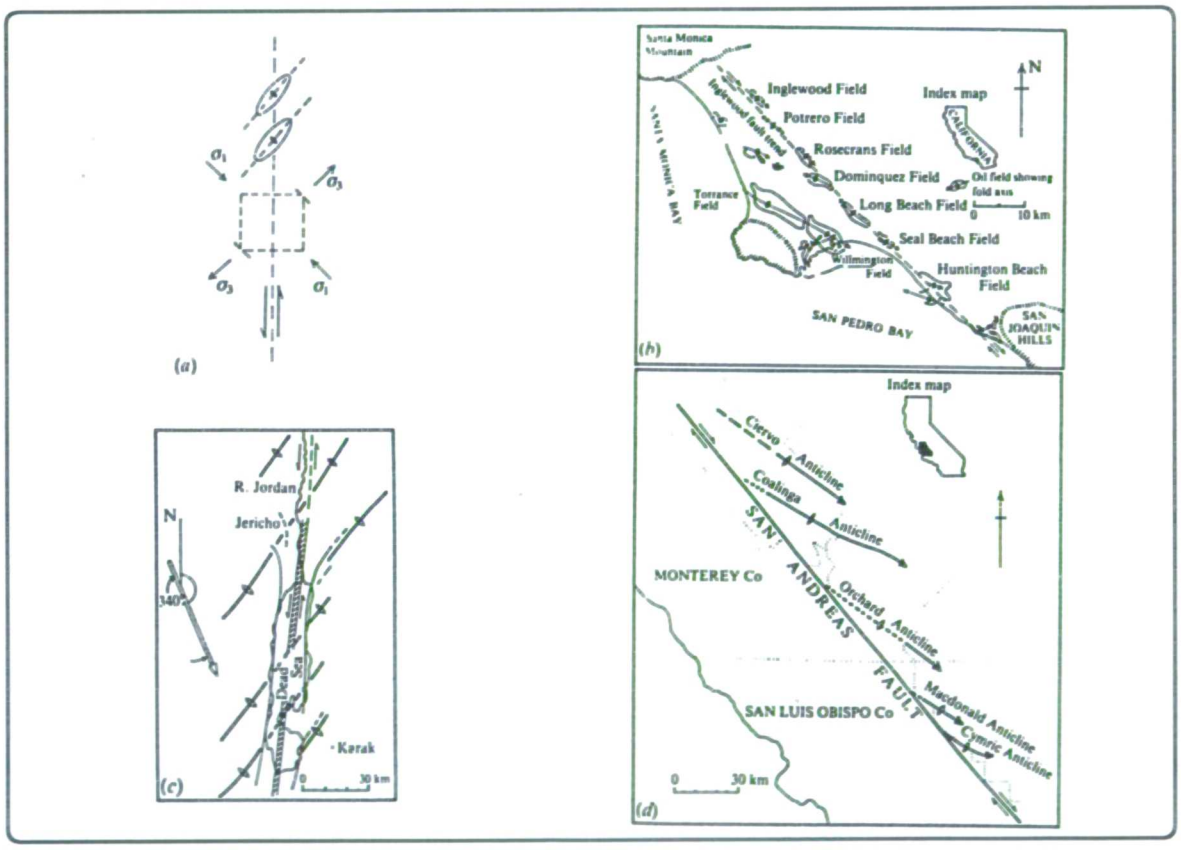


Fig. 3.18 (a) Shear in the basement induces compression in the cover rocks which produces *en echelon* folds such as are developed above (b) the Inglewood Fault (California) (c) the sinistral Dead Sea fault and (d) the San Andreas Fault (from Moody & Hill, 1956).

It should be noted that these folds have the half-wavelength/hinge length ratio in the range of 1:5, 1:10 i.e. typical of buckle folds. Inspection of the three dimensional geometry and spatial organisation of the Zagros folds using satellite images combined with field observations shows many of the characteristics discussed above. However, if the basement fault has an element of dip-slip motion then a fault scarp will develop and the geometry of the cover folds will reflect this. The aspect ratio will be considerably greater i.e. more characteristics of a '**forced fold**'.

Both '**buckle folding**' and '**different types of forced folding**', occur in the Zagros Mountain Belt. As discussed above the experimental work and field observations of these two groups of folds have provided diagnostic criteria regarding their three dimensional shape and spatial organisation which enables them to be recognised. Specific examples of these different types of folds form the Zagros belt are discussed in the following sections.

(a) BUCKLE FOLDS

The classical buckle folds, characterised by their periclinal geometry, are well represented in the Zagros folded belt. They typically have a half-wavelength/hinge length ratio of between 5 and 10 and in plan view are offset from each other in an *en echelon* manner but with no constant sense of offset. Excellent examples of folds with this aspect ratio and spatial organisation can be seen in Figs. 2.5 and 3.1. It was pointed out earlier in this chapter that the folds sometimes occur on different scales and a series of smaller buckle folds showing a random *en echelon* spatial organisation, which are enveloped within a larger periclinal structure can be seen in Figs. 3.8-3.11. It should be noted that although the aspect ratios of buckle folds range between about 1:5 to 1:10 it is possible to generate larger folds by the linking of two originally separate buckles.

The possible modes of interaction between adjacent periclines as they amplify and extend

along the fold hinge is shown in Fig. 3.19 where it can be seen that depending on the original separation of the two folds, the folds will either extend independently of each other if separation is large, block further growth if separation is around half the wavelength or link if separation is less than half the wavelength of the fold. Composite folds generated by linking will often be characterised by having a deflection in their hinge. Good example of such folds can be seen in Figs. 2.5, 3.3, 3.4, 3.7 and 3.10.

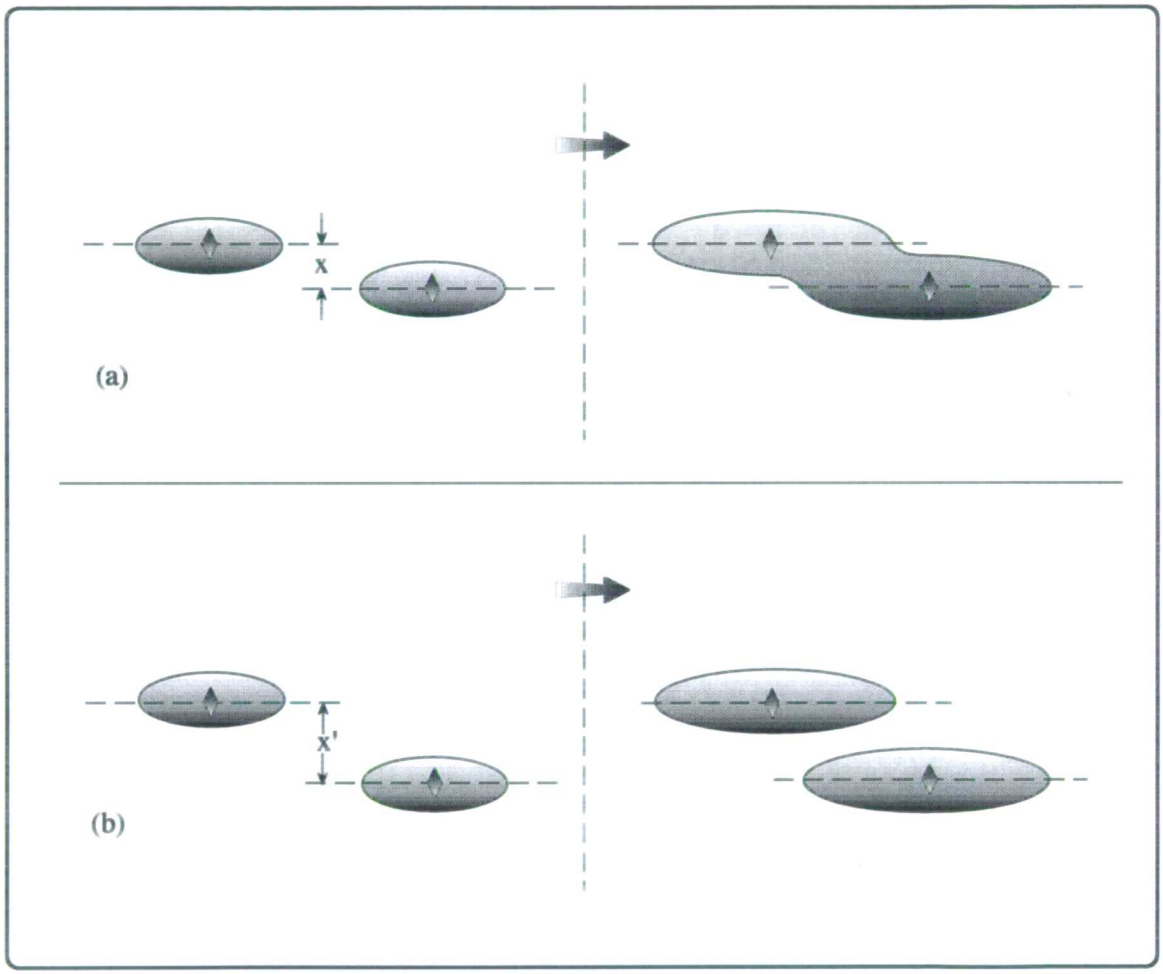


Fig. 3.19 (a) The amplification and coalescence of two periclines (shown in plan) separated by a distance X which is somewhat less than half the wavelength of the structure. (b) Two periclines separated by X' which is slightly greater than half the wavelength. The structures overlap and lock up, each preventing further propagation of the other.

(b) FORCED FOLDS ASSOCIATED WITH DIP-SLIP FAULTING

Many forced folds are generated in the fold belt and a variety of fold/fault association can be recognised. As mentioned earlier in this chapter, one of the most characteristic features of forced folds formed in association with faults is their remarkably long hinge length. Numerous examples of such folds can be found in the Zagros fold belt and one of the most impressive in the **Kabir Kuh anticline** which extends for over 200 km parallel to the fold belt (Figs. 3.1 and 3.4). It is clear from the seismic section (Fig. 3.20) that this and many other folds are generated as a result of reverse dip-slip movement on thrust of normal faults.

It is interesting to consider briefly the links between dip-slip faulting and folds, particularly thrusts and folds, with regard to the relative timing of the fault and fold formation. In '**forced folding**' it is clear that the fold is formed by movement on the fault and that the fault is the **earlier structure**. Convincing examples of this can be seen in the seismic section in Fig. 3.20. There is however the possibility that the thrusts can **post-date** the fold and good example of folding and thrusting of the beds of the 'Incompetent Group' (Fig. 2.17) are shown in Fig. 3.5.

As well as folding associated with dip-slip faulting, examples of folding linked to strike-slip faults can also be found in the Zagros fold belt.

(c) FOLDS ASSOCIATED WITH BASEMENT STRIKE-SLIP FAULTS

Folds associated with strike-slip faults are also common in the Zagros folds belt. As mentioned earlier in this chapter, pure strike-slip motion on a basement fault can generate pure buckle folds in the overlying cover sediments. These folds, which initially have the same geometry and aspect ratio of buckle folds can be recognised by their characteristic spatial organisation. They are arranged in an *en echelon* manner when viewed in plan and

there is a '*constant sense of offset*' (Fig. 3.2 b and c). Examples of this arrangement of folds can be seen in several places in the Zagros belt and these *en echelon* arrangements of folds are thought to be related to major basement wrench faults.

For example, as can be seen from 3.21 the N-S trending '**Kazerun-Borazjan fault zone**' Fig. 3.22 has associated with it a series of *en echelon* anticlines and thrust faults with a constant offset i.e. to the NE. Such arrays are characteristic of a basement wrench fault with a '*dextral*' sense of movement (Fig. 3.2 c) and it is reassuring to find that the relatively small wrench faults that have developed in the cover rocks above this proposed major basement structure have this sense of shear.

It should be noted that with progressive shear on the basement fault the folds may rotate towards parallelism to the basement fault. However, they continue to grow at approximately 45° to the fault with the result that they become sigmoidally deflected (Figs. 3.3 and 3.18b). This deflection combined with the constant sense of offset represents an important kinematic indicator relating to the position and sense of movement of the basement fault.

The existence of such major '**basement faults**', associated with the '**surface fault zones**' in the sedimentary cover have been already indicated by several authors for the 'Kazerun-Borazjan' fault zone and called as the '**Kazerun Line**' (e.g. Falcon, 1969, 1974; Ni and Barazangi, 1986 and Baker *et. al.*, 1993).

However, the present author considers that on the basis of the above mentioned '**criteria**' used to demonstrate the presence of the '**Kazerun Line**' and some additional evidence it is possible to suggests **several other** equally important basement fault systems to the NW and SE of the '**Kazerun Line**'.

Inspection of Fig. 3.21 shows that **west** of the 'Kazerun-Borazjan fault zone' is i) a series of relatively small N-S trending dextral strike-slip faults, ii) a series of *en echelon* NW-SE trending thrust faults and iii) a series of *en echelon* anticlines, offset constantly to the NE, which occur in the cover rock and are **compatible with** the dextral movement on an underlying major N-S trending strike-slip basement fault running along the **eastern margin** of the Dezful Embayment, from the 'Vanizan mountain' through 'Izeh' to Bandar-e Deylam, termed here the '**Izeh Line**' (see also Figs. 3.1 and 3.22).

The existence of this proposed basement wrench fault is also supported by the fault plane solution of the relevant earthquakes. For example an event on 2nd January 1967 at the locality (30.6°N, 50.4°E) indicated a dextral strike-slip motion at a depth of 47 km (Chandra, 1984).

As noted above, this proposed basement fault coincides with the major topographic front which defines the '**eastern margin**' of the Dezful Embayment. Not surprisingly inspection of Figs. 3.7 and 3.23 shows that the '**northern margin**' of the Dezful Embayment is also coincided with a series of strike-slip faults and a series of *en echelon* anticlines and thrust faults occur in the cover rocks with constant offsets which are compatible with the sinistral movement on an underlying major E-W trending strike-slip basement fault running along the '**northern margin**' of the Dezful Embayment from the 'Vanizan mountain' (NE of the Bakhtiari mountains) through the 'Bala Rud fault' to the area south of Mehran. This is termed here the '**Bala Rud Line**' (Fig. 3.23).

As can be seen from the Figs. 3.1, 3.21, 3.22 and 3.24, on the basis of the same criteria and evidence listed above regarding the existence of the basement 'Kazerun', 'Izeh' and 'Bala Rud' lines, **several other major basement lines** can also be detected. These are as follows:

(i) A line running along the northern margin of the 'Lorestan Fold Zone', termed here the

'**Sumar Line**' (Fig. 3.23).

(ii) A line running from the Bakhtiari mountains through Ramhormoz to the Persian Gulf, termed here the '**Ramhormoz Line**' (Fig. 3.24).

(iii) A line running along the 'Kareh Bas fault zone', termed here the '**Kareh Bas Line**' (Figs. 3.22 and 3.24).

(iv) Eight approximately parallel lines running NE-SW, NW of the Strait of Hormuz, termed here from NW to SE the '**Dashti**', '**Bastak**', '**Charak**', '**Bandar Abbas**', '**Qeshm**', and '**Larak**' lines (Fig. 3,24).

As with the proposed 'Izeh Line', the existence of these major basement wrench faults is also supported by the fault plane solutions of the relevant earthquakes.

The occurrence of several 'Hormuz salt diapirs' along some of these lines, especially those in the vicinity of the Strait of Hormuz, provides additional convincing evidence for the proposed basement lines. It is suggested that many of the Hormuz salt diapirs in this region could be controlled by these proposed basement wrench faults which created several strike-slip fault zones in the cover rocks and provided a suitable conditions for the ready salt rise in this area. The role of strike-slip faults in locating and initiating salt diapirism is discussed in more details in section 4 of this Chapter.

The present author also considers that, although some of the proposed or previously known basement line such as the 'Kazerun Line' could be pre-Zagros, i.e. early structures, their orientation is compatible with the compressive stress field that has been operating in the region since Late Cretaceous times and thus it is reasonable to suggest that they have been created and repeatedly reactivated during the evolution of the Zagros deformation. It is not surprising they also influence the geometry of the Zagros '**mountain front**' and the '**coast line**' of the Persian Gulf (Figs. 3.21, 3.23 and 3.24).

(d) FOLDS ASSOCIATED WITH BASEMENT OBLIQUE-SLIP FAULTS

An interesting example of fold development above a basement strike-slip fault can be found in association with the indentation of the Musandam block (peninsula) into the Iranian plate margin. Although the dominant sense of movement on the Minab-Zendan basement fault appears to have been strike-slip, the geometry of the folds in the overlying cover rocks indicates clearly that some dip-slip motion also occurred.

The Minab anticline (Figs. 2.12, 3.3 and 3.24) has a half-wavelength/hinge length ratio which is well is excess of the range found in ordinary buckle folds and it seems likely that the abnormally long hinge relates to a fault scarp in the basement, the result of an element of dip-slip motion on the basement fault. The *en echelon* folds associated with this linear structure which confirm the '*dextral*' component of motion on the basement fault, can still be seen (Figs. 3.3 and 3.24).

However, even these individual folds have a relatively high half-wavelength/hinge length ratio, and their offset is not as pronounced as that formed in folds above a pure strike-slip fault (Figs. 3.2b & 3.2c and 3.18c & 3.18d). At least two important faults occur in this region and there have been termed the Minab and Zendan faults (Figs. 3.22 and 3.24). The remarkably linear nature of the folds associated with these faults is very apparent from these figures. Inspection of the fold profile shows that they have a tight, chevron geometry and have clearly been amplified more than the pure buckle folds shown in Fig. 3.24.

Thus it can be concluded that the basement fault associated with the surface faults in this locality were acting in a '**transpressive**' sense during the generation of the folds. Although it is not possible to observe which side of the basement faults is the upthrown side, inspection of the geological map of Iran (Fig. 3.24) shows that the N-S trend of the Minab-Zendan fault zone links with the E-W trending thrusts which parallel the Iranian coast on

the Gulf of Oman. These north dipping thrusts are considered to be related to the northward subduction of the oceanic crust beneath Iran and Pakistan.

Thus it can be suggested that the block to the east of the Minab-Zendan fault zone will be upthrown relative to the block to the west. The fault plane solutions associated with the Minab-Zendan fault zone are compatible with this interpretation.

3. THE ZAGROS FAULTS

'**Faults**' are fractures along which there is a visible offset by shearing. They can occur as single discrete breaks, but where the rock that is faulted is weak or where faulting is especially intense, no discrete break may be evident, and instead a '**Fault Zone**' composed of countless sub parallel and interconnecting closely spaced fault surfaces is formed.

Faults and fault zones range in length and magnitude of offset from small structures visible in hand specimens to long spectacular crustal breaks extending hundreds of kilometres and accommodating displacements of tens to hundreds of kilometres. Where faulting takes place at deep levels under conditions of elevated temperature and/or confining pressure, '**shear zones**' may develop.

On the basis of the sense of movement on the fault plane, they can be divided into three end members as the '**dip-slip**', '**strike-slip**', and '**oblique-slip**' faults. Regarding the direction of movement, dip-slip faults can be divided into the normal and reverse slip (*thrust*) faults. The strike-slip faults can be divided into right-lateral (**dextral**) and left-lateral (**sinistral**) faults.

The '**Zagros Mountain belt**' of Iran is one of the worlds classical orogenic belt which provide some of the best examples of the different style of faults and fault zones. However, the intense and widespread seismicity which covers the whole mountain belt and extends well beyond the mountain front, mainly with focal depths greater than 13 km (i.e. the maximum thickness of the sedimentary cover) indicates that the '**Zagros Fault Belt**' is much deeper and broader than the Mountain Belt. The spatial distribution, geometrical characteristics, and mechanism of formation of the Zagros faults will be examined in the following sections and discussion of the seismicity is given in chapter 8.

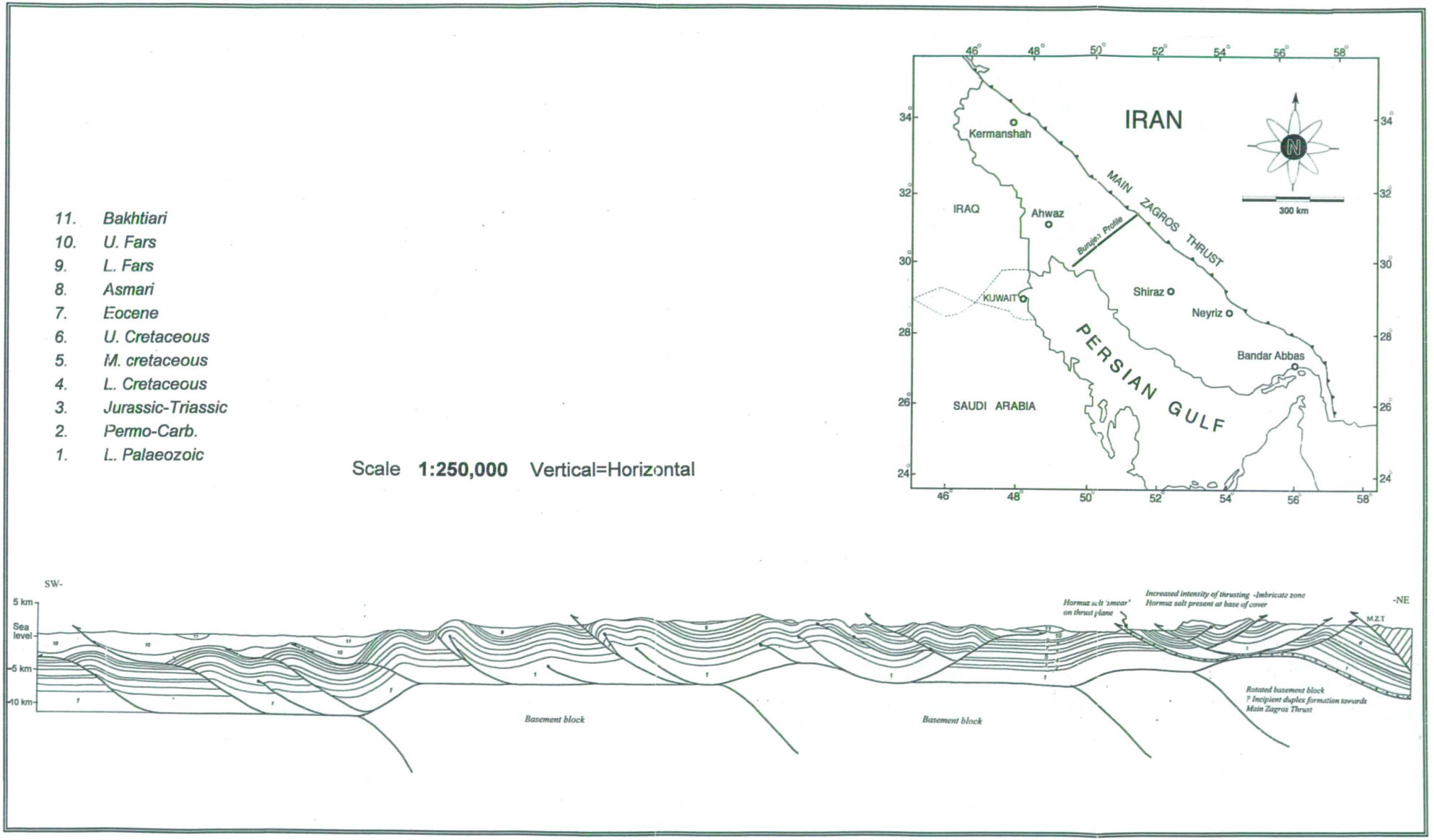


Fig. 3.20 A structural cross-section based on a seismic profile across 'Burujen' (51° 12′E- 32° 59′N), (from Payne, 1990). The location of the profile is shown in the index map.

a) SPATIAL DISTRIBUTION OF THE ZAGROS FAULTS

Thrusts are the most prevalent **mappable** faults in the '**Zagros Fault Belt**'. They generally runs parallel to the Zagros trend. Low and medium-angle thrusts are numerous in the 'Simply Folded Belt' and are generally restricted to the sedimentary cover (Figs. 3.5, 3.20 and 3.22).

As one moves from the 'Simply Folded Belt' towards the 'Imbricate' and 'Thrust' belts in the interior of the Zagros mountains, the shallow gently dipping thrusts are replaced gradually by a series of major, deep-seated, **Inverted Normal Faults**. Some of these faults have an overthrust (or nappe) appearance as a result of a remarkable bending and reduction of dip angle, in their uppermost parts. The Main Zagros Thrust is one of these major overthrusts (Fig. 2.15) (Alavi, 1980, 1994).

Strike-slip faults are less prominent mappable faults in the 'Zagros Fault Belt'. They are generally seen either as an individual fault or a series of *en echelon* faults within a fault zone. Except the '**Main Recent Fault**' which according to Tchalenko and Braud (1974) is a major strike-slip fault running parallel to Zagros trend in the vicinity of the 'Main Zagros Thrust' (Fig. 3.22) the other strike-slip faults are generally transverse faults and cross cut the Zagros Mountain belt.

Oblique-slip faults, with a combination of thrust and wrench movements are widespread in the southeastern end of the Zagros mountain belt within the Minab-Zendan fault zone, east of the Strait of Hormuz (Figs. 3.22 and 3.24).

Normal faults are rare and mostly seen in association with relatively small-scale collapse structures in the anticlinal crests (Fig. 3.25), around the salt diapirs, and within the strike-slip fault zones.

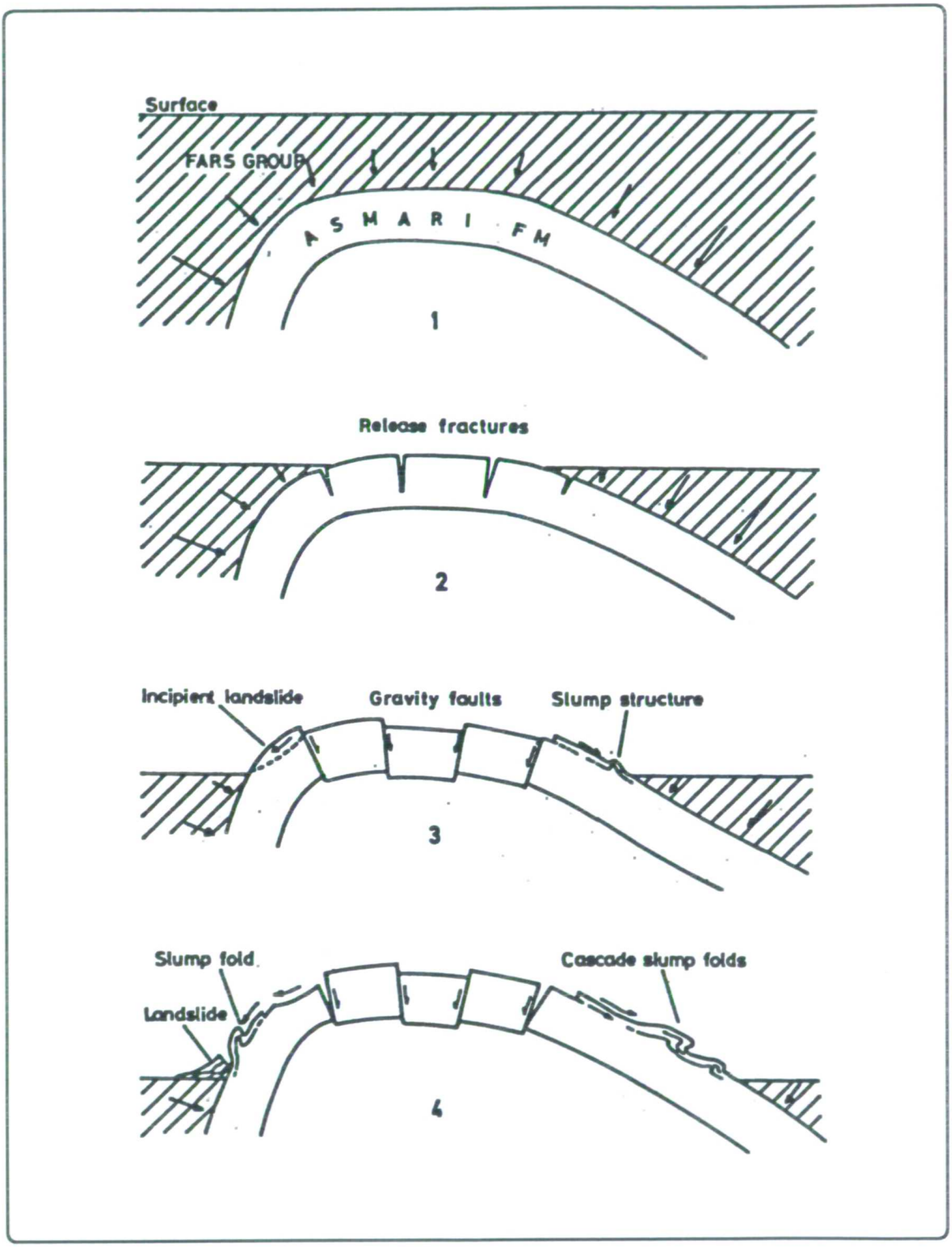


Fig. 3.25 Normal faults in the crest of the major anticlines, (from McQuillan, 1974).

b) GEOMETRY OF THE ZAGROS FAULTS

'**Thrusts**' and the '**inverted normal faults**', like the Zagros folds, have an E-W trend in the northwestern end of the belt (SE Turkey), gradually assume a NW-SE trend in NE Iraq and then extend with almost the same orientation down to the NE coast of the Persian Gulf until they swing around the Strait of Hormuz into a NNW-SSW direction (Fig. 3.22).

On the basis of their length, these thrusts and inverted normal faults can be divided into '*major*' and '*minor*' faults. **Major Faults** separate different structural and morphological zones. These are the most important elements in the structural and morphological framework of the Zagros Mountains. **Minor Faults** are smaller and distributed in different parts of a single structural zone. With a few exceptions, both types of fault dip NE towards Central Iran.

It is generally believed that the '**Main Zagros Thrust**' which strikes parallel to the Zagros NW-SE trend and marks the tectonic boundary between the Zagros Mountain Belt and Central Iran (Gansser, 1955; Falcon, 1967; Stöcklin, 1968) is the largest entirely exposed thrust fault in the Zagros Mountain belt.

Even if we ignore the confusion created by Alavi (1980) and Kashfi (1985), there is no unanimity about the origin and geometrical characteristics of this thrust. Thus Gansser (1955), Falcon (1967), Stöcklin (1968), Jaros (1981), and Berberian (1977, 1981, 1995) believe that the Main Zagros Thrust is a single, major, NE dipping, low-angle thrust. De Jong (1982), Braud and Ricou (1971), and Tchalenko and Braud (1974) take the more conventional view that the thrust line is a plate suture, and point to evidence of two NE dipping, segmented, parallel faults, one a low-angle thrust, and the other a high-angle (or vertical), right-lateral, strike-slip fault. Others, including Kashfi (1985) and Alavi (1980, 1994), argue that there is no single thrust in the Zagros Thrust Zone that can be singled out

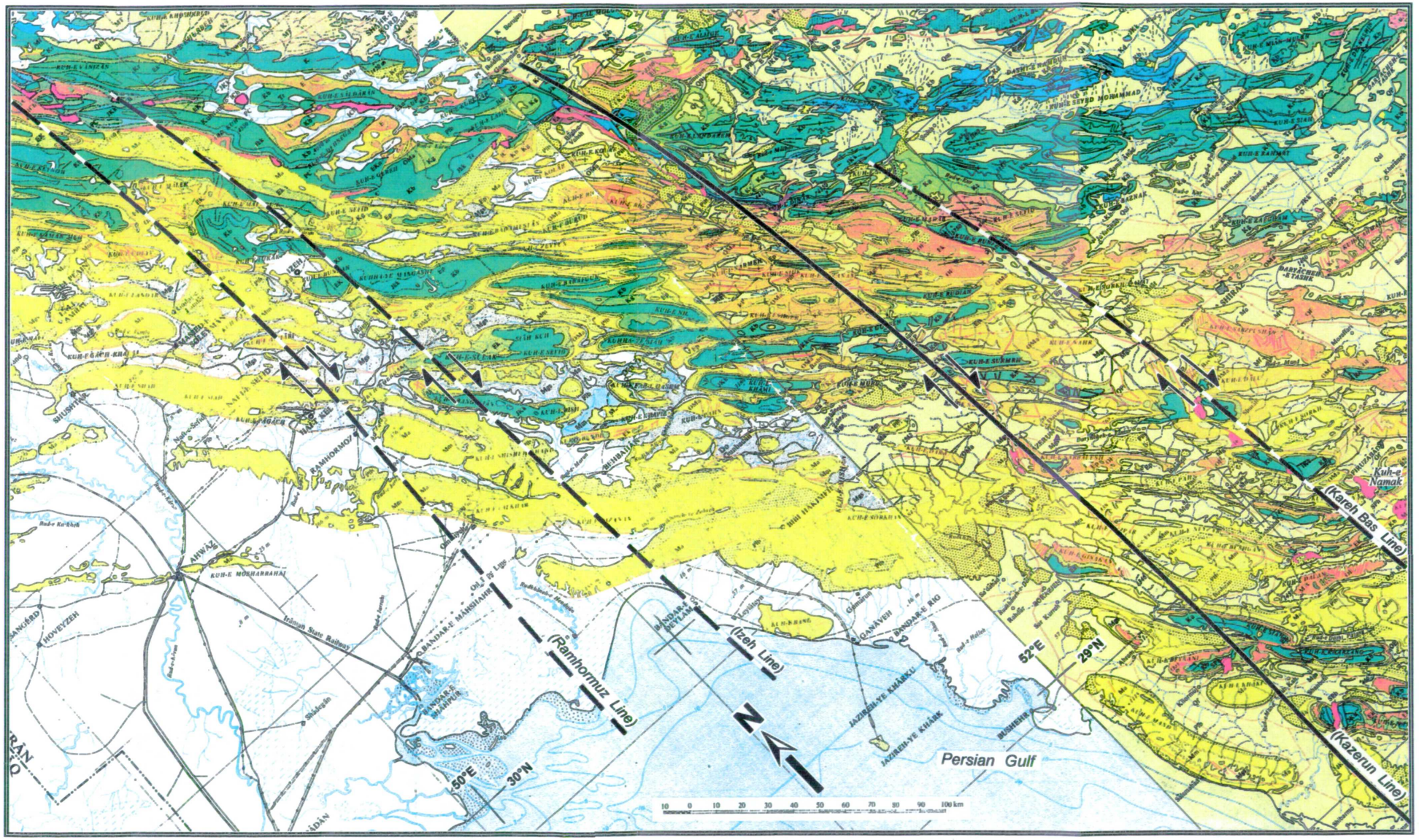


Fig. 3.21 A portion of the geological map of Iran 1:1,000,000 (NIOC, 1975) showing an *en echelon* alignment of buckle folds and thrust faults. These are used to detect the position and sense of shear on major basement strike-slip faults. The position, trend and sense of shear of these inferred faults is marked. The linear outcrop of the salt walls in the 'Thrust' zone are also shown (marked in red).

and referred to as the '*Main*' thrust. According to Alavi the troughs between the Sanandaj-Sirjan metamorphic belt and the Urmia-Dokhtar magmatic arc represents the suture zone (Figs. 2.14 and 2.15).

Southwest of the Main Zagros Thrust, within the Thrust and Imbricate zones, there are several other relatively large faults which are all of high-angles and it is generally believed that they were initially generated as normal faults and then during and after the collision of the Arabian and Central Iranian plates inverted to the reverse faults (Figs. 3.5 and 3.22).

In addition to these mappable '*thrust*' and '*inverted normal faults*', Berberian (1995) also suggested four master thrust faults which he suggests are all segmented and blind thrusts and extend almost the whole length of the belt. They also mark the boundaries between the most contrasting morphotectonic zones in the region.

The other NW-SE trending thrust faults are relatively small structures. Some of these thrusts are low-angle, fold-induced faults, and restricted to the Miocene-Holocene succession, 'Incompetent Group' while the others are of medium angles (30°-60°) and generally cut the whole thickness of the sedimentary cover to link with the Hormuz Salt detachment horizon (Fig. 3.20).

'**Strike-slip faults**' are the second prominent mappable faults in the Zagros Fault Belt. As noted earlier, except the '*Main Recent Fault*' which is a major segmented strike-slip fault and strikes parallel to the Zagros trend (Tchalenko and Braud, 1974), the other strike-slip faults generally cross cut the belt and strike either N-S or E-W (Fig. 3.22).

The **mappable** strike-slip faults occurring within the transverse fault zones are generally arranged with *en echelon* array. As mentioned earlier, in the section 2 of this Chapter, they are thought to form in association with the strike-slip motion on a major basement fault.

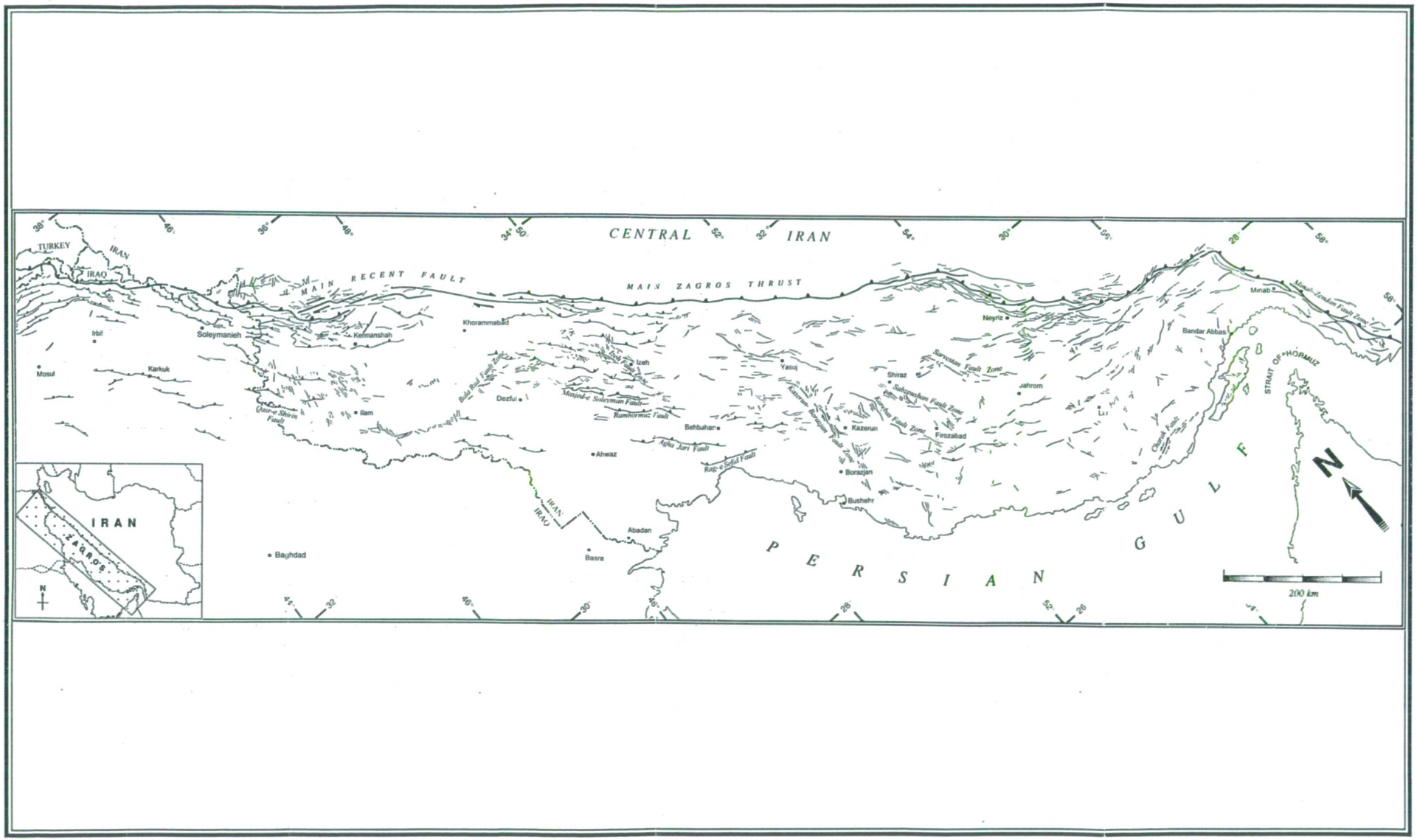


Fig. 3.22 Fault map of the Zagros mountain belt, showing the spatial distribution, trend and sense of movements of mappable faults.

The **mappable** strike-slip fault zones in the Zagros Fault Belt are from NW to SE, the Bala Rud, Izeh, Kazerun-Borazjan, Kareh Bas, Sabzpushan , Sarvestan, Bastak and Charak fault zones (Figs. 3.21-3.24). Field observations and fault plane solutions of the earthquakes around these strike-slip fault zones show that those trending approximately N-S are formed by '**dextral**' and those trending either NE-SW or E-W, '**sinistral**' faults.

'**Oblique-slip faults**' showing a combination of reverse dip-slip and dextral strike-slip movements are predominantly seen within the Minab-Zendan fault zone. The Minab fault (to the west) and Zendan fault (to the east) are two right-stepping, major faults within this zone (Figs. 3.22 and 3.24). From the available data it is not clear whether the Minab and Zendan faults extend the basement or have been developed in the cover rocks above a single basement fault with the same sense of movement. However, the *en echelon* offset and high aspect ratio of the folds developed in the vicinity of the Minab-Zendan fault zone emphasise the presence of such a major basement fault which marks the edge of the Arabian plate and separates the '**Zagros mountain belt**' (to the west) from the '**Makran range**' (to the east).

The southern extension of the Minab-Zendan fault zone is not well defined on the present geological maps. However, it seems reasonable to assume that it extends into the Gulf of Oman and separates the continental crust of the Persian Gulf from the oceanic crust of the Gulf of Oman (Fig. 2.1)

.

c) MECHANISM OF FAULTING IN THE ZAGROS MOUNTAIN BELT

The mechanics of faulting has been theoretically and experimentally examined by many authors. Anderson (1951) indicated that the normal-slip, strike-slip, and thrust-slip faults form when σ_1, σ_2, and σ_3 is vertical, respectively (Fig. 3.26). Accordingly the thrust and inverted normal faults of the Zagros Faulted belt which generally strike NW-SE have been produced by a horizontal compression (σ_1) acting in NE-SW direction.

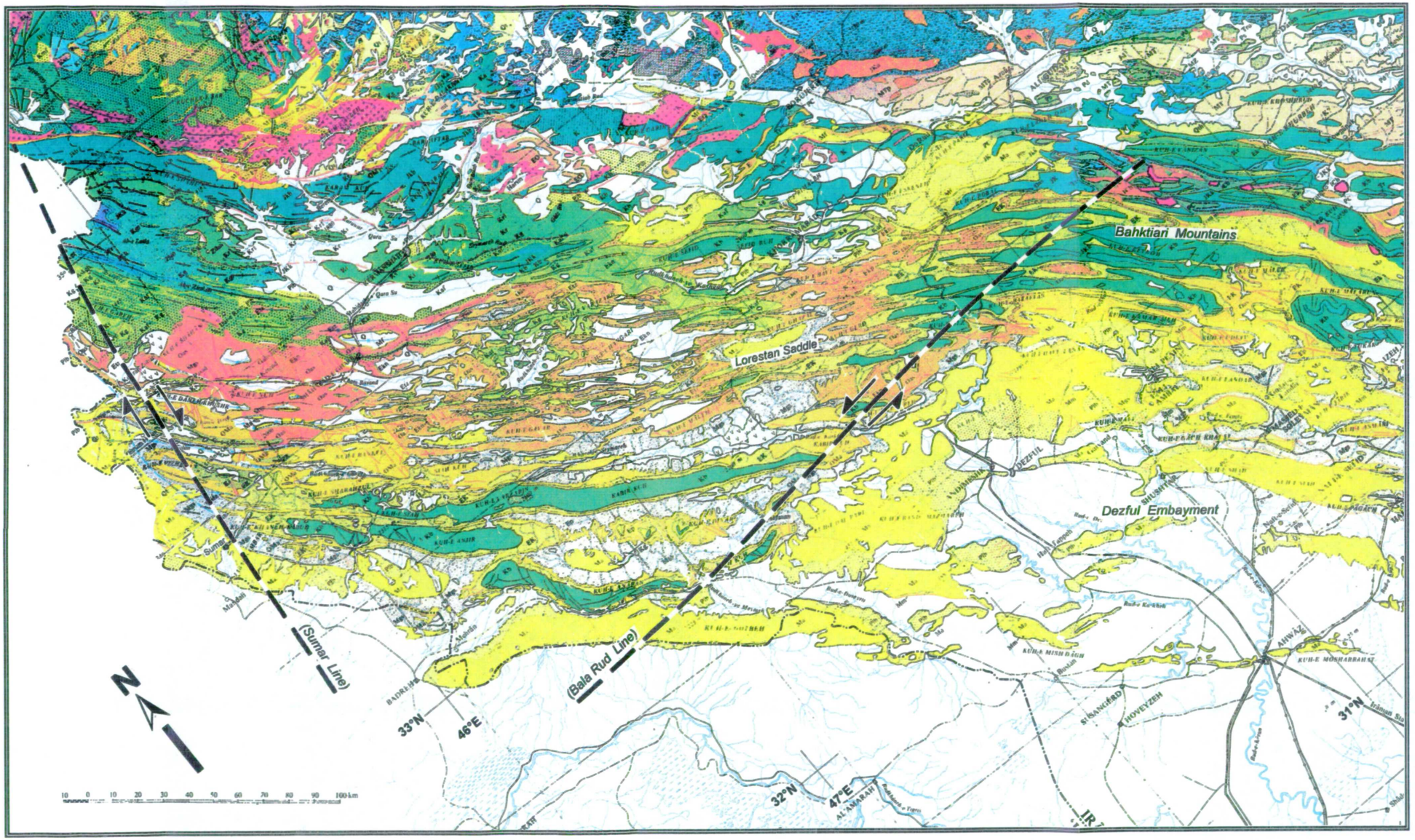


Fig. 2.23 A portion of the geological map of Iran 1:1,000,000 (NIOC, 1975), showing the large-scale **Kabir Kuh** anticline in the Lorestan fold zone, the position of inferred basement strike-slip faults (the Bala Rud and Sumar lines) and the linear outcrop of salt walls (marked in red) in the 'Zagros Thrust Zone'.

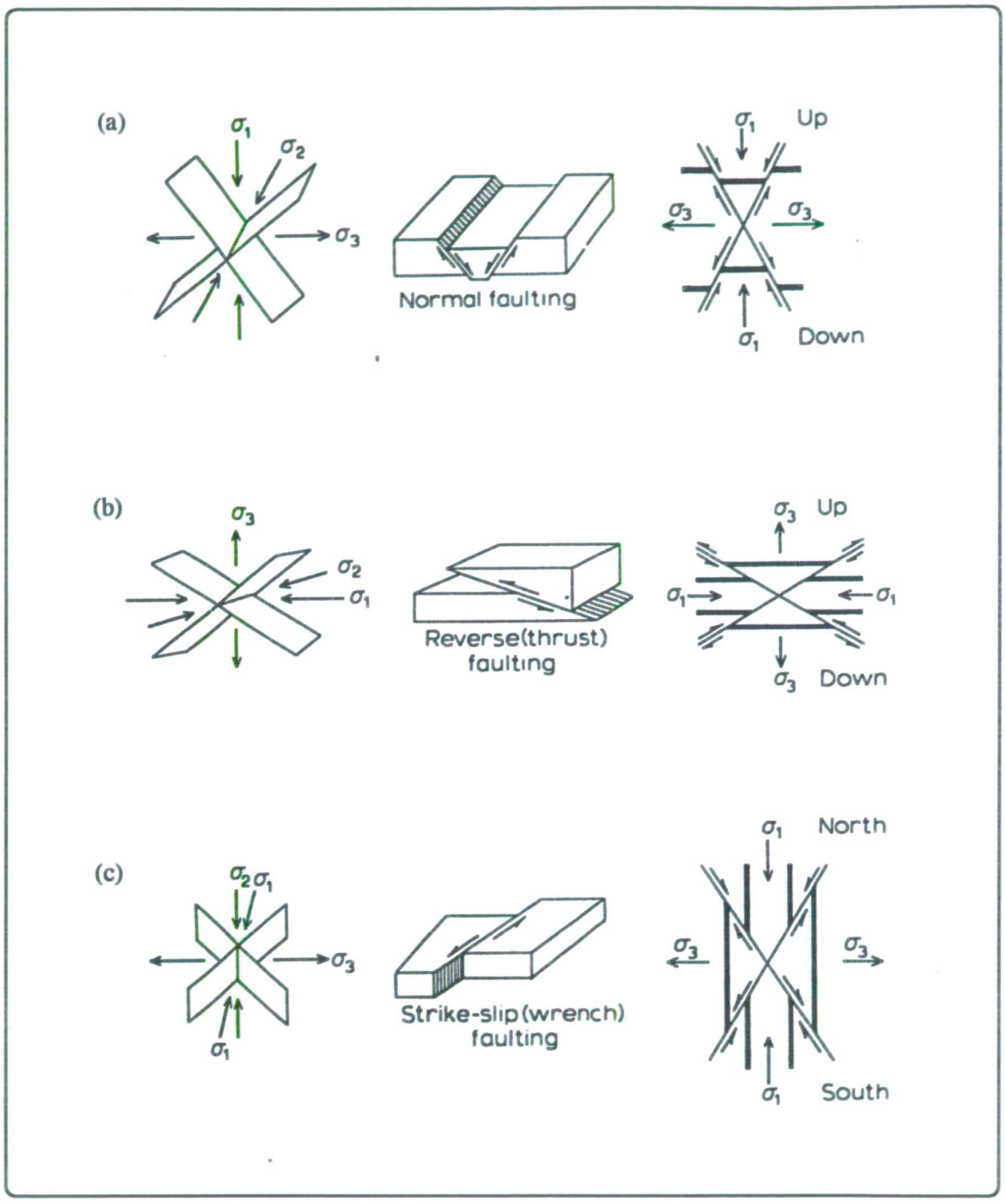


Fig. 3.26 Faulting mechanism and the initial stress distribution causing (a) normal, (b) reverse and (c) strike-slip faulting. σ_1, σ_2, and σ_3 are the maximum, intermediate and minimum principal stresses, respectively (from Hills, 1972).

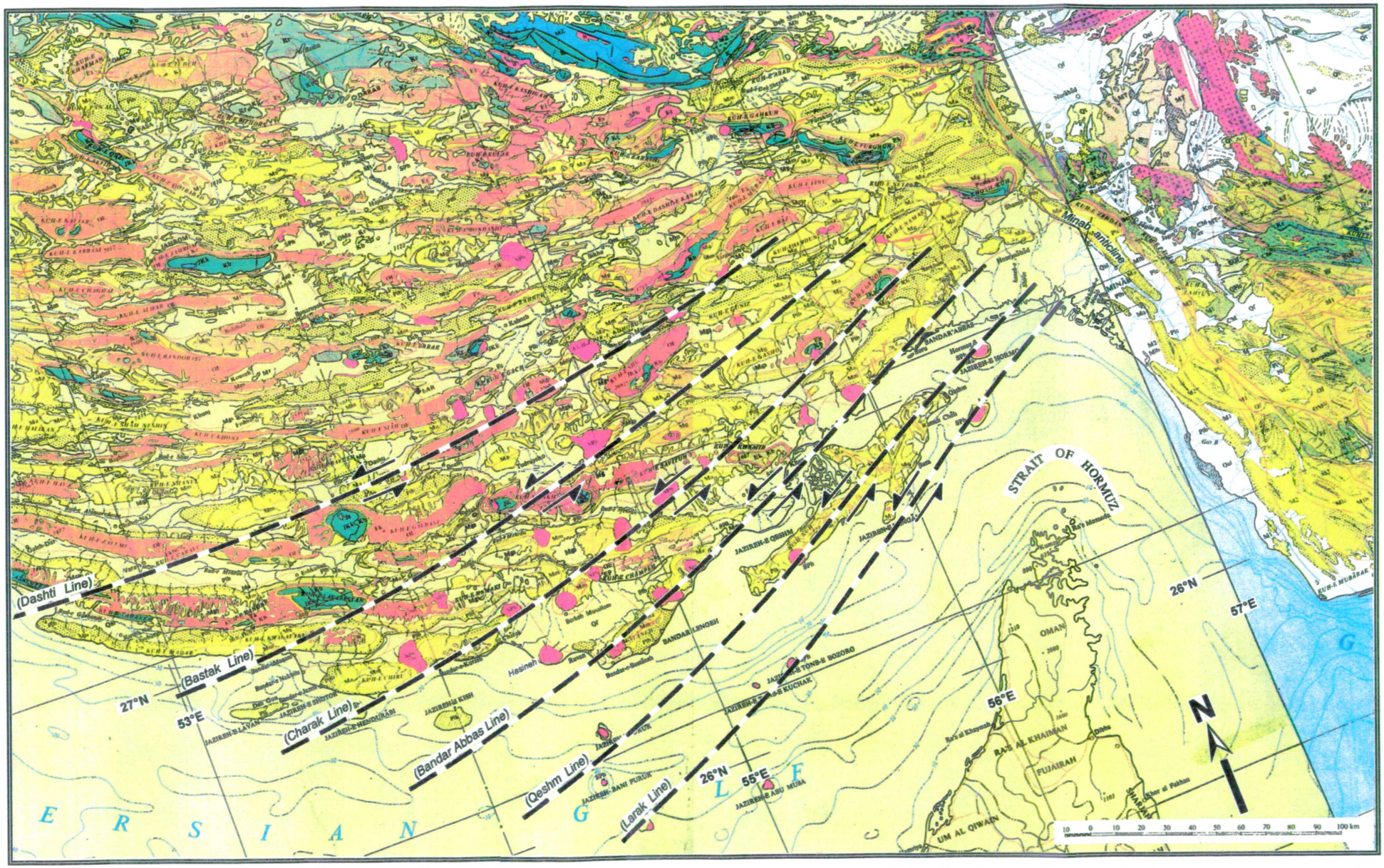


Fig. 2.24 A portion of the geological map of Iran 1:1,000,000 (NIOC, 1975), showing the marked differences in geometry of the classical buckle folds of the Fars province and the forced folding associated with the Minab-Zendan fault zone, and the Hormuz salt diapirs (marked in red) which are approximately equant and are aligned along the inferred basement strike-slip faults.

The conjugate strike-slip faults which generally strike N-S and E-W, cross cutting the Zagros trend (Fig. 3.22) are also produced and/or repeatedly reactivated by the same horizontal compression (Fig. 3.27) presumably under the influence of the considerable thickness of the overburden in some places which replaces σ_3 with σ_2. Falcon (1969, 1974) pointed out that some of the conjugate strike-slip faults cutting the Zagros sedimentary cover folds are older inherited basement structures within the Arabian Shield.

As noted earlier in section 2 of this chapter, although it is possible that some of major strike-slip faults such as those in the 'Kazerun-Borazjan fault zone' could be early structures associated with a pre-Zagros major basement wrench fault (i.e. the Kazerun Line), their '**orientation**' is compatible with the compressive stress field that has been governing in the region since the Late Cretaceous times (Figs. 3.21 and 3.27).

Strike-slip motion along the segmented 'Main Recent Fault' which according to Tchalenko and Braud (1974) strikes parallel to the Zagros trend in the vicinity of the 'Main Zagros Thrust' (Figs. 3.22 and 3.27) may be related to the anticlockwise rotation of the Arabian plate. If the maximum compression (σ_1) experienced a similar rotation, then dextral movement on some of the high-angle NW-SE trending faults such as the 'Main Recent Fault' will become possible (Fig. 3.27).

4. THE ZAGROS SALT DIAPIRS

Diapirs are features which result when a body of relatively low density pierces and rises through overlying rocks of higher density. The diapirs so formed may be composed of ice (giving rise to pingos) peat, coal, mud, clays and shales. However, the largest and most important diapirs are composed of either of salt (or other evaporites) or igneous rocks.

The terms **diapir**, **diapirism**, and **diapiric** come from the Greek word **diapeirein** which means to pierce. Generally, they are applied to geologic structures which originated, or at least appear to have originated, as the result of the movement of material from deep levels to shallower levels. Salt diapirs occur as **salt pillows**, **salt walls**, or individual **salt domes** or **stocks**. Salt diapirs have considerable economic importance not only for the salt itself but also because of the intrusion of salt frequently creates conditions which are favourable for the development of hydrocarbon reservoirs in the adjacent sediments.

The Zagros Mountain area is one of the best localities in the world for salt diapirs in the forms of *plugs* and *glaciers*. Blanford (1872) who was one of the first geologists to study the salt diapirs of the southern Zagros and their lithological characteristics and composition, did not appreciate the heterogeneous character of the igneous and metamorphic rocks associated with the evaporites, and applied the term **Hormuz Series** to the entire complex (Ala, 1974). Pilgrim (1908, 1924) also visited the region and called the salt complex the **Hormuz Salt Formation**. He was followed by many other workers who investigated the detailed tectonics of salt diapirism in the region.

a) SPATIAL DISTRIBUTION OF THE ZAGROS SALT DIAPIRS

More than 200 salt diapirs are known in southern Iran and in the Persian Gulf regions and they are largely confined to the Fars Province (Figs. 2.5 and 3.24). The density of diapirs

die out abruptly when traced NW along the Zagros mountain belt.

The absence of randomly scattered diapirs in the northwest (Figs. 3.21 and 3.23), as pointed out by Ala (1974) suggests a reduced thickness of the Hormuz Salt in that area. A complete disappearance is less likely because of the presence of folds which suggests that a detachment zone still exists in this region.

Except for the salt diapirs occurring in the Dezful Embayment in front of the higher Bakhtiari mountains, which originate from the exceptionally thick and salt rich beds of the '**Miocene Gachsaran Formation**' (Upper Mobile Group) in this locality (Figs. 3.5, 3.21 and 3.23) the other salt diapirs in the Zagros region, including those in the Persian Gulf, originate from the **Infra-Cambrian, Hormuz Salt Formation** (Lower Mobile Group).

Most of the diapirs originating from the '**Hormuz Salt Formation**' occur in the Fars province, SE Zagros, where the largest salt extrusions of the Middle East, and the best exposures of salt plugs occur (Fig. 3.24 and 3.28). Nine of the small islands off the southern Iranian coast including Hormuz, Larak, Qeshm, Hengham and Farur, are also salt plugs. Hormuz Island is the classic example. It is circular, 7 km across, with strong concentric ridges and a strongly concentric structure (Figs. 3.24 and 3.29).

As noted in section 2 of this chapter, **it can be suggested** that one of the explanations for the exceptionally widespread occurrence of Hormuz salt diapirs in the area northwest of the Strait of Hormuz could be the presence of a series of basement wrench faults which created several strike-slip fault zones in the cover rocks and provided a suitable conditions for the ready and widespread rise of salt in this area.

The surface distribution of the '**Hormuz salt diapirs**' raises some interesting and puzzling problems. They suddenly cease along the Main Zagros Thrust which marks the northeastern

margin of the Arabian plate and it has been suggested that the salt beds were either not deposited or have been removed by erosion beyond this line (Harrison, 1930). The salt diapirs north of Kerman, and the well-known salt diapirs of the Great Kavir in central Iran far away from the Zagros region, belong to separate basins (Stöcklin, 1968).

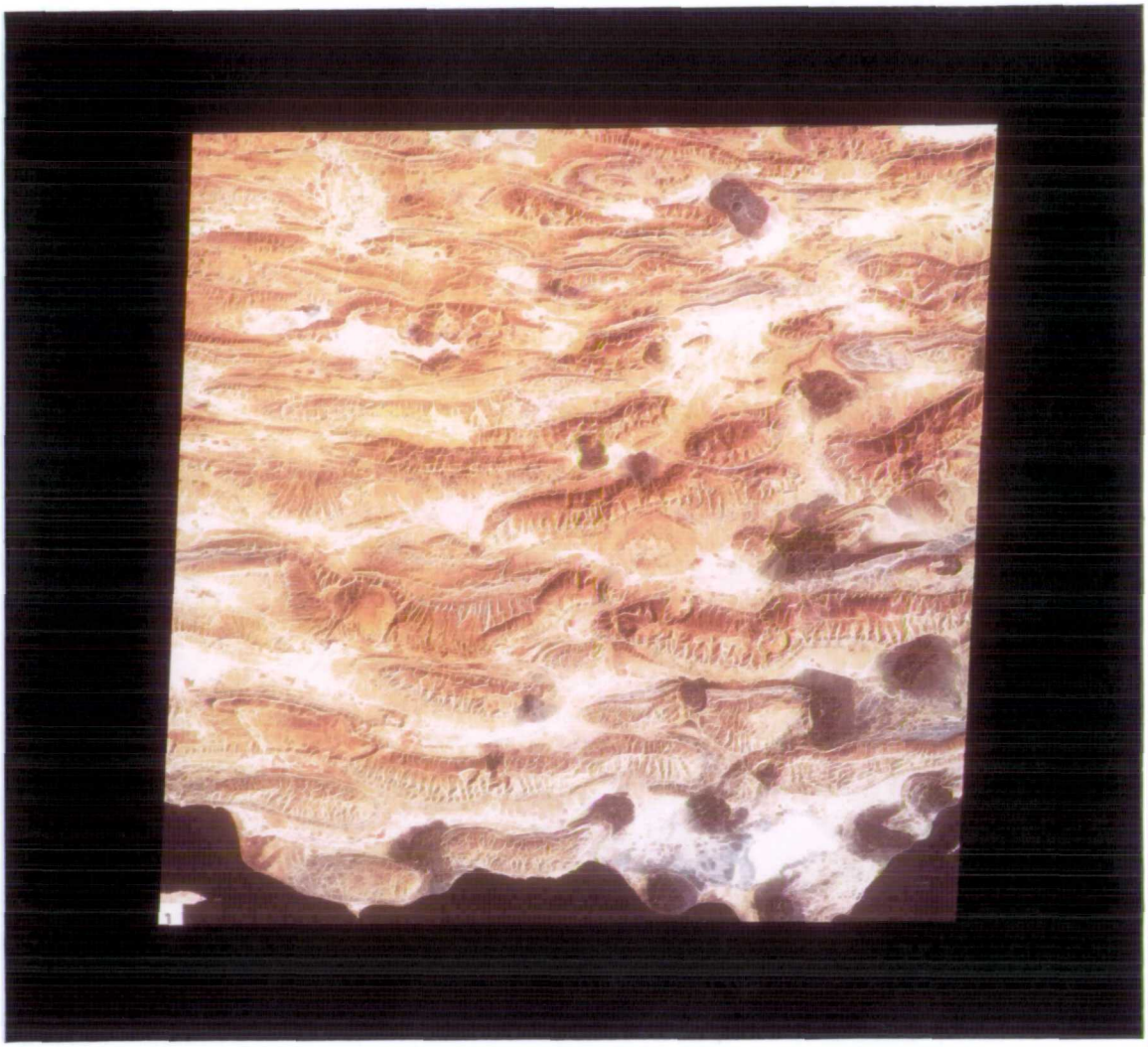


Fig. 3.28 Satellite image of the area NW of the Strait of Hormuz, showing equant salt diapirs.

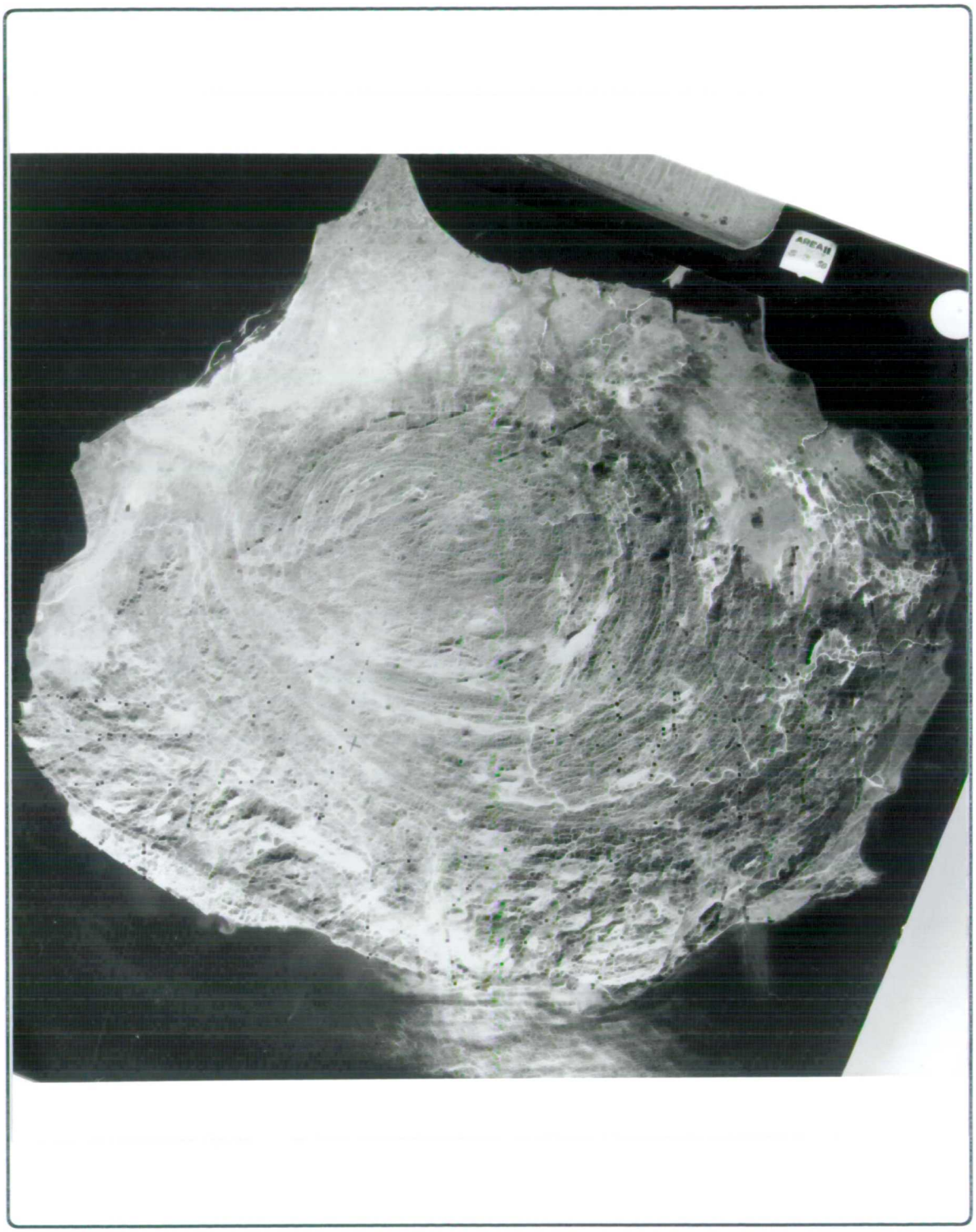


Fig. 3.29 Aerial photograph of Hormuz Island.

b) GEOMETRY OF THE ZAGROS SALT DIAPIRS

No two outcrops of the salt diapirs in the Zagros and the Persian Gulf region are identical, but there is overall uniformity throughout the region. The appearance of the *Infra-Cambrian* **Hormuz Salt diapirs** in the Zagros region, except for those occurring in the higher Bakhtiari Mountains of the central Zagros, is essentially '**plug-like**', being near circular or oval in plan (Fig. 3.24, 3.28 and 3.29), having a distinctive stock and forming a crater-like depression when the salt has been exhausted or arrested or when undue erosion has occurred (Fig. 3.10). In the Bakhtiari Mountains the salt extrusions form narrow '**slivers**' as much as 30 km long and about 1-3 km wide (Kent, 1979), following the NW-SE trace of high-angle reverse faults (Figs. 3.21 and 3.24). The **Gachsaran diapirs** of *Miocene* salt are generally in the form of '**salt bulges**' and '**flow-sheets**' along the hinge zone of mainly unroofed NW-SE trending anticlines (O'Brien, 1957) (Figs. 3.21 and 3.30).

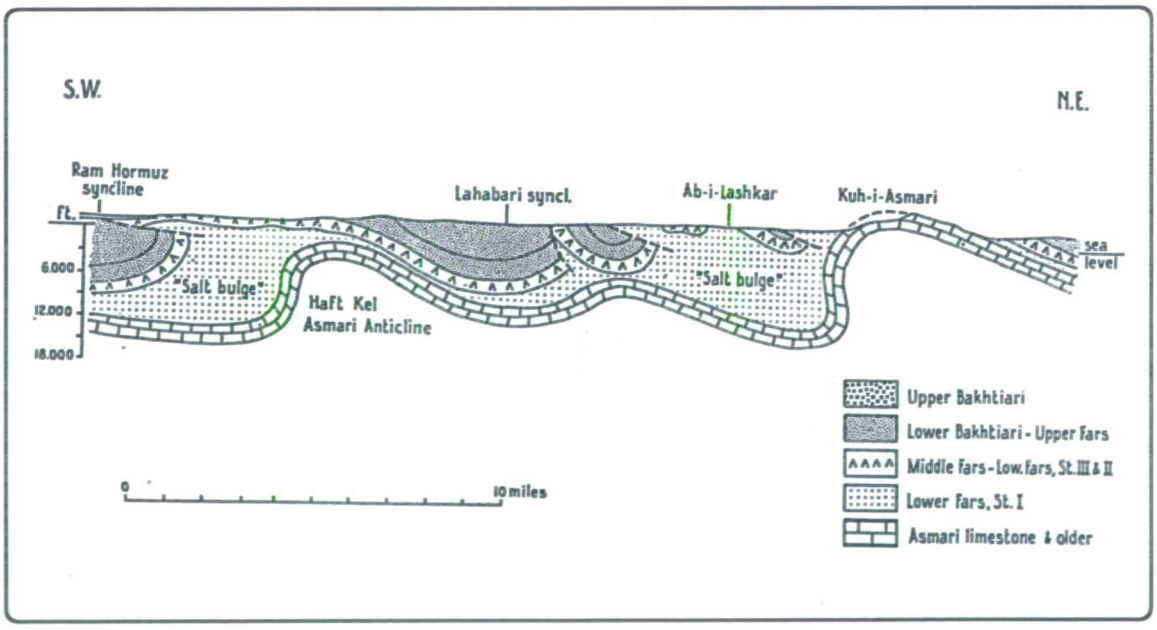


Fig. 3.30 Cross-section through the Masjed-e soleyman and Haft Kel areas, showing the Miocene Lower Fars salt rich evaporites (Gachsaran Formation) forming 'salt bulges' and 'flow-sheets' as a result of disharmonic folding (modified from O'Brien, 1957).

According to Kent (op. cit.) Hormuz salt plugs usually measure 3-11 km across, but the salt flow and mushrooming at the surface make it difficult to determine the diameter of the main salt cylinder. **Chah Benu** (55°00' E; 27°30' N), 70 km east of Lar, is one of the largest salt plugs, measuring 11 by 8 km, surrounded by low hills of Miocene and Pliocene rocks (Figs. 3.24 and 3.28). In some places the salt plugs form spectacular mountains rising up to 1220 m above the valley floor (Kent, op. cit.). The best known example of this is **Kuh-e Namak**, 113 Km east of Bushehr (Fig. 3.21).

The structural position of the Infracambrian Hormuz Salt plugs varies greatly within the Zagros Mountains. It has been suggested by Colman-Sadd (1978) that most salt diapirs pierce anticlines and occur on flanks, on crests, and at the plunging ends of anticlines because of the lower pressure in these areas. However, it has been pointed out by several workers that the diapirs are not always associated with anticlines (Harrison, 1930; Lees, 1931; Kent, 1970, 1979; De Jong, 1982). Some occur in synclines and others, for instance, the **Hasineh** and **Kuh-e Namak** diapirs (Figs. 3.21 and 3.24) are not in immediate proximity to any visible fold.

Inspection of the distribution of salt diapirs in the 'Fars Fold Zone' (Fig 3.24) confirms this view and it can be seen that the association of anticlines and diapirs is the exception rather than the rule. It is difficult to understand Colman-Sadd's statement that most salt plugs, pierce anticlines and it would seem that this statement reflects the ideas represented in Fig. 3.6 which show how he considers the folds and salt bodies to be related in profile. The more realistic profile shown in Fig. 3.24 shows that there is a much less intimate relationship between the salt and folds than is indicated in Fig. 3.6.

It can be seen that the salt horizon is situated at a depth of between 5 and 10 km below the folds and that many of the folds are related to thrusting. It is clear from this profile that the diapiric rise of salt, which was probably simulated by the tectonism which initiated the

thrusting and folding, would not generally be expected to pierce the anticlines and the lack of correspondence between the anticlines and the salt domes shown in Figs. 3.24, 3.28 and is compatible with this profile.

Indeed, there seems more evidence to support the association of faults and diapirs than folds and diapirs. As mentioned in the previous section salt extrusion in the Bakhtiari mountains forms '**narrow slivers**' up to 30 km long and approximately 1-3 km wide and are the result of salt intrusion largely along high-angle reverse dip-slip faults which extend parallel to the Zagros trend on and in front of the Zagros Thrust Zone (Figs. 3.21 and 3.23).

The distribution of the more equant salt intrusions shows that some of the salt diapirs are associated with movement on major basement strike-slip faults. For example, the marked alignment of salt intrusions along the faults can be clearly seen along the N-S trending dextral strike-slip faults within the Kazerun-Borazjan, Kareh Bas, Sarvestan fault zones as well as, the NE-SW trending sinistral strike-slip faults within the Bastak and Charak fault zones (Figs. 3.22 and 3.24).

Inspection of salt diapirs in association with the reverse dip-slip faults mentioned earlier shows that the intrusions occurred in the form of '**salt wall**' (Figs. 3.21 and 3.23) and it is interesting to speculate why the salt injection associated with the strike-slip faults has not formed similar structures rather than the discrete domes observed. It is suggested that this is probably because strike-slip motion along the fracture zones in the cover rocks, above the basement strike-slip faults is likely to generate important, **dilational jogs**, ideally suited for the intrusion of domes (Fig. 3.31). The five belts of diapirism associated with the mappable Kazerun-Borazjan, Kareh Bas, Sarvestan, Bastak, and Charak strike-slip fault zones mentioned above are immediately apparent.

In two aspects, the Persian salt plugs differ from examples in other countries. The first is

the rarity of peripheral upturning of the enclosing sediments. The other unusual feature is the absence of an annular syncline (or zone of subsidence) which is commonly recorded elsewhere in the world. It has been suggested that this may be ascribed to the mechanical properties of the country rocks, which are too strong to sag in a simple form, and also to the influence of lateral tectonic stress as well as hydrostatic pressure operating during the development of the plugs (Kent, 1958).

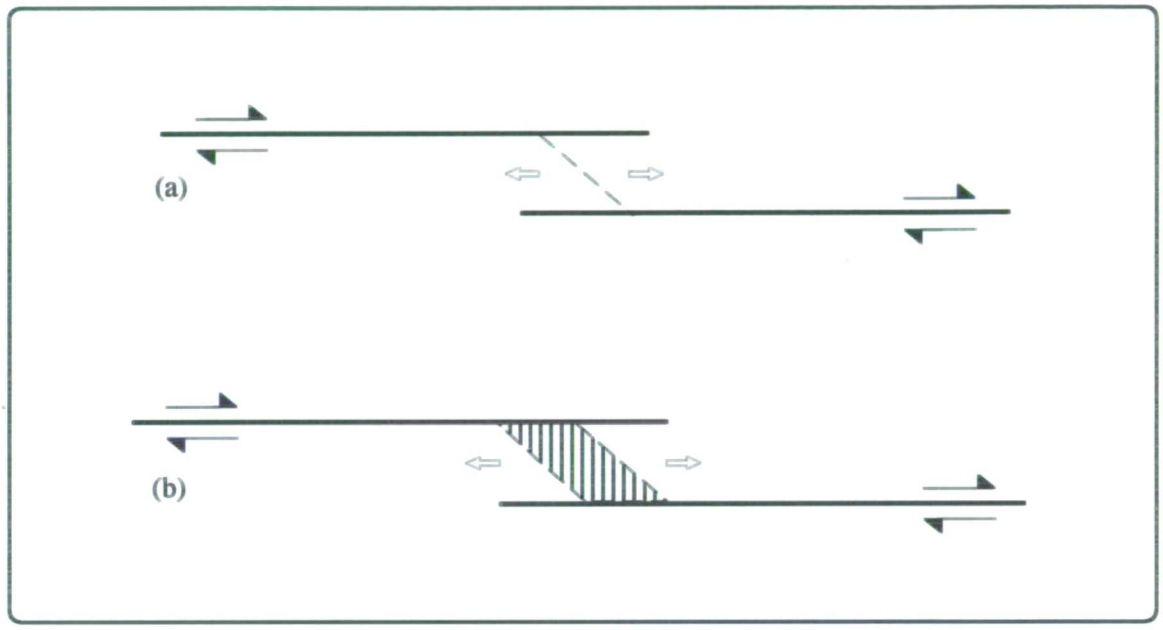


Fig. 3.31 Two stages in the development of a dilational jog in a relay area between two overlapping strike-slip faults. These jogs provide ideal sites for the initiation and intrusion of salt diapirs.

c) MECHANISM OF SALT DIAPIRISM IN THE ZAGROS MOUNTAIN BELT

A variety of suggestions have been made regarding the mechanism of injection of the Hormuz salt bodies. Harrison (1930, 1931) attributed **the initiation of the Hormuz salt rise** to the development of *irregularities* at the base of the sedimentary cover as a

consequence of folding. He pointed out that the flow of salt toward the anticlinal arches was encouraged by the growth of differential pressure resulting from the denudation of anticlines and deposition in adjacent synclines at the surface, which increased the sedimentary loading in the synclines. However, (as discussed briefly in the previous section) subsequent seismic profiles across the fold belt (Fig. 3.20) indicate that this model is naïve. Harrison recognised the inadequacy of this mechanism to explain the down-plunge or down-flank position of some of the domes, and postulated fault-controlled nuclei to account for those associated with synclines.

Many workers have attributed the surface distribution of the Hormuz salt plugs to basement fault pattern (Harrison, 1931; Ala, 1974; Kent, 1979). Some have argued that these faults affected the thickness of the evaporite itself or its local loading, controlling points of diapirism when the accumulating sedimentary column finally produced instability. Others, for example Koyi (1988) believe that the diapiric structures began to form prior to any movement along the basement faults.

Initiation of salt plug movement by igneous intrusive activity has been suggested by O'Brien (1957), who postulated that shrinkage of cracks following deep intrusion provided the first channels for upward penetration of salt. However, it was pointed out by Kent (1958) that most of the associated igneous rocks are extrusive and not intrusive. He envisaged a quite different role for volcanic activity, suggesting that 'buried topographical irregularities produced by degraded volcanic cones (probably Cambrian) could have localized and encouraged plug development when late tectonic or static loading initiated movement'.

The importance of temperature has been emphasised by Gussow (1966, 1968). He believed heat to be the *triggering mechanism*, and suggested that no flow takes place until the temperature rises to about 300°C, at which point 'the system suddenly becomes dynamic'.

Gussow further stated that even the glacier-like flow of salt at the surface took place when the salt was hot.

Ala (1974) finds this improbable. He believes that, although the Hormuz salt may have attained a temperature of 300°C at depth, it is unlikely that it could remain at this temperature during its slow rise to the surface through 6-9 km of sedimentary rock. Salt glaciers, on the contrary, show evidence of movement by solid creep.

There is a little doubt that in addition to temperature, one of the key factors that influences the mobility of salt is the thickness of the salt layer. It has been argued that at a temperature of 250-300°C salt cannot support a significant differential stress, so that the stresses in the salt are essentially hydrostatic. In order that salt may migrate laterally and so feed any salt pillow, wall, or plug, a horizontal hydrostatic gradient must be induced in the salt layer. This is most easily accomplished by a lateral variation in vertical loading on the salt layer, as indicated in Fig. 3.32.

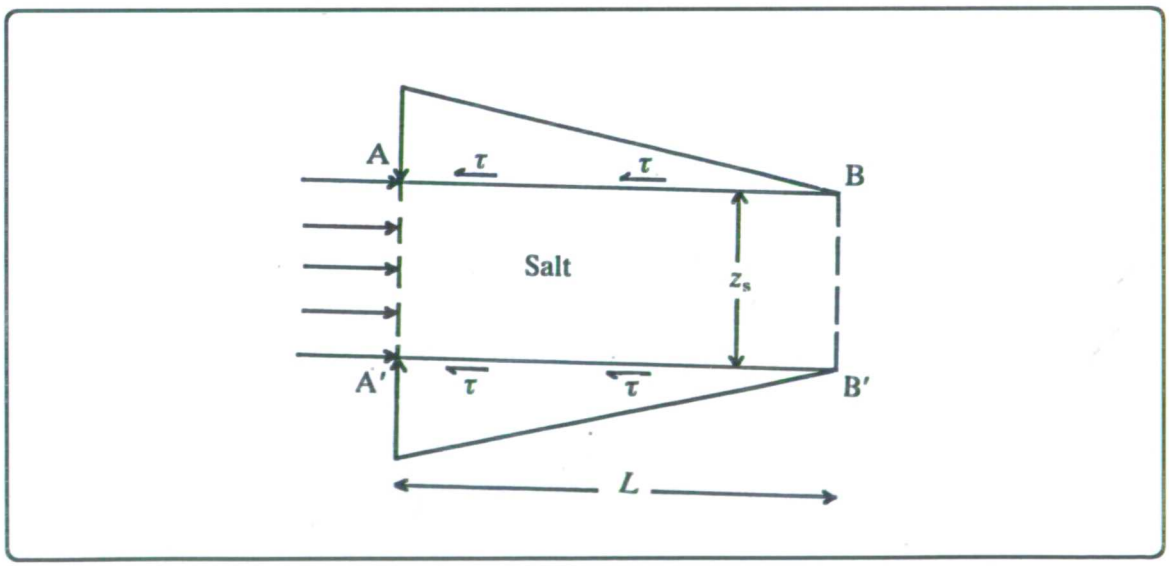


Fig. 3.32 Boundary stresses and fluid (Newtonian) flow between parallel layers see text for details (from Price & Cosgrove, 1990).

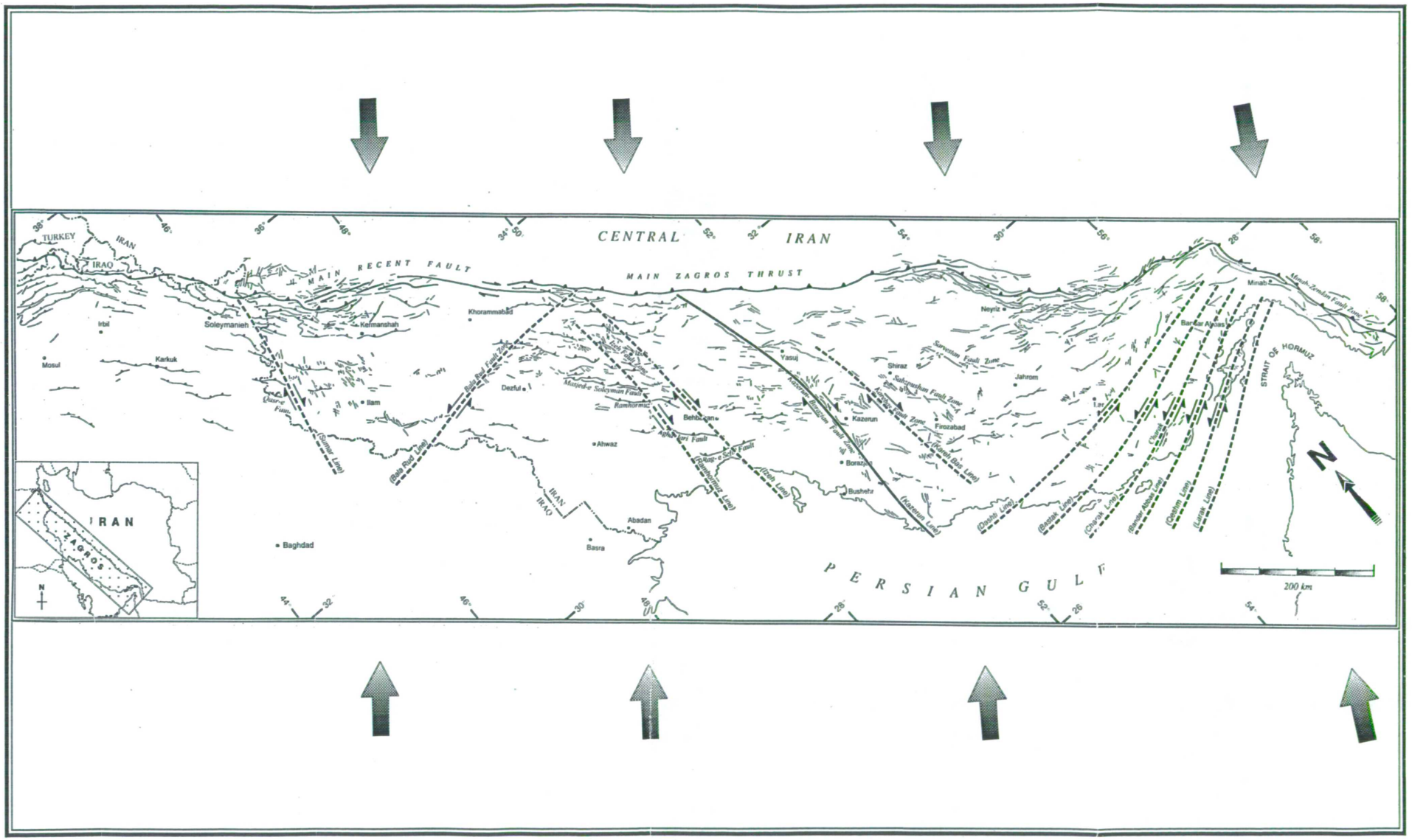


Fig. 3.27 The relationship between plate induced stresses (bold arrows) and the major known and inferred basement strike-slip faults.

Such lateral variations of loading may be induced by surface, or sub-surface topography, or lateral changes in density of the overlying sediments which result from facies changes or, of course, any combination of these factors. For simplicity, it as assumed in Fig. 3.32 that the change in vertical load varies in a linear fashion. This gives rise to a horizontal stress gradient which will tend to induce lateral migration of the salt. For equilibrium conditions, in Fig. 3.32, it follows that:

$$S_{ex} z_s = 2\tau L \tag{3.1}$$

where S_{ex} is the excess horizontal pressure acting at AA′, relative to BB′ and the linear dimensions z_s and L are as indicated. It can be shown that the average velocity (v_s) of salt, assuming it to be a Newtonian fluid, flowing between parallel planes, is:

$$v_s = \frac{\tau z_s^2}{k\eta} \tag{3.2}$$

where η is the coefficient of viscosity and k is a numerical constant (see Price and Cosgrove 1990, Chap. 3 for a fuller discussion). It follows from Eqs. (3.1) and (3.2):

$$v_s = \frac{S_{ex} z_s^3}{2\eta kL}. \tag{3.3}$$

The volume (Q) of salt that will migrate in planar flow, in a specific time, is:

$Q = v_s z_s$ so that

$$Q = \frac{S_{ex} z_s^4}{2\eta kL}. \tag{3.4}$$

That is, the mobility of a salt layer is related to the fourth power of its thickness. By using Eq. (3.4), with the data and conclusions related to the intrinsic mobility and realistic (low) values for S_{ex}, it can be shown that the salt layer needs to be of the order of 500 m thick before significant lateral migration can be achieved, even when the salt is at a temperature of 250°C. Hence, layers of salt which are only perhaps 100 m thick will not develop into salt domes. This finding is, of course, completely in keeping with the quantity of salt required to form an individual dome or plug and also their separation one from another (Price & Cosgrove, op. cit.).

The initiation of the Miocene, Gachsaran salt rise in the form of '*salt bulges*' and '*flow-sheets*', along the hinge zone of anticlines is attributed by O'Brien (1957) to the disharmonic folding of the overlying, 'Incompetent Group' of soft marls and sandstones of the Fars-Bakhtiari series, and that of the underlying, 'Competent Group' of limestones and shales which are caped with the Asmari limestone (Figs. 3.5, 3.30 and 3.33). According to O'Brien during the disharmonic folding the intervening, 'Upper Mobile Group' of Oligo-Miocene Lower Fars or Gachsaran salt and anhydrite deposits, flowed readily from zones of high pressure under the synclines to those of low pressure under anticlines and formed several salt bulges and flow sheets along the hinge zone of anticlines (Fig. 3.33).

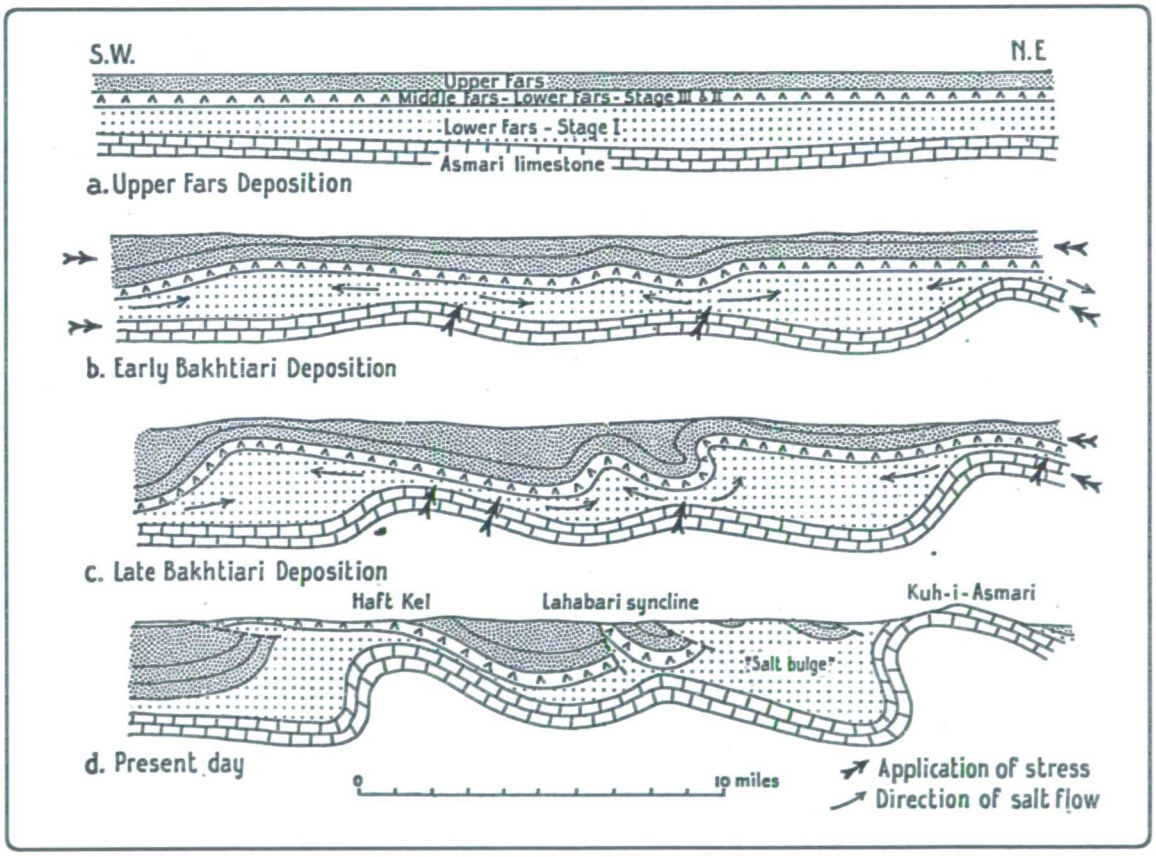


Fig. 3.33 The initiation and evolution of the Lower Fars (Miocene) Gachsaran salt diapirs in the form of 'salt bulges' and 'flow-sheets' in the Haft Kel area (see Fig. 3.21) as a result of disharmonic folding (see also Fig. 3.30) (from O'Brien, 1957).

CHAPTER 4

Geometrical analysis of the Zagros folds and sedimentary cover

1. INTRODUCTION

In order to study the geometrical characteristics of the Zagros folds in details and the variation in shortening of the whole sedimentary cover across the fold belt the following measurements were made along twenty one geological sections running approximately NE-SW across the belt (A-U, Fig. 4.1).

(i) The half-wavelength/amplitude ratio of the folds
(ii) The elevation of the median surface of the folds and
(iii) The percentage shortening of the sedimentary cover.

This study was carried out in an attempt to improve the understanding regarding the evolution of the '**Zagros deformation belt**' which is discussed in the following chapter. The results of this study are presented in both tabular and graphical format in the following sections of this chapter.

2. HALF-WAVELENGTH/AMPLITUDE RATIO OF THE FOLDS

To examine and compare the variation in fold growth along the various geological sections it was decided that, because of the variation in wavelength of the folds, the most suitable parameter to measure would be the half-wavelength/amplitude ratio.

The twenty one geological sections across the 'Zagors Mountain Belt' (Fig. 4.1) used in this study are those given in the portfolio published by British Petroleum Company (1956). Portions of eight of these sections are shown in Fig. 3.5.

a) TECHNIQUE OF MEASUREMENT

In order to measure the half-wavelength/amplitude ratio of the folds in these sections, the Lower/Middle Cretaceous contact was chosen as a **marker horizon** and copied onto tracing paper overlays. The position of the inflection points of each fold along the sections was then marked. The length of the folded marker horizon between two adjacent inflection points in each fold was measured as the **half-wavelength** (Fig. 4.2).

The amplitude of folds was measured by constructing a line parallel to the median surface of each fold (the straight line joining two adjacent inflection points) so as to touch the extremity of the fold and then the distance between the two lines was taken as the **amplitude** (Fig. 4.2). This enabled the ratio of half-wavelength and amplitude of the folds to be determined.

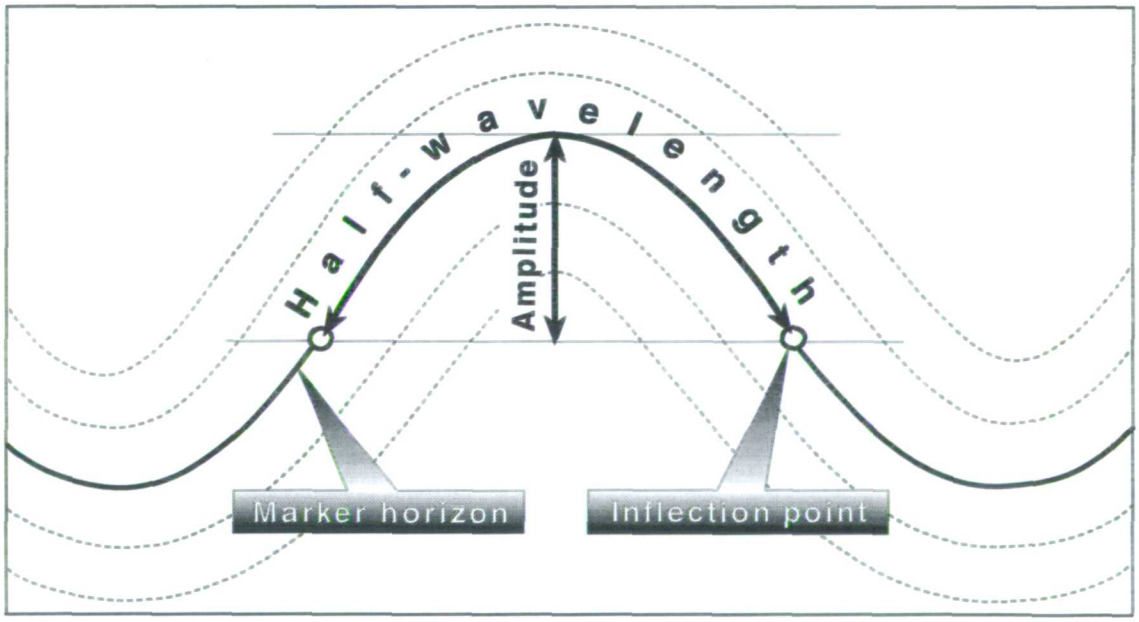


Fig. 4.2 The technique used for measuring the half-wavelength and amplitude of the Zagros folds.

In order to consider the variation in ratio in different areas, the 'Simply Folded Belt' which was already divided into 6 fold zones on the basis of morphological and structural characteristics (from NW to SE, the **Kordestan**, **Lorestan**, **Bakhtiari**, **Kohkiluyeh**, **Fars**, and **Minab** fold zones, respectively, Fig. 3.1) was subdivided again in **eleven, 20 km wide strips** parallel to the northeastern margin of the '**Simply Folded Belt**' (Fig. 4.3). It can be seen that non of the available sections fall into either the Kordestan or Minab fold zones. Consequently the analysis relates to the four central zones.

The average half-wavelength/amplitude ratio of all the individual folds within each strip was calculated for each geological section and the results are presented in the four tables shown in Figs. 4.4-4.7. Each table represents the results from the sections within a particular zone and the graph in each figure shows the average half-wavelength/amplitude ratio for each strip, for all the sections within that zone.

Finally these graphs showing the variation of half-wavelength/amplitude ratio across the fold belt in the four different zones, are combined into a single graph (Fig. 4.8) which gives the average variation across the whole fold belt.

b) RESULTS OF MEASUREMENT

The results of the measurements summarised in Figs. 4.4-4.7 show that the half-wavelength/amplitude ratio of the folds generally increase from NE to SW. This observations is compatible with the model of serial folding which argues that the folds are propagating from the NE to the SW away from the Main Zagros Thrust zone and into the relatively undeformed cover rocks of the Mesopotamian plains.

However, the variation of the half-wavelength/amplitude ratio across the belt is not uniform in the four structurally and morphologically different fold zones in which the measurements

were made (Fig. 4.1). This can be clearly seen in Fig. 4.9 which compares the variation of ratio across the fold zones.

The variation of the ratio across the 'Bakhtiari Fold Zone' (Fig. 4.1) is in particular, very different from the other three zones (Fig. 4.9). The profile gradient is much steeper in this fold zone and the fold belt is constrained to a much narrower band close to the northeastern margin of the 'Simply Folded Belt' (Figs. 3.1, 3.5 and 3.23).

It is argued that this fold distribution pattern is the result of the lack or reduced thickness of the main detachment horizon (i.e. the Hormuz Salt Formation) in the cover beneath the Dezful Embayment. This would create a strong resistance to the southwestward migrating detachment of the Zagros sedimentary sequence and would account for the localisation of intensive folding along the NE margin of the fold belt that characterise the higher Bakhtiari Mountains.

Section	strip 1 00-20	strip 2 20-40	strip 3 40-60	strip 4 60-80	strip 5 80-100	strip 6 100-120	strip 7 120-140	strip 8 140-160	strip 9 160-180	strip 10 180-200	strip 11 200-220
A		9.56	4.12	5.92	20.40						
B		7.61	5.67	6.12	6.75	7.12	11.71				
C	3.03	5.87	5.75	4.75	11.50	8.86	10.86				
D	5.53	5.62	5.74	12.71	15.70						
Average	**4.28**	**7.17**	**5.32**	**7.37**	**13.59**	**7.99**	**11.29**				

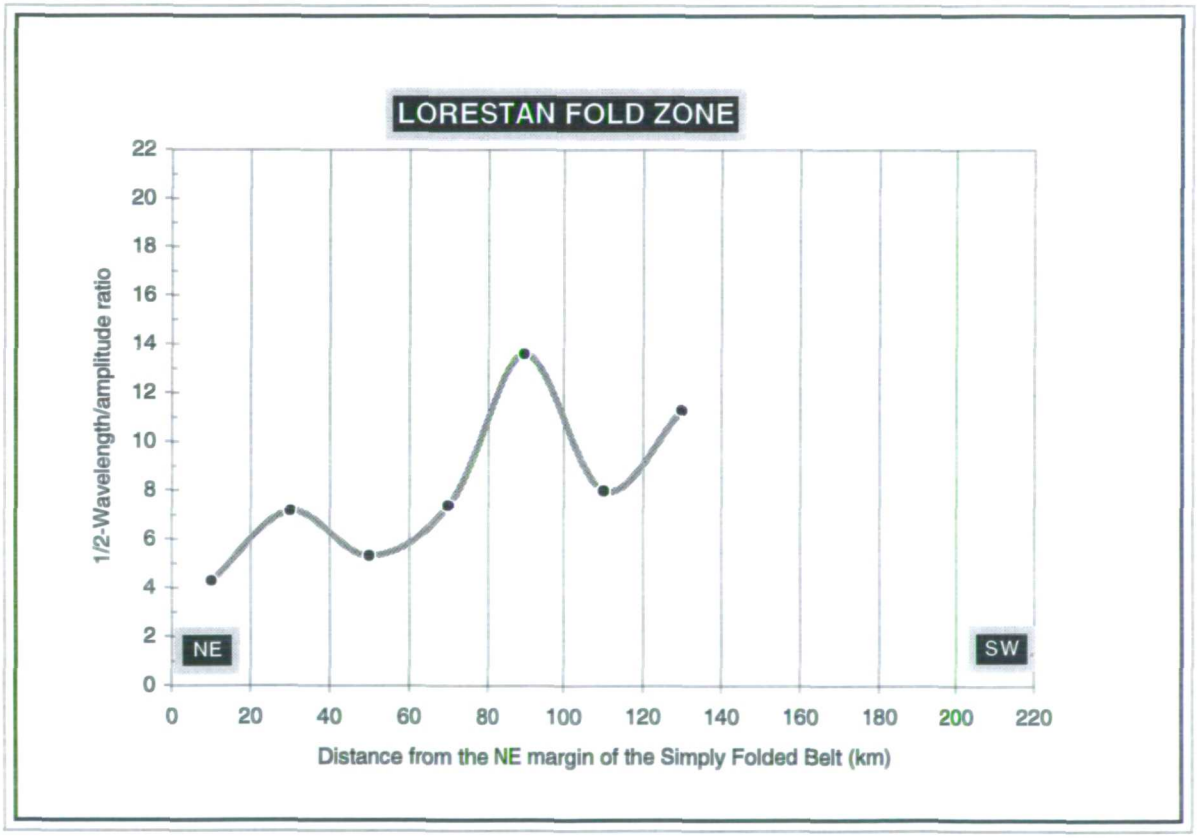


Fig. 4.4 The half-wavelength/amplitude ratio of folds within the 20 km strips parallel to the northeastern margin of the 'Simply Folded Belt' in the **Lorestan** fold zone.

Section	strip 1 00-20	strip 2 20-40	strip 3 40-60	strip 4 60-80	strip 5 80-100	strip 6 100-120	strip 7 120-140	strip 8 140-160	strip 9 160-180	strip 10 180-200	strip 11 200-220
E			3.65	6.75							
F	3.68	5.06	4.87	14.09							
G	4.82	7.72	5.15	13.16							
H		9.58	11.25	6.86							
I	4.58	5.33	8.19	5.26	10.68	18.73	22.00				
J	3.73	6.43	3.46	4.18	4.74	11.10					
Average	4.20	6.83	6.10	8.38	7.71	14.92	22.00				

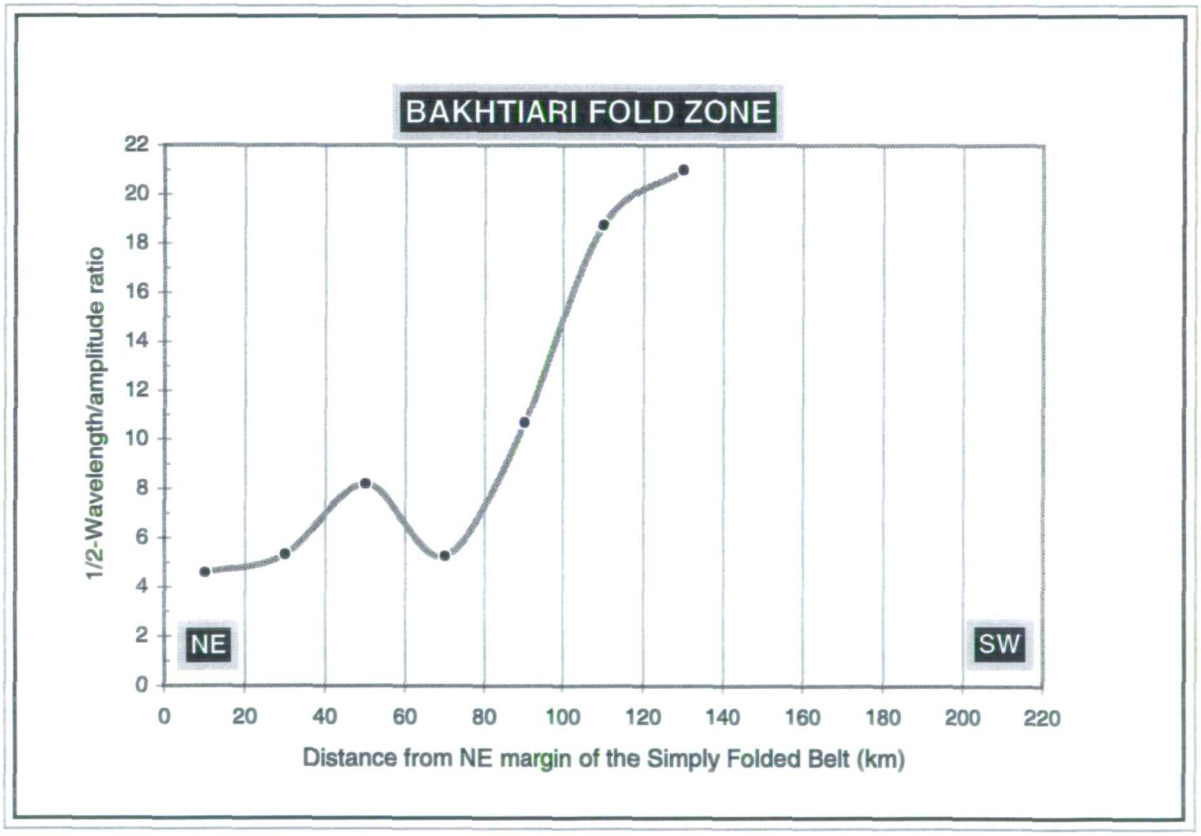


Fig. 4.5 The half-wavelength/amplitude ratio of folds within the 20 km strips parallel to the northeastern margin of the 'Simply Folded Belt' in the **Bakhtiari** fold zone.

Section	strip 1 00-20	strip 2 20-40	strip 3 40-60	strip 4 60-80	strip 5 80-100	strip 6 100-120	strip 7 120-140	strip 8 140-160	strip 9 160-180	strip 10 180-200	strip 11 200-220
K	7.36	5.88	4.44	4.95	6.09	5.77	6.20	10.22			
L	5.00	5.83	5.50	5.88	9.40	8.23	7.12				
M	6.96	6.76	6.94	4.96	7.41						
N		4.44	5.73	4.65	5.61	7.69					
Average	**6.44**	**5.73**	**5.65**	**5.11**	**7.13**	**7.23**	**6.66**	**10.22**			

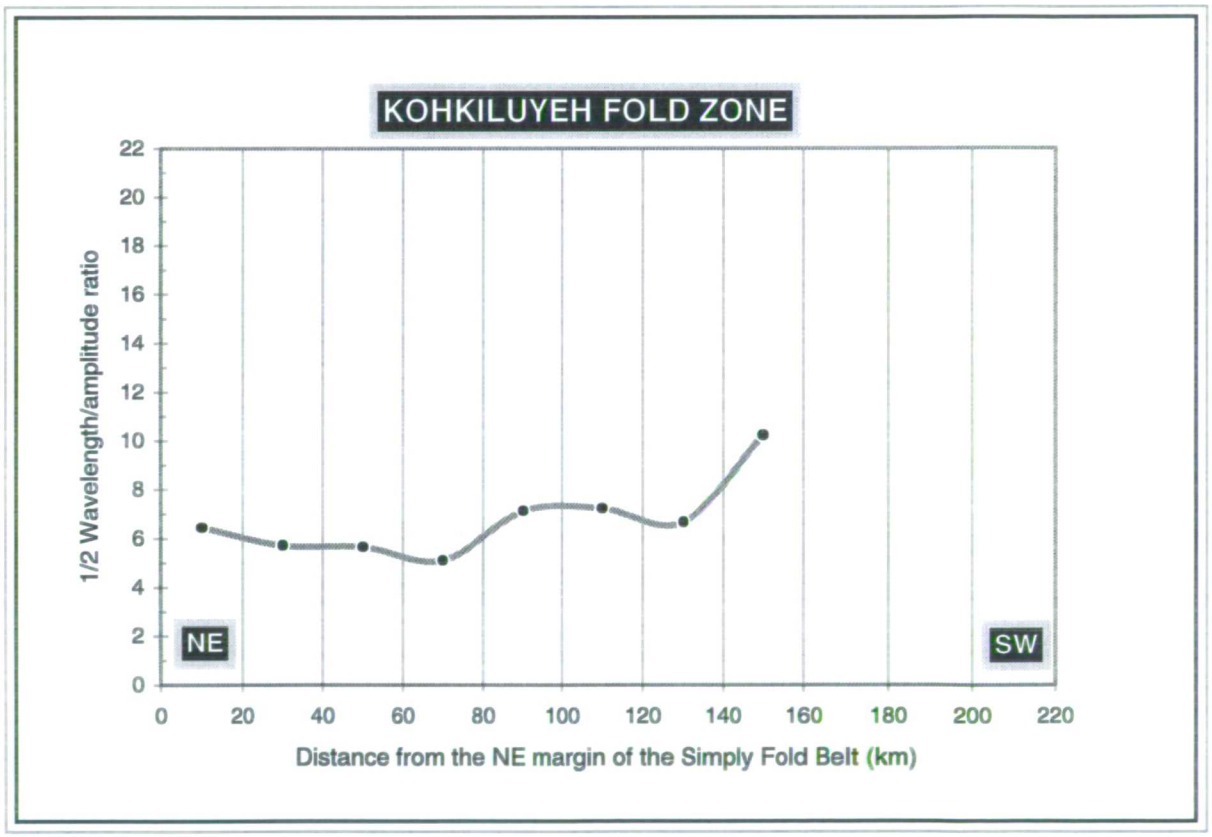


Fig. 4.6 The half-wavelength/amplitude ratio of folds within the 20 km strips parallel to the northeastern margin of the 'Simply Folded Belt' in the **Kohkiluyeh** fold zone.

Section	strip 1 00-20	strip 2 20-40	strip 3 40-60	strip 4 60-80	strip 5 80-100	strip 6 100-120	strip 7 120-140	strip 8 140-160	strip 9 160-180	strip 10 180-200	strip 11 200-220
O	4.15	6.19	9.43	6.99	6.27	5.42					
P	5.37	6.04	4.62	6.61	5.85	7.25	9.11	5.40	6.57	14.83	
Q	4.35	11.95	4.15	4.67	5.12	4.19	6.32	9.00	6.25	6.88	30.67
R	3.47	4.11	4.85	4.02	7.28	8.63	10.13	9.46	5.77	8.88	
S	5.95	5.89	4.68	4.68	11.08	3.23	4.45	7.67			
T	5.36	4.46	6.40	8.39	8.05	15.58	6.39	11.11			
U	7.33	4.36	3.04	4.74	7.36	5.23	7.20	6.00			
Average	**5.14**	**6.14**	**5.31**	**5.73**	**7.29**	**7.08**	**7.27**	**8.11**	**6.20**	**10.20**	

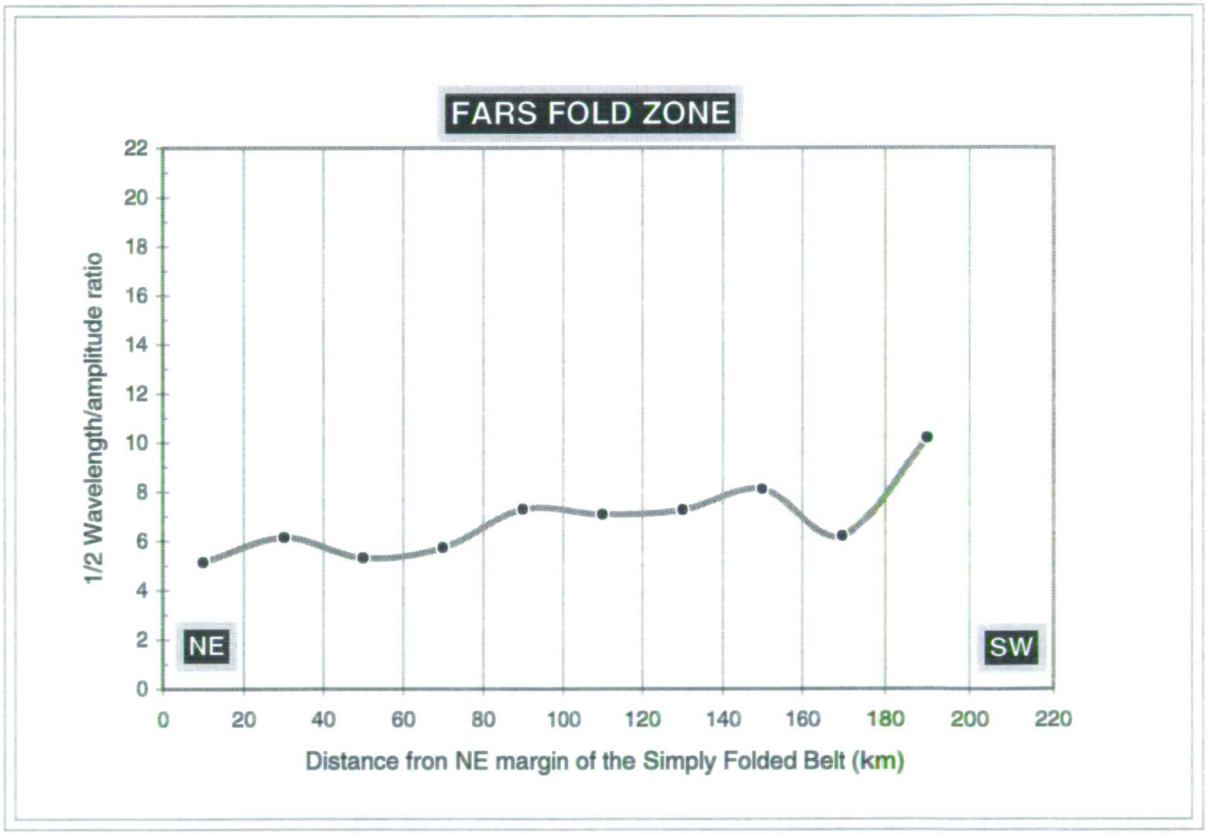


Fig. 4.7 The half-wavelength/amplitude ratio of folds within the 20 km strips parallel to the northeastern margin of the 'Simply Folded Belt' in the **Fars** fold zone.

Section	strip 1 00-20	strip 2 20-40	strip 3 40-60	strip 4 60-80	strip 5 80-100	strip 6 100-120	strip 7 120-140	strip 8 140-160	strip 9 160-180	strip 10 180-200	strip 11 200-220
Lor.	4.15	6.19	9.43	6.99	6.27	5.42					
Bak.	5.37	6.04	4.62	6.61	5.85	7.25	9.11	5.40	6.57	14.83	
Koh.	4.35	11.95	4.15	4.67	5.12	4.19	6.32	9.00	6.25	6.88	
Far.	3.47	4.11	4.85	4.02	7.28	8.63	10.13	9.46	5.77	8.88	
Average	5.04	6.43	5.60	6.68	8.78	8.36	9.14	8.41	6.20	10.20	

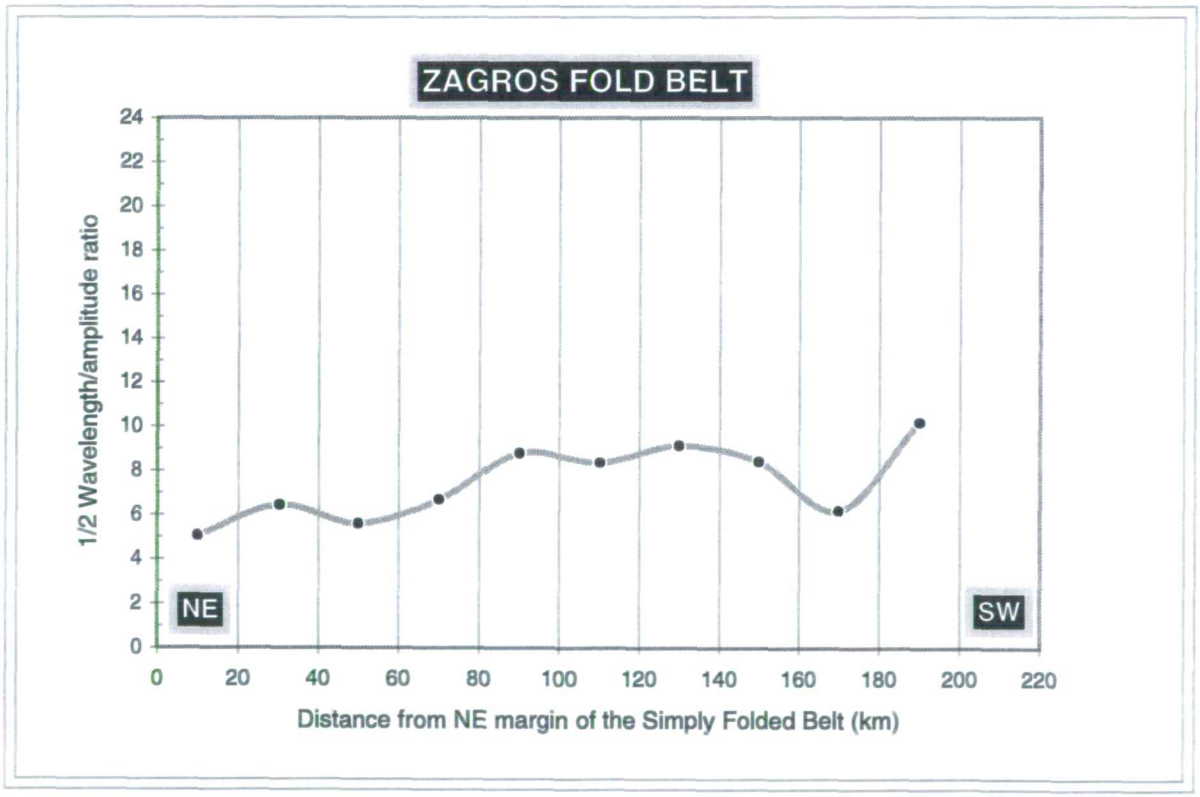


Fig. 4.8 The average half-wavelength/amplitude ratio of folds within the 20 km strips parallel to the northeastern margin of the 'Simply Folded Belt' in **the whole belt**.

3. ELEVATION AND INCLINATION OF THE MEDIAN SURFACE OF THE FOLDS

As noted earlier, the Zagros mountains as a whole have an asymmetric southwestward dipping topography. However, the gradient of topographic slope is not uniform along and across the mountain belt. There are several major culminations and depressions in different parts of the belt.

In order to investigate the origin of this complex topography and examine the effect of folding and warping of the whole Zagros sedimentary cover in the creation of the present topography and finally to understand its implications regarding the evolution of the Zagros deformation belt, a study of the elevation and inclination of the median surface of the folds in different parts of the Simply Folded Belt was carried out using the same geological sections used for determining the variation in half-wavelength/amplitude ratio across the belt (Figs. 4.3-4.7).

a) TECHNIQUE OF MEASUREMENT

As with the analysis of the half-wavelength/amplitude ratio of the folds, described in the previous section, the marker horizon chosen to carry out this median surface analysis was the Lower/Middle Cretaceous contact. The marker horizon was copied onto tracing paper for all 21 sections across the 'Simply Folded Belt'.

The inflection points of every fold along each section were then marked and their elevation from sea level and distance from the northeastern margin of the 'Simply Folded Belt' (Fig. 4.1) were measured. As in the previous section on half-wavelength/amplitude variation across the Simply Folded Belt, the data on the median surface variation has also been

subdivided into the four fold zones namely the Lorestan, Bakhtiari, Kohkiluyeh, and Fars. The average elevation of the inflection points within the 20 km wide strips, parallel to the northeastern margin of the Simply Folded Belt was then calculated.

Figs. 4.10-4.13 show the results of these measurements in tables and graphic form. Each table gives the results of the average elevation of the median surface within the 20 km wide segment along each individual cross-sections and the average for each fold zone. The graphs show the average elevation of the median surface for each strips for all the sections within that zone. Fig 4.14 summarise all these results and represents the average variation of the elevation of the median surface across the fold belt within the four fold zones.

In an attempt to illustrate the regional geometry of the median surface of the folds in three dimension, the elevation of the inflection points of the folds along the twenty one geological sections and their distance from the northeastern margin of the Simply Folded Belt together with their geographical coordinates were determined and plotted (Fig. 4.15).

b) RESULTS OF MEASUREMENT

The results of the measurements of the median surface are summarised in Figs. 4.10-4.13. As can be seen from these figures the median surface of the Zagros folds in general dips towards the southwest. However, it is not uniform in the four different fold zones along the belt (Fig. 4.14).

It can be seen that the most remarkable and sharp decrease in the inclination of the median surface of the folds is seen in the 'Bakhtiari Fold Zone' where the Middle Cretaceous/Upper Cretaceous marker horizon which has an elevation of over 2 km at the northeast margin of the Simply Folded Belt, drops below sea level at about 40 km from this margin. In contrast, in the neighbouring Lorestan and Kohkiluyeh fold zones, the elevation of the median

surface does not reach an elevation of 2 km and does not fall below sea level until it is about 100 km from the northeastern margin of the Simply Folded Belt.

The elevation of the median surface of the folds in the 'Fars Fold Zone' is very different to that of the folds in the other zones (Fig. 4.14). The marker horizon in the Fars Fold Zone is *below sea level* near the northeastern margin of the Simply Folded Belt. It rise above sea level at a distance of 40 km from the northeastern margin of the 'Simply Folded Belt' and drops below it again at 70 km. The gradient of the median surface of the folds in this zone is considerably lower than in the 'Bakhtiari Fold Zone', but approximately the same as that in the other zones.

The anomalous rise in the median surface elevation in the extreme southwest of the section (Fig. 4.13) that can be seen in the 'Fars Fold Zone' is the result of the emergence of Qeshm Island (Fig. 4.3).

Finally, as it is clear from the above results (see e.g. Fig. 4.16) that the present asymmetric and complex topography of the Zagros mountains is absolutely compatible with the geometry of the median surface of the Zagros folds which has been examined along a marker horizon within the sedimentary cover, quite deep below the earth surface.

This clear compatibility between the geometry of the median surface of the folds and the surface topography implies that the present asymmetric and complex topography of the Zagros mountain belt is a direct product of both folding and warping of the whole sedimentary cover and that its major culminations and depressions such as the Bakhtiari mountains culmination and the Shiraz-Neyriz depression have an internal and structural origin.



Fig. 4.1 The location of 21 geological sections (A-U) from British Petroleum Company Limited (1956) used by the present author for the geometrical analysis of the Zagros folds, determining of the elevation of the median surface of the folds and variation in shortening of the sedimentary cover across the belt.

Sections	Strip 1 00-20	Strip 2 20-40	Strip 3 40-60	Strip 4 60-80	Strip 5 80-100	Strip 6 100-120	Strip 7 120-140	Strip 8 140-160	Strip 9 160-180	Strip 10 180-200	Strip 11 200-220
A	1.65	1.84	0.48	0.25	-0.76	-1.78					
B	1.52	1.38	1.38	0.51	1.56	0.51	-0.76				
C	2.29	1.88	1.27	0.59	0.21	0.97	-0.25	0.00			
D	1.80	1.43	0.64	0.38	0.16	-2.03					
Average	**1.82**	**1.63**	**0.94**	**0.43**	**0.29**	**-0.58**	**-0.51**	**0.00**			

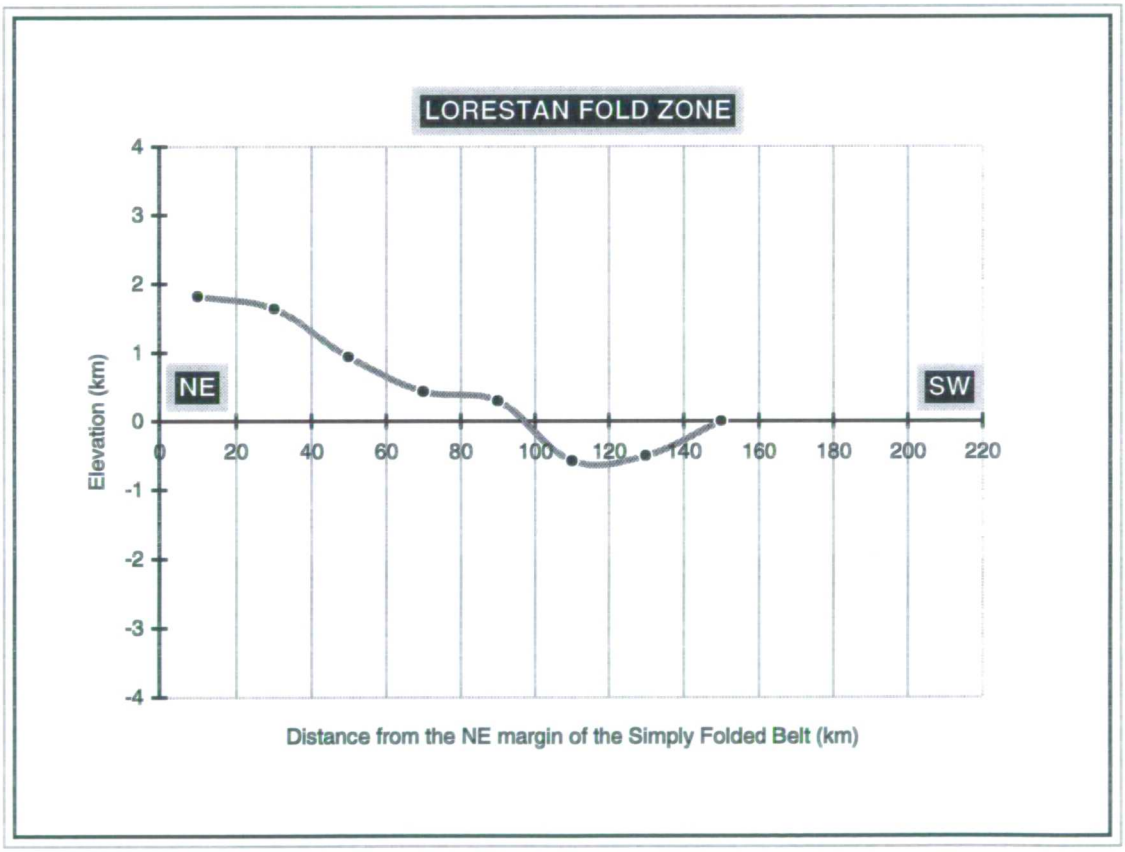


Fig. 4.10 The elevation and inclination of the median surface of the Zagros folds within the 20 km wide strips parallel to the northeastern margin of the 'Simply Folded Belt' in the **Lorestan** fold zone.

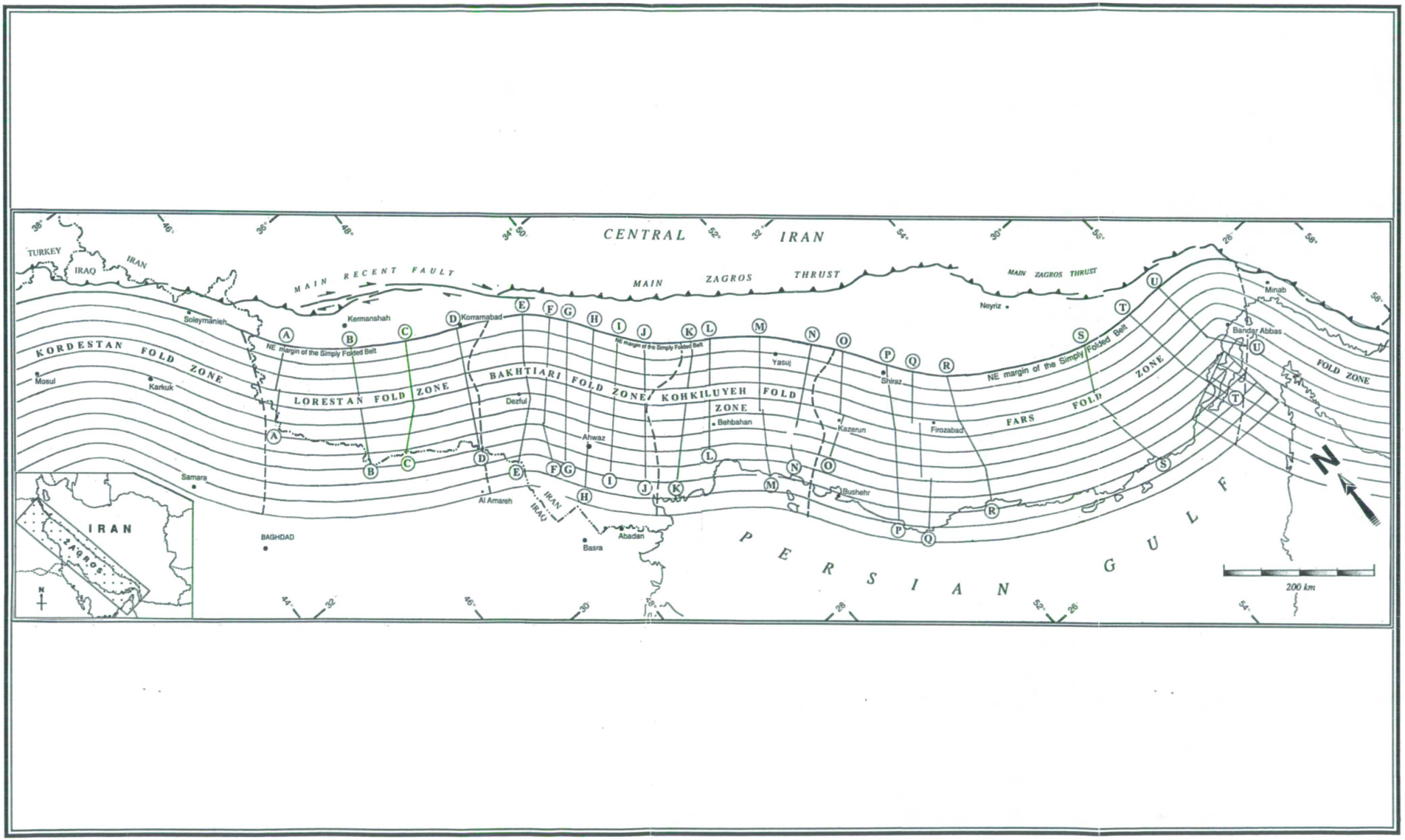


Fig. 4.3 The morphologically and structurally contrasting fold zones and eleven, 20 km wide strips parallel to the northeastern margin of the 'Simply Folded Belt'.

Section	Strip 1 00-20	Strip 2 20-40	Strip 3 40-60	Strip 4 60-80	Strip 5 80-100	Strip 6 100-120	Strip 7 120-140	Strip 8 140-160	Strip 9 160-180	Strip 10 180-200	Strip 11 200-220
E			0.42	-0.99							
F	3.23	3.37	-0.13	-4.45	-4.32						
G	2.17	3.13	0.80	-5.08	-4.32						
H	0.86	-1.05	-2.54	-3.46	-5.08						
I	1.98	1.14	-3.81	-2.79	-2.29	-2.54					
J	2.22	0.64	-0.40		-1.91	-5.08					
Average	**2.09**	**1.45**	**-0.94**	**-3.35**	**-3.58**	**-3.81**					

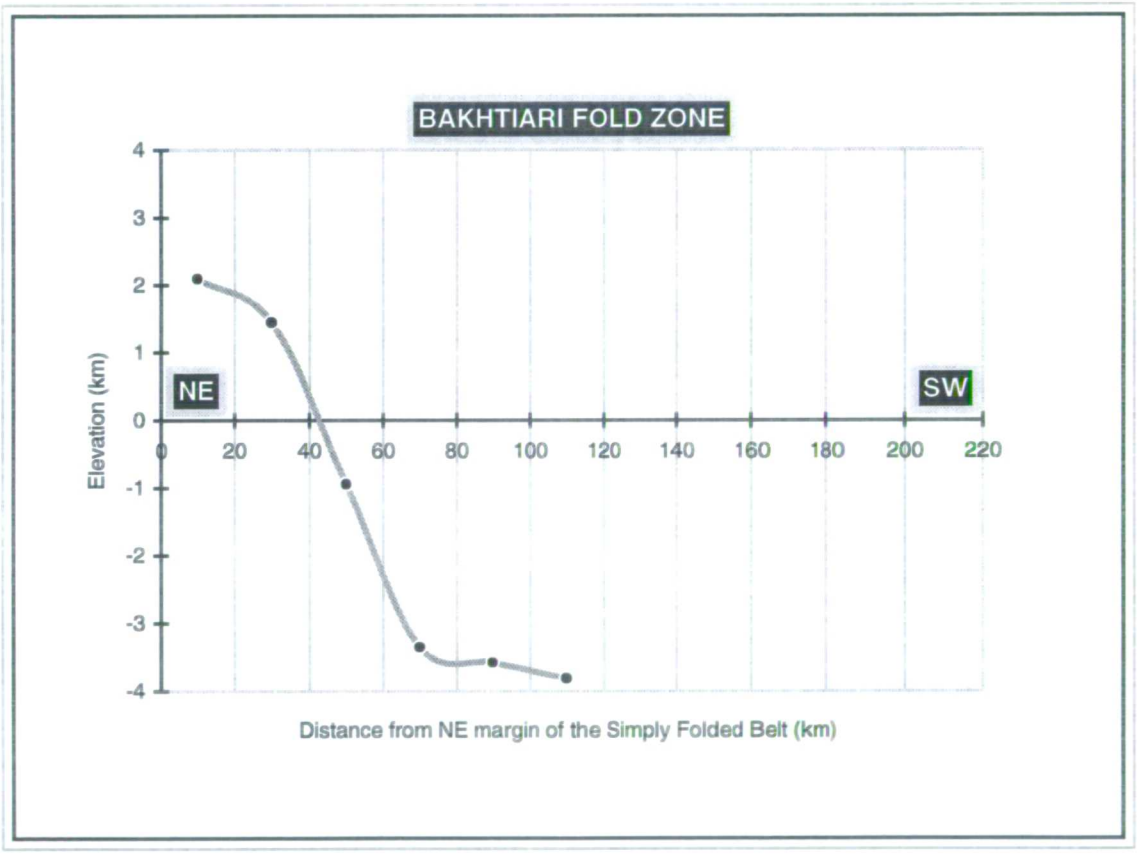


Fig. 4.11 The elevation and inclination of the median surface of the Zagros folds within the 20 km wide strips parallel to the northeastern margin of the 'Simply Folded Belt' in the **Bakhtiari** fold zone.

Section	Strip 1 00-20	Strip 2 20-40	Strip 3 40-60	Strip 4 60-80	Strip 5 80-100	Strip 6 100-120	Strip 7 120-140	Strip 8 140-160	Strip 9 160-180	Strip 10 180-200	Strip 11 200-220
K	-0.30	0.97	2.06	2.06	1.84	-1.91	-1.54		-3.81		
L	2.00	1.29	2.57	-0.15	-2.37	0.00	-2.29	-3.05			
M	0.16	0.40	1.37	2.25	1.40	-1.91					
N		1.63	1.44	1.52	-0.80	-0.59	-1.14				
Average	**0.62**	**1.07**	**1.86**	**1.42**	**0.02**	**-1.10**	**-1.66**	**-3.05**	**-3.81**		

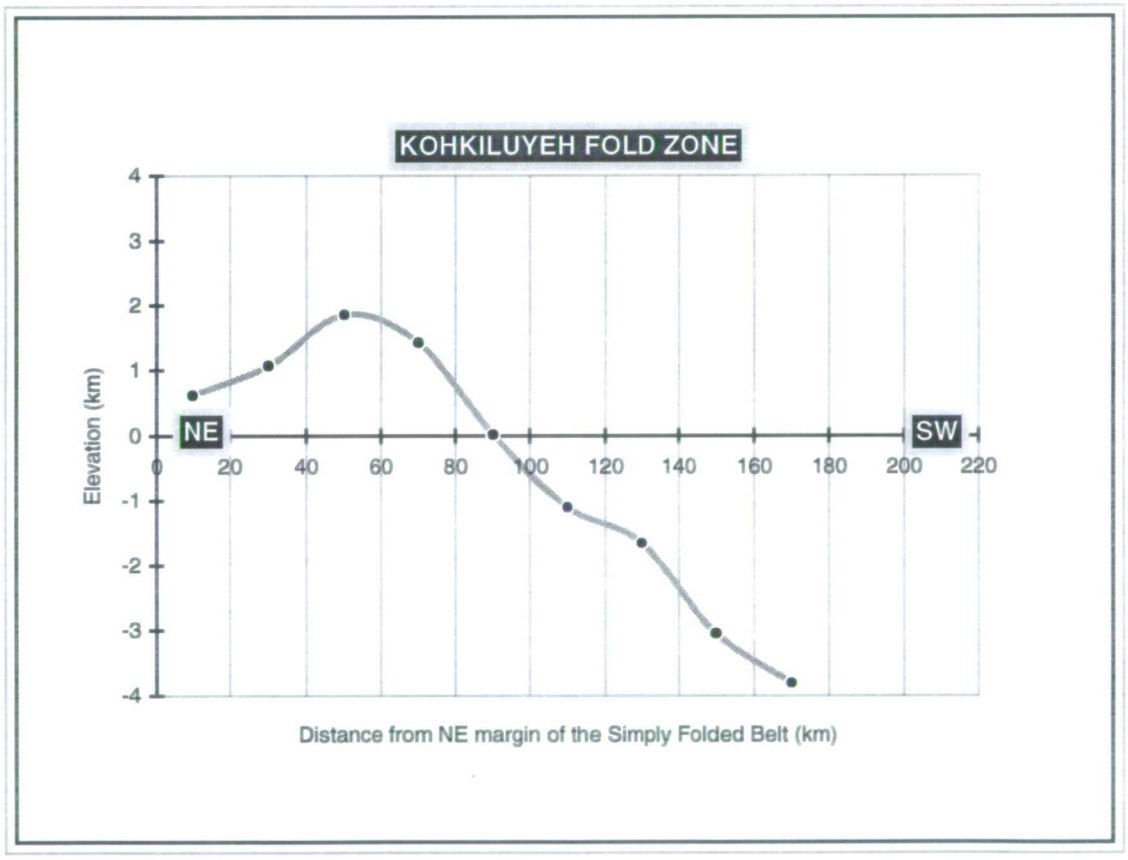


Fig. 4.12 The elevation and inclination of the median surface of the Zagros folds within the 20 km wide strips parallel to the northeastern margin of the 'Simply Folded Belt' in the **Kohkiluyeh** fold zone.

Sections	Strip 1 00-20	Strip 2 20-40	Strip 3 40-60	Strip 4 60-80	Strip 5 80-100	Strip 6 100-120	Strip 7 120-140	Strip 8 140-160	Strip 9 160-180	Strip 10 180-200	Strip 11 200-220
O	2.57	1.22	1.61	1.57	0.00	-2.24	-2.92				
P	0.24	-0.64	0.97	1.11	-0.93	-0.51	-1.12	-2.16	-0.06	-0.35	-2.79
Q	0.43	1.08	0.53	0.19	1.09	0.05	-0.51	-2.54	0.02	-0.93	
R	-0.20	-0.51	0.76	0.38	0.76						
S	-1.91	-1.02	-1.40	0.35	-0.54	-0.54	-0.38	-1.81	-1.33	2.79	
T	-1.91	-0.64	-0.34	-1.49	-2.62	-3.47	-2.29	-1.27	-3.81		
U	0.64	-1.61	0.00	-2.41	-2.54	-1.27	-2.54	-2.92			
Average	**-0.45**	**-0.30**	**0.31**	**-0.04**	**-0.68**	**-1.33**	**-1.63**	**-2.14**	**-1.30**	**0.50**	**-2.79**

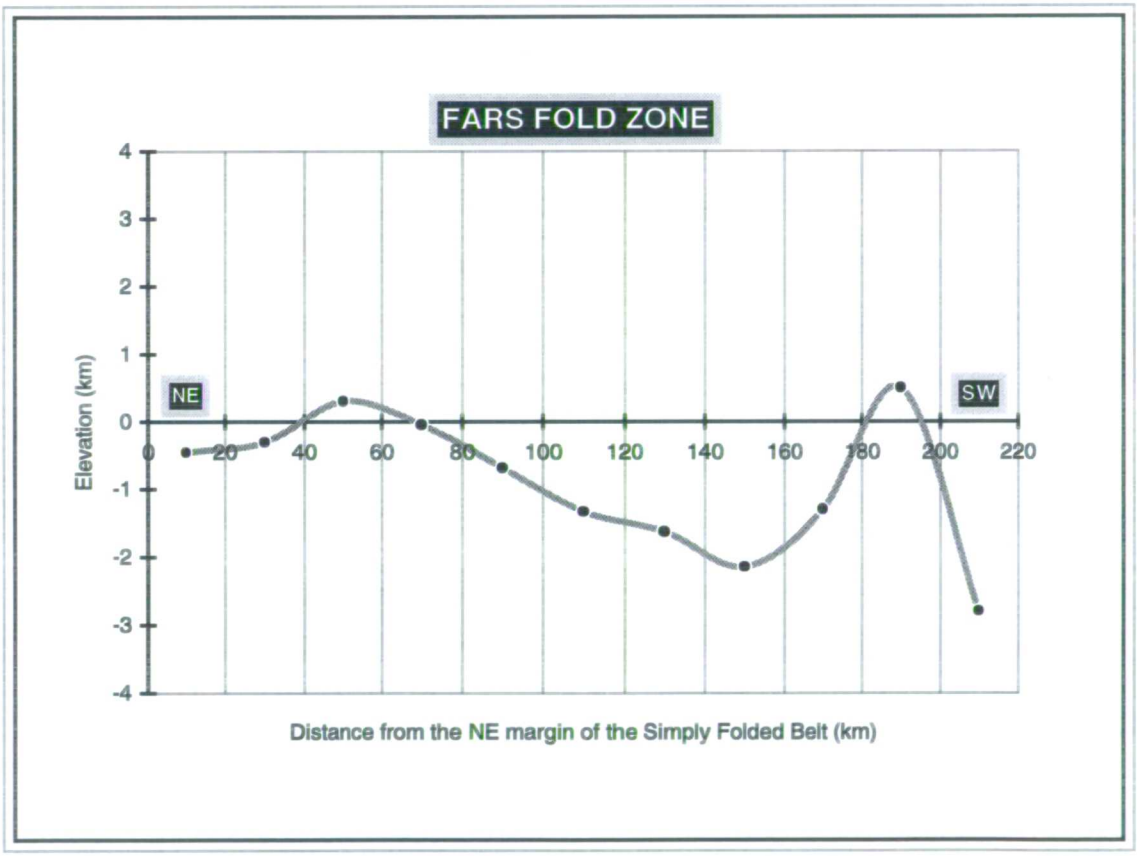


Fig. 4.13 The elevation and inclination of the median surface of the Zagros folds within the 20 km wide strips parallel to the northeastern margin of the 'Simply Folded Belt' in the **Fars** fold zone.

Zones	Strip 1 00-20	Strip 2 20-40	Strip 3 40-60	Strip 4 60-80	Strip 5 80-100	Strip 6 100-120	Strip 7 120-140	Strip 8 140-160	Strip 9 160-180	Strip 10 180-200	Strip 11 200-220
Lorestan	1.82	1.63	0.94	0.43	0.29	-0.58	-0.51	0.00			
Bakhtiari	2.09	1.45	-0.94	-3.35	-3.58	-3.81					
Kohkiluyeh	0.62	1.07	1.86	1.42	0.02	-1.10	-1.66	-3.05	-3.81		
Fars	-0.45	-0.30	0.31	-0.04	-0.68	-1.33	-1.63	-2.14	-1.30		
Average	**1.02**	**0.96**	**0.54**	**-0.39**	**-0.99**	**-1.71**	**-1.27**	**-1.73**	**-2.55**		

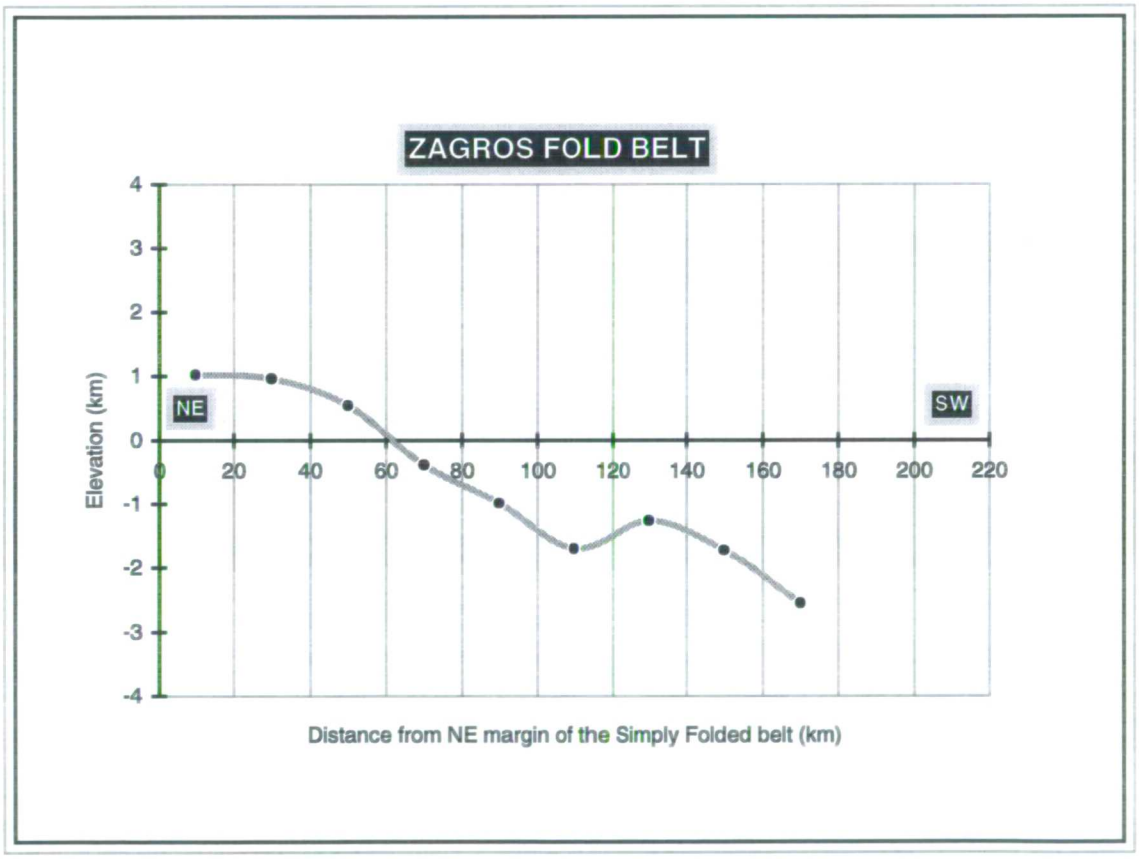


Fig. 4.14 The elevation and inclination of the median surface of the Zagros folds within the 20 km wide strips parallel to the northeastern margin of the 'Simply Folded Belt' in the **whole Zagros belt**.

4. SHORTENING OF THE SEDIMENTARY COVER

In order to examine the direction and variation in shortening of the Zagros sedimentary cover and to understand its implication to the evolution of the 'Zagros Fold Belt' it was decided to measure the percentage shortening of the sedimentary cover in different parts of the Simply Folded Belt.

As with the analysis of the half-wavelength/amplitude ratio and the median surface of the folds described in the previous sections, the geological sections prepared by British Petroleum Company (1956) were used as the database for determining the variation in shortening across the 'Simply Folded Belt'. Portions of these geological sections are shown in Fig. 3.5.

a) TECHNIQUE OF MEASUREMENT

The 'Line Length Balanced Technique' which is based on the 'Balanced Section Construction Technique' was used to measure shortening. The technique is particularly appropriate for the study area as many aspects of the balanced section methodology have been developed in geometric situations characteristic of the marginal regions of orogenic zones, an environment where a relatively thin sequence of continental shelf sediments originally deposited on a continental type basement of crystalline gneisses and igneous rocks has been deformed by horizontal shortening as a result of plate collision. In such regions the basement is often very competent compared to the overlying sediments and the cover is often mechanically detached from the basement along a décollement fault and involved in complex faulting and folding of a style not shared by the underlying crystalline basement. Such deformation is known as '**thin-skinned tectonics**' (Ramsay and Huber, 1987).

In regions of thin-skinned tectonics deformation by thrust faulting often tends to predominate over other styles, these thrusts are usually associated with local accommodation of deformation by the development of kink folds and box folds formed when the layers are transported over underlying ramp-flat surfaces. These special type of folds have been termed 'fault-bend folds' and 'fault propagation folds' (Fig. 4.17) (Suppe, 1983, 1985). The finite strain within these folds is not usually very high, and generally occurs by localized or diffuse layer parallel simple shear.

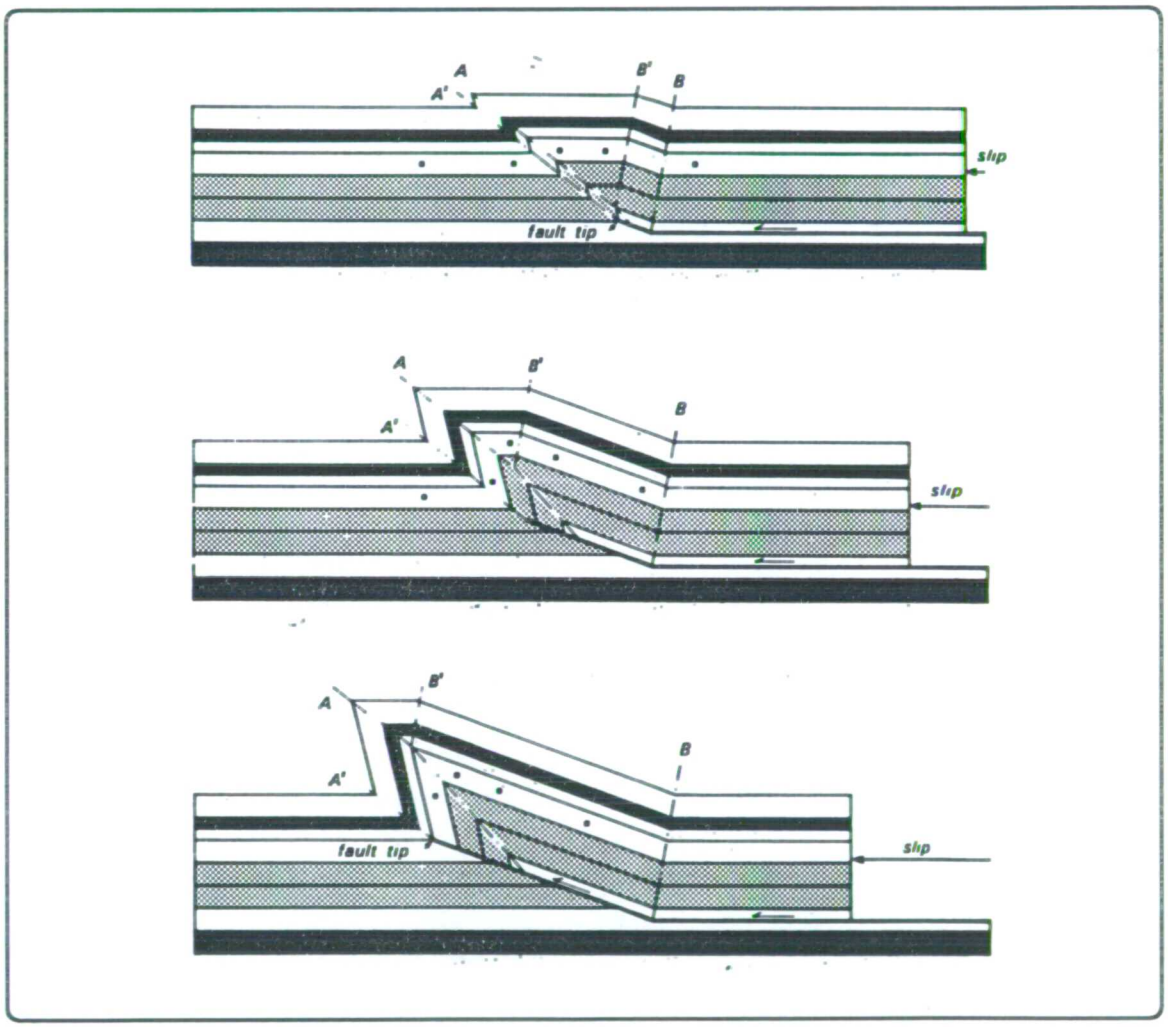


Fig. 4.17 Schematic progressive development of a fault-propagation fold at the tip of a thrust fault (from Suppe, 1985).

In such deformation the bedding surface coincides with the surface of no finite longitudinal strain of the strain ellipsoid. Profile sections through the folds will therefore show no change of bed length from that of the original bed length and, because simple shear is a plane strain deformation, the area of cross sections of the original layer will remain unchanged. The first of these geometric constraints leads to a technique known as 'Line Length Balancing' which relies on the fact that bed lengths of different layers between original fixed vertical reference lines, or pin lines, should be equal (Fig. 4.18).

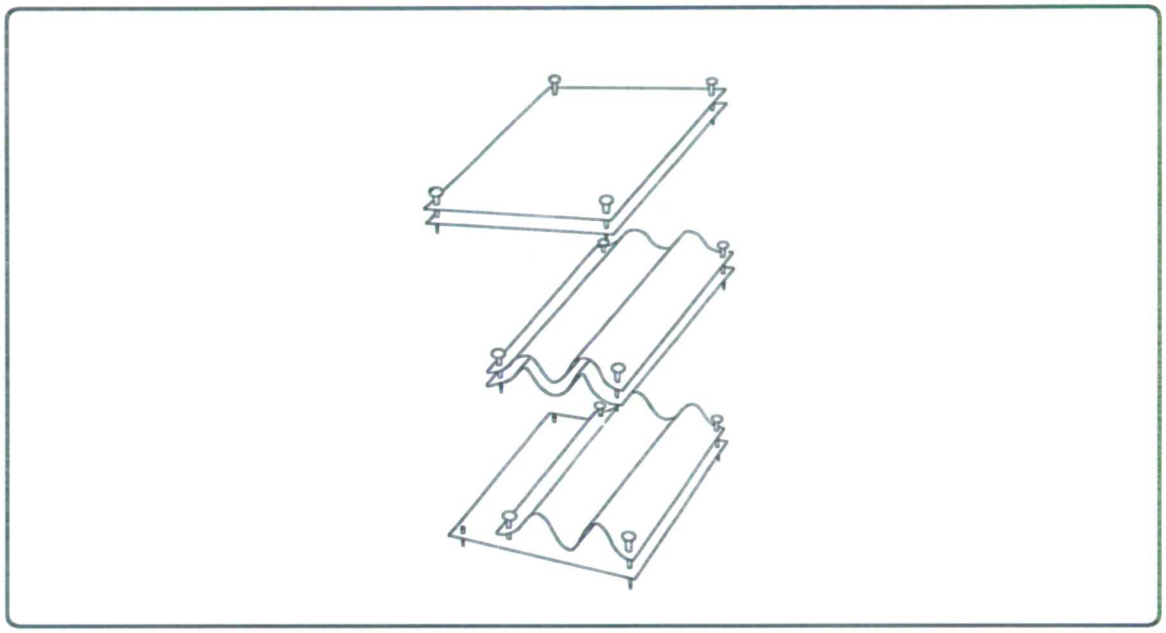


Fig. 4.18 Illustration of pin lines and the concept of constant bed length between pin lines. See text (from Dahlstrom, 1969).

As with the analysis of the half-wavelength/amplitude ratio and the median surface of the folds, the percentage shortening in different parts of the 'Simply Folded Belt was measured within the **eleven, 20 km wide strips** parallel to the northeastern margin of the belt. The northeastern margin of the 'Simply Folded Belt' was chosen as a pin point and percentage shortening was measured along the 21 geological sections (Fig. 4.3).

To determine the variation of shortening at different depths in the sedimentary cover, three marker horizons were selected; two from the 'Competent Group' (Fig. 2.16); the Jurassic/Lower Cretaceous contact, and the Middle Cretaceous/Upper Cretaceous contact, and one from the 'Incompetent Group', the Middle Fars/Upper Fars (Miocene) contact.

In order to determine the percentage shortening, a piece of soft, flexible and unstretchable telephone wire of (0.5 mm diameter) was laid down over each marker horizon within each of the 20 km wide strips and the length of the straightened wire was recorded and used to calculate the percentage shortening using the equation:

$$(L_0 - L_1) \times 100/L_1 = \% \text{ Shortening}$$

where L_0 is the original length of the marker horizon and L_1 its present length of 20 km. The shortening across the 20 km strips was calculated for three marker horizons in each geological section and the results presented in the five tables (Tables 4.1-4.5).

Tables 4.1-4.4 give the results for the geological sections in the four fold zones (Lorestan, Bakhtiari, Kohkiluyeh, and Fars), and table 4.5 gives the average shortening within each 20 km wide strip for the sections within all four fold zones.

The graphs in Figs. 4.19-4.22 show the average shortening of the three marker horizons across each 20 km wide strip for all the geological sections within each fold zone, and Fig. 4.23 summarises all these results and represents the average variation of the shortening within the four fold zones.

b) RESULTS OF MEASUREMENT

Inspection of the graphs in Figs. 4.19-4.23 shows that there is a **decrease** in the percentage

shortening across the belt from NE to SW, and this observation is compatible with the **increase** in half-wavelength/amplitude ratio in this direction (see Figs. 4.4-4.8) and the **regional dip** of the median surface of the folds to the southwest (Figs. 4.10-4.14).

Although there is a general decrease in shortening across the belt from NE to SW, the shortening profiles across the four morphologically and structurally distinct zones of the belt are not the same.

As can be seen from the graphs in Fig. 4.20 the shortening across the Bakhtiari Fold Zone is concentrated close to the NE half of the zone and as a result, the gradient of the percentage shortening graph is much steeper in this zone than in the other zones. As discussed earlier, the localisation of folding within this zone is thought to reflect the lack or reduced thickness of the salt component of the Hormuz detachment horizon in the area of the present-day Dezful Embayment which lies to the southwest of the Bakhtiari Mountains.

The variation in shortening across the 'Simply Folded Belt' was determined at three different depths within the sedimentary cover and the results from all three horizons are shown on the graphs. Two of the marker horizons occur within the 'Competent Group' i.e. in the group directly overlying the Hormuz Salt Formation which lies directly on the basement and constitutes the lower detachment horizon. The remaining marker horizon was taken from the 'Incompetent Group' which lies above the detachment horizon in the 'Upper Mobile Group' which directly overlies the 'Competent Group' (Figs. 2.16 and 3.5).

Inspection of the graphs shows that the shortening profile of the two lower marker horizon are remarkably similar. However, the upper marker horizon sometimes displays a very different shortening profile. This is particularly evident in the graphs shown in Figs. 4.19 and 4.21 which relate to the Lorestan and Kohkiluyeh fold zones. This different shortening

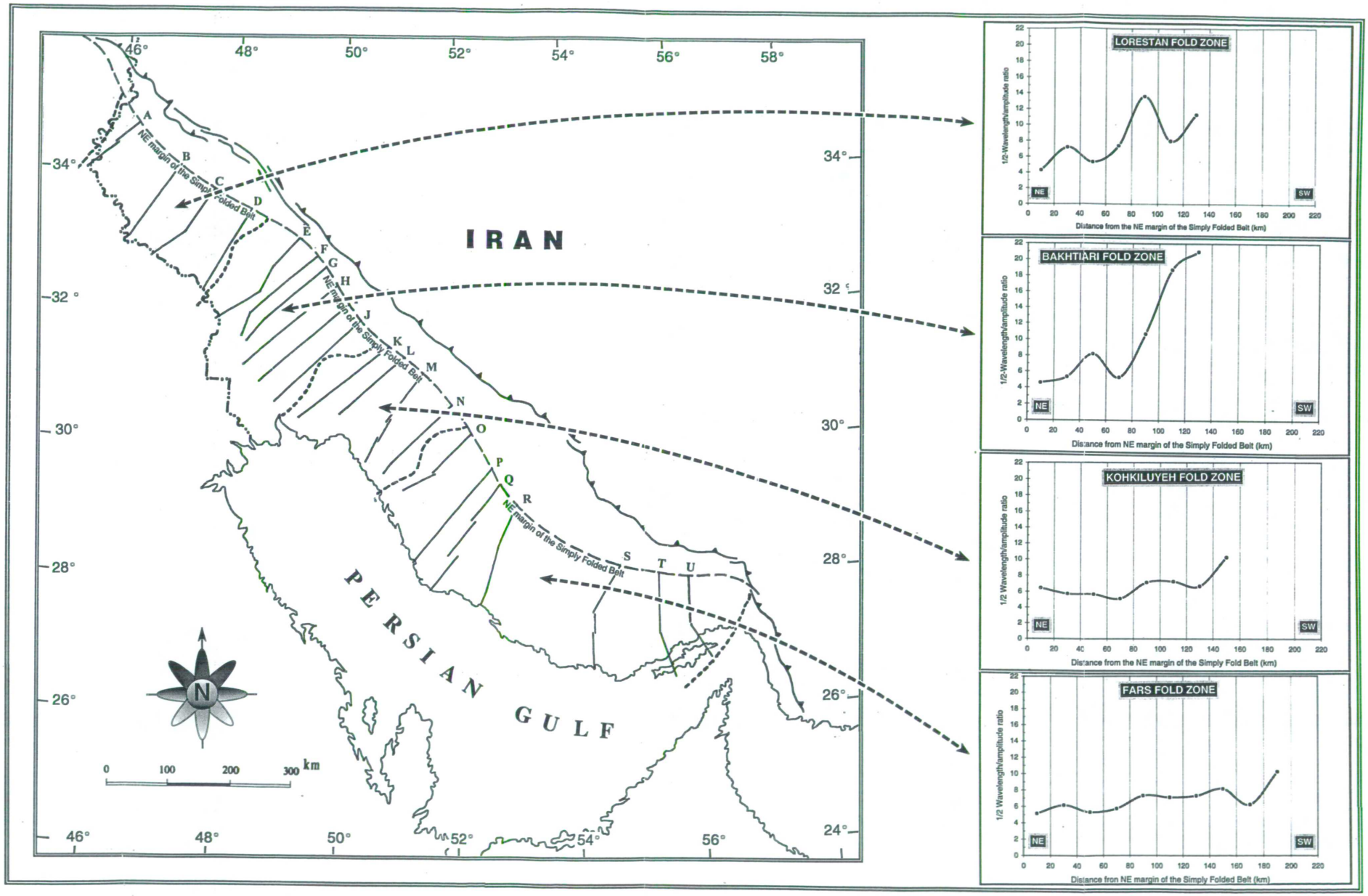


Fig. 4.9 The variation of the half-wavelength/amplitude ratio of the folds within the 20 km strips parallel to the northeastern margin of the 'Simply Folded Belt' in four of the morphologically and structurally distinct fold zones shown in Fig. 4.3.

profiles are the result of disharmonic folding between the sediments above and below the 'Upper Mobile Group' (Figs. 3.5, 3.30 and 3.33).

This is particularly marked where the thickness of the Upper Mobile Group is largest. It should be noted that although there is not apparent disharmony between the shortening profile in the three marker horizons in the Bakhtiari Fold Zone, this is only because the sections do not permit the three marker horizons to be traced across the whole of the Simply Folded Belt. However, from the sections (see for example, Fig. 3.5) it is evident that disharmonic folding does occur in the southwestern half of this fold zone.

One of the most apparent features of the percentage shortening graphs, shown in Figs. 4.19-4.22 is that superimposed on the general decrease in shortening across the belt from NE to SW is a '**periodic variation**' in shortening. It is interesting to speculate as to what gave rise to these variation.

Inspection of the geological cross sections shows that the zones of relatively high shortening can be traced from one section to the adjacent sections along strike and that in addition, these zones are generally associated with faulting as well as folding (Fig. 3.5). Thus it seems likely that these faults play an important role in controlling the localisation of folds and therefore of shortening and account for the observation that these zone have a remarkable continuity along strike, a feature uncharacteristic of simple anticlines.

The link between the zone of high shortening and faulting can be clearly seen in Fig. 3.5 which shows many of the folds to be fold bend folds associated thrusting. A study of the horse blocks between the adjacent thrusts show a decrease in deformation, both buckling and fold bend folding from NE to SW (Fig. 3.21). This is compatible with the formation of this belt by the process of '**footwall collapse**' which is discussed in the following Chapter.

Sections	Horizon	Strip 1 00-20	Strip 2 20-40	Strip 3 40-60	Strip 4 60-80	Strip 5 80-100	Strip 6 100-120	Strip 7 120-140	Strip 8 140-160	Strip 9 160-180	Strip 10 180-200	Strip 11 200-220
ABCD	1					2.47	2.46	3.64	2.46			
	2	14.69	10.64	11.68	8.86	4.50	4.24	3.06	1.86			
	3	12.15	7.79	8.52	7.30	4.22	4.24	3.64	1.86			

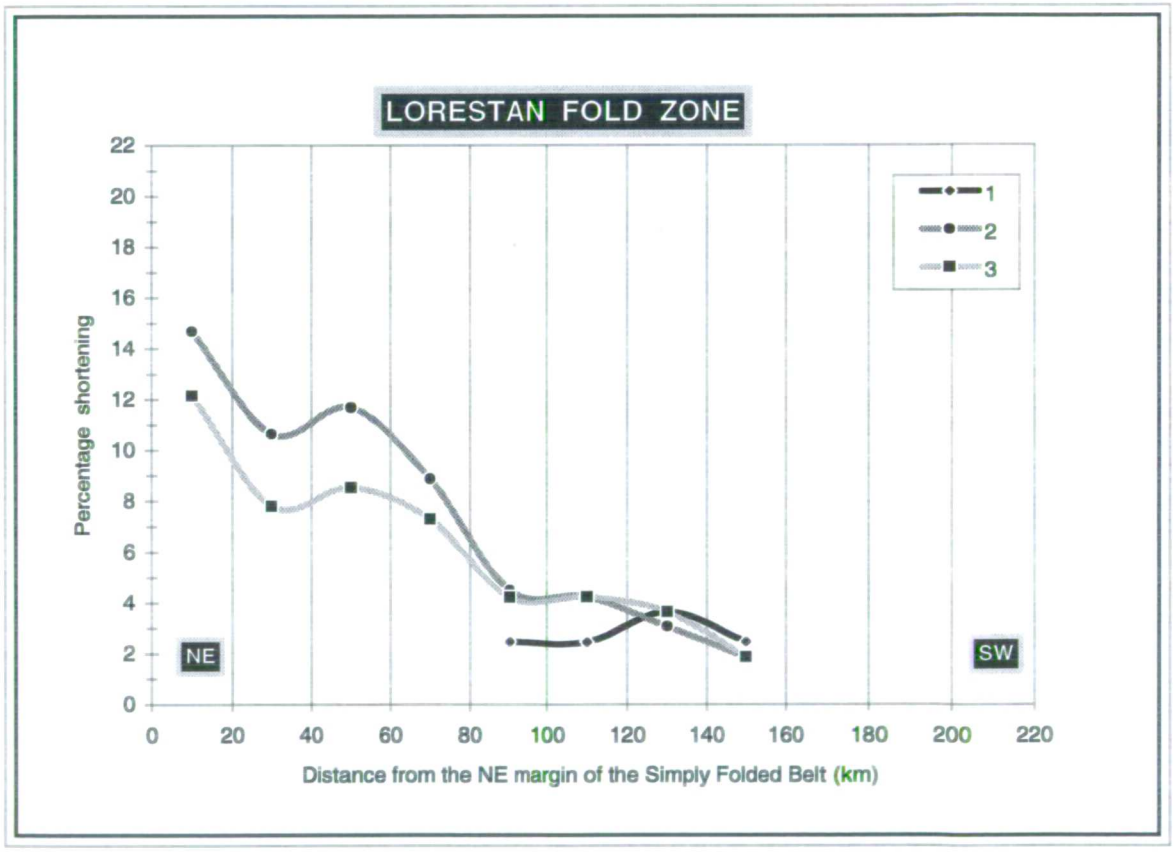


Fig. 4.19 The percentage of shortening of three marker horizons within the 20 km wide strips parallel to the northeastern margin of the 'Simply Folded Belt' in the **Lorestan** fold zone.

Sections	Horizon	Strip 1 00-20	Strip 2 20-40	Strip 3 40-60	Strip 4 60-80	Strip 5 80-100	Strip 6 100-120	Strip 7 120-140	Strip 8 140-160	Strip 9 160-180	Strip 10 180-200	Strip 11 200-220
EFGHIJ	1				11.34	9.75	2.06	2.82	3.14	4.41	2.47	
	2	21.10	15.71	19.12	10.41	8.64	1.25	1.25				
	3	19.22	14.94	16.76	9.47	7.57						

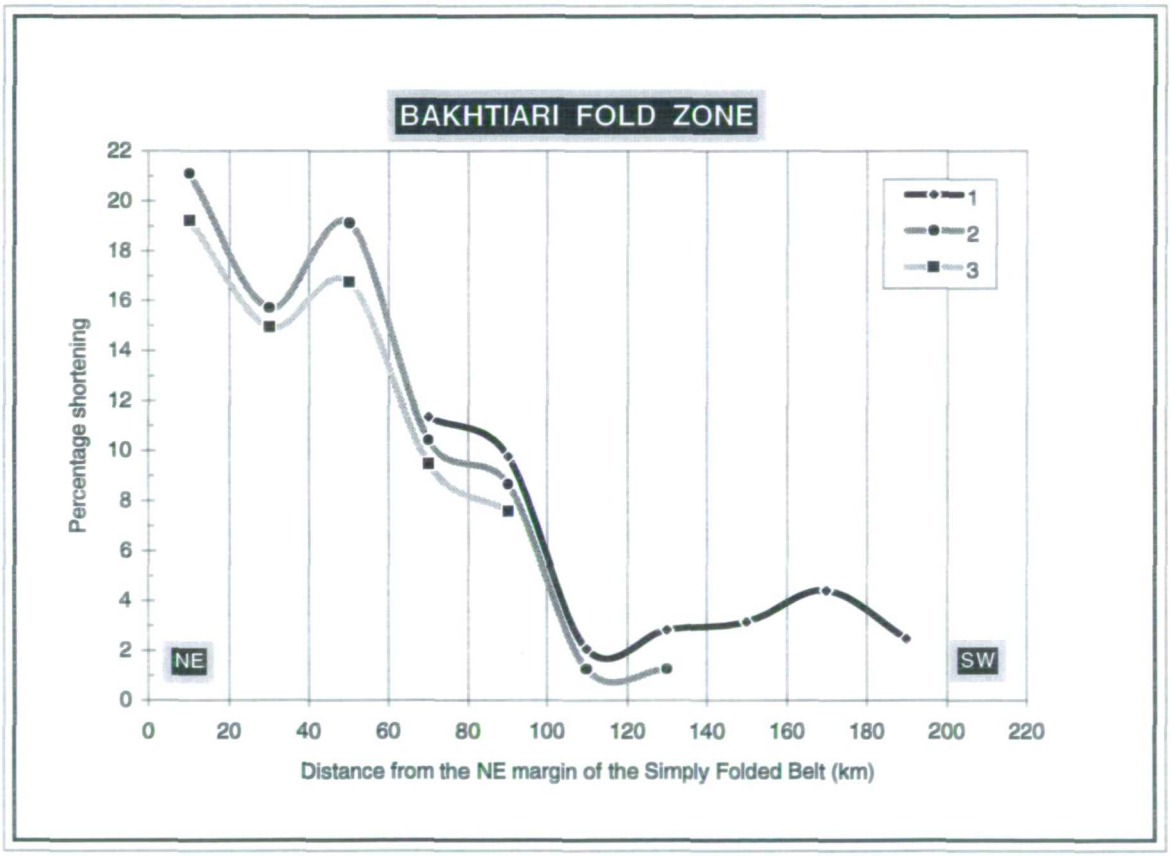


Fig. 4.20 The percentage of shortening of three marker horizons within the 20 km wide strips parallel to the northeastern margin of the 'Simply Folded Belt' in the **Bakhtiari** fold zone.

Sections	Horizon	Strip 1 00-20	Strip 2 20-40	Strip 3 40-60	Strip 4 60-80	Strip 5 80-100	Strip 6 100-120	Strip 7 120-140	Strip 8 140-160	Strip 9 160-180	Strip 10 180-200	Strip 11 200-220
KLMN	1					10.23	7.45	2.47	4.24	2.47		
	2	15.28	13.42	11.31	17.20	15.71	10.20	5.50	1.25			
	3	12.91	11.21	9.63	15.55	13.82	8.80	4.36	1.25			

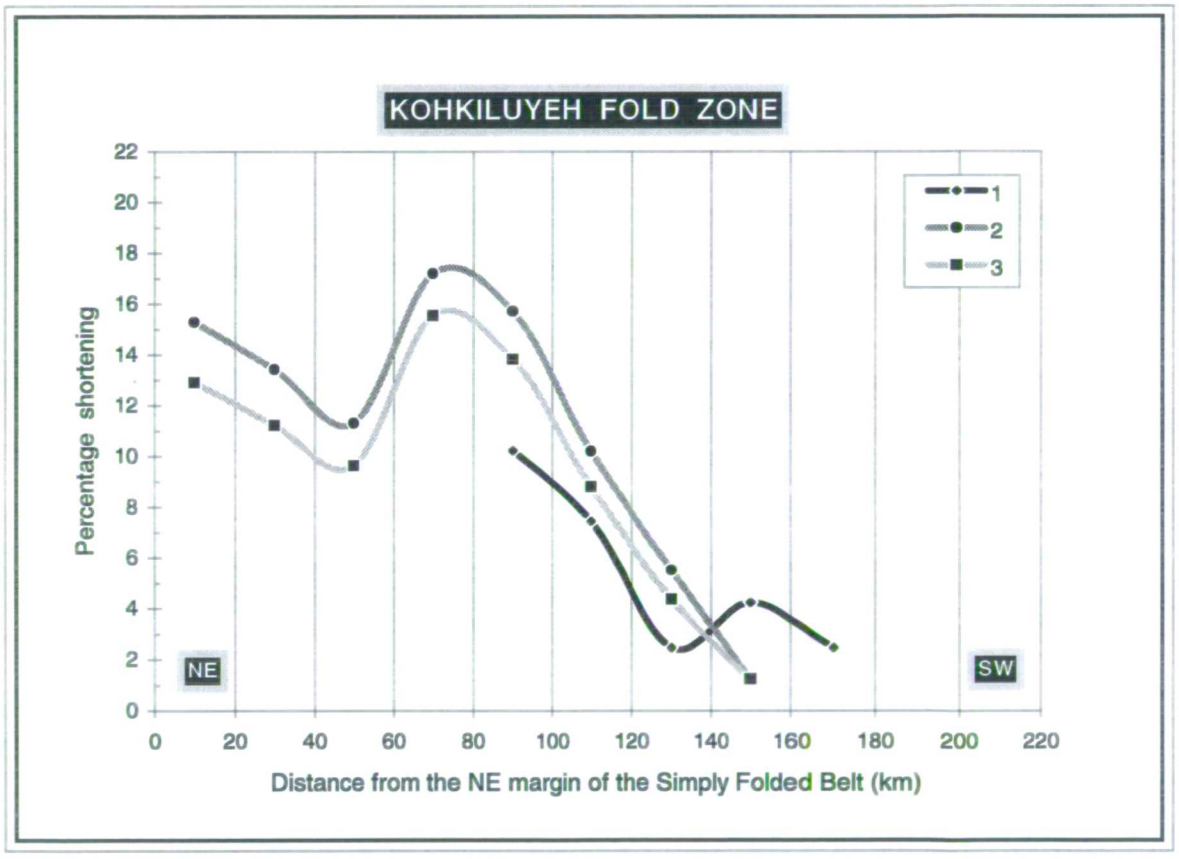


Fig. 4.21 The percentage of shortening of three marker horizons within the 20 km wide strips parallel to the northeastern margin of the 'Simply Folded Belt' in the **Kohkiluyeh** fold zone.

Sections	Horizon	Strip 1 00-20	Strip 2 20-40	Strip 3 40-60	Strip 4 60-80	Strip 5 80-100	Strip 6 100-120	Strip 7 120-140	Strip 8 140-160	Strip 9 160-180	Strip 10 180-200	Strip 11 200-220
OPQRSTU	1	15.81	14.93	15.77	14.10	5.22	10.76	7.84	7.02	12.06	5.39	1.86
	2	15.86	12.00	12.94	13.27	7.50	10.67	7.16	6.29	10.73	5.36	1.25
	3	13.87	10.06	12.42	11.74	8.34	11.17	7.41	5.71	11.64	4.81	1.25

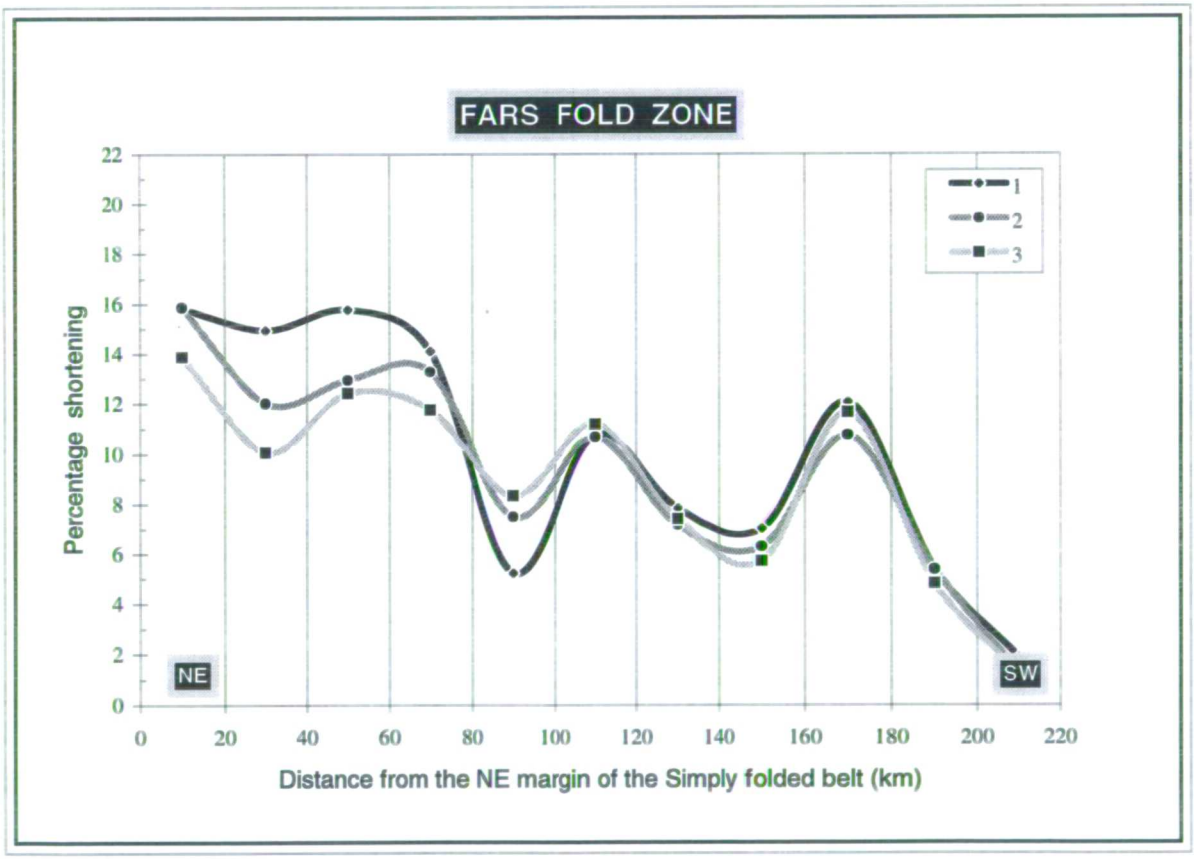


Fig. 4.22 The percentage of shortening of three marker horizons within the 20 km wide strips parallel to the northeastern margin of the 'Simply Folded Belt' in the **Fars** fold zone.

Sections	Horizon	Strip 1 00-20	Strip 2 20-40	Strip 3 40-60	Strip 4 60-80	Strip 5 80-100	Strip 6 100-120	Strip 7 120-140	Strip 8 140-160	Strip 9 160-180	Strip 10 180-200	Strip 11 200-220
A to U	1	15.81	14.93	15.77	12.72	7.49	6.38	5.14	4.07	5.79	3.44	1.86
	2	16.73	14.42	14.03	11.67	10.55	8.03	5.71	4.95	4.61	5.36	1.25
	3	14.54	12.51	12.05	9.84	9.69	9.74	6.82	4.57	4.92	4.81	1.25

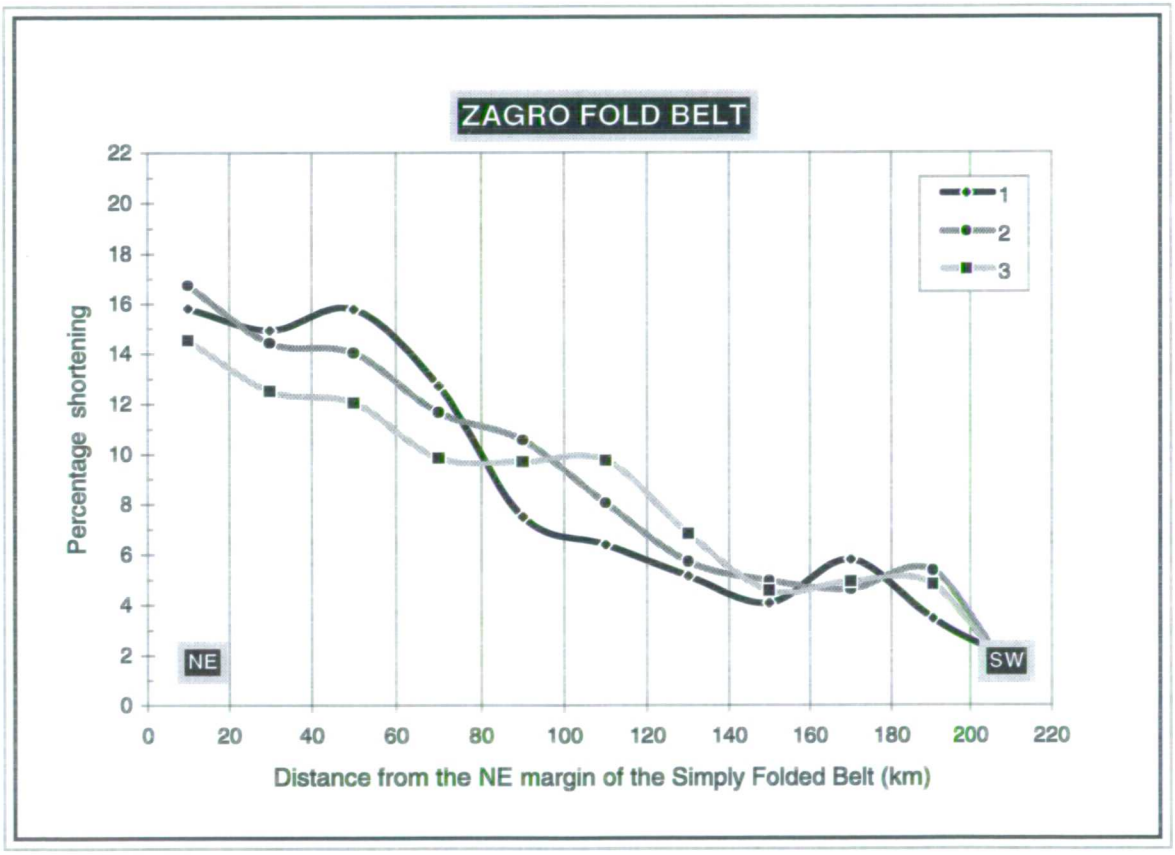


Fig. 4.23 The average percentage of shortening of three marker horizons within the 20 km wide strips parallel to the northeastern margin of the 'Simply Folded Belt' in **the whole Zagros belt.**

Section	Horizon	Strip 1 00-20	Strip 2 20-40	Strip 3 40-60	Strip 4 60-80	Strip 5 80-100	Strip 6 100-120	Strip 7 120-140	Strip 8 140-160	Strip 9 160-180	Strip 10 180-200	Strip 11 200-220
A	1					2.47						
	2	14.13	11.24	15.05	13.19	2.47						
	3	13.19	8.14	14.13	10.23	2.47						
B	1								1.25			
	2	9.20	5.95	11.24	7.06	7.06	4.82	2.47	1.25			
	3	8.14	3.66	4.82	5.95	5.95	4.82	2.47	1.25			
C	1						3.66	4.82	2.47			
	2	17.71	11.24	9.20	8.14	4.82	3.66	3.66	2.47			
	3	12.22	9.14	5.95	7.06	4.82	3.66	4.82	2.47			
D	1						1.25	2.47	3.66			
	2	17.71	14.13	11.24	7.06	3.66						
	3	15.06	10.23	9.20	5.95	3.66						
Average	1					**2.47**	**2.46**	**3.64**	**2.46**			
	2	**14.69**	**10.64**	**11.68**	**8.86**	**4.50**	**4.24**	**3.06**	**1.86**			
	3	**12.15**	**7.79**	**8.52**	**7.30**	**4.22**	**4.24**	**3.64**	**1.86**			

Table 4.1 The results of measurements of the variation in percentage shortening of three marker horizons within the 20 km wide strips parallel to the northeastern margin of the 'Simply Folded Belt' in the **Lorestan** fold zone.

Section	Horizon	Strip 1 00-20	Strip 2 20-40	Strip 3 40-60	Strip 4 60-80	Strip 5 80-100	Strip 6 100-120	Strip 7 120-140	Strip 8 140-160	Strip 9 160-180	Strip 10 180-200	Strip 11 200-220
E	1					1.25	2.47	1.25	0.00	5.95	2.47	
	2				10.22							
	3	22.55	19.39	20.20	10.23							
F	1				11.24	7.06	2.47	4.82	5.95	4.82	2.47	
	2	22.55	17.71	24.04	3.66							
	3	19.39	16.84	15.05	3.66							
G	1				5.95	17.71	3.66	3.66	2.47	2.47		
	2		13.19	15.05	3.66							
	3	18.56	12.22	15.05	3.66							
H	1					2.47	1.25	0.00	2.47			
	2	22.25	14.13	4.82	11.24							
	3	18.56	12.22	4.82	9.20							
I	1			16.84	16.84	13.19	1.25	1.25	4.82			
	2	14.13	19.39	8.14	15.96	7.06	1.25	1.25				
	3	12.22	17.71	4.82	14.13	5.95						
J	1					16.84	1.25	5.95				
	2	25.47	14.13	43.57	17.71	10.23						
	3	24.04	11.24	40.60	15.96	9.20						
Average	1				**11.34**	**9.75**	**2.06**	**2.82**	**3.14**	**4.41**	**2.47**	
	2	**21.10**	**15.71**	**19.12**	**10.41**	**8.64**	**1.25**	**1.25**				
	3	**19.22**	**14.94**	**16.76**	**9.47**	**7.57**						

Table 4.2 The results of measurements of the variation in percentage shortening of three marker horizons within the 20 km wide strips parallel to the northeastern margin of the 'Simply Folded Belt' in the **Bakhtiari** fold zone.

Section	Horizon	Strip 1 00-20	Strip 2 20-40	Strip 3 40-60	Strip 4 60-80	Strip 5 80-100	Strip 6 100-120	Strip 7 120-140	Strip 8 140-160	Strip 9 160-180	Strip 10 180-200	Strip 11 200-220
K	1						11.24	2.47	3.66			
	2	8.14	13.19	17.71	24.04	16.84	12.22	9.20	1.25			
	3	5.95	12.22	13.19	21.00	15.05	10.23	8.14	1.25			
L	1							2.47				
	2	12.22	10.23	10.23	11.24	11.24	10.23	3.66				
	3	10.23	9.20	8.14	10.23	10.23	10.23	2.47				
M	1								4.82	2.47		
	2			7.06	23.30	28.83						
	3			5.95	21.78	24.04						
N	1					10.23	3.66	2.47				
	2	25.47	16.84	10.23	10.23	5.95	8.14	3.66				
	3	22.55	12.22	11.24	9.20	5.95	5.95	2.47				
Average	**1**					**10.23**	**7.45**	**2.47**	**4.24**	**2.47**		
	2	**15.28**	**13.42**	**11.31**	**17.20**	**15.71**	**10.20**	**5.50**	**1.25**			
	3	**12.91**	**11.21**	**9.63**	**15.55**	**13.82**	**8.80**	**4.36**	**1.25**			

Table 4.3 The results of measurements of the variation in percentage shortening of three marker horizons within the 20 km wide strips parallel to the northeastern margin of the 'Simply Folded Belt' in the **Kohkiluyeh** fold zone.

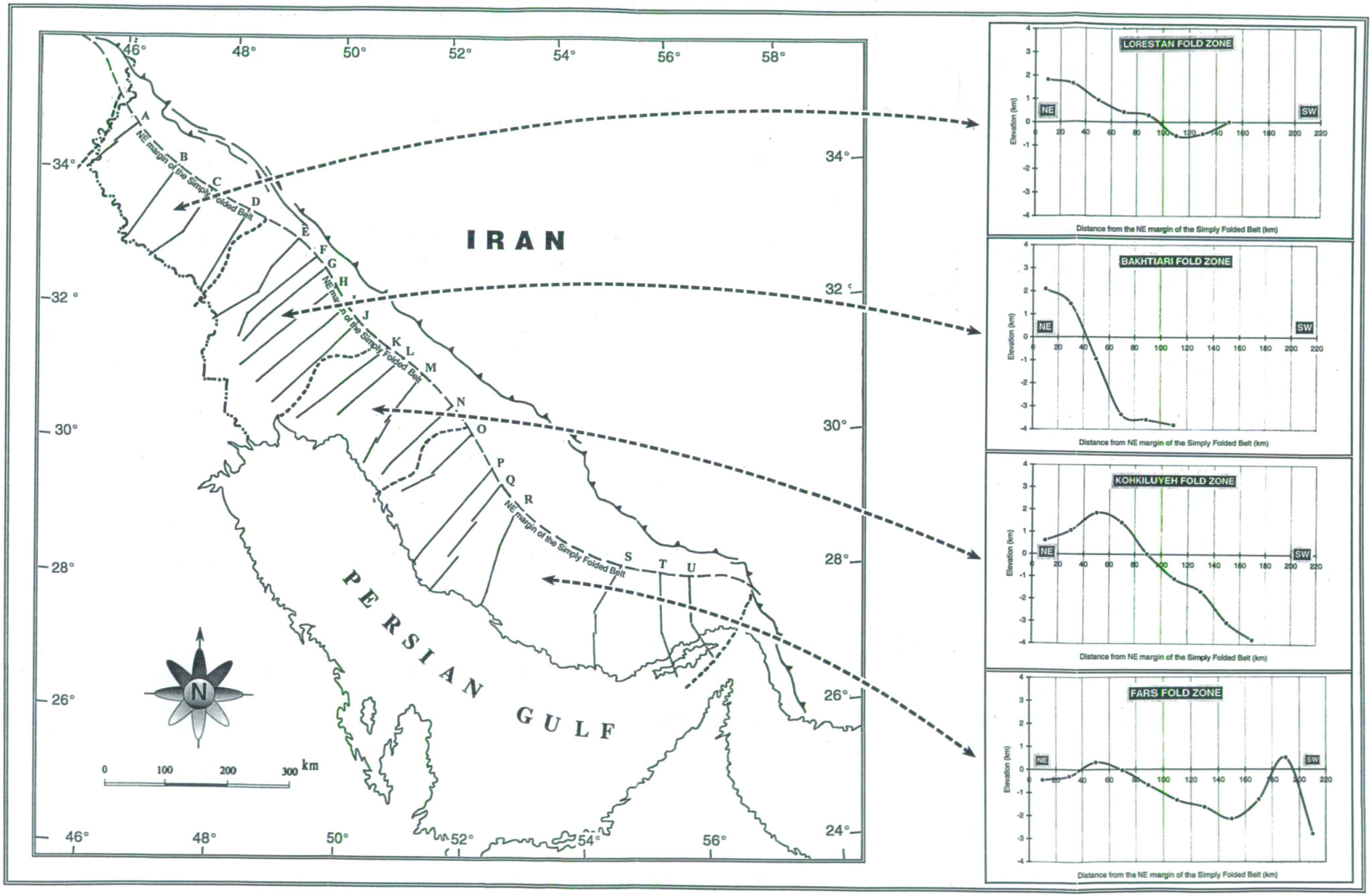


Fig. 4.16 The contrasting southwestward inclination of the median surface of the folds within the four adjacent fold zone.

Section	Horizon	Strip 1 00-20	Strip 2 20-40	Strip 3 40-60	Strip 4 60-80	Strip 5 80-100	Strip 6 100-120	Strip 7 120-140	Strip 8 140-160	Strip 9 160-180	Strip 10 180-200	Strip 11 200-220
O	1						10.23					
	2	15.96	9.20	4.82	10.23	7.06	9.20					
	3	15.05	7.06	3.66	9.20	5.95	7.06					
P	1						15.05	8.14	7.06	17.71	4.82	1.25
	2	17.71	14.13	8.14	12.22		14.13	7.06	7.06	15.96	3.66	1.25
	3	14.13	5.95	8.14	10.23		10.23	7.06	5.95	14.13	3.66	1.25
Q	1						15.05	9.20	9.20	13.19	5.95	2.47
	2	15.96	3.66	18.56	13.19	13.19	14.13	8.14	8.14	12.22	7.06	1.25
	3	10.23	3.66	17.71	12.22	12.22	12.22	7.06	7.06	11.24	5.95	1.25
R	1						4.82	4.82	8.14	17.71		
	2	13.19	15.05	14.13	15.05	7.06	4.82	3.66	8.14	15.96		
	3	12.22	15.05	13.19	16.84	7.06	4.82	3.66	7.05	14.13		
S	1	12.22	12.22	17.71	15.96	2.47	17.71	14.13	8.14	9.20		
	2	10.23	10.23	16.84	16.84	2.47	17.71	12.22	5.95	7.06		
	3						18.56	12.22	4.82	7.06		
T	1	19.39	13.19	7.06	14.13	5.06	1.25	4.82	3.66	2.47		
	2	18.56	13.19	7.06	14.13	7.06	2.47	4.82	3.66	2.47		
	3											
U	1		19.39	22.55	12.22	8.14	11.24	5.95	5.95			
	2	19.39	18.56	21.00	11.24	8.14	12.22	7.06	4.82			
	3	17.71	18.56	19.39	10.23	8.14	14.13	7.06	3.66			
Average	1	**15.81**	**14.93**	**15.77**	**14.10**	**5.22**	**10.76**	**7.84**	**7.02**	**12.06**	**5.39**	**1.86**
	2	**15.86**	**12.00**	**12.94**	**13.27**	**7.50**	**10.67**	**7.16**	**6.29**	**10.73**	**5.36**	**1.25**
	3	**13.87**	**10.06**	**12.42**	**11.74**	**8.34**	**11.17**	**7.41**	**5.71**	**11.64**	**4.81**	**1.25**

Table 4.4 The results of measurements of the variation in percentage shortening of three marker horizons within the 20 km wide strips parallel to the northeastern margin of the 'Simply Folded Belt' in the **Fars** fold zone.

Fold zone	Horizon	Strip 1 00-20	Strip 2 20-40	Strip 3 40-60	Strip 4 60-80	Strip 5 80-100	Strip 6 100-120	Strip 7 120-140	Strip 8 140-160	Strip 9 160-180	Strip 10 180-200	Strip 11 200-220
Lor.	1					2.47	2.46	3.64	2.46			
	2	14.69	10.64	11.68	8.86	4.50	4.24	3.06	1.86			
	3	12.15	7.79	8.52	7.30	4.22	4.24	3.64	1.86			
Bakh.	1				11.34	9.75	2.06	2.82	3.14	4.41	2.47	
	2	21.10	15.71	19.12	10.41	8.64	1.25	1.25				
	3	19.22	14.94	16.76	9.47	7.57						
Kohk.	1					10.23	7.45	2.47	4.24	2.47		
	2	15.28	13.42	11.31	17.20	15.71	10.20	5.50	1.25			
	3	12.91	11.21	9.63	15.55	13.82	8.80	4.36	1.25			
Fars	1	15.81	14.93	15.77	14.10	5.22	10.76	7.84	7.02	12.06	5.39	1.86
	2	15.86	12.00	12.94	13.27	7.50	10.67	7.16	6.29	10.73	5.36	1.25
	3	13.87	10.06	12.42	11.74	8.34	11.17	7.41	5.71	11.64	4.81	1.25
Average	1	**15.81**	**14.93**	**15.77**	**12.72**	**7.49**	**6.38**	**5.14**	**4.07**	**5.79**	**3.44**	**1.86**
	2	**16.73**	**14.42**	**14.03**	**11.67**	**10.55**	**8.03**	**5.71**	**4.95**	**4.61**	**5.36**	**1.25**
	3	**14.54**	**12.51**	**12.05**	**9.84**	**9.69**	**9.74**	**6.82**	**4.57**	**4.92**	**4.81**	**1.25**

Table 4.5 The results of measurements of the variation in percentage shortening of three marker horizons within the 20 km wide strips parallel to the northeastern margin of the 'Simply Folded Belt' in **the whole Zagros belt**.

CHAPTER 5

Plate tectonic and geomorphological evolution of the Zagros mountain belt

1. INTRODUCTION

In this chapter the plate tectonic and geomorphological evolution of the entire Zagros Mountain belt up to the end of the latest orogenic movements in Pliocene times is considered. A more detailed consideration and discussion on the evolution of the '*Zagros Deformation Belt*' including the fold and fault belts and salt diapir provinces, during and after the Pliocene Orogeny is given in the following Chapter. The recent development and changes in the tectonic and morphological elements of the belt are considered in chapter 7, on neotectonics.

2. PLATE TECTONIC MODELS

Over the last 70 years and especially since the emergence of the theory of plate tectonics as a framework for understanding the motions of the earth's lithosphere, and explaining the tectonic evolution of mountain belts, several investigators have studied the geological, geophysical, and morphological aspects of the Zagros belt and have proposed various tectonic models to explain its plate tectonic evolution (for example, Stöcklin 1968, Takin 1972, Haynes & McQuillan 1974, Falcon 1974, Kashfi 1976, Farhoudi 1978, Iranpanah & Esfandiari 1979, Alavi 1980, 1994, and Jaros 1981).

Some of these models such as those proposed by Kashfi (1976) and Stöcklin (1968) are based on the now out dated '**geosynclinal theory**', while others such those proposed by Haynes & McQuillan (1974) and Alavi (1980) are based on the '**plate tectonic theory**'.

Kashfi (1976) argued that Africa, Arabia, as well as India have been integral parts of Europe and Asia and have been in fixed position since Late Proterozoic time. He suggested that the arguments of the supporters of plate tectonic theory regarding horizontal motion of Africa

by about 1,500 to 2,000 km since Jurassic time towards the Persian plate, and its collision and the resulting uplift of the Zagros region were meaningless and unscientific speculation. According to Kashfi, there was no plate tectonic collision in the Tethys area at least in the Late Proterozoic and possibly also in earlier times, and the *geosynclinal theory* provides the means for producing the Zagros geosynclinal without invoking plate tectonics. However, the weight of scientific evidence for the occurrence of 'plate tectonics' and its role in the formation of the Zagros mountain belt is now so overwhelming that it is difficult to lend credence Kashfi's to these ideas.

The various plate tectonic models proposed for the formation of the Zagros Mountain Belt have many points in common. The major differences between these models relate to:

i) The existence, position and geometrical characteristics of the fault structure known as the 'Main Zagros Thrust' extending along the northeastern margin of the Arabian plate.
ii) The position of the subduction zone and the suture line between the Arabian and Iranian continents.
iii) The number, nature, origin and boundaries of the major structural zones in the Zagros region.
iv) The timing of the various tectonic events.

According to Alavi (1980, 1994) the so-called 'Main Zagros Thrust' (Figs. 2.14 and 2.15) which has been traditionally considered to be **a single reverse fault** at the boundary between the 'Sanandaj-Sirjan Zone' and the 'Thrust Zone', and the suture line between the collided continents, **is not a single fault**, nor does it represent the boundary between the two plates. He considers the Main Zagros Thrust to be one of a series of low-angle thrusts dipping NE. These faults he claims are indistinguishable from those mapped in the Sanandaj-Sirjan Zone, and are geometrically part of the Sanandaj-Sirjan Zone structures. No single thrust among them that can be singled out and referred to as the '**Main**' thrust.

Alavi argued that the Zagros thrust is a repeatedly reactivated fault zone which, as originally suggested by Harrison (see Wells, 1969), has been acting as a buffer between the southwestern and northeastern parts of the continental shelf along the northeastern margin of the Arabian continent (Fig. 2.15).

Alavi considers that the position of the *Cretaceous* subduction zone i.e. the plate margin between the Arabian and central Iranian plates is situated on the southwestern margin of the 'Urmia-Dokhtar magmatic arc' (Figs. 2.14, 2.15 and 2.17).

Stöcklin (1968) and Kashfi (1976) have argued that the Zagros region is restricted to the area southwest of the Main Zagros Thrust and contains only two major structurally contrasting zones, namely the 'Folded Belt' and the 'Thrust Zone'. Whereas, Oberlander (1965) and Falcon (1967, 1974) believe that there is a third zone between them which they call the 'Imbricate Zone' (Fig. 2.14).

In contrast, Alavi (1980) groups all three zones lying southwest of the Main Zagros Thrust, into the 'Simple Folded zone' and considers that, both the 'Sanandaj-Sirjan metamorphic belt' and the 'Urmia Dokhtar magmatic arc', to the northeast of the Main Zagros Thrust to be two other major structural zones of the Zagros Belt (Fig. 2.15).

Haynes & McQuillan (1974) recognise four structurally distinct zones to the southwest of the Main Zagros Thrust (the 'Simply Folded belt', the 'Imbricated zone', the 'Trench zone', and the 'Crush zone'), and only one to the northeast, the 'Stable Block' (the Sanandaj-Sirjan metamorphic zone).

There is also disagreement over the timing of the successive tectonic events. For example, Wells (1969) considers that the Zagros orogeny started towards the end of the Miocene, while Jaros (1981), Takin (1972), Haynes & McQuillan (1974), Falcon (1974), Alavi

(1980), and Stöcklin (1968) favour the Upper Eocene-Oligocene, the Late Tertiary, the Late-Miocene-Pliocene, the Late Pliocene, Pliocene, and the Plio-Pleistocene respectively.

Despite these differences between the various models and interpretations, they share many similarities as regards the nature, origin, and sequence of tectonic and geomorphological events.

Using the main points of these models and interpretations which are compatible with the results of the present study **a comprehensive and updated model** for the plate tectonic and geomorphological evolution of the '*Zagros mountain belt*' in the northeastern margin of the Arabian plate **is proposed**.

3. PLATE TECTONIC EVOLUTION

Palaeogeographic maps which are prepared on the basis of palaeomagnetism indicate that in **Early Mesozoic** times the continental masses of Africa, Arabia, central Iran, Australia and Antarctica were all part of a great mass of continental crust named '*Gondwanaland*' (Fig. 5.1) which was separated from '*Laurasia*' by the ocean crust of the '*Tethys Sea*'. The Sea of Tethys was a wide seaway that spread far over the margins of the continental crust so that much of the crust of Arabia and parts of central Iran, for example, were submerged by it (Shearman, 1976).

According to Stöcklin (1968) early orogenic movements in Iran resulted in the consolidation of a **Precambrian**, shield-like basement and the formation of a vast Iranian platform as an extension of the Arabian shield and part of great Gondwanaland. The 'Assyntic Orogeny' occurred in **Late Precambrian** time, and resulted in the intensive folding and metamorphism of the Iranian platform (Iranpanah & Esfandiari, 1979), including what was to become the basement of the present-day Zagros Mountain Belt.

This was followed by a long period of remarkable tectonic calm during most of the interval from **Infra-Cambrian** to **Middle Triassic** times (Stöcklin, 1968). The rock sequences deposited during this time interval, are shallow water sediments and include the Infra-Cambrian Hormuz Salt Formation. They all have the characteristics of a true platform cover (Fig. 2.16). No orogeny affected this platform during the *Palaeozoic* Era (Fig. 5.2 a) and only epeirogenic movements occurred (Stöcklin, 1968).

During the **Mesozoic**, Gondwanaland began to break up into new smaller continents, and during this time central Iran, which forms part of Iranian platform, separated from Afro-Arabia by sea-floor spreading, an event sometimes referred to as the opening of the 'Neo-Tethys Sea' (Shearman, 1976; Alavi, 1980) (Fig. 5.1). According to Alavi rupturing of the Iranian platform occurred in the **Late Triassic** but may even have been initiated in **Late Permian** times (Fig. 5.2 b). The resulting normal faults define several 'horsts' and 'grabens'.

In the northeastern part of the continent the depositional environment changed from marine to continental (Shemshak Formation, Fig. 5.2 b), but in the southwest shallow-water marine sedimentation continued resulting in the deposition of the Khaneh-Kat Formation (Figs. 2.16 and 5.2 b) in the newly generated 'sedimentary basins'. All of this was accompanied by upward movement of magma along the fault planes and emplacement of diabase sheets within the sedimentary prisms (Fig. 5.2 b).

In **Early Jurassic** times, the main graben deepened, while block faulting was still occurring elsewhere, and developed into a spreading centre (the New Tethys Sea) between the two now-separated continents Arabia to the southwest and central Iran to the northeast, along which volcanic activity occurred, generating oceanic crust and developing Red Sea-type structures (Fig. 5.2 c). Continuous shallow-water marine sedimentation occurred along the shelf zone with a zone of transition represented by the Neyriz Formation, between the two sedimentary environments (Alavi, 1980).

In **Late Jurassic** times, the central Iranian and Arabian blocks moved away from each other, as the ocean developed and deep sea sediments (radiolarites and pelagic limestone) and volcanic and volcaniclastic materials was deposited on the ocean floor (Fig. 5.2 d). Two shallow basins were formed as the sea transgressed onto the neighbouring continents. The one on the Iranian block was relatively shallow and received clastic sediments represented by the Hojadk Formation. The basin on the Arabian block was somewhat deeper and received continental shelf-type marine carbonates represented by the Surmeh Formation (Alavi 1980).

In **Early Cretaceous** times, as a result of the opening of the Atlantic ocean (Fig. 5.3) westward motion of the Arabian plate ceased (see, Fig. 5.2 e) (Iranpanah & Esfandiari, 1979). In addition, the eastward motion of the central Iranian plate also stopped as a result of the closing of the Tethys Sea (Fig. 5.1). Thus the relative motion of the Arabian and central Iranian plates reversed and subduction of the oceanic crust beneath the central Iranian plate was initiated (Fig. 5.2 e).

As a consequence an oceanic trench formed in front of the Iranian continent (Fig. 5.2 e) and the Arabian plate moved northeastward as the trailing edge of a continent attached to the subducting oceanic crust. High-pressure, low-temperature metamorphism occurred below the trench, as indicated by the glaucophane-jadeite mineral assemblage in the Zagros ophiolites. Uplift of the southwestern edge of the central Iran continent occurred because of pressure exerted by the downgoing oceanic crust, and a foreland basin formed on its former continental shelf (Fig. 5.2 e). Shallow-water sedimentation on the Arabian continental shelf represented by the Sarvak Formation was continuous during this period (Alavi, 1980).

In **Late Cretaceous** times, the development of the subduction zone was accompanied by progressive loss of oceanic crust along the trench, leading to the early phases of collision

of the Iranian block and the Arabian continent (Fig. 5.2 f). Several high-angle reverse faults formed along the edge of the Arabian continent, and southwest obduction of slices of oceanic crust along these faults caused ophiolitic mèlange complexes to form. These events were followed by the intense folding, uplift, and short-lived erosion of the deep-ocean sediments, more plutonic activity on the edge of Iranian continent, a second phase of metamorphism (high-pressure, high-temperature), and migration of the deformation front into the undisturbed Zagros sedimentary basin, causing pre-buckling thickening and some scattered salt intrusions further to the southwest.

During the **Palaeocene**, further subduction of the oceanic crust resulted in a late-phase and much stronger collisional events and in the formation of several high-angle reverse fault zones, including the future Zagros thrust line (Fig. 5.2 g). These affected the continental shelf sequence and the basement complex of the northeastern part of the Arabian continental shelf area. Uplift of the thrust blocks occurred, and a flysch basin represented by the Amiran Formation, developed in front of the elevated area on the shelf sediments (Alavi, 1980).

In **Eocene** times, intense plutonic and volcanic activity along the edge of the Iranian continent originating from the subducted oceanic crust of the Neo-Tethys Sea resulted in the development of the Urumieh-Dokhtar magmatic arc (Figs. 2.14 and 2.15). According to Takin (1972), a pause in compression when sea-floor spreading in the Indian ocean was slow or had stopped, facilitated plutonic and volcanic activity and the development of the Urmia-Dokhtar magmatic arc.

In **Pliocene** times, the elevated Sanandaj-Sirjan zone changed from highlands to lowlands, and Alavi (1980) suggests that this is because of the structural pull exerted by the downgoing attached oceanic crust (Fig. 5.2 h). Sedimentary basins developed on both sides of the much expanded magmatic arc. The high angle reverse faults that had originated in

Late Cretaceous times in the Sanandaj-Sirjan zone were then reactivated, especially along the Main Zagros Thrust.

Finally, the accelerated motion of the underlying basement complex related to the opening of the Red Sea, initiated in Miocene times (Laughton, 1966), resulted in intense folding and faulting of the whole Zagros sedimentary sequence which overlay a rigid metamorphic and igneous basement complex, in the Pliocene times. (Fig. 5.2 h).

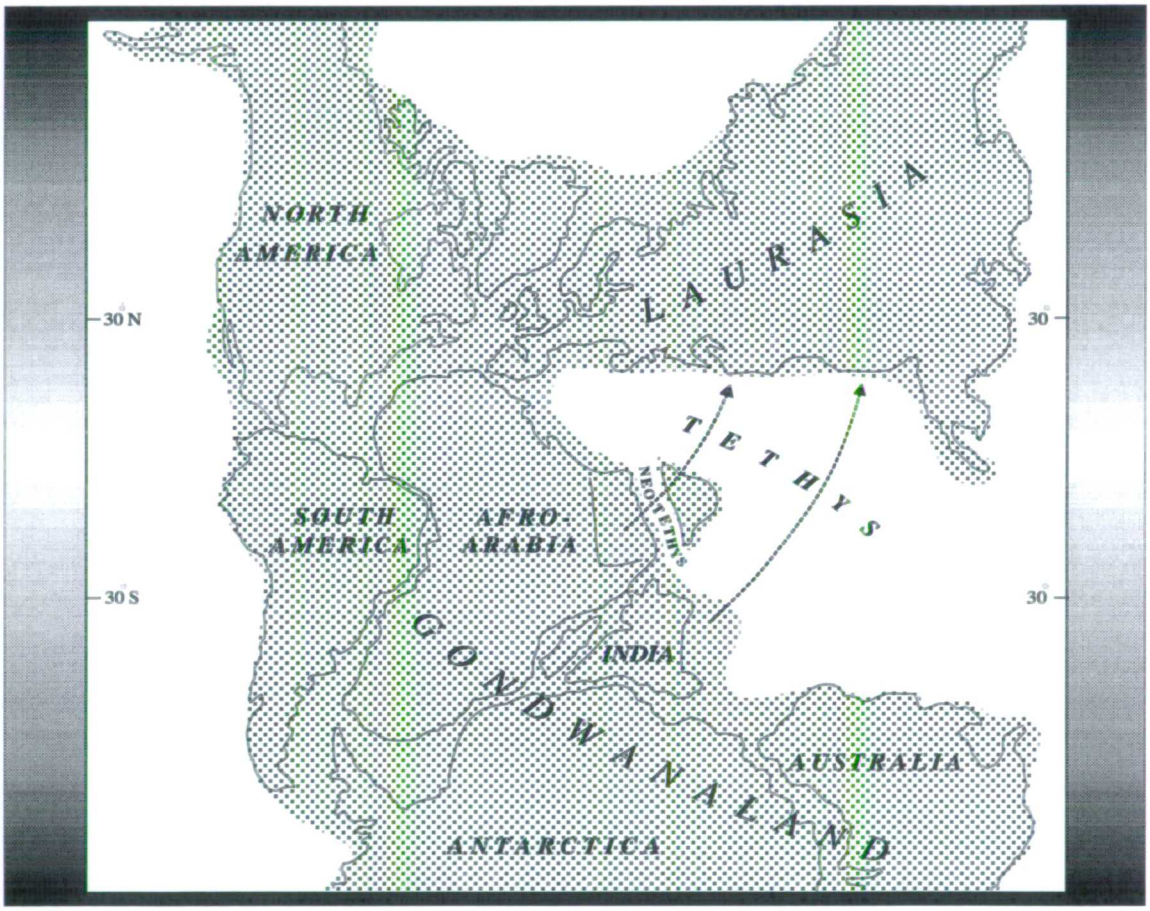


Fig. 5.1 Palaeogeographic map showing the possible distribution of continental crust (stipple) and ocean crust thought to have existed in Early Mesozoic era. The position of the Tethys and Neo-Tethys sea between Laurasia and Gondwanalad are shown (modified from Shearman, 1976).

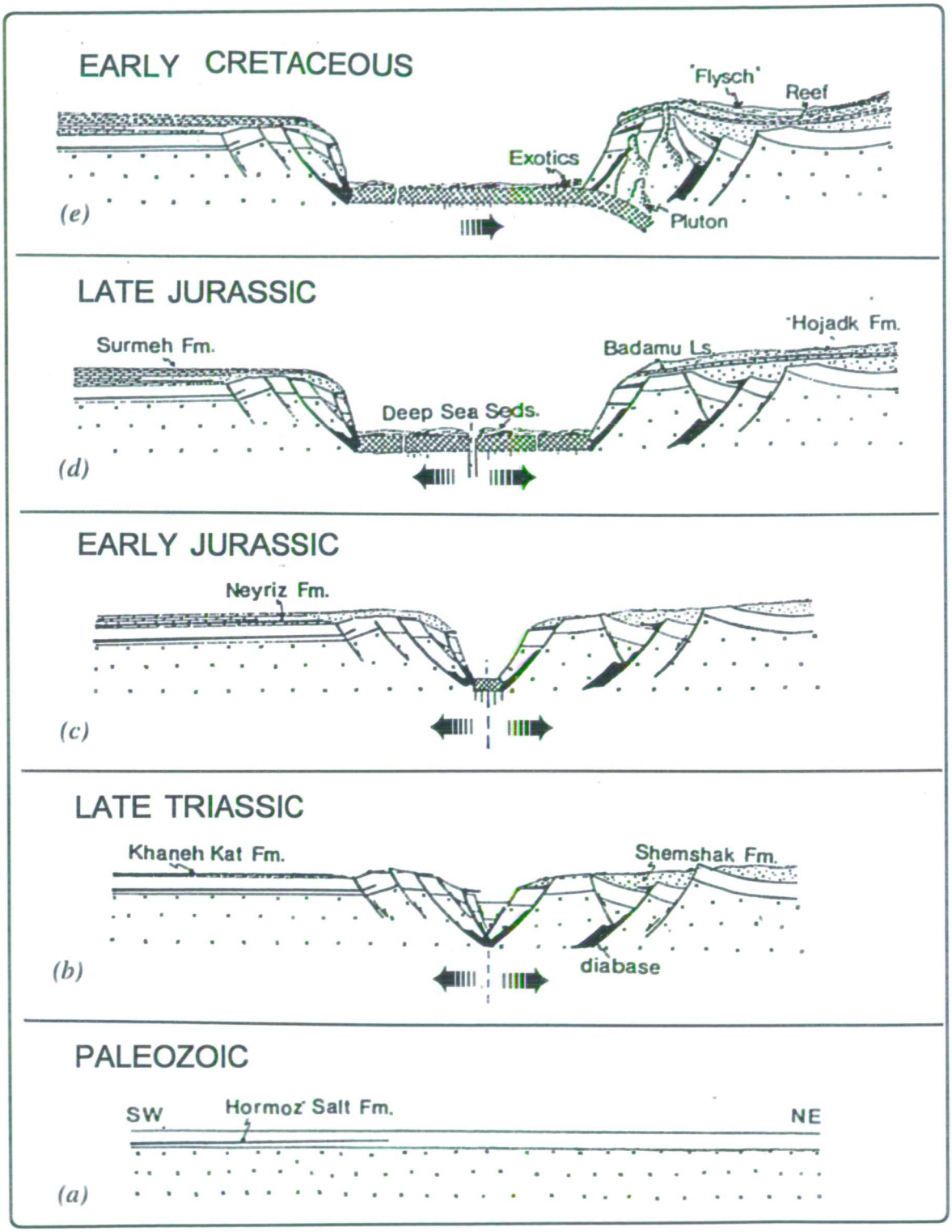


Fig. 5.2 Plate tectonic evolution of the Zagros Mountain Belt (modified from Alavi, 1980).

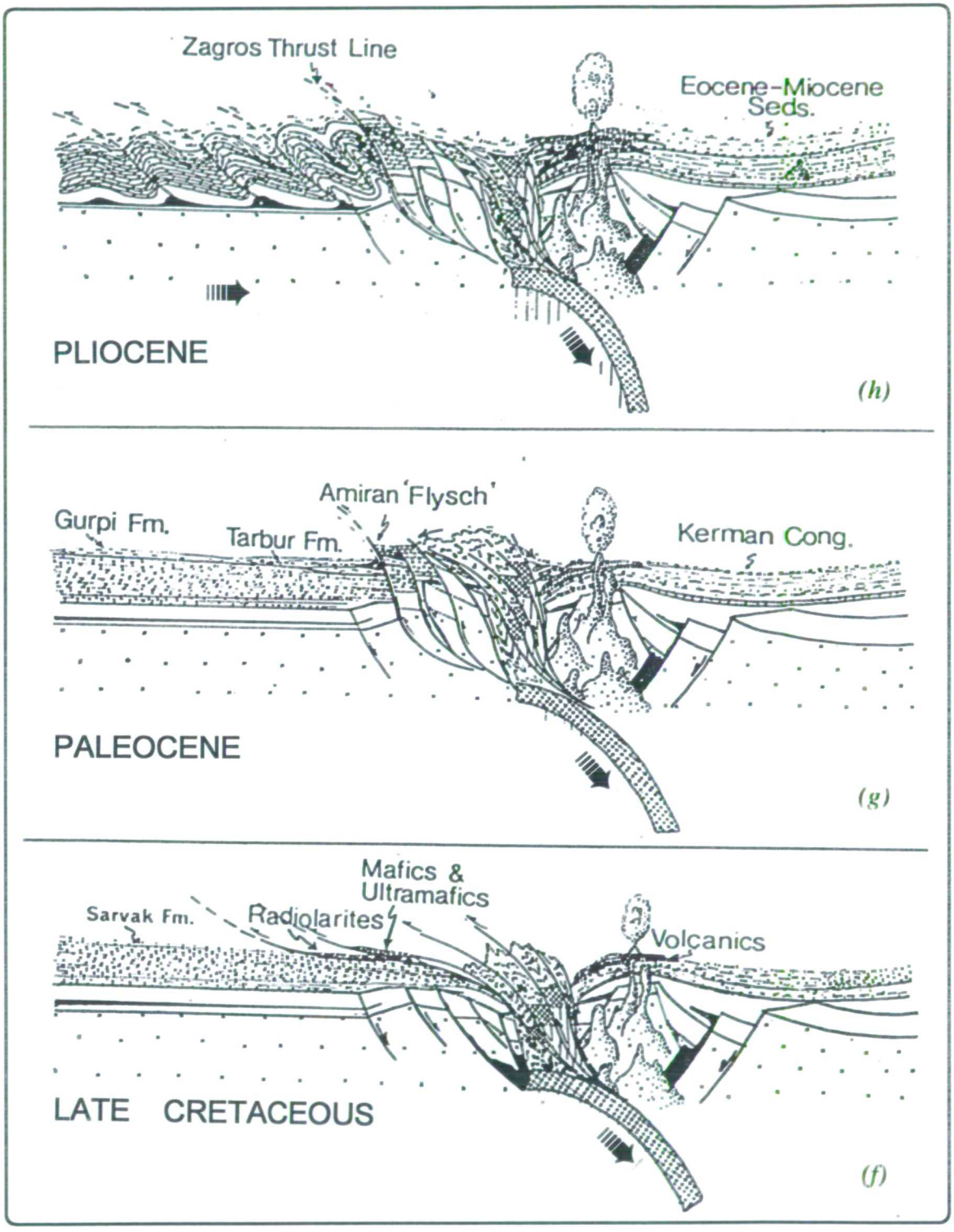


Fig. 5.2 Continued.



Fig. 5.3 Plate tectonic map, showing the opening of the Arlantic Ocean and separation of the Arabian and African plates by seafloor spreading in the Red Sea and the Gulf of Aden.

4. GEOMORPHOLOGICAL EVOLUTION

The present regional geomorphological configuration of the Zagros mountain belt relates to the major orogenic event linked to the opening of the Red Sea in the Miocene. As mentioned earlier in this chapter this event caused an increase in plate velocity and the propagation of deformation SW into the Arabian plate. The associated formation of folds and thrusts played a key role in geomorphological evolution of the region.

The Miocene event mentioned above led to the generation of a pulse of deformation referred to as the Pliocene orogeny and it was in fact during the Pliocene orogeny that the fundamental framework of the present-day structural and morphological setting of the Zagros Mountain Belt took shape. Before this orogeny most of the Zagros belt was below sea level and consequently exogenetic processes had only a minor role in the creation of topography.

During the Pliocene orogeny the generation of major anticlines and the uplift of many Imbricate slabs in the vicinity of the Main Zagros Thrust led to a rapid emergece of the mountain front and its migration towards the southwest. As a result of this process the Zagros sedimentary basin was broken into several smaller troughs all of which migrated towards the SW. As a result of this process most of the relatively small basins dried out or become restricted to form small lakes within the structural depressions (e.g. the Bakhteghan, Maharlu and Tashk lakes, Figs. 2.13 and 2.18) and the main basin driven to the SW to form the present day **Persian Gulf**. The gradual emergence and the southwestward migration of the '*Mountain Front*' initiated by the Pliocene orogeny exposed the belt increasingly to external processes.

This deduced southwestward migration of the mountain building process is supported by

several lines of the structural and geomorphological evidence. These are:

i) The disharmony between the drainage pattern and the geological structures in the Zagros mountains which is seen most strikingly in the transverse gorges resulting from the collision of discordant drainage pattern with individual structural barriers particularly major folds. Examples of these transverse drainage system and gorges are seen in Figs. 2.9-2.12.

ii) The increasingly youthful characteristics of the Zagros gorges in a downstream direction which is suggestive of through-flowing drainage that originated on the protaxis of the highland and maintains itself as deformation and the associated uplift spread to the southwest (Oberlander, 1965).

iii) The constituents of the Early Pliocene Upper Fars and Lower Bakhtiari formations in the outer Zagros which are clearly derived from the interior of the mountain belt. For example, the significant percentage of quartzite and other metamorphic siliceous rocks can only have come from the region of metamorphic and ultramafic rocks, far to the northeast of the Fold zone (Oberlander, 1965).

iv) The abundant sandstone layers of the Lower Bakhtiari Formation, as compared to the siltier Upper Fars, which indicates increasing relief in the emergent orogen (Oberlander, 1965).

v) The northeastward increase in the age and erosional state of the fold structures and their constituent rocks units. This can be clearly seen in Fig. 2.3 and in the satellite image (Fig. 2.5).

vi) As indicated in Chapter 4, The elevation of the median surface of the Zagros folds measured along a marker horizon within the sedimentary cover in 21 geological sections

drawn across different parts of the fold belt, generally decreases from NE to SW.

vii) The precentage shortening of the sedimenatry cover also show a gradual decrease in the same direction which is compatible with the southwestward progress of the mountain building processes.

In addition to the evidence listed above confirming the southwestward migration of the mountain front, there are several other lines of evidence which indicate that *local* uplift related to earlier emergence of some of the structures in the outer Zagros, occurred in addition to the more regional SW migration of the mountain front.

For example, on the basis of isopach maps Oberlander (1965) pointed out that submarine anticlines were forming in the outer Zagros as early as the *Eocene*. He considered that these primal features should not be regarded as mountains, but as barely perceptible swells pushed above the level of marine sedimentation and only occasionally above sea level.

The great barrier of 'Kabir Kuh' in Lorestan (Figs. 3.4 and 3.7) is one of the earlier folds which appeared at least in an embryonic state during the Oligocene, probably well before the lesser folds on the northeast, whose drainage it now deflects so uniquely. The possibility that Kabir Kuh emerged as an island at least in its long and severely stripped crestal region, is supported by its strong deflecting effect on drainage from the interior (Fig. 3.7).

In short, the conclusion which can be drawn from these different geomorphological observations is that the emergence of the mountain belt generally started from the NE and then gradually, but unevenly, migrated towards the southwest. However, the amplification and emergence of some individual, probably fault-induced, larger folds could have taken place independently from the southwestward advancing mountain front.

Thus, although there is a general drop in topography across the belt from NE to SW this simple pattern is modified by local uplift zones. The detailed topographic profiles across the belt can vary dramatically. For example, the NE-SW section across the Bakhtiari mountains shows a rapid drop in elevation from this major culmination in the Zagros range to the lowlands of the Dezful Embayment. This is in marked contrast to the profile through the adjacent depressions i.e. the 'Shiraz-Neyriz Depression' to the SE and 'Lorestan Saddle' to the NW, have much more gently inclined profiles.



CHAPTER 6

Evolution of the Zagros deformation belt

1. INTRODUCTION

In this chapter the results of the studies concerning, (i) the geographical and geological setting of the Zagros mountain belt, (ii) the spatial distribution, geometrical characteristics, and formation mechanism of the Zagros large-scale folds, faults, and diapirs, (iii) the geometrical analysis of folds, the shortening of the sedimentary cover and (iv) the plate tectonic and geomorphological evolution of the Zagros mountain belt which are discussed in detail the foregoing chapters, are used in an attempt to analyse the processes responsible the '**evolution of the Zagros deformation belt**' particularly the Zagros fold and fault belts and salt diapir provinces.

2. PROCESS OF FOLDING AND EVOLUTION OF THE ZAGROS FOLD BELT

The geometrical characteristics of the Zagros folds have been considered by previous workers, especially petroleum geologists in association to the oil and gas reserves. However, their studies are concerned with the role of folds as potential reservoirs and do not generally consider the evolution of the fold belt as a whole.

A few geologists however, have considered the tectonic implication of this spectacular fold belt. Lees (1952) was probably the first to considered the possibility of lateral shortening of the whole sedimentary cover by a pressure from the NE and of sliding over an unfolded basement with the Hormuz Salt acting as lubricant. However, as a result of his study he concluded that the folds were generated by an alternative mechanism, namely that each anticline owed its existence to a separate basement flexure.

Shearman (1976) expressed the view that the Zagros folds did not all form at one and the

same time, but developed '*Serially*'. Mann & Vita-Finzi (1989) tested the assumption that the process of folding was serial and obtained an average rate of advance for the fold front from NE to SW of about 17 mm/yr.

The concept of *serial folding* was introduced by Blay (1974) and developed by Price (1975), Blay *et al.*, (1977), Cosgrove & Price (1987), and Price & Cosgrove (1990) as a process of mountain building by detachment folding above a décollement zone.

'Serial folding' is a special case of the buckling process in which the development of adjacent folds in layered materials such as a bedded succession is not synchronous. The adjacent folds initiate and amplify sequentially. Two types of 'non-synchronous fold development' have been recognised by Blay *et al.* (1977). In the first type, adjacent folds initiate and amplify sequentially (*serial folding*) (Fig. 6.1) and in the second type, folds amplify randomly at different times and at different points within the multilayer (*stochastic folding*).

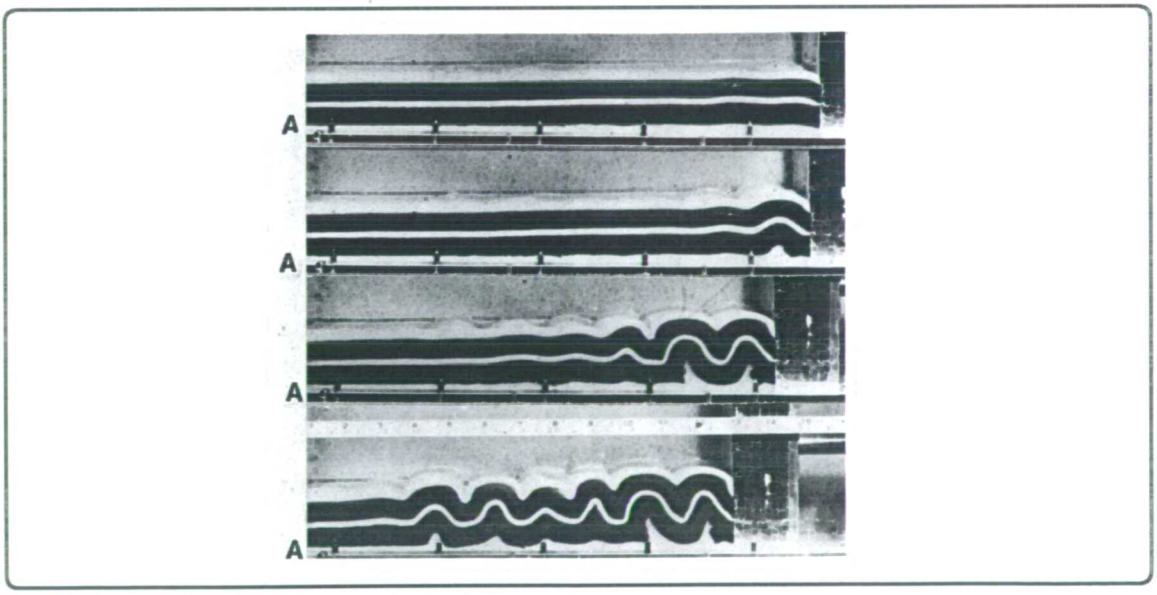


Fig. 6.1 The serial development of folds in a lubricated gelatine multilayer, as the result of the piston moving from right to left (from Blay *et al.*, 1977).

Experiments by Blay *et al.* (op. cit.) indicate that process of *pre-stressing* during the early stages of an experiment, i.e. before the initiation and the amplification of the folds, may play a key role in serial folding. Because of the importance of '*serial folding*' to the generation of folds within the Zagros fold belt, a brief discussion of the model work and results described by Blay *et al.* are presented. For a more detailed discussion the reader is referred to Blay *et al.*, (op. cit.) and Price & Cosgrove (1990).

The three types of apparatus used in the experiments are illustrated in Fig. 6.2. Each type of apparatus allows a particular set of boundary displacements to be applied to a horizontally layered model. In apparatus (a) and (b) a section of the base of the multilayer was slowly raised to simulate basement uplift beneath a sedimentary pile. Structures developed as a result of down-slope gravity gliding of the uplifted section of the model on a thin, lubricated base layer.

In these experiments, the development of thrusts and folds was generally confined to the flat-laying section of the model. In order to study the development of structures in this region more closely, a third type of apparatus ((c) in Fig. 6.2) was used, in which lateral compression produced by gravity gliding was simulated by the action of a vertical piston face driven horizontally against the end of a multilayer by a geared electric motor.

The multilayers were composed of layers of gelatine with identical mechanical proportion but different colours separated from each other and the walls of the apparatus by thin layers of the lubricant, liquid paraffin. Before describing the results of individual experiments, some remarks should be made about the initial development of compressive strain along the length of the models.

Initial lateral compression, whether produced by gravity gliding or by piston movement, did not cause an immediate lateral loading of the whole length of the multilayer. During the

early stages of an experiment, the model could be divided into a section which had become stressed by the source of lateral compression (stippled region in Fig. 6.2 d-g) separated by a stress front (s.f.) from the remainder of the model. This stress front gradually propagated down the length of the model until it reached the fixed end wall of the apparatus at which point the whole length of the multilayer had become stressed.

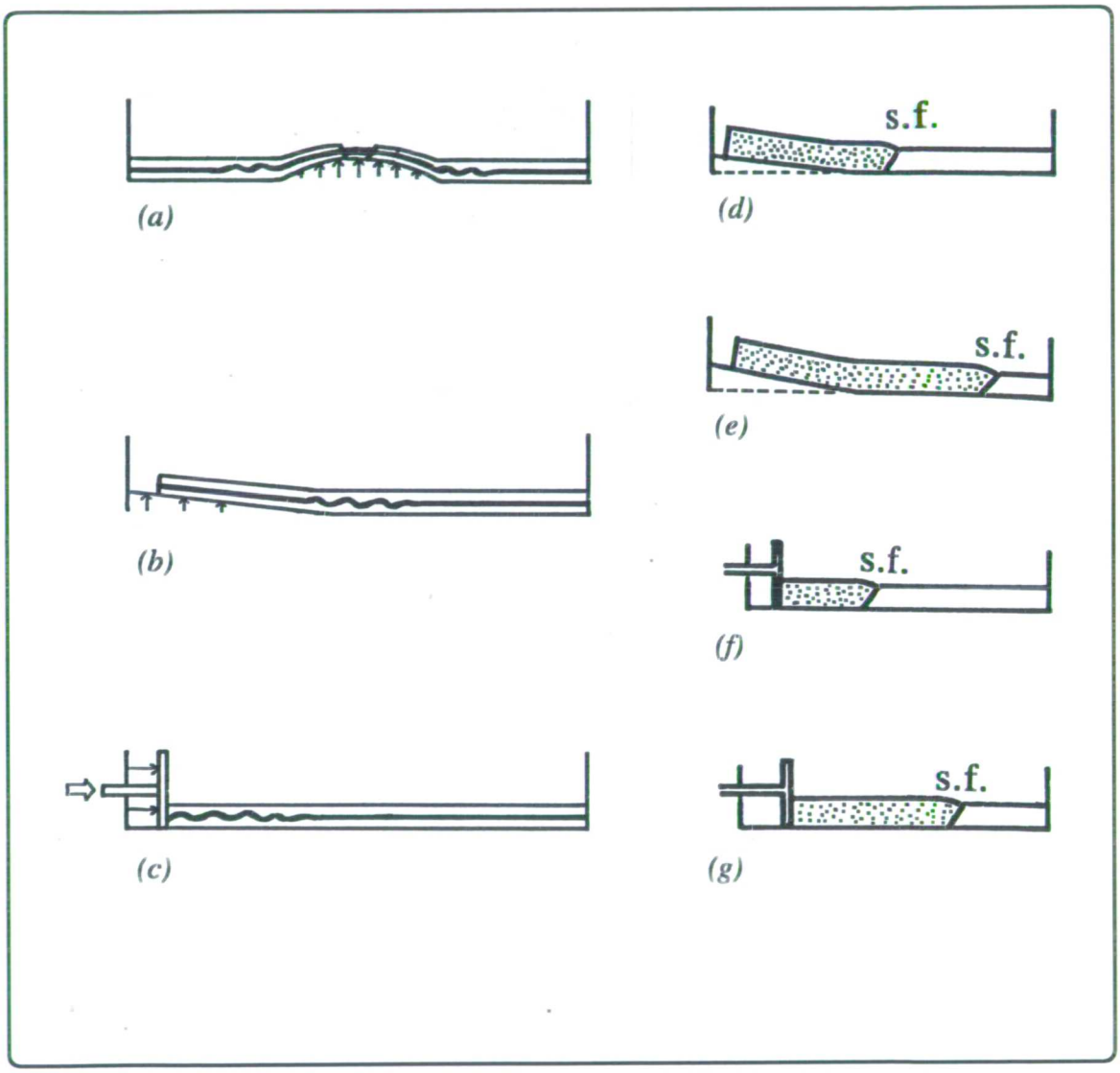


Fig. 6.2 (a), (b) and (c) Three types of apparatus used in experiments on folding. (d-g) A diagrammatic representation of the propagation of the stress front (s.f.) in the apparatus shown in (b) and (c) (from Blay *et al.*, 1977).

The experiment shown in Fig. 6.3 illustrates the role that the stress front played in certain experiments, in the initiation of folds. The experiment is an example of the development of structures on either side of a zone of progressive uplift. Tensile failure of the model occurred at the crest of the uplift together with the initiation of gravity gliding down both flanks of the basement arch. Lateral compressive stress, derived from the gravitational potential of the zone of uplift, propagated through the model behind a slow-moving stress front. However, the relationship between fold development and initial stress development to the right of the basement arch was very different from that to the left.

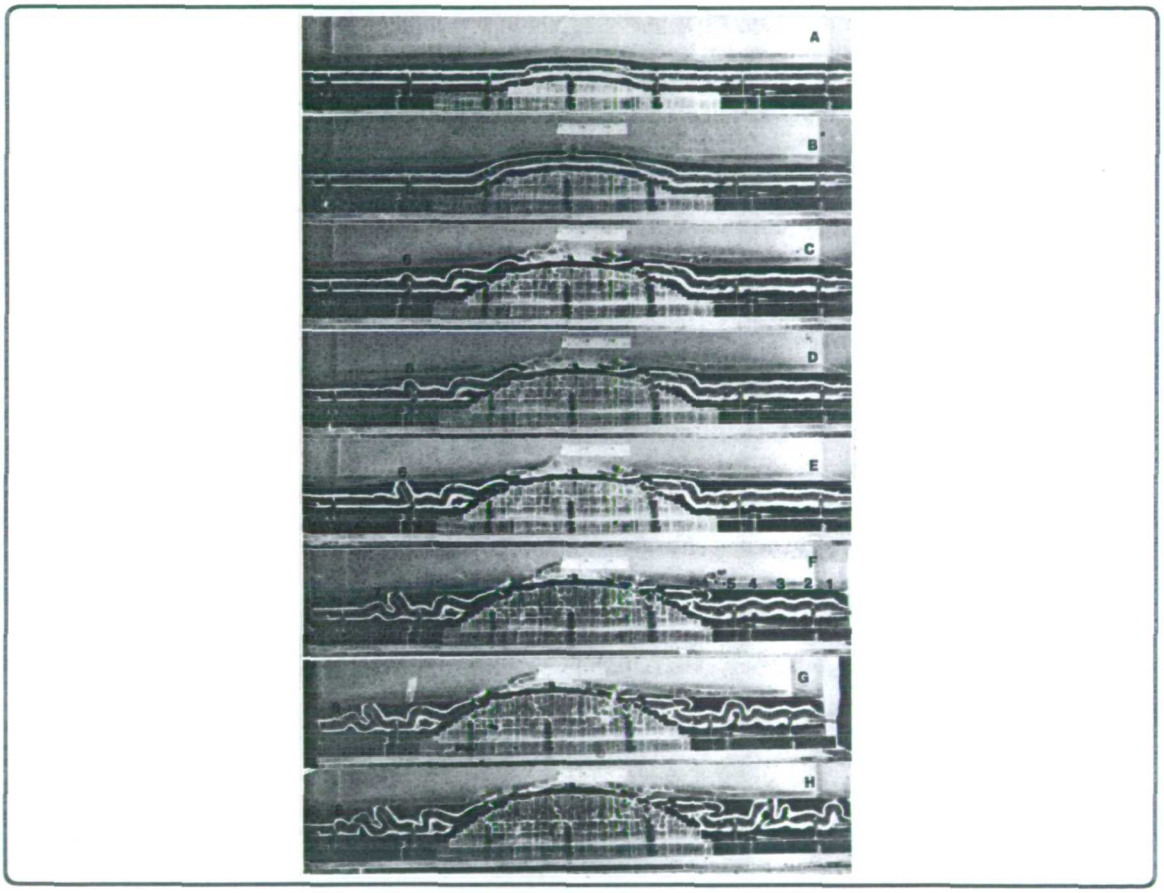


Fig. 6.3 Eight stages in the deformation history of a model multilayer. To the right of the 'basement' uplift, folds develop synchronously as a wave-train in a pre-stressed region of the multilayer. To the left of the uplift, the folds are developed serially at the wave-front as it propagates by a stick-slip mechanism through the multilayer (from Blay *et al.*, 1977).

To the right, the stress front propagated through almost the whole length of the multilayer (Fig. 6.3 a and b) before there was any significant development of the folds. The folds were then initiated as a uniform train of buckles, (folds 1-5, Fig. 6.3 e and f). This is the type of folding that is assumed to occur in most theories of folding where it is implicitly assumed that the whole of the layered system becomes pre-stressed before folds are initiated.

With continued uplift, three of these buckles were selectively amplified (Fig. 6.3 g and h, folds 4, 1 and 3). In contrast, to the left of the basement arch, the stress front became arrested during its propagation and a fold was initiated and amplified at this point of arrest (fold 6 Fig. 6.3 c, d and e). The stress built up behind the arrested wave-front until it was of sufficient magnitude to overcome the local resistance to shear on the décollement, probably an area of little, or no, lubrication. Renewed propagation of the stress front then occurred and a repetition of this process generated a series of folds (Fig. 6.3 e, f, g and h, folds 6, 7 and 8), each fold having developed at the temporarily static stress front.

The observations that folding occurred before the whole of the multilayer and had been pre-stressed and that individual anticlines become amplified at different times during the course of an experiment was typical of the majority of the experiments. Such non-synchronous (but serial) fold development was not always associated with fold initiation at the stress front and, in a number of experiments, occurred after the whole length of the multilayer had been laterally stressed.

A good example of this can be seen in Fig. 6.1, where the stress front reached the fixed end wall of the tank before the folds developed serially from the advancing piston face. Price and Cosgrove (1990) pointed out that the serial development of folds, although a neglected concept, is not a novel idea in geology. For example, it is implicit in Buxtorf's reconstruction of the development of two folds in the Jura Mountains (Fig. 6.4).

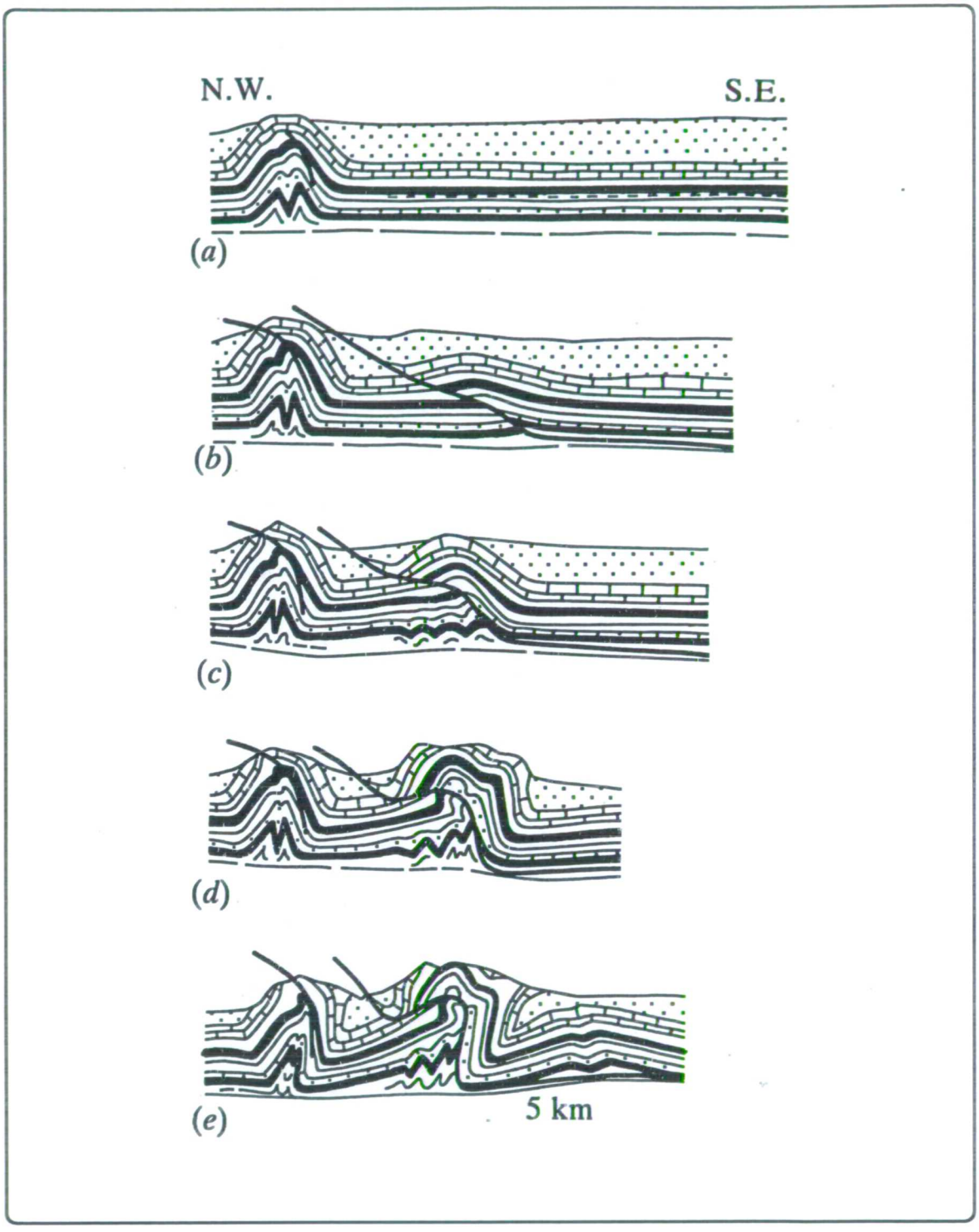


Fig. 6.4 The serial development of structures in the Jura Mountains deduced from field observations (from Buxtorf, 1916).

The rate of migration of the wavefront through a material is given by:

$$v = \frac{Eh_1h_2}{2\eta L} \qquad (6.1)$$

where v is the velocity of the wavefront, E the young's modulus of the layered succession, η the velocity of the viscous décollement and h_1 and h_2 the thickness of the layered succession and décollement horizon respectively (see Price & Cosgrove, 1990). It can be seen that the rate of advance of the wavefront will be directly related to the thickness of the décollement horizon. This is a point we shall return to in Chapter 9, when discussing the effect of variation in thickness of the Hormuz Salt on the Zagros folding.

It is interesting to contrast the non-synchronous, serial development of folds in the experiment shown in Fig. 6.1 with the stochastic, non-synchronous development of isolated anticlines in the experiment shown in Fig. 6.5. In the latter experiment the folds developed randomly within the multilayer after the wave-front had passed right across the model and fold initiation was not caused by the amplification of an adjacent fold, as is the case in serial folding. The cross section through the Jura structures (Fig. 6.5 b) shows the close similarity between the geometry and spatial distribution of the model and natural folds.

It can be seen from the above discussion that the **main conditions required** for the formation of **serial folding process** are:

i) The presence of an undisturbed and mechanically anisotropic sedimentary cover/sequence over a rigid basement block.

ii) The presence of a mechanically ductile layer of sufficient thickness and mobility to act as a décollement horizon between the basement and overlying sedimentary cover.

iii) The presence of a horizontal compression acting from one end of a multilayer sedimentary cover.

iv) The presence of mechanical conditions for classical buckling of the sedimentary cover, leading to the generation of folds by either flexural slip or tangential longitudinal strain mechanisms.

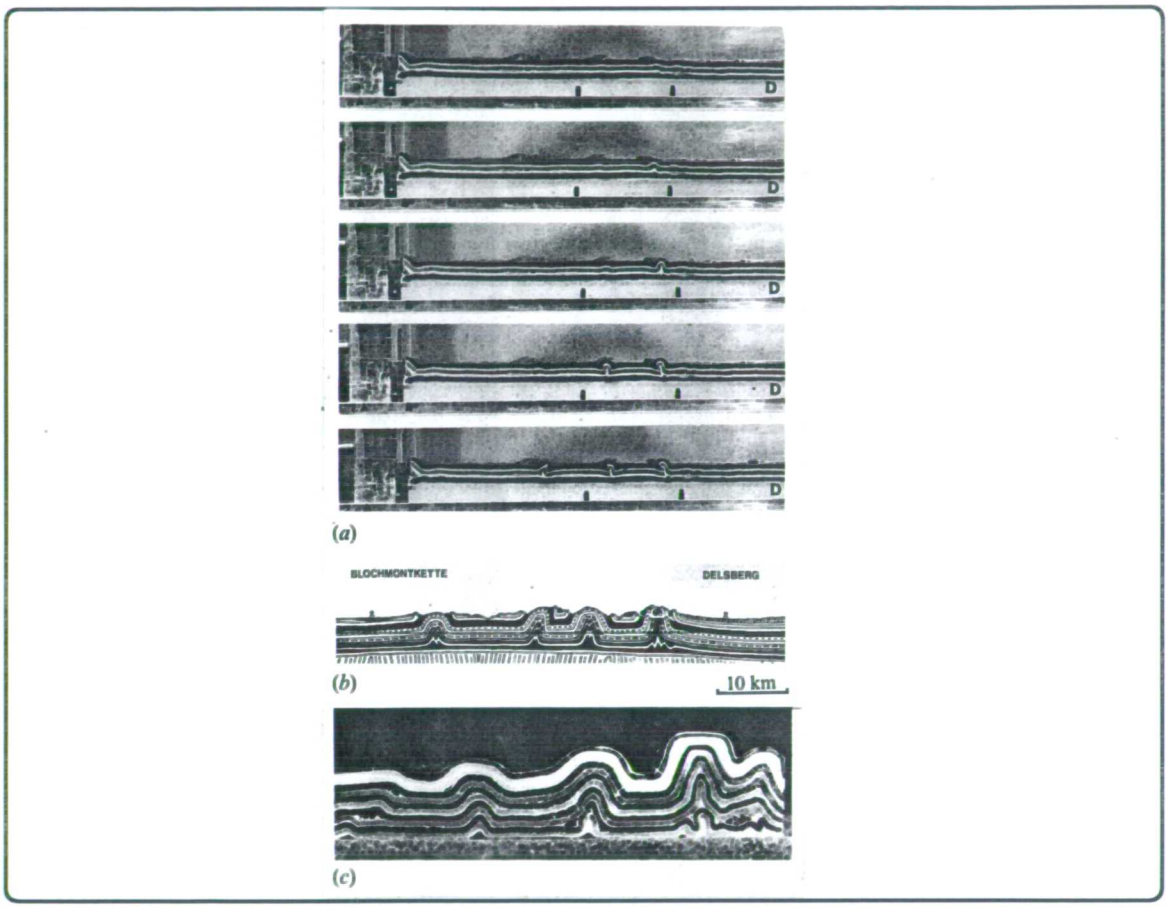


Fig. 6.5 (a) The stochastic development of isolated folds in a compressed gelatine multilayer (from Blay *et al.*, 1977) and (b) a cross section through the Jura mountains between Blochmontkette and Delsberg (from Buxtrof, 1916) which shows close similarity to the model structures. (c) Isolated, straight limbed conjugate folds in a wax multilayer (from Summers, 1979).

A consideration of the previous discussion on, i) the stratigraphy of the Zagros region, ii) the plate tectonic and geomorphological evolution of the Zagros mountain belt, iii) the spatial distribution, geometrical characteristics, and the mechanism of formation of the regional structures, and iv) the results of geometrical analysis of folds and the study of the distribution of shortening of the sedimentary cover, reveals that all the conditions required for the serial folding process are present in the Zagros region and the results of different studies and analyses are all compatible with suggestion by Shearman (1976) that the Zagros folds developed in a '**serial**' manner.

However, as noted earlier, there are many lines of evidence indicating that some of the folds for example, the Kabir Kuh anticline in the Lorestan (Figs. 3.1, 3.3 and 3.7) were generated before the arrival of the fold front. This atypical fold together with other folds in different part of the fold belt which do not seem to have been generated by the serial folding process, are thought to have been initiated as a result of the generation or propagation of a large dip-slip reverse fault.

Nevertheless, In general it can be argued that the generation of the Zagros folds and the evolution of the fold belt started from the NE in the vicinity of the collision zone and then gradually migrated to the southwest.

3. PROCESS OF FAULTING AND EVOLUTION OF THE ZAGROS FAULT BELT

As with the Zagros folds the process responsible for the successive generation of the Zagros faults has been almost overlooked by previous workers.

The review of the tectonic and geomorphological evolution of the Zagros mountain belt (Chapter 5) shows that except for the deep-seated high-angle reverse faults in the Imbricate and Thrust zones which were initiated as normal faults during the opening of the Neo-Tethys sea in Triassic time (Fig. 5.2 b), almost all other Zagros faults, mainly thrust and strike-slip faults, were created during and after the collision of the Arabian and central Iran plates and the ensuing Pliocene orogeny (Fig. 5.2 h).

The thrusts can be divided into two groups. Those of low angle and restricted to the beds of the 'Incompetent Group' above the 'Upper Mobile Group' (Figs. 2.16, 3.5 and 3.30) and those of relatively higher angles that are initiated in the Hormuz salt and cut all the overlying succession (Fig. 3.20). The relationship between the folds and these two groups of thrusts is different.

In the Incompetent Group which is situated above the Upper Mobile Group, it is clear that the initial structures are the buckle folds and that the formation of low-angle thrusts on the steeper flank of the folds occurs subsequently as the folds become progressively more asymmetric towards the SW. Thus if as has been argued, the folds develop serially then the faults would also form in a **serial** manner.

The second group of thrusts are larger, medium-angle dip-slip reverse faults which generally cut the whole thickness of the sedimentary cover and link to the Hormuz salt

décollement zone. On the basis of the geometry and location of the folds associated with these thrusts it is suggested that the folds are '**fault-bend folds**' (Fig. 6.6). Thus in contrast to the fold thrust association in the 'Incompetent Group', discussed in the previous paragraph, the folds associated with the thrusts in the 'Competent Group' post-dates the faults. It is interesting to speculate regarding the relative age of the thrusts shown in Fig. 3.20 and to try to find evidence to support the suggestion that the thrusts propagated from NE to SW by the process of '**Footwall Collapse**'.

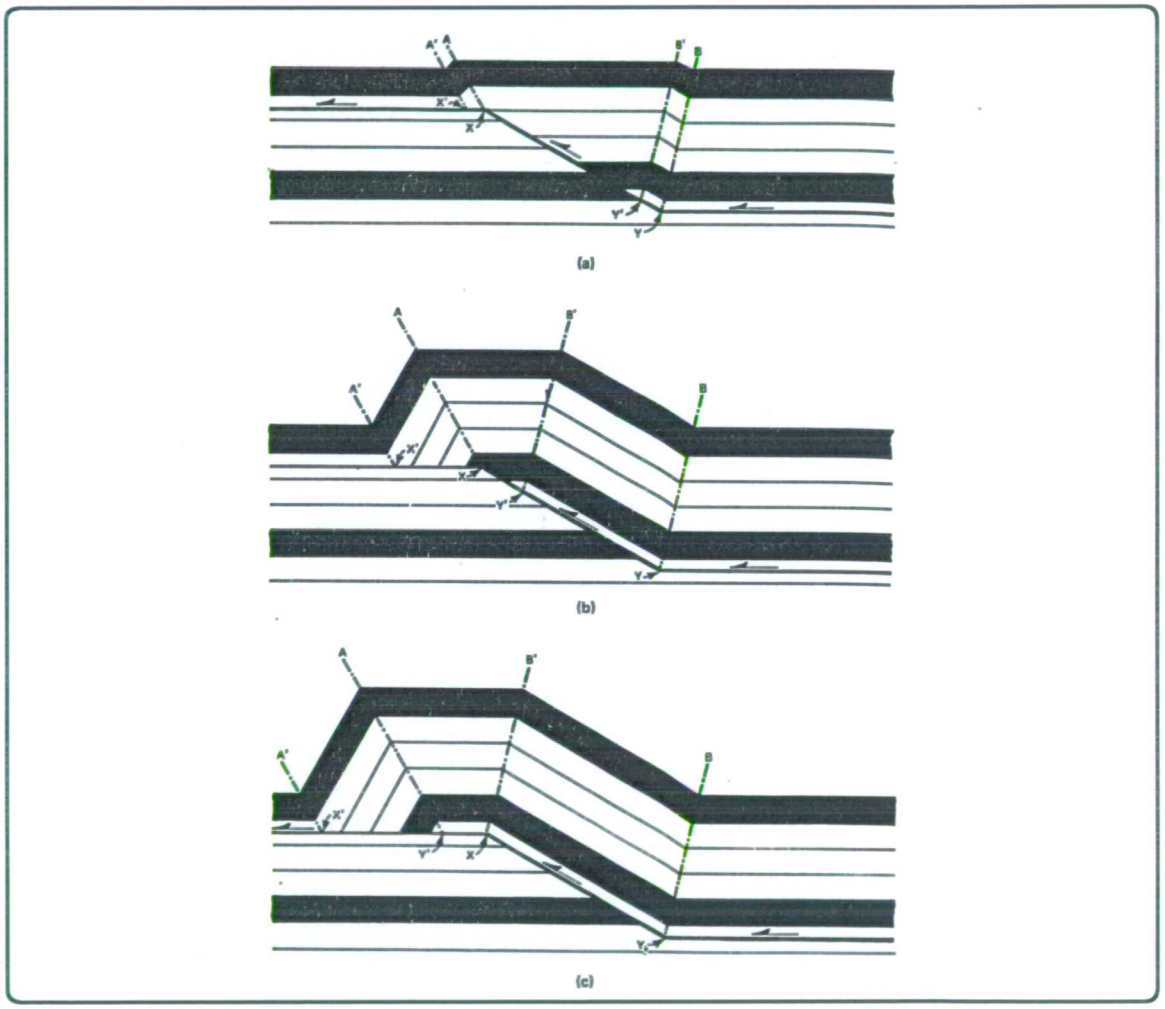


Fig. 6.6 Schematic progressive development of fault-bend folds as a thrust sheet rides over a step in décollement (from Suppe, 1983).

It is commonly observed that a thrust front migrates into a relatively undeformed region by footwall collapse. As a thrust moves along a ramp cutting through a succession of beds, the overlying beds become progressively more deformed (Fig. 6.6). It become more and more difficult for slip to occur and eventually the thrust is abandoned for another thrust which initiates in the footwall. As this new thrust moves it becomes more difficult for slip to occur and the process is repeated (Fig. 6.7).

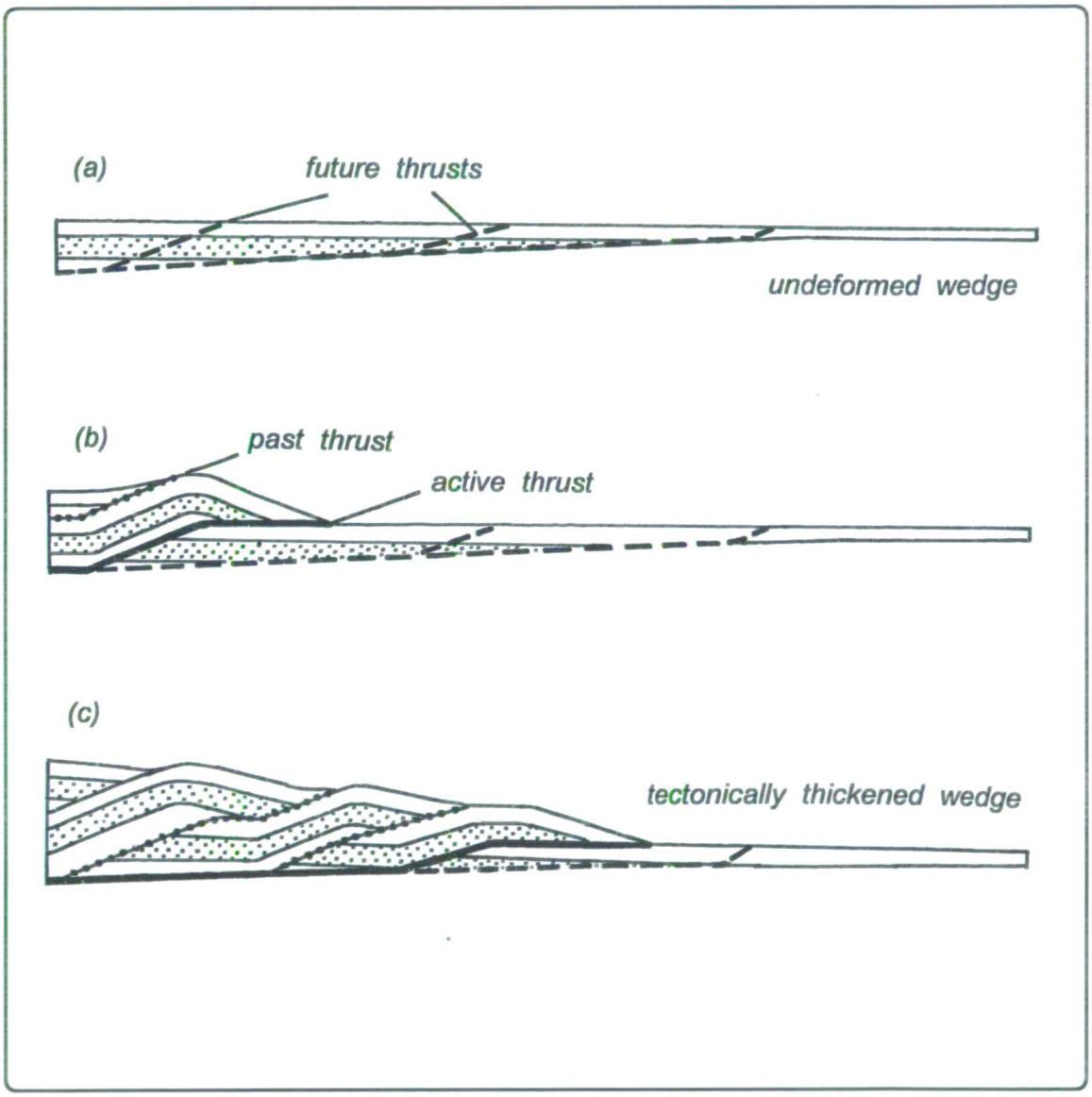


Fig. 6.7 The process of footwall collapse.

It would be expected that the displacement along the thrust and deformation of the thrust block would decrease when traced from older to younger thrusts. Such a decrease can be seen in the Zagros belt, (Fig. 3.20) the least deformed thrusts occurring at the SW margin of the fold belt and the amount of slip and deformation of the thrust blocks increases to the NE. It can be seen from this figure that there are two buckle folds within the section and that these form in horse blocks between adjacent thrusts as a result of continued tectonic compression. The process of '**Footwall Collapse**' can be considered to be the brittle equivalent of '**serial folding**'. The fault-bend folds associated with footwall collapse, will of course also develop sequentially and, in the case of the Zagros belt from NE to SW in exactly the same way that would occur by the process of serial folding (Fig. 6.1).

In conclusion the occurrence of footwall collapse in the Zagros region is indicated by several lines of evidence, i) the presence of a series of reverse dip-slip faults (with dips between 30-60°) which are restricted to the Phanerozoic sediments and which generally link to the Hormuz Salt detachment horizon (Fig. 3.20), ii) the presence of some folds with an abnormal high aspect ratio ($\frac{\lambda}{h}$ wavelength/hinge length ratio), characteristic of forced folds, e.g. the Kabir Kuh in Lorestan (Fig. 3.1, 3.4 and 3.23), i.e. folds initiated over faults which occur amongst the folds with aspect ratios more typical of buckle folds, and iii) the excellent seismic profiles which allows detailed geological cross sections (e.g. Fig. 3.20) to be constructed.

In addition to the thrust faulting that characterises the sedimentary cover, the fold belt is intersected by several major **strike-slip faults** (Figs. 3.22 and 3.27). As mentioned in Chapter 3, the age of these faults is controversial. However, the sense of displacement on these fractures indicates that they are conjugate faults generated by a regional NE-SW compression and are thus compatible with the plate motions that have characterised the region since Late Cretaceous times. As has been discussed in Chapter 3, these faults have played an important role in controlling salt diapirism (Fig. 3.27).

4. PROCESS OF SALT DIAPIRISM AND EVOLUTION OF THE ZAGROS DIAPIR PROVINCES

Despite a controversy concerning the age of intrusions of the salt diapirs, most authors consider that, at least some of the diapirs date back to the Early Cretaceous, or perhaps even Triassic times (Harrison, 1930 1931, Kent 1979, Ala 1974, Falcon 1974, Koyi 1988) which considerably pre dates both the **Late Cretaceous major collision** and **Pliocene orogeny**.

Harrison (1930, 1931) and Kassler (1973) also pointed out that whilst some intrusions have only moved during one epoch, others have moved at least twice, and some have continued moving until almost recent times.

According to Ala (1974) by the Jurassic-Early Cretaceous times a significant number of the present plugs had already been initiated as '**large mounds**' capable of influencing sedimentation on the Middle Cretaceous-Lower Tertiary sea floor and of generating substantial relief. Some of the mounds grew sufficiently to reach sea level during the Middle-Late Cretaceous, and formed islands in the ancient sea like the present-day salt-dome islands (Figs. 3.24 and 3.29) in the Persian Gulf. This is evidenced by the presence of derived Hormuz material in the sediments peripheral to the salt body.

Nevertheless, the **main period of massive salt rise** as indicated for example by Harrison (1930, 1931), Kassler (1973), Ala (1974), Kent (1979), Koyi (1988), and Talbot and Alavi (1996) accompanied or followed the Pliocene Orogeny as the direct consequence of décollement folding over a considerably thick (about 1 km) evaporitic substrata (the Infra-Cambrian Hormuz Salt Formation).

Based on the ideas relating to the tectonic evolution of the Zagros Mountain Belt discussed earlier in chapter 5, the writer supports the suggestions by Kent (1958), Ala (1974), Jackson

& Vendeville (1994) and Talbot & Alavi (1996) that diapirs of the Hormuz Salt did not reach to sea level until the Late Cretaceous. This it is suggested is because of the existence of a thick stiff carbonate overburden (Fig. 2.16) which inhabited salt movement in the absence of any compressional tectonic movement in the region.

The present author considers that the **first generation of salt diapirs reached to sea level** during the Late Cretaceous times as a result of initiation of a horizontal compression from the northeast due to closure of the Neo-Tethys Sea and the collision of the Arabian and Central Iranian plates. It is argued that the this NE-SW trending horizontal compression resulted in generation of many thrust and strike-slip faults and they played an important role in triggering most of the salt rises during and after the collision (Figs. 3.21, and 3.24).

This early phase of diapirism continued through the Paleocene until, as a result of the opening of the Red Sea the plate velocity increased and the horizontal stress rose. This resulted in the Pliocene orogeny, the effect of which are shown schematically in Fig. 5.2 h. The increased compression drove the deformation front SW into the Arabian plate. This initiated a series of folds and new faults within the cover rocks above the Hormuz Salt which flowed into the anticlinal cores and fault planes to form **the second and massive generation of salt diapirs** as plugs and walls. Clearly salt diapirs associated with the first episode of salt intrusion which was triggered by faulting, will not be related to specific folds.

It has already been noted earlier in this chapter that both the folds and the faults of the cover rocks developed in serial (non-synchronous) way. The close link between the onset of diapirism and the formation of the folds and faults in the cover rocks (Figs. 3.21, 3.23 and 3.24) show clearly that, if the folds and faults developed serially, the associated salt intrusions into fold closures and along fault planes must also develop '**serially**'.

In addition to this serial initiation of salt diapirs it seams highly likely that diapirs were initiated stochastically, i.e. at various times and various positions throughout the fold belt, as in result of the random initiation of either folds and faults. Thus two types of non-synchronous diapirism (*serial* and *stochastic*) probably occurred.

The salt diapirs originated from the Upper Mobile Group (Gachsaran Formation) were also generated during the Pliocene orogenic movements. This is particularly so in areas where the salt was thickest or where the process of disharmonic folding generated significant lateral migration of salt to generate local areas of great thickness (Figs. 3.5, 3.30 and 3.33). As mentioned in chapter 4 the general form of the diapirs from this Miocene halite is that of **sult bulges** and '**flow-sheets**' which form along the hinge zones of the NE-SW trending anticlines.

Many lines of evidence indicate that a large number of Hormuz and Gachsaran diapirs are still active and that as a result of continuous compression in the region salt intrusion is still in progress. This is further discussed in Chapter 7, on neotectonics.

CHAPTER 7

Neotectonic activity in the Zagros mountain belt

1. INTRODUCTION

There is some controversy about the scope and purpose of '**Neotectonics**' and especially about how far back in time the prefix 'neo' indicates (Vita-Finzi, 1986).

The term was introduced by Obruchev (1948) to describe 'the study of the young and recent movements taking place at the end of the Tertiary and the first half of the Quaternary' (Pavlides, 1989). Slemmons (1991) writes: 'Neotectonics can be broadly described as tectonic events and processes that have occurred in post-Miocene time'.

Stewart and Hancock (1994) defined 'neotectonics' as the branch of tectonics concerned with understanding earth movements that both occurred in the past and are continuing at the present day. The above definition takes account of much current usage and attempts to avoid arbitrarily restricting the stratigraphic scope of the subject.

Vita-Finzi (1986) also believes that the word 'neotectonics' generally stands for the study of Late Cainozoic deformation and undoubtedly reflects interest in crustal movements which are 'recent' enough to permit detailed analysis and the assessment of rates of changes.

For the purpose of this present study the end of the latest orogenic movements which occurred in the Pliocene times has been chosen as the starting point of neotectonic activity. Accordingly, recent tectonic instability in the Zagros deformation belt during the post-orogenic period up to the present time is considered in the present study to represent the 'Neotectonic activity in the Zagros belt'.

This chapter focuses on the origin and effects of recent earth movements and the evidence for neotectonic activity in the Zagros Mountain Belt. The **seismic activity** in the Zagros region which is one of the most reliable and informative manifestation of the neotectonic activity is considered separately in the following chapter on the seismotectonic activity.

2. ORIGIN OF NEOTECTONIC ACTIVITY

As discussed in Chapter 5, on the plate tectonic and geomorphological evolution of the Zagros mountain belt, the onset of tectonic instability in this region dates back to Precambrian times. During this long time span at least three important regional tectonic events and several local events have affected this region severely.

The 'Assyntic Orogeny' in Late Precambrian times, which affected only the Zagros basement complex and led to a regional metamorphism was **the origin of the first intensive tectonic activity** in the Zagros region.

The opening of the 'Atlantic Ocean' which commenced in Late Jurassic-Early Cretaceous times and led to the closure of the Neo-Tethys Sea, subduction of its oceanic crust, the collision of the Arabian and Iranian continents and the onset of deformation along the northeastern margin of the Arabian plate, in Late Cretaceous time, was **the origin of the second intensive tectonic activity** in the Zagros region.

The opening of 'Red Sea and the Gulf of Aden', during the latest stage of the 'Alpine Orogeny' which led to separation of the African and Arabian plates, the addition of a rotational component to the eastward motion of the Arabian plate, and the formation of the 'Zagros mountain belt' along the northeastern margin of the Arabian plate in the Pliocene was **the origin of the third intensive tectonic activity** in the Zagros region.

The **continuation** of the sea-floor spreading in the Red Sea and the Gulf of Aden, during the post-orogenic times i.e., since the end of Pliocene which caused the 'continuous' rotational drifting of the Arabian plate towards the central Iranian plate and the southwestward migration of deformation into the Arabian plate is considered to be **the origin of the neotectonic activity** and responsible for the **'present seismicity'** and **'active deformation'**.

3. EFFECTS OF NEOTECTONIC ACTIVITY

The continuation of the regional tectonic activity during the post-Pliocene orogenic movements has caused many changes and developments in both the structural and morphological elements of the Zagros region. The structural developments are manifested by further shortening, thickening, and warping of both the sedimentary cover and the basement complex which generally takes place by a combination of coseismic (faulting) and aseismic (folding and salt diapirism) processes. The geomorphological developments are mainly manifested by the recent alterations in the width, depth, course and direction of streams/rivers, and the slope, erosional state, and general configuration of the landscape.

4. EVIDENCE OF NEOTECTONIC ACTIVITY

Evidence of neotectonic activity in the Zagros region consists of a variety of geological, morphological, archaeological, seismological and historical items. The **'seismic activity'** which is the most reliable and informative source of information on neotectonic activity and the **'rates of neotectonic activity'**, will be considered and discussed in the following chapter on the seismotectonic activity of the Zagros Mountains.

a) GEOLOGICAL EVIDENCE

Like most records, the geological evidence from which earth movements are constructed is often ambiguous and always open to more than one interpretation. The three major items at issue are the nature of the deformation, its age and the mechanism responsible for it. The first of these is just as likely to provoke disputes as the other two (Vita-Finzi, 1986).

Nevertheless, the geological evidence of recent earth movements in the Zagros region often involves little ambiguity, since each piece of geological evidence can often be confirmed by non-geological evidence, such as morphological and archaeological evidence.

The most important geological evidence for the neotectonic activity in the Zagros region is provided by recent shortening and thickening due mainly to recent folding, faulting, diapirism. Other evidence includes warping of the folded sedimentary cover in the form of a major anticlinorium, isostasy and the occurrence of unconformities. This geological evidence for the neotectonic activity in the Zagros region are discussed below.

'Recent shortening and thickening' of the Zagros crust, both the Precambrian metamorphic basement complex and its Phanerozoic sedimentary cover, has been in progress since the collision of the Arabian and Iranian plates in Late Cretaceous times. This was intensified during the folding of the Zagros sedimentary sequence in Plio-Pleistocene times.

Recent shortening and thickening in the **basement** generally takes place by very slight warping and the occasional reactivation of inverted normal faults. Snyder and Barazangi (1986) indicated that the Moho dips about 1° to the northeast beneath the Zagros Simply Folded Belt and increases in dip to about 5° near the Main Zagros Thrust. The Moho depth also increases from 40 km beneath the leading edge of the foreland basin to 65 km beneath the Main Zagros Thrust.

Makris *et al.* (1981) using gravity and seismic data, deduced an increase in crustal material of approximately 15 km under the Zagros belt and pointed out that, since the crustal thinning at the spreading zone of the Red Sea is by volume compatible to that of the crustal thickening under Zagros, there is at present no lithospheric destruction by subduction under the Zagros Ranges.

Recent shortening and thickening in the Phanerozoic **sedimentary cover** takes place by a combination of warping, folding and faulting processes. The process of regional warping of the whole sedimentary cover generally takes place as a result of decoupling above the Hormuz salt detachment horizon. The amount and rate of warping, however, is not uniform throughout the mountain belt.

'Recent folding' is manifested by the initiation of new folds along the fold front and the amplification of older folds. Uplift of historical canals in the Shaur anticline (Fig. 3.1), the tilting of Quaternary terraces on the limbs of anticlines and the warping of some of the recent beaches on the Zagros coast were ascribed by Lees and Falcon (1952) to recent anticlinal folding. Intervening drowned valleys were linked to synclinal development.

Kassler (1973) also indicated that on several coastal islands (Kharg, Hendurabi, and Sheikh Shuaib) the Plio-Pleistocene Kharg Limestone is gently arched over the culmination of the underlying Zagros anticlines.

According to Vita-Finzi (1986) at Khomsokh, west of Bandar Abbas, the modern wave-cut platform has a seaward dip of 2° or less, late Pleistocene marine sediments now 20 m above sea level rest on an ancient platform which dips about 10° and the underlying Tertiary beds, truncated by the platform, have dips of about 20°. The position of this sequence on the limb of the Nam anticline parallel to the coast suggests that tilting is a product of progressive anticlinal growth.

'Recent faulting' in the form of the initiation of the new faults and reactivation of old faults is manifested superbly by the widespread **recent seismic activity** which is discussed in details in the following chapter on the seismotectonic activity. However, the evidence of recent faulting is also manifested by the **mappable recent faults** observed in the Quaternary deposits. For example, Vita-Finzi (1975) for the first time, indicated that the *'Chah Shirin fault'* at locality (56°57′ E, 27°22′ N), near the Minab-Rudan road Junction, 40 km north of Minab, is a recent thrust fault affecting Sadaich Alluvium, deposited 7,000-7,300 years ago (Fig. 7.1) and the underlying Aga Jari (Late Miocene-Pliocene) beds.



Fig. 7.1 Chah Shirin fault, southern Iran, in Neogene beds and gravels laid down c. 30 000-7000 years ago. As a second set of deposits dating from 1250-300 years ago is undisturbed, faulting dates from 7000-1250 years ago. Note the dip in the skyline where the fault outcrops (from Vita-Finzi, 1986).

The '*Teleng fault*' which is also a recent reverse-slip fault was found for the first time in the Teleng area of southern Iran by Vita-Finzi (1986). The fault which strikes N20°E and dips 30°NW affects Neogene beds overlying Late Quaternary gravel. The northwestern block of the fault has been thrust over the southeastern by 5.5 m (Vita-Finzi, 1986).

In addition to these recent faults and the other known recent faults from different parts of the region several new faults were also found by the present author in the area east and west of the Strait of Hormuz during the stereoscopic examination of aerial photographs (Figs. 7.2 and 7.3). As can be seen from the photographs these faults affect the recent alluvium deposits and offset the drainage system. The offsets indicate sinistral and dextral strike-slip movements respectively, which is compatible with the regional stress field and the sense of movement in the underlying major basement strike-slip faults proposed in Chapter 3.

'Recent salt diapirism' is manifested by the present altitude of the salt diapirs and the occurrence of the salt glaciers around some of the Hormuz salt diapirs. Despite the fact that vast quantities of salt are dissolved and washed away from the salt domes every year during winter rains, many of the domes stand higher than the rocks that immediately surround them (Shearman, 1976). Nine Persian Gulf islands which are made of salt diapirs (Kent, 1979) are also higher than the surrounding water (see for example the Hormuz Island, Fig. 3.29).

The salt glaciers which occur around some of the Hormuz salt diapirs and which according to Kent (1979) is a phenomenon perhaps unique to Iran, also provide one of the most reliable lines of evidence for active diapirism and neotectonic activity.

The salt glaciers have been studied by several workers such as Lees (1927, 1931), Harrison (1930, 1956), Kent (1958, 1970, 1979) and Ala (1974). Fig. 7.4 shows a large fan of a salt glacier around one of the Zagros salt diapirs in the area northwest of the Strait of Hormuz.



Fig. 7.4 The aerial photograph of the area NW of the Strait of Hormuz, showing an example of a salt glacier around a Zagros salt diapir.

'Recent warping' of the whole Phanerozoic sedimentary cover is manifested by a gentle southwestward, post-depositional tilting of the Plio-Pleistocene Bakhtiari conglomerate, (Fig. 2.3) uplifted terraces as evidenced by incised river systems in the foothills of the central Zagros (Falcon, 1961) and the development of many incised rivers and transverse gorges in the interior Zagros especially in the Bakhtiari Mountains (Figs. 2.9-2.12) (Oberlander, 1965).

'Recent isostasy' is manifested by localised uplift and subsidence. Before 1952 it was widely accepted that deltaic deposition had shifted the head of the Persian Gulf seawards during prehistoric and historic times by over 200 km. Lees & Falcon (1952) then suggested that gradual, although not necessarily continuous *subsidence* had characterized the area as a concomitant of folding of the Zagros belt and that this subsidence had accommodated the bulk of the sediment brought down by the Karun, Tigris, and Euphrates rivers. The evidence cited by Lees & Falcon (1952) included archaeological records, i.e. traces of ancient irrigation canals, rejuvenated stream channels inland, and faunal remains obtained from boreholes.

In contrast, Vita-Finzi (1982) indicated that there is no incontrovertible evidence for recent subsidence, and the one ^{14}C age indicates either stability or uplift. According to Vita-Finzi the volume of fluvial sediment brought down by the Tigris and Euphrates has been drastically reduced at least during the period 30,000-10,000 years B.P. (Vita-Finzi, 1969), and the present sediment load of these rivers gives a misleading impression of the totals laid down in the delta during the Holocene.

'Recent unconformities' provide one of the most prevalent lines of evidence for neotectonic activity in the Zagros region. Massive conglomerates of the 'Upper Bakhtiari Formation' in the central Zagros overlie everywhere the conglomerates of the 'Lower Bakhtiari Formation' with a marked angular unconformity (Oberlander, 1965). Most of the Iranian coastal islands also clearly demonstrate Quaternary movements and the resultant unconformities. On Kharg island, the Kharg Limestone, which is Plio-Pleistocene in age

according to its micro and macro fauna, rests unconformably on Tertiary formations (Vita-Finzi, 1986).

b) GEOMORPHOLOGICAL EVIDENCE

The present topography in the Zagros Mountains is a joint product of both endogenetic (tectonic) and exogenetic (e.g., erosional) processes. The continuation of these two processes after the major Pliocene orogeny, resulted in many new changes and developments in both the structural and morphological configurations of the region, each of which can be used as evidence of neotectonic activity.

'Tilted and uplifted river and marine terraces' are common geomorphic features in the southeastern parts of the Zagros belt. Uplifted marine terraces (fossil shorelines or raised beaches) have been reported from the Iranian Makran for several decades.

Similar terraces to those in the Makran have also been identified in many places along the Persian Gulf coast and its southern islands, particularly on the islands of Kharg and Qeshm by Harrison (1941) and Falcon (1947). Kashfi (1984) suggested that the river terraces in the Mehran river west of the Qeshm Island in the Strait of Hormuz (Figs. 2.7 and 7.5) and marine terraces along the shoreline of the Persian Gulf owe their present elevations to vertical uplift which has taken place in three stages with a variable increase in elevation.

Vita-Finzi (1986) also studied the uplift history of the raised terraces at Tujak (about 200 km SE Bandar Abbas) and pointed out that uplift has been sufficiently rapid for Holocene terraces to be raised by as much as 28.6 m above present-day high water.

A series of tilted and uplifted marine terraces were identified along the eastern coast of the Strait of Hormuz by the present author during the stereographic examination of aerial photographs of the Hormuzghan Province (Fig. 7.5).

As can be seen from Fig. 7.5 b the inland extent of the marine terraces is dramatically influenced by the local structures. In the centre of this figure where the N-S trending Sukaron anticline is parallel and close to the coast, the terraces are restricted to a narrow band near the present shore line. However, to the north and south of this fold the terraces have progressed considerably further inland.

The age and height of the terraces tend to increase inland. They show an uniform slope towards the sea of about 20°- 40°, depending on their original slope, the amount of uplift and their position with respect to the underlying structural grain.

The present height and slope of the terraces however, does not show with any accuracy the amount of uplift and tilting. This is partly due to continuous deposition of beach sands during uplift and partly due to the original slope of the shore.

'A major raised delta' at the mouth of the Mehran River along the Persian Gulf coast (Fig. 7.6), also provides convincing evidence for recent vertical movement. According to Kashfi (1984), the Mehran River is a relatively small river with an often large seasonal discharge. It derives its sedimentary load from the rapidly rising Zagros Range, and deposits it into a shallow and usually quiet body of water in an arid region. The river forms the largest single delta of the Iranian coast, built out into the Persian Gulf as an arcuate feature.

In many modern large deltas, subsidence takes place at the mouth of the rivers where the sediments are accumulating. However, the Mehran River Delta differs from normal subsiding deltas which existed in the geologic past or from modern deltas which are underlain by a great thickness of Quaternary sediments. As indicated by Kashfi (1984), on the Mehran River Delta the sediments are usually oxidized to a tan, light yellowish colour as a result of subaerial exposure, a further indication of uplift rather than subsidence.

'Meanders' along the rivers draining to the Persian Gulf, are a common features of the drainage pattern in the Zagros region (Fig. 2.7). However, in some places along the Persian

Gulf coast for example, east of the Strait of Hormuz meanders have been produced or intensified by local uplifts due to amplification of anticlinal structure, probably the Band-e Lengeh Anticline (Fig. 7.6). The local negative topographic gradient generated by such uplift may become negative and cause anomalous deflections of the rivers:

'**Landslides**' which are the product of rapid and localized earth movements and which usually cause remarkable changes to the regional topography, are sometimes triggered by endogenetic processes. The enormous Saidmarreh Landslide which covers 166 km^2 of the Saidmarreh Valley at the Kashgan confluence and which developed on the southwestern flank of the major Kabir Kuh anticline (Figs. 2.3-2.4), probably formed when a seismic shock jolted this area (Oberlander, 1965).

'Cuestas' which are asymmetric ridges with one face (dip slope or back slope) long and gentle and conforming with the dip of the resistant bed or beds that form it, and the opposite face (scarp slope) steep or even cliff-like and formed by the outcrop of the resistant rocks, are considered to be evidence of recent progressive tilting. The backslope of a conglomerate cuesta composed of the Plio-Pleistocene Bakhtiari Formation, in front of the high Bakhtiari Mountains in the central Zagros, could be the result of neotectonic activity (Figs. 2.3 and 7.7).

This immense mass of detrital materials derived from the erosion of the rising mountain mass in Pliocene times has been stripped back from the mountain front in some areas as a result of post-Pliocene uplift.

The conglomerate cuesta facing the mountain front is best developed in the Dezful Embayment, particularly where it is crossed by the deeply incised Dez and Karun rivers (Figs. 2.3, 2.7 and 7.7) (Oberlander, 1965).

'Transverse gorges' commonly seen north of the 30°N, are also convincing evidence of post-orogenic movements and the southwestward migrating warping of the central Zagros.

Disharmony between drainage and geological structure (Figs. 2.9 and 2.12) in the Zagros mountain is most strikingly seen in the gorges resulting from the collision of the discordant drainage pattern with the individual structural barriers i.e. folds. Some of the most notable of these gorges occur in the 'mountain front' , where the runoff from the interior finally exits onto the detrital foreland (Oberlander, 1965).

As pointed out by Oberlander (op. cit.), the increasingly youthful characteristics of the Zagros gorges in a downstream direction is suggestive of through-flowing drainage that originated on the protaxis of the highland and maintained itself through succeeding orogenic spasms as deformation spread to the southwest.

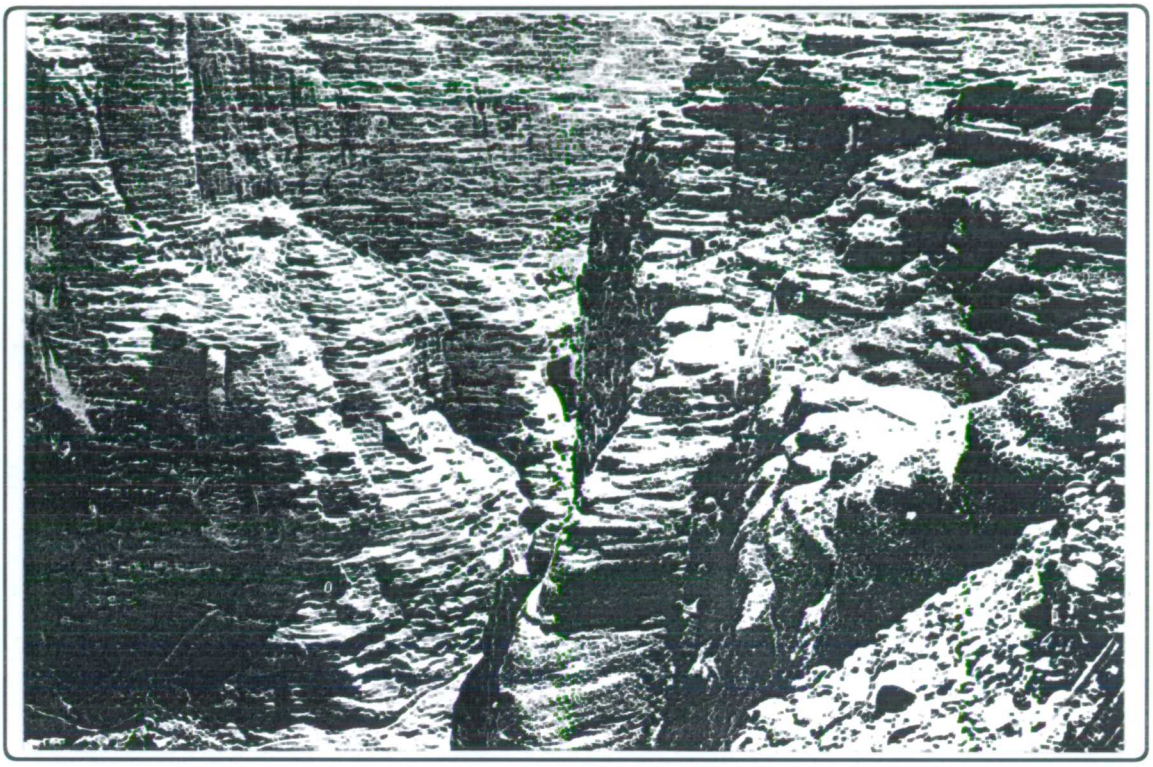


Fig. 7.7 The Dez River canyon through the Upper Bakhtiari Conglomerate cuesta facing the mountain front. The gorge is some **1,500 feet** depth at this point. The Dez Dam is just out of sight behind the projecting wall on the right. The lower half of this canyon is occupied by the reservoir (from Oberlander, 1965).

c) ARCHAEOLOGICAL EVIDENCE

In some special circumstances archaeological evidence can be used as one of the most reliable indicators of recent ground movements. When dated accurately, it plays an important role in the evaluation of ancient earthquakes and ground movements (Vita-Finzi, 1986). In the Zagros Mountains archaeological evidence of neotectonic activity consists of ancient canals, submerged irrigation works, displaced qanats, and ruins.

'Two ancient canals' dug across the Shaur anticline, between Dezful and Ahwaz (Fig. 3.1)

period (first and second century AD) (Lees & Falcon, 1952). In 1955 it was found that one of the canals, which still carried water, had cut down some 4m below its original bed (i.e., a little over 2mm/yr), supposedly because its erosive power had kept pace with uplift.

The other, a qanat, which crossed a higher part of the anticline and whose middle section originally ran in a tunnel, was either too feeble in flow or too poorly maintained to survive, but at the crest of the anticline its bed had risen about 18m in 4km, equivalent to 10 mm/yr (Less & Falcon, 1952; Lees, 1955; Falcon, 1974; Vita-Finzi, 1982).

'**Submerged irrigation canals**' at the head of the Persian Gulf indicated by Lees and Falcon (1952) are further archaeological evidence of recent earth movements in the Zagros region.

'**Qanats**' are water gathering systems for supplying both drinking and irrigation water. A qanat consists of a series of water wells, dug along a straight or bent line which are connected to each other by an artificial underground canal (Figs. 7.8 and 7.9). Qanats, like ancient canals, can be used as evidence of recent movements if they show any departure from their original position, or if the linear alignment of wells shows an obvious offset (Vita-Finzi, 1986).

Qanats are very common in the Zagros and can be detected around most inhabited places, especially at the vicinity of the Persian Gulf, where the temperature is high and precipitation restricted mainly to the winter and spring. However, no offset due to recent faulting was detected by the author during the stereographic examination of the aerial photographs of the Hormuzghan Province.

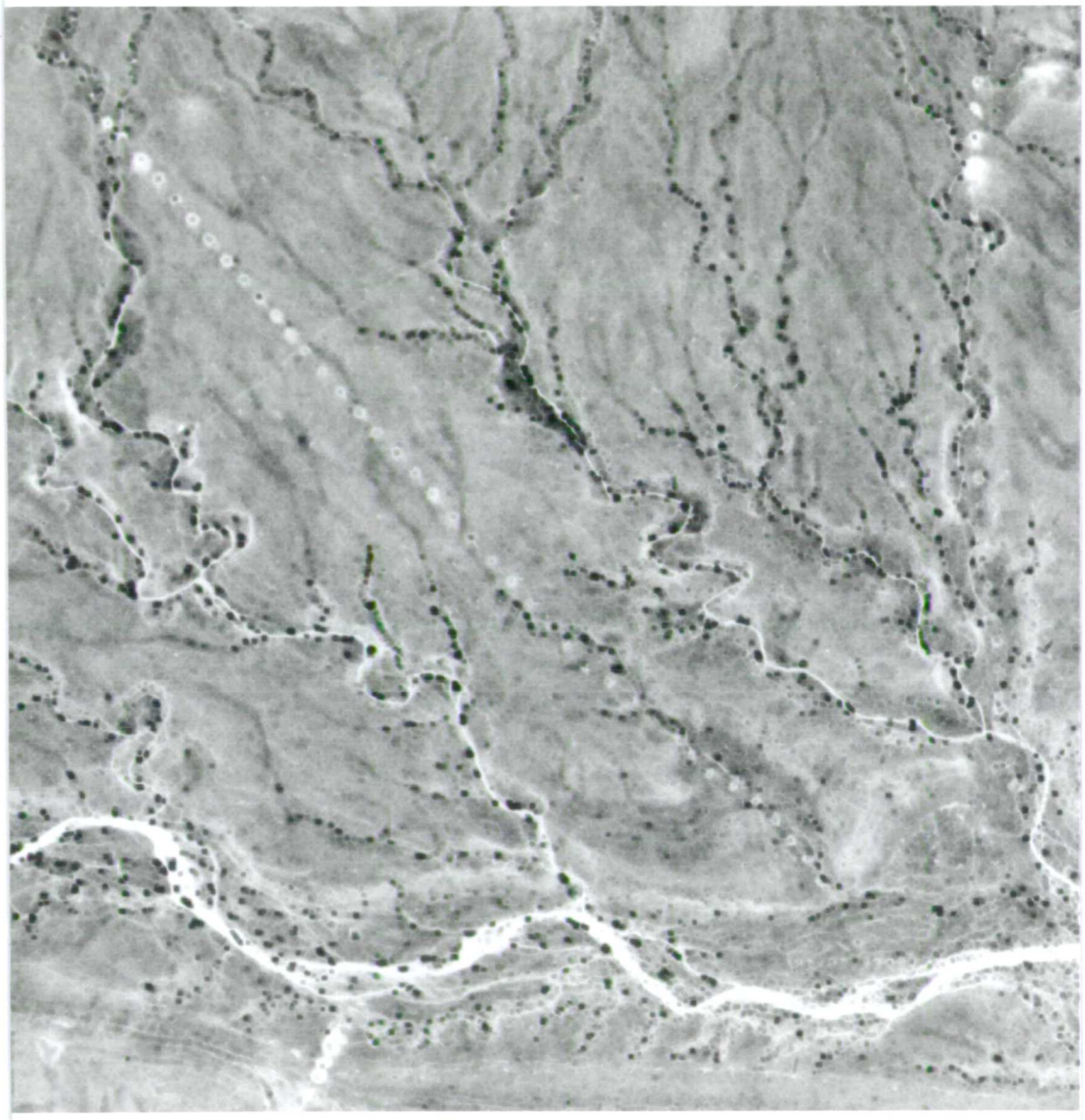


Fig. 7.8 The aerial photographs of the area NW of the Strait of Hormuz showing the strings of well associated with qanats.

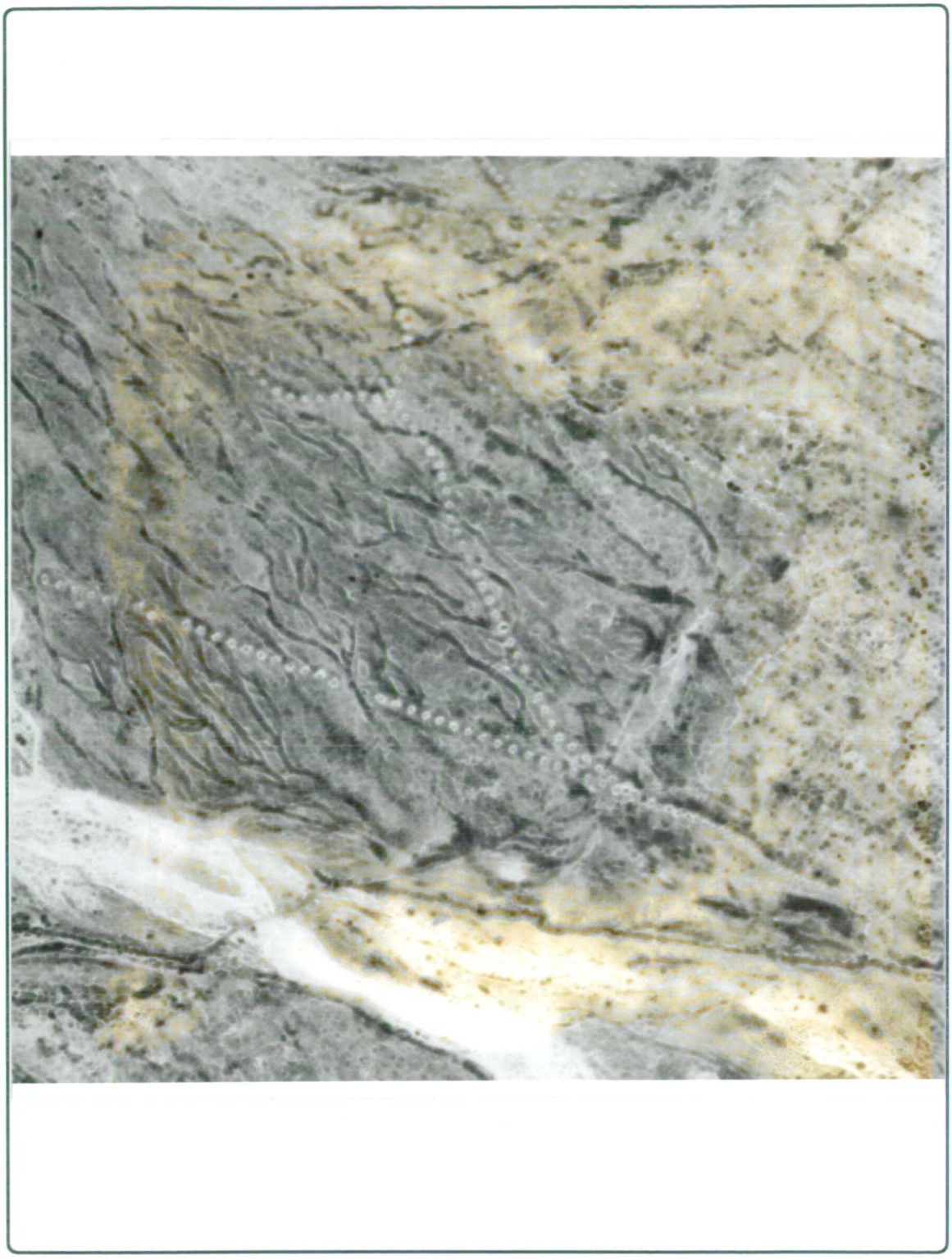


Fig. 7.9 The aerial photographs of the area NW of the Strait of Hormuz showing the strings of well associated with qanats.

'**Ruins**' whose original form is unambiguous, on occasion supply useful limiting ages and also information on the geometry of deformation (Vita-Finzi, 1986). The stereographic examination of aerial photographs of the Zagros Mountains sometimes reveals the traces of small ancient ruined once inhabited places in the vicinity of the present habitat which were most likely ruined by a severe seismic event. The importance of these ruins as evidence of recent earth movements will certainly grow as their interpretation moves from merely demonstrating that seismic activity occurred to contributing new data on the character of the activity.

d) HISTORICAL EVIDENCE

Historical sources can also provide remarkable evidence of neotectonic activity and recent earth movement. Although, like the archaeological evidence, there are many difficulties with historical sources other than eyewitness reports of earthquakes or other ground movements. Even where artifacts are being used for dating geological features their function as well as their age may raise problems of interpretation. The problems are multiplied when the evidence for earth movements is entirely a matter of inference (Vita-Finzi, 1986).

Historical sources benefit greatly from being combined with skilled mapping from air photographs and on the ground even if centuries have elapsed since the earthquake struck. The value of such historical reports, once their reliability has been tested, lies not only in the activity but also in the gaps and pauses they reveal. These gaps however, could be the indication of missed and unrecorded events rather than the absence of events (Vita-Finzi, 1986). For this reason, in dealing with historical events one should always bear in mind an old English adage, *"absence of evidence is not evidence of absence*".

Transmission and survival of historical evidence of neotectonic activity depends very largely on historical or geographical circumstances, which are not necessarily consistent for all regions over different periods in the past. The existing historical evidence therefore must

be reviewed in the light of the circumstances in which they were recorded (Ambraseys & Melville, 1982).

Seismic and coseismic events including, landslides, liquefaction, and damage or offset of archaeological artifacts are the most useful evidence of recent earth movements in the historical sources.

In their book entitled 'The History of the Persian Earthquakes' Ambraseys & Melville (op. cit.), using almost all the available historical sources, reviewed the seismic and coseismic events which have occurred in the whole of Iran since 700 AD up to the mid 1970s.

Using this reference the present author has listed the historical events that occurred in the Zagros region in chronological order and plotted their epicentral locations in a seismicity map of historical events (Fig. 7.10) as **a record of the historical evidence of neotectonic activity** in the Zagros mountain belt.

According to Ambraseys & Melville the first historical record of an earthquake in the Zagros region goes back to the Pre-Islamic period, to the birth of the prophet Muhammad (traditionally in November 570 AD) in **Baghdad**. This earthquake destroyed thirteen towers of the palace of the Khusraus at Ctesiphon south of Baghdad. According to Ambraseys and Melville the occurrence of the earthquake may be admitted, but its symbolic coincidence with the birth of Muhammad need not to be taken seriously. This historical seismic event was followed by many other seismic and coseismic events as follows:

658, **Basra**. A shock that caused no damage.

840, **Ahwaz**. There was a destructive earthquake in the Zagros. In Ahwaz many houses were destroyed and people left the city. The hill overlooking Ahwaz was fissured.

859, **Baghdad**. Baghdad and Mada'in were shaken by an earthquake.

872, June 22, **Samara**. An earthquake devastated the region of Samara, following a damaging foreshock the previous day. The walls fell down and 20,000 people were killed. The shock was also responsible for large-scale landslides in the Samara valley.

902, June, **Baghdad**. A series of earthquake shocks and thunderstorms caused some concern in Baghdad.

958, April, **Hulvan**. An earthquake destroyed Hulvan, modern **Sar-i Pul-i Zuhab**, killing many people in the Jibal, and affecting underground water supplies in the Zagros.

978, June 17, **Siraf**. A locally destructive earthquake occurred at the port of Siraf in Fars. Most of the houses in the town were damaged or destroyed and more than 2000 people were killed.

1008, April 27, **Dinavar**. There was a destructive earthquake in central Zagros. Damage was concentrated in the important city of Dinavar which was totally destroyed with the loss of more than 16,000 people, apart from those who were overwhelmed by landslides.

1008, **Siraf**. There was earthquake at Siraf and along the coast of the Persian Gulf. Many people were killed and a number of ships were sunk, probably by seismic sea-wave (*tsunami*).

1052, **Khuzestan**. A destructive earthquake shock Arrajan and the region around Ahwaz causing walls to collapse and battlements to be thrown from castles. A large mountain there was fissured, possibly by landslides.

1058, December 8, **Western Zagros-Hamrin**. A widely felt earthquake in the western Zagros caused considerable damage, killing many people.

1069, **Jahrom**. An earthquake at Khurshah near Jahrom allegedly caused a loss of water

in the castle, thus forcing its defenders to sue for peace.

1085, May, **Arrajan**. Arrajan and districts bordering it were shaken by an earthquake, causing many deaths and the collapse of the Masjed-e- Jami. Crowds of men and beasts were buried beneath the wreckage.

1118, April 3, **Western Zagros**. An earthquake in the western Zagros was widely felt in Kordestan and in Iraq.

1130, February 27, **Jibal**. There was a destructive earthquake in the western Zagros. The shock caused widespread damage in al-Jazira, in Iraq as far as Mosul and in the Jibal.

1135, July 25, **Kordestan**. A destructive earthquake in Kordestan caused a large number of casualties.

1144, May, **Baghdad**. A strong shock was felt without damage in the city.

1150, April 1, **Hulvan**. There was a destructive earthquake in the region of Hulvan (*Sar-i Pol-i Zuhab*), causing ground deformations in the mountains.

1156, February, **Northern Iraq**. An earthquake shock was felt in northern Iraq possibly in areas bordering with Kordestan.

1179, April 29, **Irbil**. A destructive earthquake ruined castles and villages in the region of Irbil. Large-scale landslides dammed the river for two years.

1226, November 18, **Shahrizur**. A destructive earthquake in Kordestan ruined Shahrizur and destroyed six other castles in the area and many villages.

1291, **Shiraz**. It is alleged that an earthquake caused some damage to the Masjed-e Nau in

Shiraz.

1361, **Qeshm Island**. An earthquake caused much damage to the Island of Qeshm.

1400, **Lar**. An earthquake in Lar destroyed 500 houses.

1440, **Karzin-Qir**. A destructive earthquake in southern Fars caused considerable damage and loss of life at Karzin, and also in other parts of the district of Shiraz, killing nearly 10,000 people.

1495, **Jibal**. There was an earthquake in the Jibal in 900 H. It was felt in Hamadan, Isfahan and Ray. In the region of Hamadan the shock caused a large landslide.

1497, **Hormuz**. a whole town in the vicinity of Hormuz, most probably Gambrun (modern Bandar Abbas), was destroyed and its inhabitants perished in the ruins.

1503, **Hakkari**. There was a major earthquake in the Hakkari region. in the district of Mosul many houses were destroyed.

1506, **Shiraz**. An earthquake in Shiraz caused the collapse of the roof of the library in the Shah Chiragh mausoleum.

1593, September, **Lar**. A destructive earthquake affected Lar in the late summer. Three shocks occurred in forty-eight hours. The second of these, in the early evening, destroyed all of large houses and major buildings. The ground opened up, in some places by as much of two to three metres. The third shock dislodged great boulders from the mountains at the foot of which Lar is situated, and landslides overwhelmed the rest of the town. the earthquake destroyed more than 1200 houses and caused the death of 3,000 people.

1604, June 18, **Basra**. A great earthquake at Basra destroyed most of the houses both inside

and outside the city.

1622, October 4, **Bandar Abbas**. A damaging earthquake in Bandar Abbas and on the Island of Hormuz ruined many houses and caused the collapse of a tower of the fortress.

1623, **Marv-dasht**. An earthquake destroyed Shikasteh and Istakhr castles, among other places. It is probable that this shock was responsible for the collapse of a number of columns in *Perspolis* and for the damage caused in the area of *Nagsh-i Rostam*.

1666, **Zagros**. A destructive earthquake in upper reaches of the Karun river to the northwest of Haft-Tanan decimated the local tribes. The shock brought down massive rockfalls, blocked mountain passes and dammed streams.

1677, **Lar**. Several settlements and caravanserais on the road north from Lar to Bunaru were destroyed by two earthquakes.

1705, **Basra**. A strong earthquake was felt in the region of Basra.

1765, April 23, **Shiraz**. An earthquake in Shiraz caused considerable damage to houses as well as to the structure of Masjed-e Nau.

1766, **Lar**. In The district of Lar an earthquake damaged Lar and triggered landslides that overwhelmed a village and its inhabitants.

1769, May 1, **Baghdad**. During a damaging thunderstorm a number of shocks were felt in the city.

1784, March 1, **Shiraz**. A strong earthquake was felt in Shiraz, without causing damage. To the southeast of the city the shock triggered rockfalls and landslides from the mountains.

1812, **Shiraz**. Shiraz suffered considerable damage from earthquake which partly threw down the Bazaar-i Karim Khan Vakil and shattered the walls of the city, which in collapsing nearly filled up the ditch. Perspolis and Imamzadeh-yi Shah Mir may have been damaged by the earthquake.

1824, June 2, **Kazerun-Shahpur**. The shock destroyed many villages and triggered rockfalls that entirely filled up the mountain pass of Tang-i Dokhtar between Kamarij and Kazerun. Kamarij and the whole village of Diris were totally ruined.

1824, **Northwest Shiraz**. A destructive shock occurred in the district of Shiraz causing serious damages on houses and public buildings. The earthquake also caused a permanent rise in the underground water table in the region of Shiraz, and it was followed by aftershocks for six months.

1825, October, **Shiraz**. A strong shock ruined a number of buildings in Shiraz.

1823, May 5, **Shiraz**. A series of foreshocks began to cause progressive damage in Shiraz. Then at noon on 5 May the main shock almost totally destroyed the city. The shock triggered rockfalls on the road to Ardakan and caused widespread liquefaction of the ground to the southeast of the city.

1862, December 21, **Shiraz**. Preceded by two very strong foreshocks, an earthquake caused extensive damage in the region of Shiraz. The ground slumped and mountain was cleft in two.

1894, February 26, **Shiraz**. A destructive shock destroyed many villages around Shiraz killing many people.

1909, January 23, **Silakhur**. A catastrophic earthquake devastated the Silakhur valley, southeast of Burujird in the Zagros. Damage was particularly heavy. In all, 128 villages

were affected, of which 64 were totally destroyed with a loss of life estimated between 6,000 and 8,000. The earthquake was associated with faulting which extended for a distance of forty-five kilometres from near Kalanganeh to the south of Sarvand.

1929, July 15, **Izeh-Anika**. A damaging earthquake shock the southeast provinces of Khuzestan and Bakhtiari. On the southeast face of Kuh-i Landeh the earthquake triggered a landslide and in places rockfalls that produced a discontinuous scarp about one kilometre long.

1972, April 10, **Qir-Karzin**. Throughout March 1972 a swarm of shocks in the districts of Hingam and western Karzin had forced the people to live outside their homes. Early on the morning of 21 Farvardin 1351 a destructive earthquake shock central Fars, almost totally destroyed the town of Qir, Karzin and Afzar. The earthquake was associated with minor and discontinuous ground deformations.

CHAPTER 8

Seismotectonic activity in the Zagros mountain belt

1. INTRODUCTION

'Seismotectonics' is a branch of geoscience that is concerned with the relationship between the seismological characteristics of present-day earthquakes and tectonics. Accordingly, this chapter examines the earthquake data in the context of the evidence for **neotectonic activity**.

Two catalogues of earthquake data from the National Earthquake Information Centre (NEIC) and the International Seismological Centre (ISC) along with a catalogue of historical data provided by Ambraseys and Melville (1982) are used for the examination of the epicentral location, magnitude, and focal depth of historical and modern events. A subset of available fault plane solutions of the Zagros earthquakes obtained from different publications are also considered for determining the sense of movements on the active faults and the state of regional stress.

2. THE QUALITY OF THE ZAGROS EARTHQUAKE DATA

Earthquake data are always considered to be evidence of neotectonic activity and informative clues regarding the state of regional stress, and the position, geometry, and sense of movement of active faults. Nevertheless it is essential to take into account the quality of the data over different time spans when interpreting the regional pattern.

The evidence used in this chapter includes a set of 'Macroseismic data' bearing on historical events and obtained from historical sources, and two subsets of 'Instrumental data', bearing on modern shocks. Both types of data involve errors.

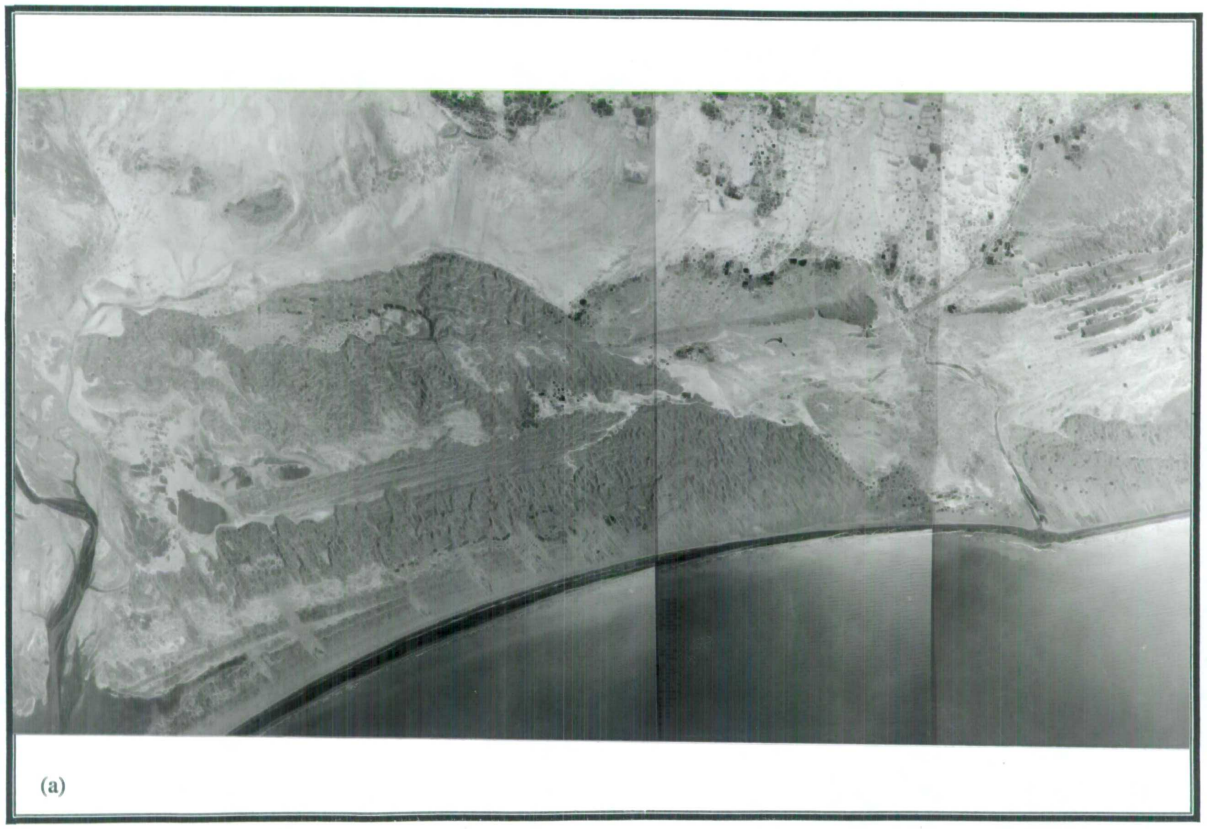
According to Ambraseys and Melville (1982), the quality, transmission and survival of macroseismic data depends very largely on the following parameters: i) historical and geographical circumstances, which are not necessarily consistent for all regions over different periods of the past, ii) the distribution and density of settled population and

major routes, and the geographical proximity of an urban centre to epicentral region, iii) fluctuations in the importance of urban centres and routes, iv) the existence of local records, and v) the personal, religious, and political views of the local authors or travellers and their understanding of seismic phenomena.

Since, according to Ambraseys and Melville (1982), the study of historical earthquakes based on the observations over a period more than ten times longer than the ninety-six years that have elapsed of this century, leads to better understanding of the generic cause of earthquakes, the epicentral distribution of historical events are examined in this chapter, despite the lack of ideal precision. The imprecision of instrumental data, especially for the period before 1963, originates mainly from the lower quality and poor distribution of recording instruments, as well as the techniques used for determining the earthquake parameters.

The first earthquake in Iran to be recorded by an instrument occurred in **Tabriz** at 19 hours 49 minutes on 4 October 1856. It triggered a Cacciator-type seismoscope in the observatory of Tabriz, which was established by the Russian Consul N. Khanikoff early in 1855. However, it was the larger earthquake of 8 July 1895 that was first recorded by practically all the seismographs in operation (mainly in Europe), at the time. At that time there were only about ten stations equipped with seismographs and these by modern standards were very imperfect. In 1903 there were 69 seismological stations in all, most of them in Europe and by 1910 the number of stations had increased to almost 200 (Ambraseys and Melville 1982).

Attempts at the instrumental location of '**epicentres**' in Iran, date from the turn of the century. In the following decades the number of seismological observations increased rapidly and epicentre location errors gradually decreased. Following the installation of the World-Wide Standardized Seismograph Network (WWSSN) in 1962, with special stations in about 60 countries around the world, the United State Geological Survey (USGS) began a systematic magnitude determination program in the Preliminary Determination of Epicentres in 1963. Since then the location errors have decreased



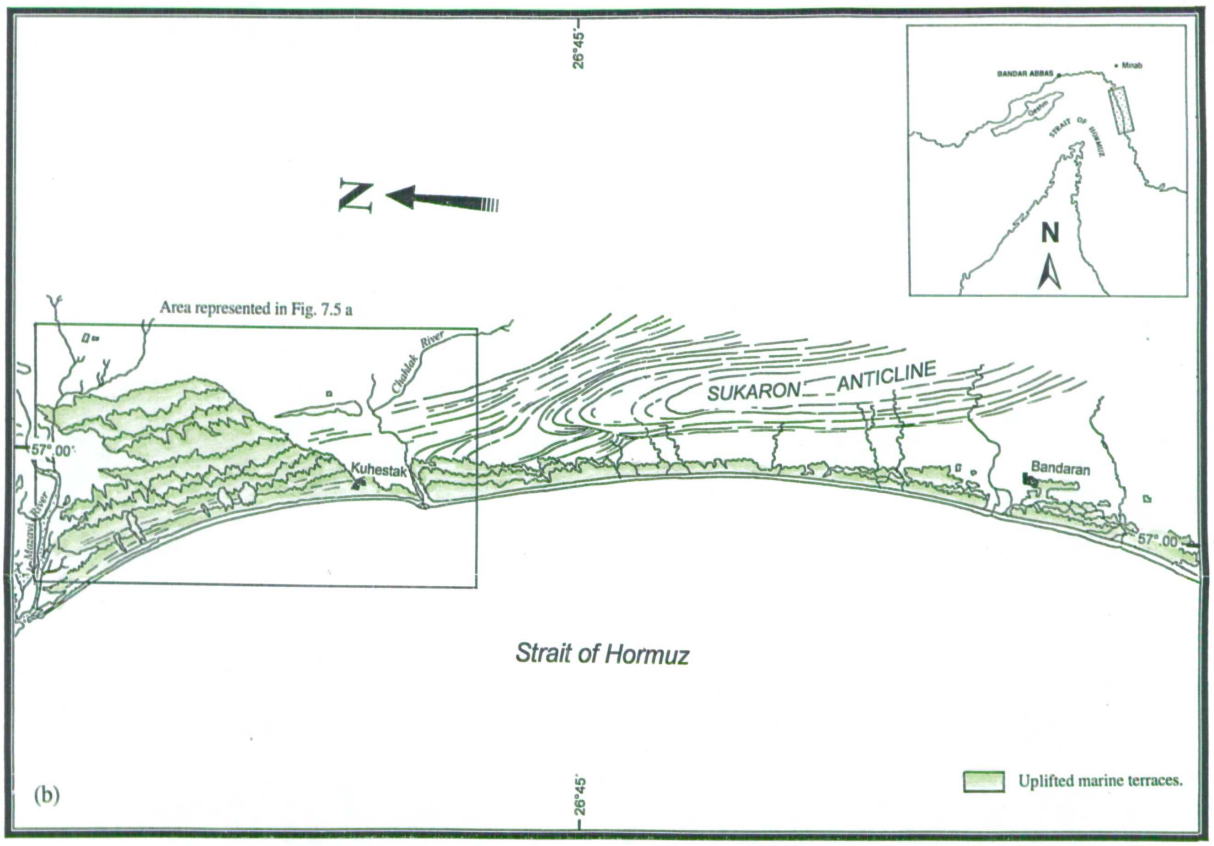


Fig. 7.5 (a) Aerial photograph of the area along the eastern coast of the Strait of Hormuz, showing uplifted marine terraces along the coast. (b) Aerial photograph interpretation of a larger area of the eastern coast of the Strait of Hormuz, showing the influence of the Sukaron anticline on the development of the uplifted marine terraces.

rapidly but remain on average in excess of about 10 kilometres which is just above the limit of macroseismic location (Ambraseys and Melville 1982).

The present difficulties in determining the accurate location of earthquake epicentres and the correlation of earthquake events to any known surface fault in Iran, especially in the Zagros region arise from the following imperfections in the seismic and geological data:

1. Shortage of well documented historical data.
2. Considerable location error in the instrumental data.
3. Limited number of regional seismological stations
4. Poor azimuthal coverage.
5. Lack of adequate micro-earthquake surveys.
6. Systematic and random reading errors.
7. Lack of adequate fault maps.
8. Absence of Quaternary faulting from most of the geological maps.
9. A lack of adequate knowledge of the structural setting of the Precambrian metamorphosed basement at depth, where most earthquakes occur.
10. Presence of a considerably thick (about 1 km) mechanically ductile evaporitic décollement horizon (the Hormuz Salt Formation) between the sedimentary cover and basement together with several other minor horizons within the sedimentary cover, each of which act as a zone of slippage, disconnecting the sedimentary cover from the basement and its different rock units/lithological groups from each other (Fig. 2.16).

Instrumental determination of the '**focal depths**' of earthquakes involved even greater errors mainly due to some additional difficulties arising from the technique utilized, inaccuracy in the arrival time and many other deficiencies. During the last three decades, remarkable improvements have been achieved in modifying the focal depths of past earthquakes. However, many events were relocated for a **fixed focal depth of 33 km** as the inaccuracy of arrival times did not permit valid depth determination.

The present data concerning the '**magnitudes**' of the events also involves some errors and discrepancies. This is, of course, due to the fact that the determination of earthquake magnitude in its present-day concept dates from as recently as in 1967.

No magnitudes are available for earthquake events in Iran before 1909, and for the period up to 1930 Gutenberg and Richter assigned magnitudes to only half the events of magnitude greater than or equal to 6. For smaller shocks magnitudes remain unknown. For the period 1931 to 1948 these authors assigned magnitudes to all the earthquakes greater than 6, but only to very few below this value. Magnitudes estimated by individual stations in the period 1949-60 are quite numerous but very heterogeneous (Ambraseys and Melville 1982).

In short, the available Zagros earthquake data for the events prior to 1963 involves gross errors and cannot be considered reliable. Even more recent data, which are usually determined using the records of sophisticated and computerized instruments and more advanced techniques, involve some common and standard errors.

The present standard errors of the earthquake data, reported by several international agencies, are 1/4-1/2° in the epicentre location, 2-25 km in the focal depth, about 0.2-0.3 units in magnitude, and around a second in the origin time (Båth, 1979).

However, despite the present imperfections in the seismic and geological data, examination of these data can still reveal many important and meaningful results. Several authors, for example Nowroozi (1971, 1972, 1976), Berberian (1976, 1977, 1979, 1981, 1995), Ni and Barazangi (1986), and Jackson and McKenzie (1984, 1988) have examined the available Zagros earthquake data sets and attempted to correlate the better located seismic events to the known surface or subsurface faults.

3. ANALYSIS OF THE ZAGROS EARTHQUAKE DATA

In an attempt to obtain a better understanding of the seismicity of the Zagros region the present author drew extensively the National Earthquake Information Centre (NEIC), and the International Seismological Centre (ISC) data sets for the period 1963-1988. These provided data on 1075 and 1560 seismic events within the Zagros region respectively. In addition data was also gleaned from the literature.

For example, data for the analysis of earthquake events during the period 1900-1950 from a catalogue of over 600 relocated earthquakes for the period 1900-1975, prepared by Nowroozi (1976), and data for the analysis of the historical events for the period 700-1900 AD, prepared by Ambraseys and Melville (1982).

The results of these studies are presented in a number of graphs and maps. The distribution of earthquake epicentres, magnitudes and focal depths are considered and the information provided by fault plane solutions (taken from Nowroozi 1972, Jackson and McKenzie 1984, Chandra 1984, and Ni and Barazangi 1986) discussed in terms of the Zagros tectonics.

a) EPICENTRES OF THE ZAGROS EARTHQUAKES

An '**earthquake epicentre**' is defined as a point on the earth's surface vertically above the earthquake focus, which is a small volume of several cubic kilometres and regarded for most practical purposes as a point. Earthquake epicentres are usually specified in terms of geographical coordinates, *latitude* and *longitude*, and routinely determined by using the arrival time of the earthquake waves (Båth, 1979).

As noted in the previous section, the accurate determination of epicentre locations and the correlation of the earthquake events to any known surface fault has always been a difficult task in Iran and the Zagros region in particular, and the available data sets

regarding the earthquake epicentres are not totally reliable. Nevertheless, the examination of the available data still provides significant information which can be summarized as follows:

i) Two seismicity maps prepared by the author, based on NEIC and ISC data sets for the period 1963 to 1988 (Figs. 8.1 and 8.2), and one seismicity map prepared by Ni and Barazangi (1986) (Fig. 8.3) indicate that the entire Zagros Mountain Belt is a region of relatively high seismicity. The epicentre distribution of earthquakes, however, as can be seen from these figures, is not uniform throughout the belt.

ii) Most of the seismic activity related to the Zagros belt terminates along the Main Zagros Thrust but a zone of high activity extending NE of it occurs in the vicinity of 34°N, 48°E, where the NW-SE trending Main Zagros Thrust changes its trend and joins to the NNW-SSE trending Minab and Zendan transpressive faults (Figs. 8.1- 8.3).

White and Ross (1979) detected a large basement ridge on multichannel seismic reflection and gravity profiles to the west of the Minab-Zendan fault zone, and suggested that this ridge could be a subsurface continuation of the Musandam Peninsula beneath the Strait of Hormuz. Almost the same conclusion has been reached by Chandra (1981) and Kadinsky-Cade and Barazangi (1982). As discussed later in this chapter, this anomalous zone of seismicity is probably related to the indentation of the Musandam block into the Central Iranian plate.

iii) To the southwest the seismic activity extends beyond the 'mountain front' as far as the middle of the Persian Gulf and into Iraq (Fig. 8.1 and 8.2), demonstrating that the width of the seismic belt is greater than that of the mountain belt.

iv) Like the Zagros Mountain Belt, the seismic belt is relatively narrow in the northwest but gradually widens towards the southeast, with a corresponding increase in seismicity (Figs. 2.1, 2.4, 8.1 and 8.2). The most active point within the Zagros mountain belt is the area north of the Strait of Hormuz and associated with the indentation of the

Musandam Peninsula.

v) As can be seen from the seismicity maps, based on NEIC and ISC data sets for the period 1963-1988, the concentration of epicentres occurs along a wave-shaped zone which coincides approximately with the '**sinuous**' map view of the Simply Folded Belt (Figs. 3.1, 8.1, 8.2, and 8.3). However, within this zone of high concentration, the spatial distribution of the events is not uniform and the much higher concentrations are seen along several seismic trends which coincide with most of the mappable fault zones and major topographic fronts (Figs. 3.22, 8.1 and 8.2).

vi) In contrast to the'Simply Folded Belt' the 'Thrust' and 'Imbricate' belts, especially to the SE have a relatively low level of activity (Figs. 8.1-8.3). The writer considers that this could be due to presence of dominantly high-angle dip-sip reverse faults in these belts which may be too steep for reactivation or will require a much higher stress level to reactivate compared to the lower-angle dip-slip reverse faults within the Simply Folded Belt.

vii) Comparison of the epicentre distribution of the large historical earthquakes for the periods from 700 to 1900 AD (Fig. 8.4 a), with that of the first half of the twentieth century from 1900 to 1950 (Fig. 8.4 b), and modern events from 1963 to 1988 (Fig. 8.4 c) shows that the epicentre distribution of Zagros earthquakes has a similar pattern through time

viii) The seismicity maps of the Zagros region reflects the distribution of both the exposed and blind active faults and indicates a close relationship between seismicity and other manifestations of the neotectonic activity in different parts of the Zagros belt.

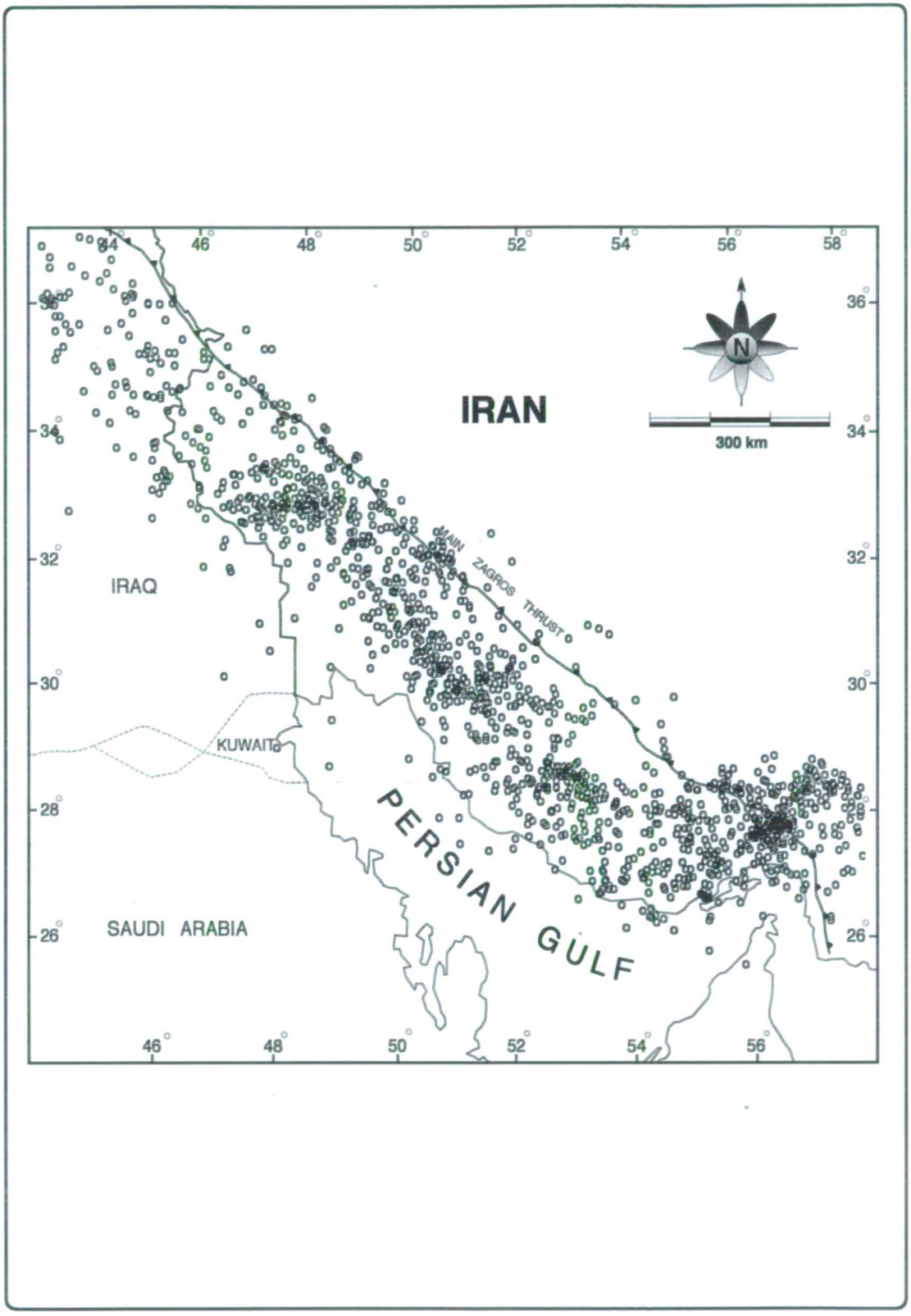


Fig. 8.1 Epicentre distribution of the Zagros earthquakes of magnitude (3-7.1) for the period 1963-1988 (based on the NEIC data set).

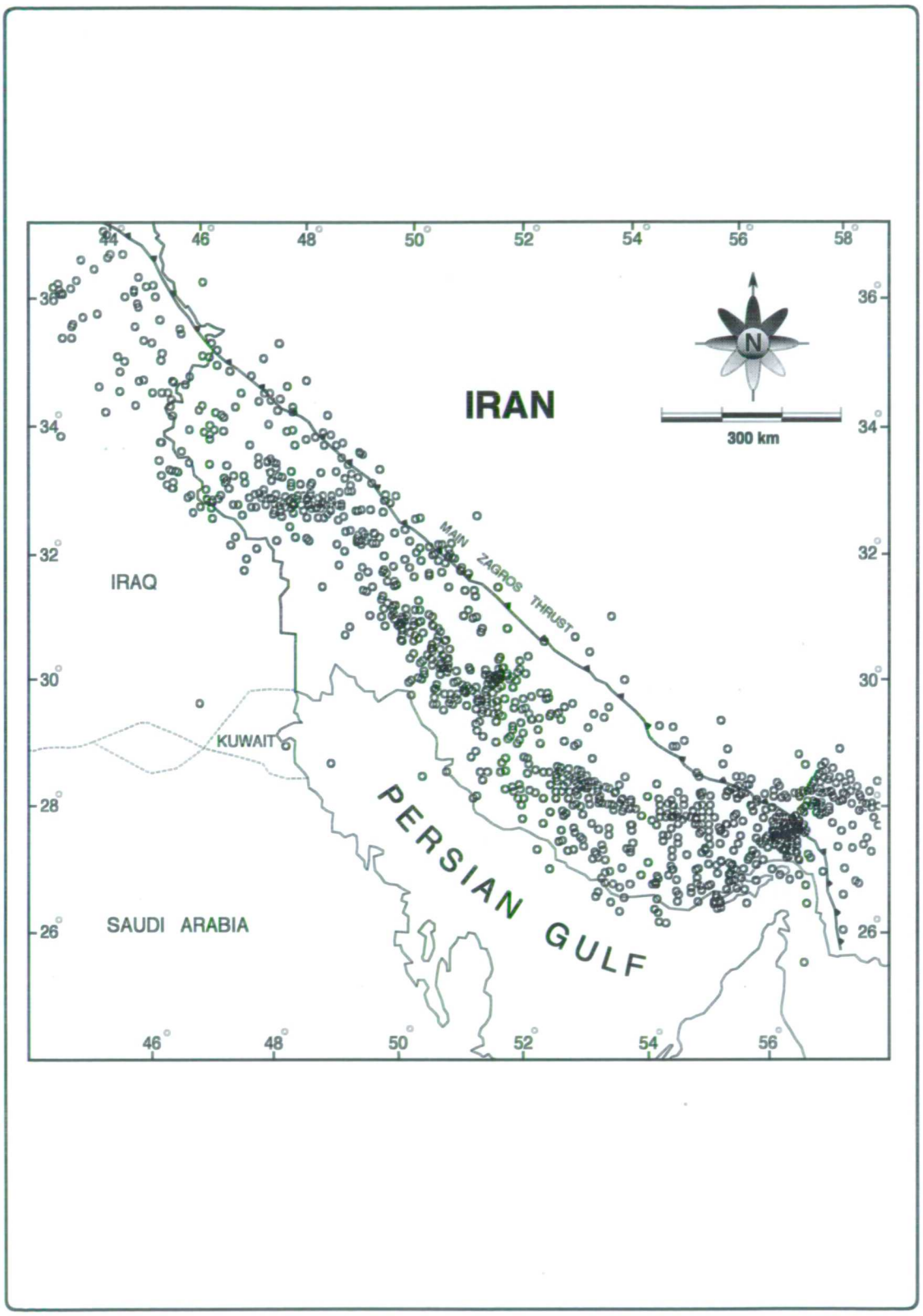


Fig. 8.2 Epicentre distribution of the Zagros earthquakes of magnitude (3-7.3) for the period 1963-1988 (based on the ISC data set).

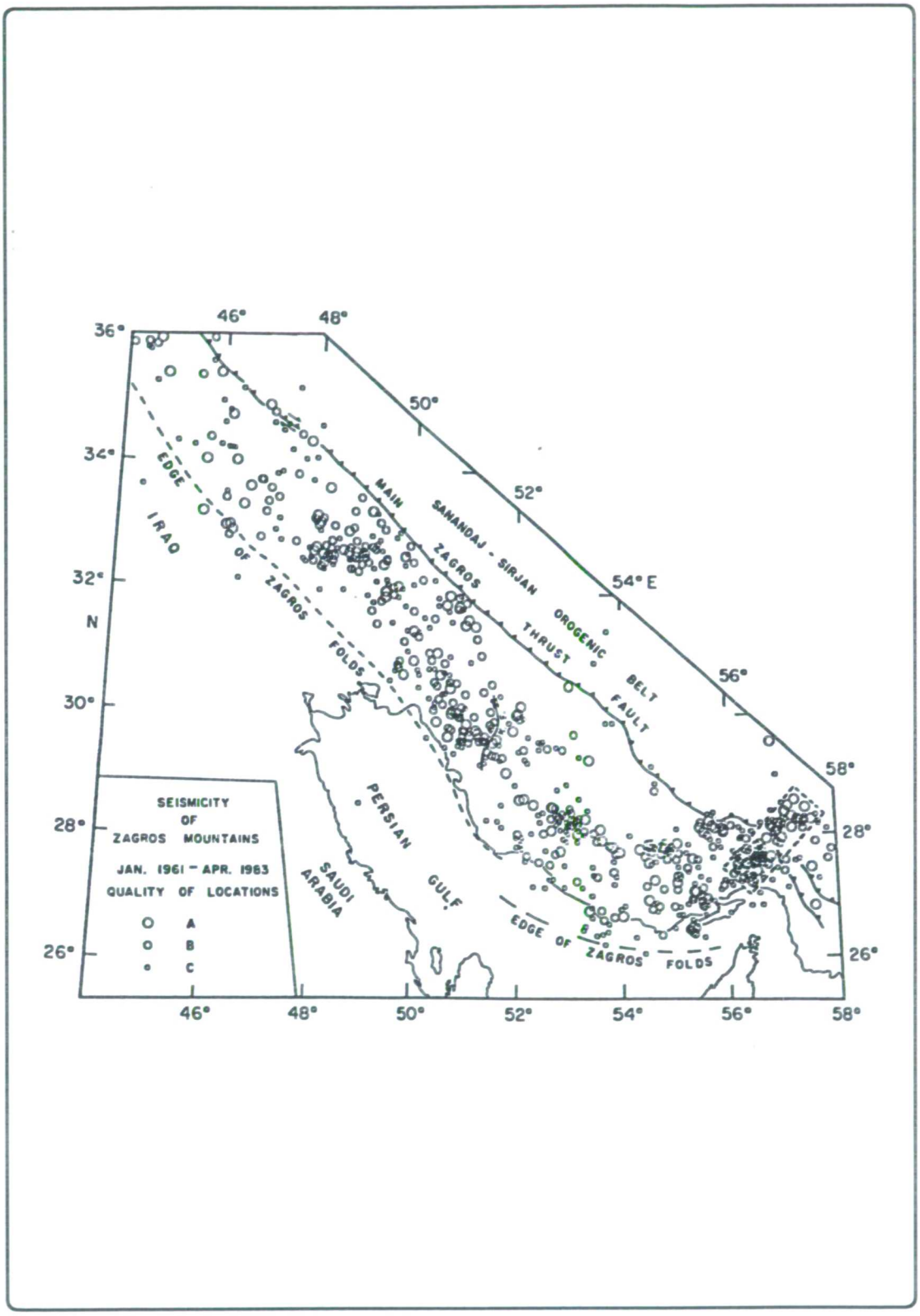


Fig. 8.3 Seismicity map of the Zagros mountain belt for the period from January 1961-April 1993 (from Ni & Barazangi, 1986).

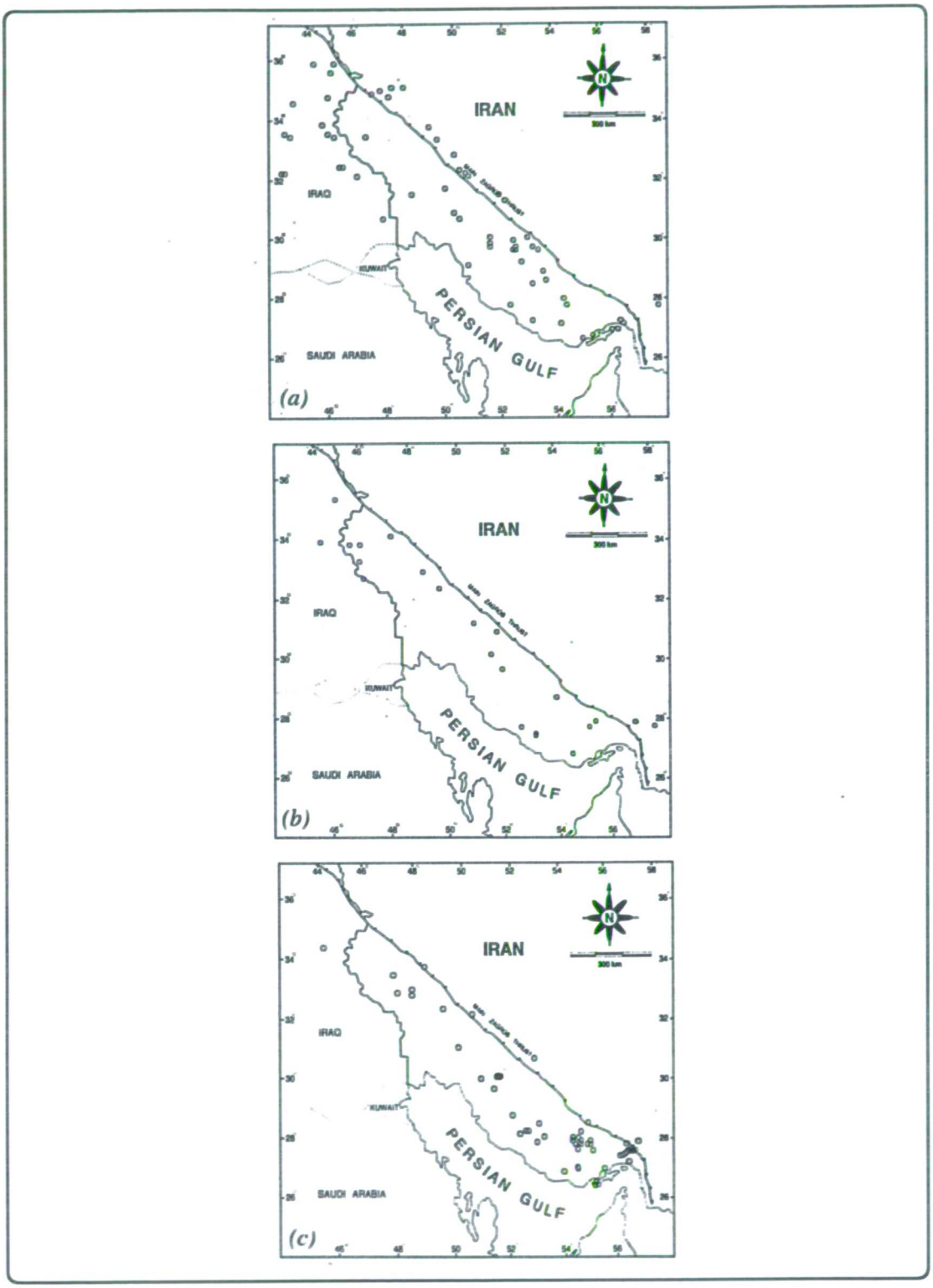


Fig. 8.4 Epicentre distribution of **large earthquakes** within the Zagros belt for the periods, (a) 700-1900, (b) 1900-1950 and (c) 1950-1988 (based on Ambraseys & Melville 1982, Nowroozi 1976, and the NEIC data set).

b) MAGNITUDE OF THE ZAGROS EARTHQUAKES

Earthquakes usually occur where tectonic strain accumulates and sudden seismic slip takes place, releasing the stored strain energy. Earthquake magnitude is an absolute measure of the size of an earthquake and is directly related to the strain energy released when over-strained rocks fracture and slip.

The concept of **earthquake magnitude** was for the first time introduced by the American seismologist Richter in 1930's. In general, it can defined in the following way:

$$M_L = log_{10} \frac{a}{T} + f(\Delta, h) + C_s + C_r \qquad (8.1)$$

where M_L = magnitude of local shocks based on surface waves, a = ground amplitude (expressed in microns; 1 micron = 0.001 mm), T = wave period (secs), Δ= epicentral distance (degrees), h = focal depth (km), C_s = station correction, which corrects for special conditions at the station (local structure, etc), C_r = regional correction, different for different earthquake areas and depending on the earthquake mechanism and wave propagation.

The original magnitude (M_l) introduced by Richter in 1935 was defined so as to be used for **local shocks** in southern California. Since then, a number of other definitions and equations of earthquake magnitude have been formulated.

A magnitude scale based on **surface waves** (M) developed in 1945 by Gutenberg considerably, making it applicable to any epicentral distance and to any type of seismograph. By limiting the period range considered to 20±2 sec, further by indicating only earthquakes of a normalised depth (h constant) and finally by stating that the function f for surface waves is proportional to log Δ, equation (8.1) is simplified to the following form:

$$M = log\, a + C_1\, log\, \Delta + C_2 \qquad (8.2)$$

where C_1 and C_2 are constants.

(m) is magnitude based on body waves and defined by the same equation (8.1).

In 1945 Gutenberg extended magnitude determinations also to '**body waves**' (P, PP, S) and to earthquakes of any depth. The magnitude based on body waves (m_b) is defined by the same equation (8.1). Later, (m) was called the '**unified magnitude**' by Gutenberg (see, Båth, 1979).

As magnitude is a quantity characteristic for each shock, determinations from different stations and also from different waves at the same station should agree within error limits, i.e. within about ± 0.2-0.3 units. Unfortunately for a number of reasons the variations are often larger. These include inaccurate seismographs, poorly known station corrections constants, and the use of surface waves from shocks of greater depth than normal without proper correction for depth (Båth, 1979).

Dziewonski and Woodhouse (1983) have shown that earthquake size is best described by its seismic moment (M_o), a spectral amplitude scale factor. These authors have demonstrated that there is generally a weak link between magnitudes based on surface and body waves and an earthquake and its true size (i.e., the amount of energy released) and they believe that M_o is the most reliable measure of the energy and size of an earthquake. Seismic moment is defined as: $M_o = \mu \bar{u} A$ (8.3)
where μ is the rock rigidity and $\bar{u}$ is the average slip over the fault area A.

Magnitudes of destructive historical events in Iran, including the Zagros region, have been assigned by Ambraseys and Melville (1982) using the recorded intensity of the events from at least two known points around the epicentral areas. The magnitude of instrumentally recorded events during the period prior to 1963 is not reliable. Thus only the magnitude of events after 1963 are examined in the present study, and for the sake of uniformity the present analysis of the magnitude is based on body-wave magnitudes derived from the NEIC and ISC catalogues. The results can be summarized as follows:

i) Zagros earthquakes occur in all ranges of magnitude up to a maximum of 7.1. Most

of the events however, are of magnitudes between 4 and 5. For example, in the examined NEIC data set including **1075 earthquakes**, 3.3 % of events (36 events) are of magnitudes between (3-4), 74.5 % (801 events) between (4-5), 20.8 % (224 events) between (5-6), and 1.3 % (14 events) over 6. This implies that a great portion of the brittle and semi-brittle deformation takes place by more frequent but relatively smaller coseismic faulting.

ii) The longitude/magnitude and latitude/magnitude plots of the Zagros earthquake on the basis of the NEIC data sets (Figs. 8.5 and 8.6) show that the earthquake magnitudes generally increases from N to S and W to E. This observations imply that **in general** the greater events occur in the southeastern end of the Zagros mountain belt. The present author considers that this to be the effects of several important factors including, 1) a southeastward increase in the relative plate velocity, 2) the indentation of the Musandam Peninsula into the Zagros mountain belt, and 3) the presence several major deep seated basement wrench faults on the east and west of the Strait of Hormuz which require large stresses to reactivate them and are consequently associated with larger seismic events.

The association of the larger events with the major basement strike-slip faults can be seen from Fig. 8.6 which shows that the greater events generally occur in the areas close to the mappable and blind major strike-slip faults. As can be seen from the comparison of Figs. 3.21, 3.23 and 3.24 with Fig. 8.6 the large events in the NW occur in association with the '**Main Recent Fault**' and the proposed '**Bala Rud** and **Sumar Lines**'. In the SE the large events occur along the '**Kazerun line**' and the **other** basement strike-slip fault lines, proposed in Chapter 3.

iii) The time/magnitude plot of the historical events, constructed from a database provided by Ambraseys and Melville (1982) (Fig. 8.7) indicates that reoccurrence interval for the larger historical earthquakes of magnitudes greater than 7, prior to 1900 was 250-350 years. This considerably long recurrence interval indicates that the occurrence of the more frequent smaller earthquakes associated with relatively low-angle dip-slip faults decreases the stored energy and increases the recurrence time

interval of the larger events.

iv) It can be seen from the depth/magnitude plot (Fig. 8.8) the earthquake magnitudes greater than 6.00 range in depth between 17-47 km and those with magnitudes greater than 6.5 between 28 and 38 km. On the basis of this observation it can be argued that the dominant '**coseismic brittle deformation**' within the Zagros crust takes place in the upper part of the basement within a band ≈ 10 km thick 28-38 km below sea level. Most deformation above and below this horizon takes place as semi-ductile or ductile deformation and involves considerably less brittle deformation and therefore generates smaller earthquakes.

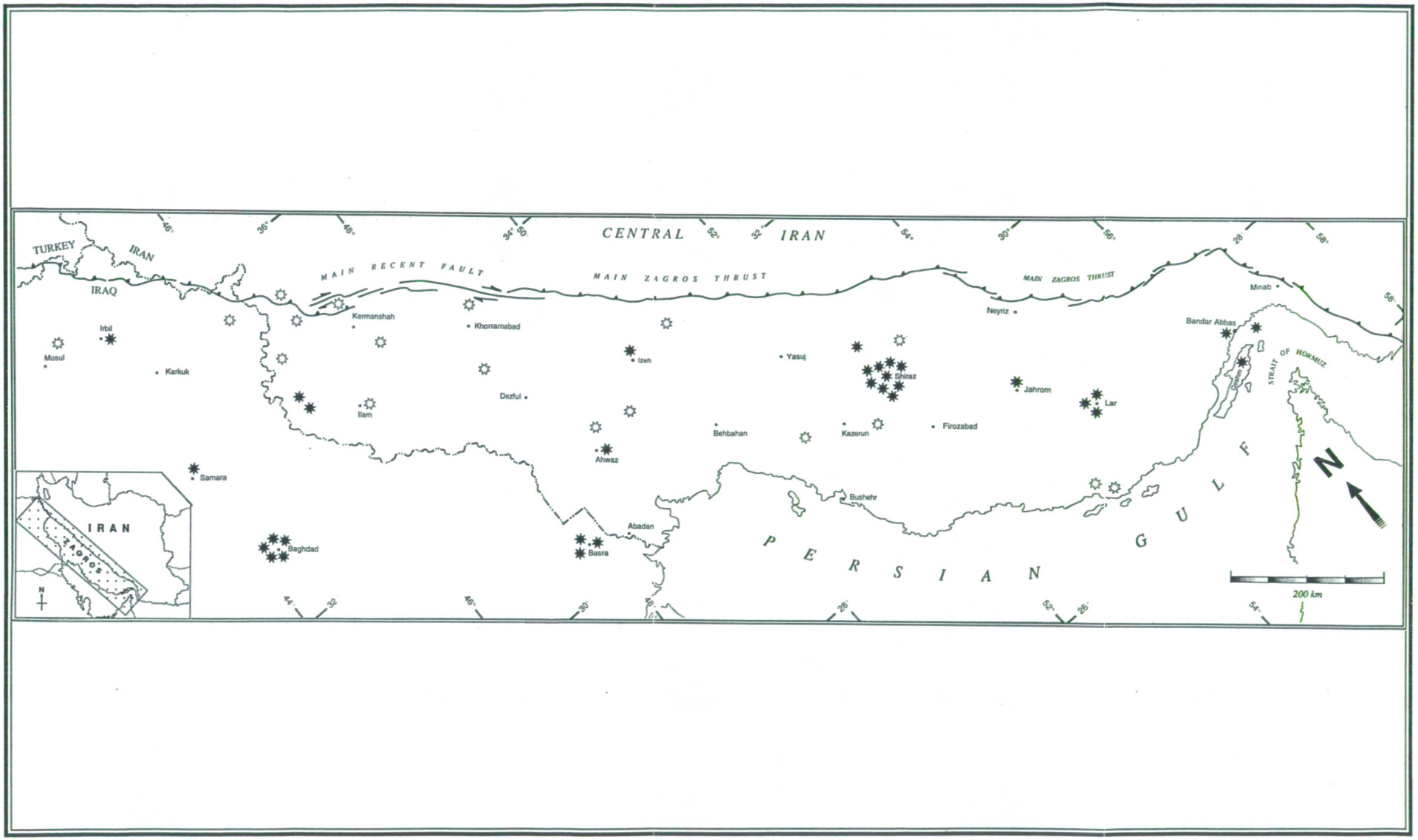


Fig. 7.10 Seismicity map of the Zagros mountain belt, based on information from historical sources. Solid stars show the precise location; open stars show imprecise locations.

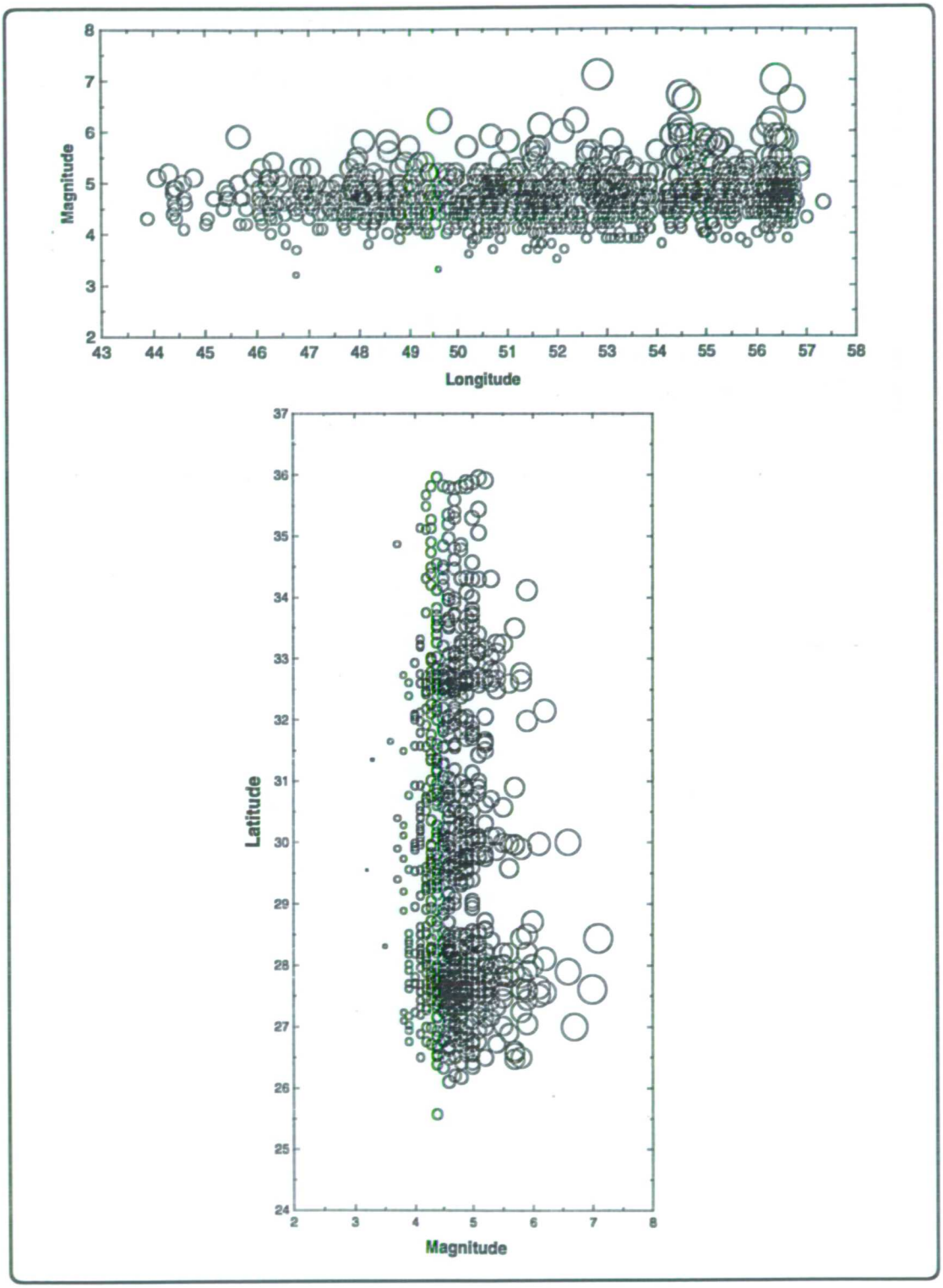


Fig. 8.5 The latitude and longitude/magnitude plots for the entire data set shown in Fig.8.1. It should be noted that neither represents a normal profile across the deformation belt.

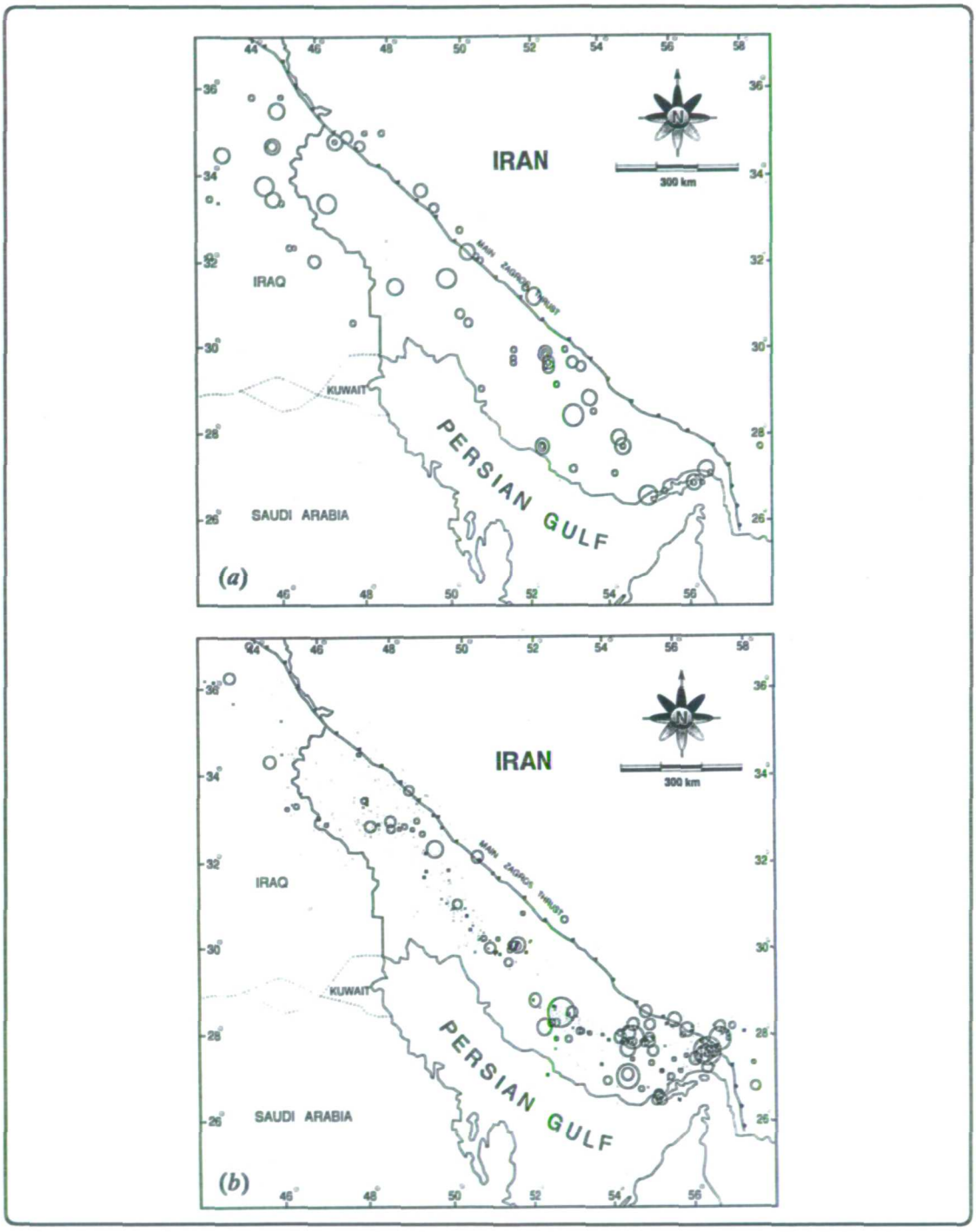


Fig. 8.6 The epicentre distribution/magnitude plots of the large magnitude earthquakes along the Zagros belt. (a) Historical earthquakes for the period 700-1900, and (b) modern events from 1963 to 1988 (based on a data set from Ambraseys & Melville 1982 and the NEIC data set). There is clear correlation between the location of the major earthquakes and the major strike-slip faults shown in Fig. 3.27).

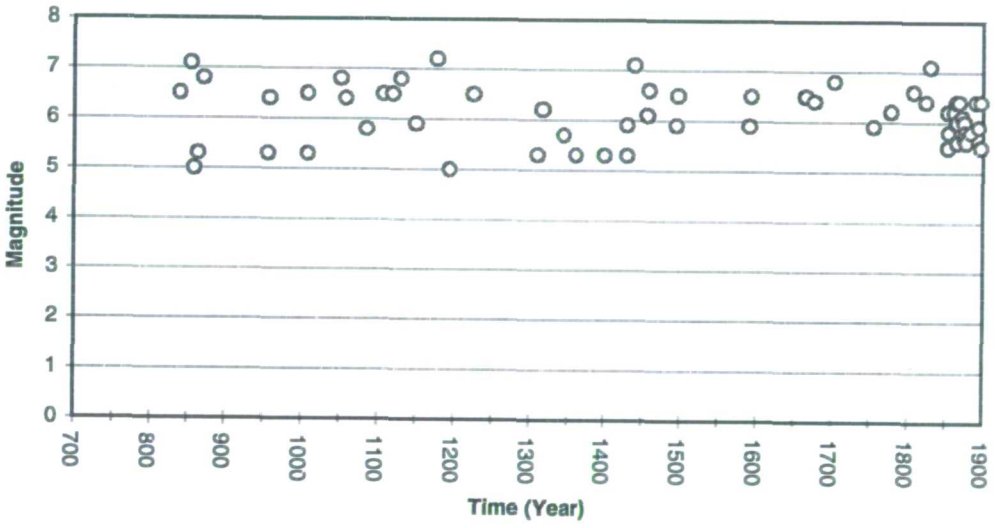


Fig. 8.7 The time/magnitude plot of the Zagros historical earthquakes (based on a data set from Ambraseys & Melville, 1982).

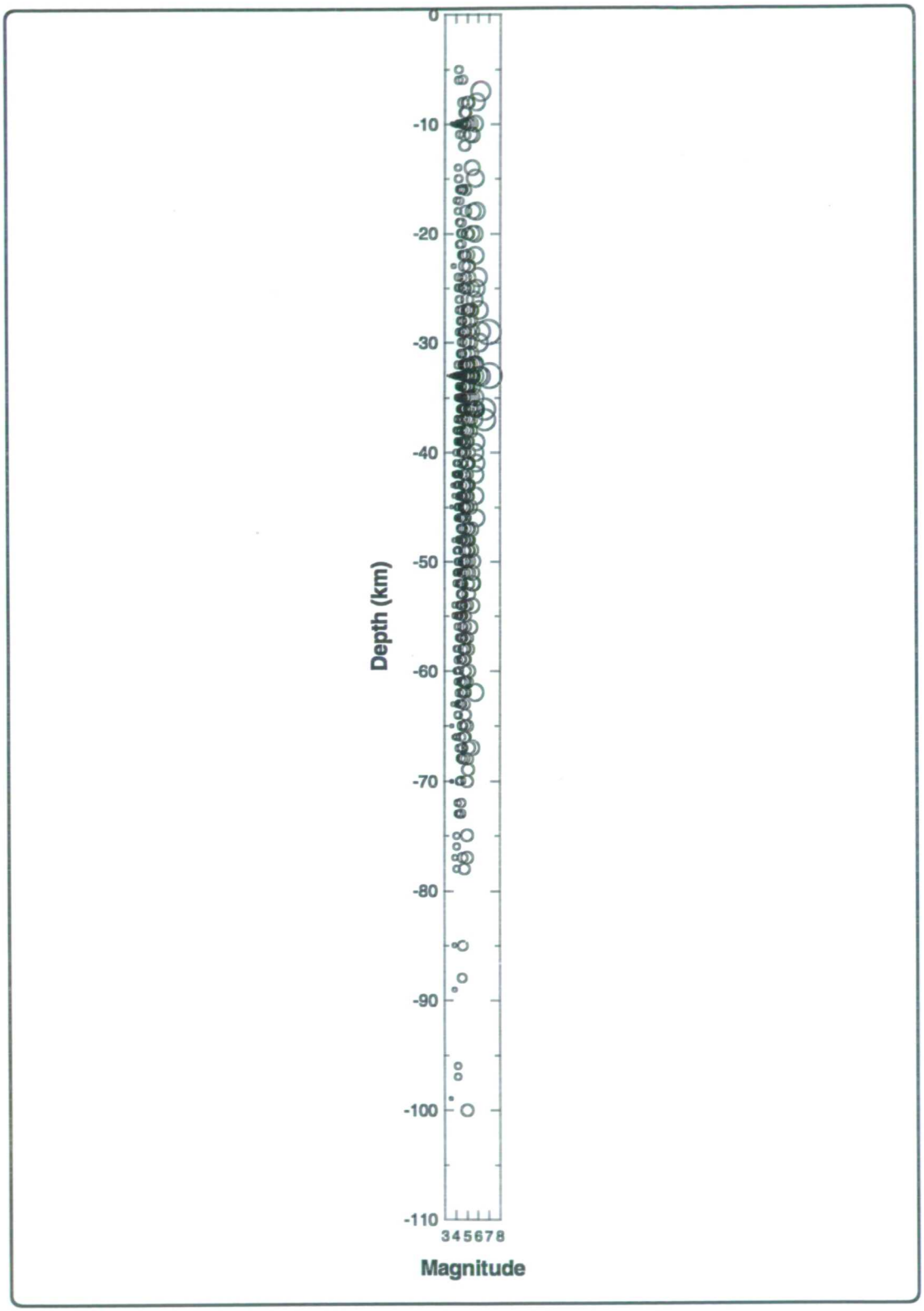


Fig. 8.8 The focal depth/magnitude plot of the Zagros modern earthquakes (based on the NEIC data set).

c) FOCAL DEPTHS OF THE ZAGROS EARTHQUAKES

The focal depth of an earthquake is the vertical distance between the hypocentre and its epicentre above it at the earth's surface. Determination of the focal depth of earthquakes usually involves some errors and ambiguities, originating from different sources. For example, misreadings of poorly recorded arrivals and the existence of only a few stations can generate large errors.

Jackson (1980a) pointed out that the smaller shocks tend to have greater errors in depth estimation than the larger, because the number of recording stations detecting increases with the size of the earthquake. As the number of recording stations detecting the shocks decreases so the station distribution, which is crucial in determining the quality of a hypocentre location, deteriorates.

According to Jackson (op. cit.) the focal depths of the smaller earthquakes in Iran (which include all the published smaller ones in the Zagros) are unreliable, while the focal depths for the larger events are likely to be much better.

This is especially so for instrumentally recorded events prior to the installation of the World-Wide Standardized Seismograph Network (WWSSN) in 1962. Despite the present discrepancy in the quality of the hypocentral locations, the available data concerning the focal depths of the events from 1963 to 1988 were analyzed in the present study and the results which are presented graphically (Fig. 8.9) led to some important findings which can be summarized as follows:

i) The focal depth/Longitude and focal depth/Latitude plots based on the NEIC data (Fig. 8.9) show that most of the earthquake '**hypocentres**' are located between 5-70 km below the sea level. The dense concentration however, is between 33- 43 km. It should be recalled however that the exceptionally dense concentration of hypocentres at **33 km** is the result of assigning this focal depth all the events with arrival times that are too

inaccurate to allow the focal depth to be determined. Despite the fact that most of the examined focal depths, especially those of smaller events, as indicated by Jackson (1980), are not reliable, the spatial distribution of '**hypocentres**' in general is compatible with the crustal structure of the Zagros region covering the northeastern margin of the Arabian plate.

ii) Analysis of the NEIC data also show that the larger Zagros earthquakes of magnitudes greater/larger than 6.00 and 6.5 occur between 17-47 km and 28-38 km below the sea level, respectively (Fig. 8.8). It is suggested that the concentration of larger events in uppermost basement is due to both the presence of very large scale, steeply dipping dip-slip or strike-slip faults which generally require large stresses to reactivate them and as a consequence produce earthquakes of large magnitude.

iii) The number and magnitude of the earthquake events decrease downwards (Figs. 8.8 and 8.9). Most of the events in deeper parts of the basement (below 50 km) are of smaller magnitudes and it is suggested that this is due to the fact that the downward progressive increase in earth's temperature gradually modifies the deformation conditions from brittle to ductile, and the current deformation here takes place generally by creep.

iv) It is interesting to note that other studies of the range of focal depths of the Zagros **larger events** yield significantly different results to those of the present study shown in Figs. 8.8 and 8.9. For example, Berberian (1981) proposed a range between 8-12 km, Jackson and McKenzie (1984) 10-20 km, and Baker *et al.* (1993) 8-20 km.

v) In addition, nearly all of the workers on the basis of teleseismic microearthquake studies demonstrate that there is no evidence for subcrustal seismicity in the Zagros region (e.g. von Dollen *et al.*1977, Savage *et al.* 1977, Niazi *et al.* 1978, and Jackson & McKenzie 1984), despite data shown in Figs. 8.8 and 8.9.

vi) Nowroozi (1972) believes that Zagros earthquakes are confined to a possible

lithospheric slab nearly 60 km thick dipping 10° to 20° toward the NE and this considerable thickness, almost twice the thickness of continental crust suggests that the northeastern boundary of the Arabian plate is being thrust under the folded foothills.

vii) In contrast to the upper part of the basement the sedimentary cover (Max. 13 km) shows a relatively low seismicity (Figs. 8.8 and 8.9). Most of the earthquakes here are of relatively smaller and magnitudes of less than 5, and generally nucleate as a result of either the reactivation of relatively small, low or medium angle thrust faults. In addition in the sedimentary cover the high strain release rate due to active folding process makes the faults incapable of bearing higher stresses and producing larger destructive earthquakes.

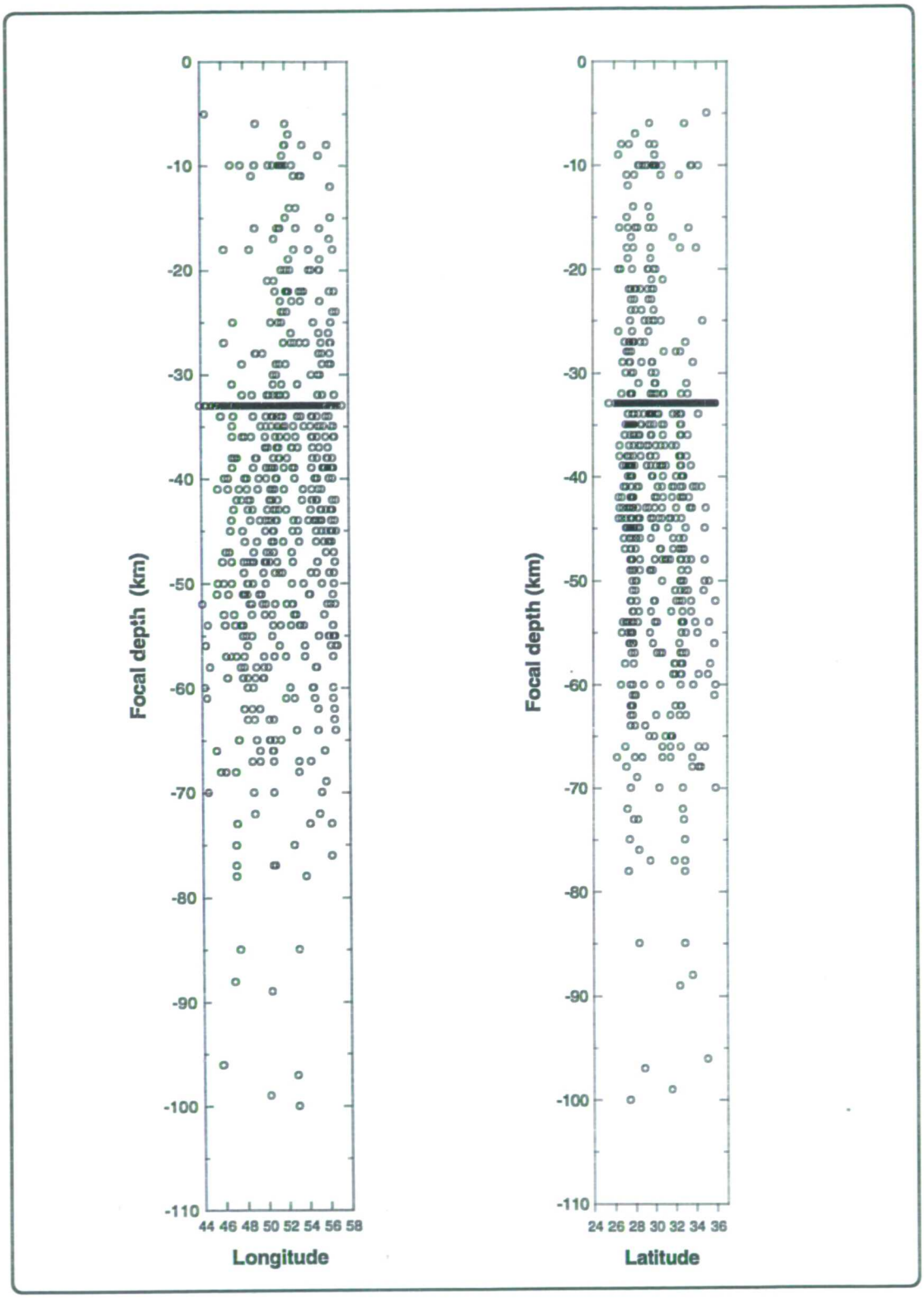


Fig. 8.9 The latitude and longitude/focal depth plots of the Zagros earthquakes (based on the NEIC data set).

d) FAULT PLANE SOLUTIONS OF THE ZAGROS EARTHQUAKES

The method of finding the fault plane associated with an earthquake is called '**fault plane solution**'. The polarity of first motions of *P* and *S* waves was used by Byerly (1928, 1938) to determine the nature of the forces at the source of an earthquake. Since then, many of his students and other workers have refined this technique.

The importance of focal mechanism and its relevance to tectonics was highlighted by Sykes (1967) when he showed that earthquakes along mid oceanic ridge crests have predominantly normal faulting solutions whereas earthquakes on the seismically active part of fracture zones predicted by Wilson's hypothesis of transform faulting (Wilson, 1965) have strike-slip faulting solutions (Fig. 8.10). This work stimulated a flood of research on the subject.

The 'Centroid Moment-Tensor' method for determining the focal mechanism of earthquakes which have recently been developed by workers at Harvard University, depends on the moment of the energy released and yields solutions superior to first-motion solutions.

The examination of the fault plane solutions of the Zagros earthquakes presented by different workers such as Nowroozi (1972), Jackson and McKenzie (1984), Chandra (1984), and Ni and Barazangi (1986) yield useful information regarding the orientation of the regional stress and the sense of movement along the active faults, which can be summarized as follows:

i) Fault plane solution of the Zagros earthquakes are generally divided into three groups: strike-slip faults, purely dip-slip thrusting, and oblique thrust faults with a considerable component of strike-slip motion.

ii) As indicated by several workers for example, Chandra (1984), Jackson and

McKenzie (1984), and Ni and Barazangi (1986) the pure thrust faulting, is the predominant fault plane solutions for the Zagros earthquakes (Figs. 8.11-8.13). Most of these solutions show nodal planes with strikes parallel to the trend of the Zagros Simply Folded Belt, and the compressional axes are approximately perpendicular to this trend. This is compatible with the distribution and orientation of major thrust faults.

iii) Fault plane solutions with pure strike-slip movements generally have a vertical or near vertical nodal plane which is oblique to the Zagros trend but again compatible with the distribution and orientation of the '**mappable**' strike-slip faults in the cover rocks and the major deep seated '**blind**' strike-slip faults in the in the basement including those proposed by the present author in section 2 of Chapter 3.

iv) Strike-slip solutions with nodal planes parallel to the Zagros trend are only seen along the 'Main Recent Fault' (Figs, 3.22, 8.11, 8.12 and 8.13) which according to Tchalenko and Braud (1974) is a large segmented strike-slip fault parallel and close to the Main Zagros Thrust. The compressional axes responsible for the generation and reactivation of the Main Recent Fault is compatible with the opening of the Gulf of Aden (Fig. 2.1) which, along with the opening in the Red Sea cause a counterclockwise rotational motion of the Arabian plate.

v) The greatest principal stress is always horizontal and generally oriented NE-SW. However, there are pronounced local discrepancies especially in the SE end of the belt due to counterclockwise rotational movement of the Arabian plate towards Iran (Figs. 2.1, 8.11, 8.12, and 8.13) and the indentation of the Musandam Peninsula into the Zagros mountain belt.

vi) As noted earlier in section 2 of Chapter 3, the fault plane solutions of the Zagros earthquakes provide a convincing evidence for the presence of several major basement strike-slip faults which cross cut the Zagros mountain belt and probably played a key role for the triggering of many salt diapirs in the Zagros region, especially in the area west of the Strait of Hormuz (Figs. 3.24 and 3.27).

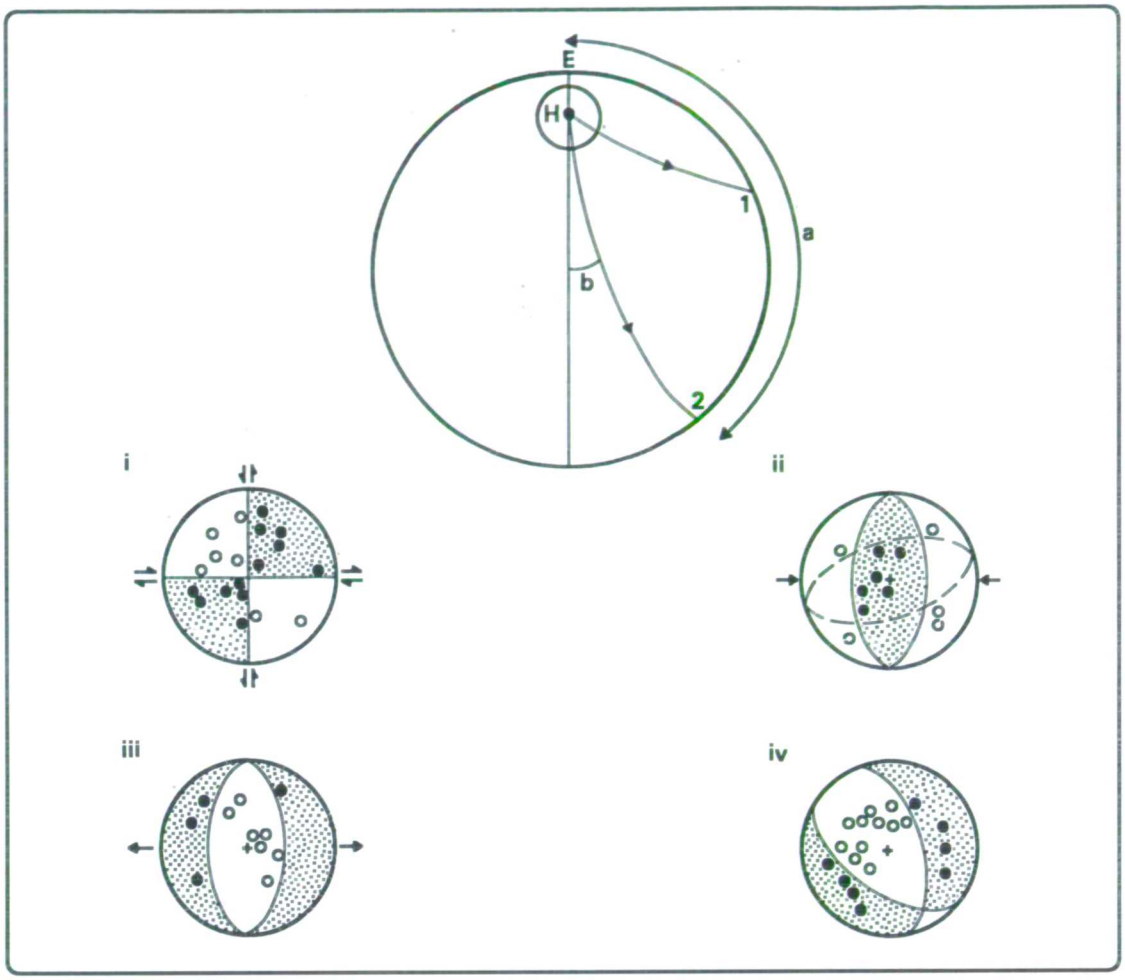


Fig. 8.10 The focal sphere is shown surrounding the hypocentre (H). Note also the epicentre (E), the path of two earthquake waves (1 and 2), the epicentral distance (a) and the corresponding angle of emergence (b). The intersection of the seismic rays with the focal sphere permits the polarity observed at a station such as 2 in the figure to be plotted. It is usual to do so on either a stereographic or an equal-area projection of the lower hemisphere. Based on account in Kasahara (1981). The lower figures are idealized focal plane solutions. (i) Strike-slip; (ii) dip-slip reverse, (iii) dip-slip normal, (iv) normal with a small strike-slip component. Note that the data for (ii) are insufficient to constrain the solution unambiguously. The alternative (broken line) also indicates reverse faulting but on an ENE-WSW strike. At the nodal lines separating the compressive and dilational sectors the amplitude of the initial P-pulse tends towards zero. Open circles = dilational arrivals; solid circles and stipple = compression (from Vita-Finzi, 1986).

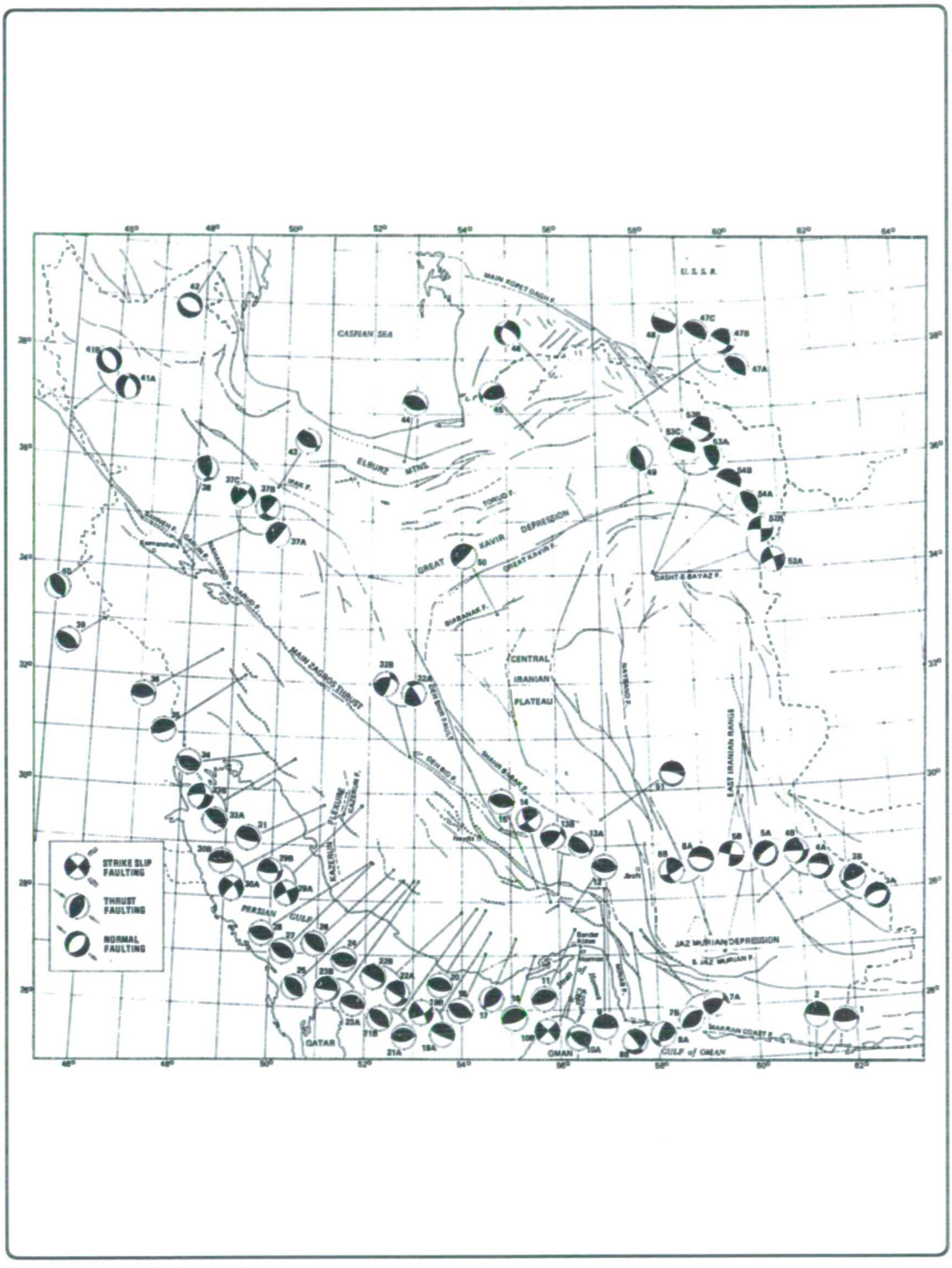


Fig. 8.11 Focal mechanism solutions for earthquakes in Iran. P-wave compression quadrants are shown by dark regions and the rarefraction quadrants by plane regions. The location of faults and other tectonic features are adapted from Berberian (1976) (from Chandra, 1984).

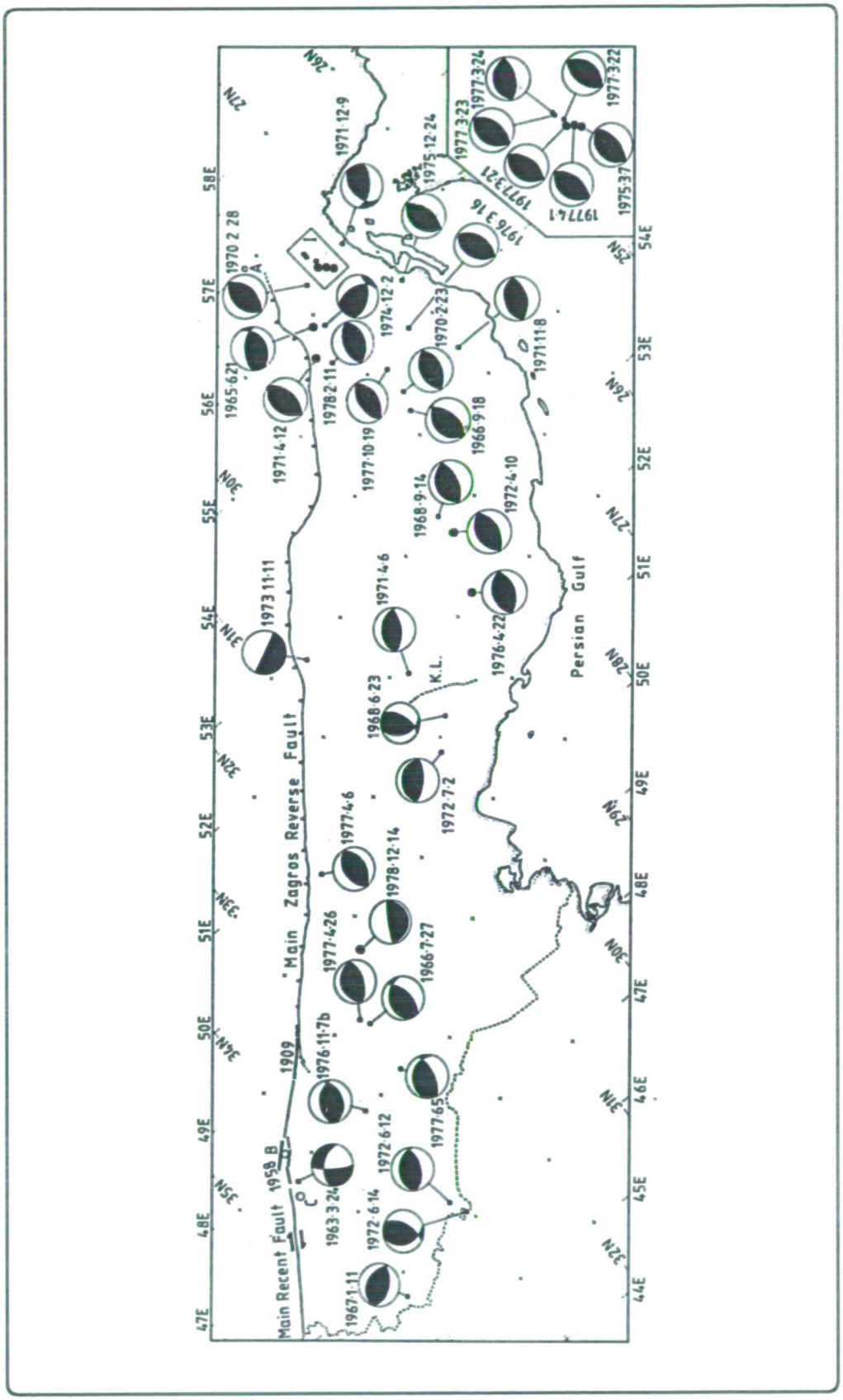


Fig. 8.12 Fault plane solutions in the Zagros (from Jackson & McKenzie. 1984).

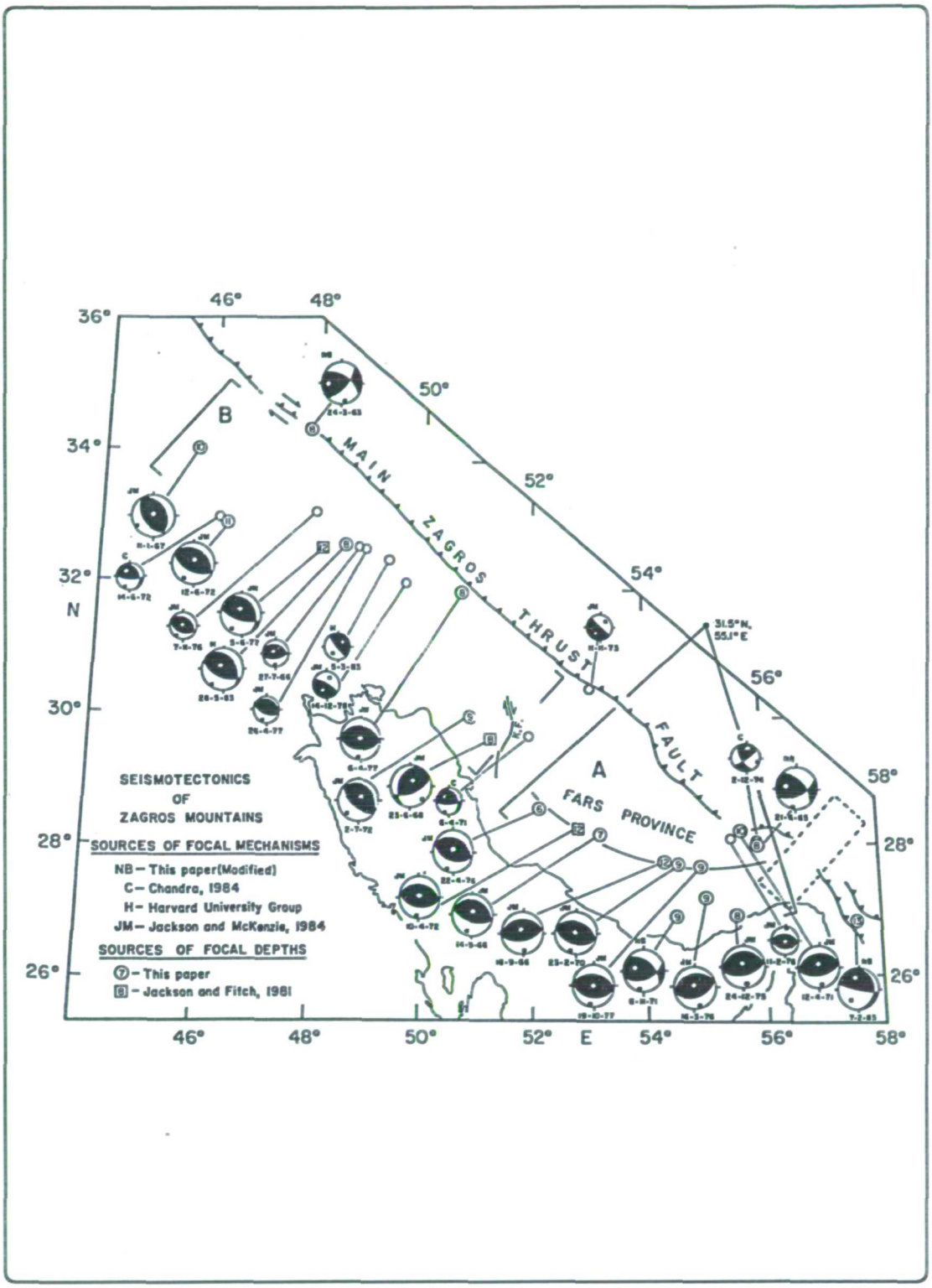


Fig. 8.13 Seismotectonic map of the Zagros showing epicentres of larger events and their fault plane solutions. Darkened regions in fault plane solutions indicate compression (from Ni & Barazangi, 1986).

4 CHARACTERISTICS OF THE SEISMIC ACTIVITY IN THE ZAGROS MOUNTAIN BELT

The study of present day seismicity shows it to be compatible with deformation of the type deduced from the study of structures within the Zagros belt described in the previous chapter and the synchronous occurrence of thrust and wrench faulting associated with plate convergence, discussed in Chapter 3, is confirmed by the seismic evidence. In addition the indentation of the Musandam Peninsula into the Iranian plate and the associated transpressive tectonics indicated by the fold geometry associated with the Minab-Zendan fault zone, is supported by the occurrence of oblique-slip fault plane solutions of the earthquakes in the region.

Everywhere in the Zagros region is earthquake prone and liable to seismic and coseismic hazards. The areas along the fault zones and major topographic fronts are of higher potential for the occurrence of these hazards. **Landslides** are the most common coseismic hazard in the Zagros mountain belt. This is because of the presence of alternatingly mobile and competent rock units which form the steep limbs of the Zagros anticlines. The areas along the Persian Gulf coast are also susceptible to coseismic **liquefaction** hazard due to the vast accumulation of the sand and alluvium deposits eroded from the rising Zagros mountains to the NE. Since a large amount deformation along the northeastern margin of the Arabian plate covering the Zagros Mountain Belt, takes place by as ductile deformation and the strain release rate is relatively high throughout the region, the chance of the occurrence of more destructive earthquakes with magnitudes greater than 6.5 is very low.

5. RATES OF NEOTECTONIC ACTIVITY

As discussed earlier in section 2 of Chapter 7 on the neotectonic activity of the Zagros mountain belt, the seafloor spreading in both the Atlantic Ocean and the Red Sea is the main cause and origin of the neotectonic activity in the Zagros mountain belt which is situated along the northeastern margin of the Arabian plate.

These two superimposed movements lead to on going convergence, shortening, uplift, and structural development in the form of both **coseismic** (faulting) and **aseismic** (folding and salt diapirism) processes in the Zagros mountain belt.

The **rate of seafloor spreading** in the Atlantic Ocean and the Red Sea have been estimated on the basis of palaeomagnetic data by Chase (1978) as 23-40 and 18 mm/yr, respectively (Fig. 8.15). Since these two seafloor spreading events are still in progress the compressional deformation along the northeastern margin of the Arabian plate is also in progress.

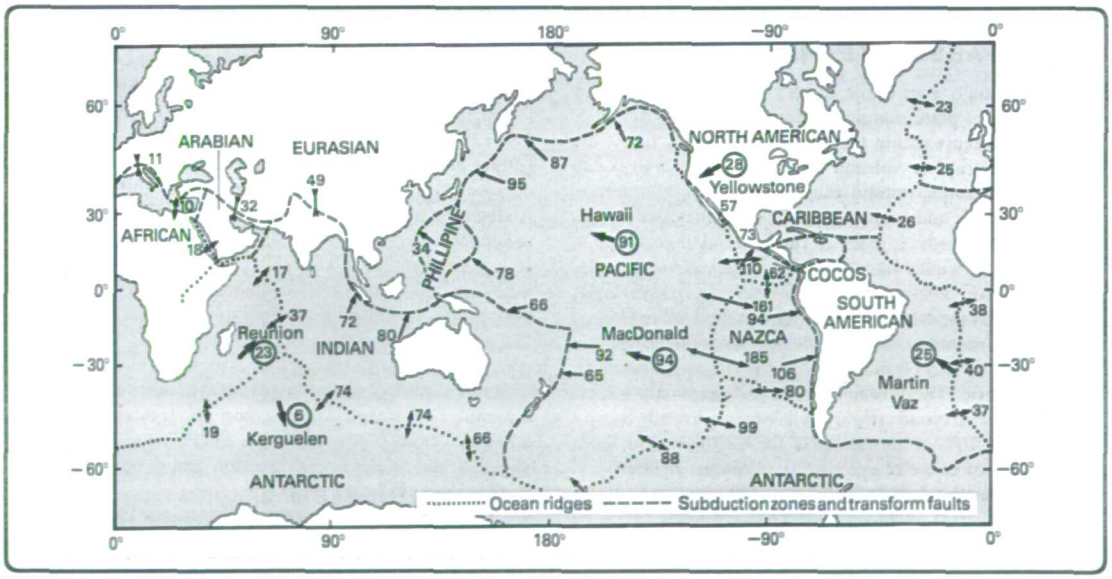


Fig. 8.14 Direction and rates (in mm a^{-1}) of relative motion of the earth's major plates shown at selected points on their boundaries. Circled numbers represent absolute motions (in mm a^{-1}) of plates relative to the hotspot reference frame (from Chase, 1978).

The **rate of convergence** between Arabian and Iranian continents during the Pliocene time was suggested by Le Pichon (1968) as 47 mm/yr, on the basis of '*palaeomagnetic*' data (see, Farhoudi, 1978). Tchalenko (1975) also proposed 45 mm/yr as the rate of convergence over the last 10 m.y. derived from ocean-floor magnetic studies.

Chase (1978) also on the basis of '*palaeomagnetic*' data suggested 32 mm/yr (Fig. 8.15) and pointed out that the convergence between the Arabian and Central Iranian plates is caused partially by a counterclockwise rotation of the Arabian plate relative to Africa around a pole 3500 km to the northwest, at lat. 34.9°N, long. 7.2°E, in Syria.

Westaway (1990) on the basis of '*seismic*' data suggested the rate of convergence in the Late Cenozoic as to be approximately 30 mm/yr. According to Westaway 20 mm/yr of this convergence rate was predominantly aseismic shortening (folding) taking place in the Zagros Mountains. The remaining 10 mm/yr occurred predominantly as coseismic shortening (faulting) farther north in the Alborz Mountains area (see also Bushara, 1995).

Jackson and McKenzie (1988) also on the basis of '*seismic*' data estimated it amounts to 15 mm/yr in the NW and 28 mm/yr in the SE part of the central Zagros. These different rates of convergence obtained by Jackson and McKenzie suggests that the rate of convergence is not uniform everywhere along the northeastern margin of Arabian plate and generally increases from NW to SE, an observation compatible with the counterclockwise rotation of the Arabian plate suggested by Chase (1978).

As is clear from the above mentioned estimates the convergence rates calculated from the Palaeomagnetic data are generally higher than that of seismically based results and as pointed out by Tchalenko (1975), this suggests that a major portion of the deformation is taken up by viscoelastic processes such as creep or by aseismic ductile deformation by folding.

Jackson and McKenzie (1988) also indicated that the seismicity could only account for

a slip-rate of about 1.0 mm/yr, and that perhaps as much as 90% of the deformation within the upper crust of the Zagros occurs aseismic. Similar ideas also have been expressed by several other workers, for example, North (1974) and Shoja-Taheri & Niazi (1981).

An interesting point that emerges from these studies is that the rate of sea-floor spreading in the Red Sea which is generally believed to be responsible for the whole deformation in the Zagros belt, is less than the estimated rate of convergence between the Arabian and central Iranian plates. This is because the convergence stems from two superimposed motions, originating from the sea-floor spreadings in the Atlantic Ocean and Red Sea.

The **amount of shortening** within the Zagros sedimentary cover, associated with the continent/continent convergence has been calculated by Falcon (1974) as about 50 km since the beginning of the Zagros Orogeny in Early Pliocene times. This is approximately the same as that postulated for the separation of Arabia and Africa. Falcon also indicated that the bulk of the shortening takes place by folding and that the average shortening in a NE-SW direction in the Simply Folded Zone is much less than that in the Imbricate and Thrust zones.

According to Falcon (op. cit.) an accurate estimate of basement shortening is not possible, owing to lack of information at depth. However, the slip rate within the basement based on cumulative seismic movements of medium and large Zagros earthquakes for a period of over 1000 years has been estimated to be about 0.4-1.2 mm/yr (Ambraseys & Melville 1982, North 1974, Shoja-Taheri & Niazi 1981).

According to Ni and Barazangi (1986) these estimates of crustal basement shortening are about an order of magnitude smaller than those of overlying sedimentary cover and than the convergence rate of Arabia and Iran based on global plate movements (e.g., Minster & Jordan, 1978). Ni & Barazangi (op. cit.) suggested that this apparent discrepancy between the rates of shortening in the sedimentary cover and the underlying

basement may be explained by basement shortening through aseismic processes.

Lees and Falcon (1952) reported a **rate of uplift** of about 12 mm/yr during the past 1700 years for the Shaur anticline, near the head of Persian Gulf (Fig. 3.1), compared to a general uplift rate for the major geo-flexure in central Zagros of about 1 mm/yr (Falcon, 1974). The rate of Holocene uplift on the Persian Gulf coast around the Straits of Hormuz was determined by Vita-Finzi (1979b) as 7.4 mm/yr for one section and 1.9 mm/yr for two others. As pointed out by Vita-Finzi (1979b) these figures lie between the minimum average of 1mm/yr that has been proposed for general uplift of the Zagros Mountains, since the early Pliocene, and the rate of about 12 mm/yr obtained for the Shaur anticline.

It will be recalled from the discussion of the regional topography that the general decrease in elevation from NE to SW is modified by the amplification of local anticlines which correspond to areas of relatively rapid uplift. It is clear from the above discussion that various sites of anomalously high uplift rate such as the Shaur anticline and the 7.4 uplift recorded for the coast around the Strait of Hormuz are indeed related to the local growth of anticlines.

CHAPTER 9

Discussion and conclusions

1. INTRODUCTION

As mentioned in the introduction to this thesis (Chapter 1), the Zagros mountain belt, which is situated along the NE margin of the Arabian plate, represents one of the most spectacular exposed continent/continent collision zones in the world and displays unparalleled examples of major folds, faults and salt diapirs. As a result of associated oil and gas reservoirs it has attracted the attention of numerous geologists (see, Previous work in Chapter 2) who have studied the plate tectonic evolution of the region and formation of many of major folds, faults and salt diapirs.

A considerable amount of work has been carried out on the individual structures within the Zagros belt. However, prior to the work described in this thesis, very little study had been made of the deformation processes associated with the evolution of the Zagros deformation belt as a whole. Oberlander (1965) considering the evolution of the Zagros drainage system concluded that transverse streams originated on the protaxis of the highland and maintained itself through succeeding orogenic spasms **as deformation spread to the SW**.

A similar idea was also suggested by Haynes & McQuillan (1974) and Alavi (1994). However, non of these workers comments on the processes that might give rise to this deformation gradient. Shearman (1976) also writing on the geological evolution of the southern Iran, suggested in passing, the possibility of **serial folding** in the Zagros region but provided no evidence to support his contention.

In an attempt to understand the details of the deformation processes occurring along the NE margin of the Arabian plate, the present author embarked on several studies which included:

i) a study of the stratigraphy of the Zagros region;

ii) a study of the spatial distribution, geometrical characteristics, and mechanism of formation of the large-scale geological structures;

iii) a geometrical analysis of the Zagros folds and the distribution of shortening across the whole folded sequence;

iv) a study of the plate-tectonic evolution of the belt; and

v) a study of the seismotectonic activity.

The insights these studies provided into the deformation processes associated with the evolution of the Zagros deformation belt, are summarised in this final chapter where they are compared, wherever possible, with previous work and ideas.

2. DISCUSSION

The study of the plate tectonic evolution of the Zagros region, described in Chapter 5, reveals that this mountain belt is the product of deformation of the NE margin of the Arabian plate. This collision was initiated in Late Cretaceous times as a result of collision between the Arabian and Central Iranian plates and the post-collision continuation of the convergence between these two plates caused the **migration of a deformation front** from collision zone towards the SW, into the almost undisturbed Zagros basin. The opening of the Red Sea which began in the Miocene (Laughton, 1966) and was associated with the addition of a counterclockwise rotation to the previous eastward motion of the Arabian plate (Chase, 1978), led to the initiation of both a differential plate velocity and deformation along the NE margin of the Arabian plate (both the plate velocity and deformation increasing from NW to SE) and the creation of the Zagros mountain belt.

This model is supported by several lines of evidence. For example the different convergence rate along the plate margin (15 mm/yr in the NW and 28 mm/yr in the SE part of the central Zagros calculated by Jackson and McKenzie 1988) and the results of the studies of the distribution of the present-day seismicity by the present author, which also increases from NW to SE (Figs. 8.1-8.3, Chapter 8).

The result of the studies described in this thesis show that the type and distribution of the deformation within the Zagros deformation belt, as well as its geometry, is controlled not only by **plate velocity** but also by a number of other factors, the most important being the regional **stratigraphy.**

As pointed out in Chapter 2, from a mechanical point of view the **stratigraphic column** of the Zagros region (Fig. 2.16) can be considered to be made up of a **rigid basement** under a **sedimentary cover** made up of four distinct litho-structural units. These are in ascending

order the **'Lower Mobile Group'** made up predominantly of the thick Hormuz Salt Formation (about 1 km thick), the **'Competent Group'** made up of mainly carbonate rocks, the **'Upper Mobile Group'** consisting predominantly of salt rich evaporitic rocks and the **'Incompetent Group'** which contains a variety of thin-bedded marles, shales, sandstones and conglomerates with minor anhydrite.

The **Lower Mobile Group**, is the main detachment horizon and allows the complete decoupling of the basement and cover and facilities the south-westward migration of the stress and deformation fronts from the plate margin. Although there is no accurate information about its distribution and thickness, it has been possible to deduce these from a study of surface structures. For example, the presence of classical buckle folds, almost everywhere along and across the belt, indicates that the detachment horizon, which is one of the essential requirements for the development of the classical buckle folds in a detached sedimentary sequence, is present almost everywhere in the belt.

However, when the wave-form geometry of the belt is viewed in plan, this, together with the presence of major culminations and depression along and across the belt, and the uneven distribution of the Hormuz salt diapirs within the belt, shows that the spatial distribution and thickness of the Hormuz salt is not uniform everywhere in the belt. The thickness of salt is known to play an important role in salt mobilisation and it has been argued (Price & Cosgrove, 1990) that a minimum thickness of 500 m is required before the initiation of the salt rise. Thus the absence of Hormuz salt diapirs NW of the Kazerun Line (except a few salt-walls intruded along reverse faults in the higher Bakhtiari mountains of central Zagros) can be attributed to a reduced thickness of the salt.

In addition to the Lower Mobile Group, the other major litho-structural units of the Zagros stratigraphic column have a significant influence in the style and distribution of deformation and the geometry of both the deformation belt as a whole and of geological structures in particular. For example, in places where the Upper Mobile Group is very

thick and salt rich, the Competent and Incompetent Groups which it separates fold disharmonically and deformation above and below this mobile horizon becomes completely decoupled (Figs. 3.5, 3.30 and 3.33).

The **geometrical analysis of folds in the present study**, in particular a study of i) the geometry of individual folds, ii) their spatial distribution and iii) the change in geometry of folds across the deformation belt, has also provided insights into the deformation mechanisms operating in the Zagros deformation belt. As pointed out in Chapter 3, the geometry and spatial distribution of the **individual folds** provide information regarding their **style** and **mechanism of formation** which enables one to differentiate between classical buckle folds, buckle folds associated with basement wrench faults and forced folds associated with thrusts. For example, the **aspect ratio** of a fold (its half-wavelength/hinge-length ratio) provides a clear indication as to whether the folds are classical buckle or forced folds related to faults.

Experimental work and field observations have shown that buckle folds have an aspect ratio of ranging between 1:5-1:10 (see e.g., Price & Cosgrove, 1990) and many of the Zagros folds have the aspect ratios that fall within this range (see e.g., Figs. 2.5 and 3.1). Nevertheless, inspection of geological cross-sections derived from seismic profiles across the belt (Figs. 3.5 and 3.20) show that many folds are linked to thrusts and several excellent examples of folds with anomalously high aspect ratios can be seen. The most impressive is the **Kabir Kuh anticline** which extends for over 200 km along its length. Work by Ameen (1991) on the Taurus-Zagros belt of NE Iraq, also indicates that some of the Zagros folds in this region are **forced folds** controlled by block faulting in the basement.

Examples of folds **linked to the basement wrench faults** can also be seen in the Zagros deformation belt. As discussed in Chapter 3., when folds are viewed in plan view, the classical buckle folds tend to be arranged in an *en echelon* manner with the sense of offset

being **randomly** to left or right. If however, the folding is associated with movement on an underlying wrench fault, the buckles are arranged in an *en echelon* array with a **constant** sense of offset. Such arrays can be recognised within the Zagros deformation belt and together with the several other lines of evidence (such as i) the presence of thrust faults arranged *en echelon* with constant offset similar to that of folds, ii) the presence of relatively small mappable strike-slip faults in the cover rocks, iii) the presence of salt domes aligned along the strike of the deduced basement strike-slip faults, and vi) focal plane solution of the major Zagros earthquakes) have been used by the author to suggest the occurrence of **several major blind basement strike-slip faults**, previously unrecognised.

The evidence listed above for the existence of major basement strike-slip faults is admittedly circumstantial. Nevertheless, a major strike-slip basement fault, the Kazerun Line, has been recognised (Fig. 3. 21). Although in the area NW of the Strait of Hormuz, the orientaion of the proposed basement strike-slip faults seems to have been modified by the indentation tectonics associated with the Musandam Peninsula, the majority of the proposed basement strike-slip faults are either parallel or conjugate to the Kazerun line. In addition, the orientation of the proposed faults are compatible with the known regional plate-tectonic stress field.

The study of the geometry of folds and their spatial distribution in the Minab Fold Zone (see, Fig 3.1) also provides an important insight into the deformation mechanism and process of deformation. As pointed out in Chapter 3, a relatively high aspect ratio of the folds in this fold zone together with their *en echelon* array with a constant offset to the NE reflects the formation folds over a basement **oblique-slip fault(s)**, with a combination of reverse dip-slip and dextral strike-slip movements. It is clear from the proceeding discussion that **folding, faulting** and **salt diapirism** within the belt **are linked** in both **time** and **space.**

Further insights into the deformation processes operating within the belt have been obtained from the analysis of the 21 geological sections across the fold belt (Fig. 4.1). The detailed geometrical analysis of these sections, described in chapter 4, reveals that there is a change across the belt of a variety of parameters. These include i) the **half-wavelength/amplitude ratio of folds**, ii) the **elevation and inclination of the median surface of the folds,** and iii) the **percentage shortening of the sedimentary cover.**

As noted in Chapter 4, because the **wavelength** of the folds along the sections is quite variable, the ratio of half-wavelength/amplitude was measured as this provides a normalised value which relates directly to the stages of development of the fold and is independent of absolute size of the structure. As can be seen from the graph of Figs. 4.4-4.8, the **half-wavelength/ amplitude ratio** of the Zagros folds increases in value from NE to SW, and this implies that the folds becoming progressively less developed in this direction.

The study of the **geometry of the median surface of the folds** in different zones also shows that although variation in the elevation of the median surface of the folds is not uniform in different fold zones, there is a general drop in elevation of this surface from the NE to SW, everywhere in the belt (Fig. 4.16).

Similarly the results of measurements of the **percentage shortening** of the sedimentary sequence across the fold belt along the geological sections, at three different horizons within the stratigraphical column, indicate a south-westward decrease and show a drop in shortening from around 16% along the NE margin to 2% along the SW margin.

These **results** are **all compatible with** the **south-westward migration** of the deformation front by the process of **serial folding** which it is argued is responsible for the progressive generation of the Zagros classical buckle folds. During the serial folding process, folds develop one after the other as a deformation front propagates through a sedimentary

sequence (Blay 1974, Price 1975, Blay *et al.* 1977, Cosgrove and Price, 1987). This process has been fully discussed in Chapter 6 where it was shown that the main condition required for this process to occur are all satisfied in the Zagros region.

Other convincing evidence for the south-westward migration of the deformation and serial folding in particular, comes from a study of the geomorphology. For example Oberlander, 1965, 1985) discussed the morphology of **transverse gorges** in the limestone fold structures and the Pliocene conglomerate masses and noted successive highly significant changes in gorge characteristics as the rivers, which drain across the Zagros mountain belt, are traced from SW to their sources in the NE .

In the SW, i.e. the outer Zagros, covering the **Simply Folded Belt**, it is noted that:

- There is no significant **local variations** in gorge character.
- Gorges have in common the characteristics of extreme youth or strong recent rejuvenation.
- The streams passing through them are invariably swift and turbulent.
- The canyon walls are characterised by angular mechanical weathering under joint and bedding control.
- The cuts of the trunk streams through the Mountain Front Detrital Apron are as precipitous, constricted, and deep as most of the exit gorges through the Mountain Front anticlines.

In the NE, i.e. the inner Zagros, covering the **Imbricate** and **Thrust Zones**:

- Gorges show **no sign of** the very recent strong **rejuvenation** that characterises the dissection of the outer Zagros.
- The near-vertical lower story of transverse gorges which occur in the outer Zagros in hard rocks, disappears.
- Gorges in this zone, though unmatched in depth and still youthful in physiognomy, are either **V-shaped** throughout, or cyclic with a deep V-shaped inner story. This

implies that these gorges have been cutting down at a **uniform rate** for considerable period.

- In the interior Detrital Belt (about 65 Km from the Mountain Front Detrital Apron to the NE), the gorges of the same streams through deposits of the same age are more than twice as deep as those of the Mountain Front Apron, but are far more open, often rising by stages separated by broad erosional shelves. These gorges are clearly late or post Pliocene since they dissect late Pliocene synclinal and piedmond deposits.

On passing from the **Imbricate** zone into the **Thrust Zone,** even more striking changes in gorge morphology immediately appears. In this zone:

- Although the **multi-story character** of the gorges is often preserved, along with the steep declivity of their walls, the gorges are seen to be in almost all cases **heavily alluviated**.
- The canyon walls are **widely separated** at the base either by lateral planation, cliff back-wearing, or aggragational filling of the canyons.
- These walls frequently rise from heavy talus accumulations, and are themselves more **strongly weathered** than any found on hard rocks in the fold belt.
- Their surfaces evidence chemical as well as mechanical disintegration, their resistant outcrops being round and pitted, **in marked contrast to** the fresh angular outcrops of the exterior ranges.

Oberlander (1965) conclude that the increasingly **youthful characteristics** of the Zagros gorges **in a downstream direction** are suggestive of through-flowing drainage the originated on the protaxis of the highland and maintained itself through succeeding orogenic spasms **as deformation spread to the southwest**.

It is interesting to note that the distribution of shortening across the deformation belt is often non-uniform and marked **periodic variations in shortening** are seen to be

superimposed on the general NE to SW decrease in shortening across the belt. Examination of the geological cross sections shows that the zones of relatively high shortening can be traced from one section to another along strike and that these zones are generally associated with **thrusts** as well as **folds** (Fig. 3.5). Thus it seems likely that these faults play an important role in controlling the localisation of shortening and account for the observation that these zones have a remarkable continuity along strike, a feature uncharacteristic of classical buckle folds.

The **dip** and **displacement** on **these thrusts** increases systematically across the belt from SW to NE, a trend compatible with them being formed by the process of **Footwall Collapse**. This process can be considered to be the brittle equivalent of serial folding. The fault-bend folds (Suppe, 1983) associated with footwall collapse, will of course also develop sequentially from NE to SW in exactly the same way that would occur by the process of serial folding.

It is clear from the above discussion that a deformation front is migrating south-westward into the Arabian plate from its NE margin, by both **ductile** and **brittle** deformation. This illustrates a possible interplay between folds and faults and shows the role of both **Serial Folding** and process of **Footwall collapse** in the evolution of the Zagros deformation belt.

Two conflicting models have been presented for the distribution of deformation within the basement and cover rocks of the Zagros mountain belt. The first by Jackson & Fitch (1981) is based on seismic evidence and proposes that shortening in the basement occur by inversion of old normal faults. They argue that shortening in the sedimentary cover occur by folding and that the two deformation regimes are separated by the detachment horizon of the Hormuz salt. **In contrast**, a model has been proposed by Berberian (1995) based on seismic and topographic evidence in which he suggests that several important basement thrusts propagate through the detachment horizon into the cover and are expressed at the surface as major topographic steps. Because the seismic lines and well data on which the

geological sections are based, do not penetrate the Hormuz salt, they provide no insight regarding the transmission of faults from the basement into the cover. The geometrical analysis of folds and faults in the cover rocks shows that there are locations of intense local shortening along the various cross-sections and that these are related to thrusts and can often be traced considerable distances along strike from section to section. However, it is found that the locatities of intense shortening do not in general coincide with master trusts proposed by Berberian. In addition, a study of the elevation of the median surface of folds across the Zagros deformation belt (Fig. 4.16) generally shows a smooth decrease in elevation across the belt from NE to SW. If major thrusts from the basement cut up through the cover as proposed by Berberian, these would be apparent from the median surface profile, which would be stepped.

Although the analysis of the geological sections across the belt does not provide evidence to support Berberian's contention that basement faults propagate into and effect the cover rocks, nevertheless the present author has argued that movement on basement faults can influence the generation of structures and indeed has used the spatial organisation of surface structures such as folds and faults to determine the location of major wrench faults in the basement.

Work by the present author based on 21 geological cross-sections across the Zagros deformation belt (BP, 1956) indicates that the thrusting within the cover is the result of footwall collapse which accompanied the south-westward migration of deformation from the NE margin of the Arabian plate. In such a model these thrusts would lie within the deforming wedge and would not penetrate below the basal detachment horizon. Such a model is compatible with model proposed by Jackson & Fitch (1981) in which there is a complete decoupling of the basement from the cover across the Lower Mobile Group.

The above discussion illustrates an **important link** between folding and faulting during the deformation of the plate margin in both the cover and basement. In addition, the study of

geometry and spatial distribution of the major geological structures (folds, faults, and salt diapirs) in the cover rocks reveals that links also exist between folds, faults and salt diapirs.

As mentioned in section 4 of Chapter 3, the position of the Infra-Cambrian **Hormuz Salt diapirs** in relationship to the large-scale folds varies greatly within the Zagros Mountains. It has been suggested by Colman-Sadd (1978) that most salt diapirs pierce anticlines and occur on flanks, on crests, and at their plunging ends because of the lower pressure in these areas. However, the results of present study, discussed in Chapter 3, as well as the studies carried out by several other workers (for example, Harrison 1930, Lees 1931, Kent 1970, 1979, De Jong 1982) indicate that the diapirs are not always associated with anticlines. Some occur in synclines and others, for instance, the **Bustaneh** and **Kuh-e Namak** diapirs are not in the immediate proximity to any visible fold (Figs. 3.21 and 3.24).

The inspection of the distribution of salt diapirs in the Fars Fold Zone (Fig. 3.24) confirms this view and it can be seen that the association of anticlines and diapirs is the exception rather than the rule. The more realistic profiles shown in sections based on seismic profile (e.g. Figs. 3.5 and 3.20) show that there is a much less intimate relationship between the salt and folds than is indicated in Fig. 3.6.

The studies of **neotectonic activity** also provide important insights into the **present state of deformation** in the Zagros region. For example, the results of analysis of the **seismic activity** in the Zagros region, which is considered as one of the most reliable and informative lines of evidence of neotectonic activity, show that seismic activity is occurring almost everywhere within the mountain belt and even further to the SW beyond the mountain front. The seismic activity along the belt increases from NW to SE and the zones of higher activity generally coincide with the location of major basement faults. The larger magnitude earthquakes generally occur either along the major basement relatively higher-angle thrusts or strike-slip faults both of which generally have high reactivation energies.

As can be seen from the Figs. 8.8 and 8.9 the analysis of the Zagros earthquake data also shows that the higher seismic activity and the large magnitude earthquakes are generally concentrated in the upper parts of the basement and that the deformation above and below this higher seismicity horizon takes place mainly as **aseismic ductile deformation**. These observations are **compatible** with the results of **previous works** by Jackson *et al.* (1995) who suggested that earthquakes between 1909 and 1992 can account for only a small part (~10-20%) of the total deformation required by the convergence between the Arabia and Eurasia plates, and Sobouti & Arkani-Hamed (1996) who on the basis of a numerical modelling argued that in the Zagros the crust is deforming by a creep process, whereas in northern Iran most of the present-day deformation is being accommodated seismically.

A consideration of the available fault plane solutions for the Zagros earthquakes also indicates that thrust faulting with nodal planes parallel to the Zagros trend is the predominant and widespread coseismic movement in the Zagros region; strike-slip movements, both dextral and sinistral, are restricted to a few N-S and E-W trending mappable or blind strike-slip faults (see, Figs. 3.27 and 8.6).

The pattern of **neotectonic activity** outlined above is **compatible** with the deformational processes discussed earlier in this chapter associated with south-westward migration of a deformation front. Other aspects of neotectonic activity in the region related to geology (recent folding, faulting, salt diapirism, unconformities), geomorphology (uplifted marine terraces and transverse drainage system), and archaeology (differential uplift of two ancient canals dug on the flank of the Shaur anticline) discussed in Chapters 7, also show that the Zagros mountain belt along the NE margin of the Arabian plate is still a **tectonically active belt** and the deformation processes deduced from the different studies, discussed above, **is still going on.**

3. CONCLUSIONS

On the basis of the proceeding discussion the following conclusions can be drawn regarding the deformational processes associated with the evolution of the Zagros deformation belt and the present state of deformation.

- The regional **plate velocity** and **stratigraphy** play key roles in determining the amount and distribution of deformation and mountain belt.

- The Lower Mobile Group (the Hormuz Salt Formation) as the main detachment horizon between the basement and sedimentary cover **facilitates decoupling** of these two units and the migration of the deformation front from the collision zone towards the SW. The distribution and thickness of the Hormuz salt can be deduced from a study of the distribution of folds and salt diapirs.

- The decoupled basement and sedimentary cover often deform independently and by different mechanisms.

- The second detachment horizon, within the stratigraphic column in the cover (the Upper Mobile Group) also allows another decoupling to occur which can lead to the disharmonic folding of the overlying and underlying groups.

- The results of the **geometrical analysis** of the individual folds, their spatial distribution, and change in geometry across the deformation belt provide significant insights into the deformation mechanism and processes operating along the NE margin of the Arabian plate and strongly support the idea of a south-westward migration of the deformation by the processes of **serial folding** and **footwall collapse**.

- The compatibility of the geometry of the median surface of the folds, shown by a marker horizon quite deep below the Earth's surface and the present day Zagros topography also implies that the present asymmetric and complex topography of the Zagros mountain belt is structurally controlled.

- The distribution of folds and thrusts within the cover rocks suggest the existence of important basement strike-slip faults.

- Brittle and ductile deformation occur together within both the **cover** and **basement** during the deformation of the Zagros belt. **In the cover** the process of footwall collapse (brittle) and serial folding (ductile) occur synchronously and at the same level. **In the basement** the coseismic brittle deformation by faulting occurs predominantly in a zone (about 20 km thick) immediately below the sedimentary cover and the rocks in deeper levels deform mainly in a more ductile manner.

- Geological, geomorphological and archaeological evidence of neotectonic movements confirms active nature of the SW margin of the Zagros belt and demonstrate that the deformation that has been occurring since the Pliocene, is continuing today.

In summary, **the overall contribution of this study** (thesis) to our understanding of tectonics of the Zagros region is the demonstration that deformation is migrating from the NE edge of the Arabian plate towards the SW by a variety of mechanisms. The two most important in the cover rocks are serial folding and footwall collapse and it is clear that both ductile and brittle deformation are going on concurrently and at the same level. It is also clear from seismic evidence that this deformation which was initiated in the Pliocene, is continuing today.

However, the study has revealed a number of issues which remain unsolved and which require further investigations. Such investigations might involve:

- a detailed studies of the neotectonics of the region. This would enable the model of deformation proposed above to be further refined. For example in Chapter 7 on neotectonic activity, the majority of the evidence for neotectonic activity relates to the SW margin of the deformation belt. A comparison of neotectonic activity across the belt would enable one to determine whether the whole belt is still undergoing deformation in a **uniform manner** or whether the deformation is **focused** along the SW margin of the belt.
- The geomorphological studies discussed in Chapter 2 are mainly based on geological and topographical maps and aerial photographs. A detailed study of the high resolution remote images now available exploiting advanced computer softwares would certainly reveal a more detailed picture of the topographical evolution of the region, which could be used to check some of the conclusions of the present work.

REFERENCES

REFERENCES

Adib, D. 1978. Metamorphic complex situated along the southwestern margin of the Central and Eastern Iran microplate. *Neuves Jahrbuch für Paläontologie Abhandlungen* **156**, 393-409.

Ala, M. 1974. Salt diapirism in southern Iran. *Bull. Am. Ass. Petrol. Geol.* **58**, 1758-1770.

Ala, M. 1979. *Framework of petroleum geology of the Zagros sector of Middle East Basin with special reference to source rock geochemistry*. Unpublished Ph.D. thesis, University of London.

Ala, M. 1982. Chronology of trap formation and migration of hydrocarbons in Zagros sector of southwest Iran. *Bull. Am. Ass. Petrol. Geol.* **66**, 1535-1541.

Alavi, M. 1980. Tectonostratigraphic evolution of the Zagrosides of Iran. *Geology (Boulder)* **8**, 144-149.

Alavi, M. 1994. Tectonic of the Zagros orogenic belt of Iran: new data and interpretations. *Tectonophysics* **229**, 211-238.

Ambraseys, N. N. & Melville, C. P. 1982. *A History of Persian Earthquakes*. Cambridge University Press, Cambridge.

Ameen, M. S. 1988. *Forced folding of layered cover due to dip-slip, basement faulting*. Unpublished Ph.D. thesis, University of London.

Ameen, M. S. 1991. Possible forced folding in the Taurus-Zagros belt of northern Iraq. *Geol. Mag.* **128**, 561-584.

Anderson, E. M. 1951. *The dynamic of faulting* (2nd. edn). Oliver & Boyd, Edinburgh.

Baker, C., Jackson, J. & Priestley, K. 1993. Earthquakes on the Kazerun line in the Zagros Mountains of Iran: strike-slip faulting within a fold-and-thrust belt. *Geophys. J. Int.* **115**, 41-61.

Blanford, W. T. 1872. Notes on the geological formations seen along the coasts of Baluchistan and Persia, from Karachi to the head of the Persian Gulf, and some of the Gulf islands. *India geol. Surv. Recs.* **5**, 41-45.

Båth, M. 1979. *Introduction to seismology* (2nd edn). Birkhäuser Verlag, Basel.

Berberian, M. 1976. Contributions to the seismotectonics of Iran, II. *Iran geol. Surv. Rep.* **39**.

Berberian, M. 1977. Contributions to the seismotectonics of Iran, III. *Iran geol. Surv. Rep.* **40**.

Berberian, M. 1979. Evaluation of the instrumental and relocated epicentres of Iranian earthquakes. *Geophys. J. R. astr. Soc.* **58**, 625-630.

REFERENCES

Berberian, M. 1981. Active faulting and tectonics of Iran. In: *Zagros, Hindu Kush, Himalaya Geodynamic evolution* (edited by Gupta, H. K. & Delany, F. M., Geodyn, S.). *Am. Geophys. Union* **3**, 33-69.

Berberian, M. 1995. Master 'blind' thrust faults hidden under the Zagros folds: active basement tectonics and surface morphotectonics. *Tectonophysics* **241**, 193-224.

Bird, P., Toksoz, M. N. & Sleep, N. H., 1975. Thermal and mechanical models of continent-continent convergence zone. *J. Geophys. Res.* **80**, 4405-4416.

Blay, P. K. 1974. *A model study of gravity tectonics*. Unpublished Ph.D. thesis, University of London.

Blay, P., Cosgrove, J. W. & Summers, J. M. 1977. An experimental investigation of the development of structures in multilayers under the influence of gravity. *J. geol. Soc. Lond.* **133**, 329-342.

Braud, J. & Ricou, L. E. 1971. Tectonique-L, accident du Zagros ou Main Thrust, un charriage et un coulissement. *C. R. Acad. Sc. Paris* **272**, 203-206.

British Petroleum Company Limited (BP) 1956. *Geological Maps and Sections of south-west Persia. Six geological maps (Scale 1:1,000,000), four sheets of geological cross sections, seven sheets of stratigraphical columns*. Edward Stanford, London.

Buxtorf, A. 1916. Prognosen und Befunden beim Hauensteinbasis und Grenchenbergtunnel und die Bedeutung der Letzteren fuer die Geologie des Jurasgebirges. *Verl. Natur. Ges. Basel.* **27**, 185-254.2

Byerly, P.1928. The nature of the first motion of the Chilean earthquake of November 11, 1922. *Am. J. Sci.* **5**, 232-236.

Byerly, P. 1938. The earthquake of July 6, 1934, amplitudes and first motion. *Bull. seism. Soc. Am.* **28**, 1-13.

Chandra, U. 1981. Focal mechanism solutions and their tectonic implications for the eastern Alpine-Himalayan region. In: *Zagros-Hindu Kush-Himalaya Geodynamic Evolution* (edited by Gupta, H. K. & Delany, F. M.). Geodynamics Series, copublished by *Am. Geophys. Union* and *Geol. Soc. Am.* **3**, 243-271.

Chandra, U. 1984. Focal mechanism solutions for earthquakes in Iran. *Physics of the Earth and Planetary Interiors* **34**, 9-16.

Chase, C. G. 1978. Plate kinematics: the Americas, East Africa, and the rest of the world. *Earth Planet. Sci. Lett.* **37**, 355-368.

REFERENCES

Colman-Sadd, S. P. 1978. Fold development in Zagros simply folded belt, SW Iran. *Bull. Am. Ass. Petrol. Geol.* **62**, 984-1003.

Cosgrove, J. W. & Price, N. J. 1987. The deformation of well-bedded sediments with particular reference to the buckling of accretionary prisms. *China geol. Soc. Mem.* **9**, 275-304.

Dahlstrom, C. D. A. 1969. Balanced cross sections. *Can. J. Earth Sci.* **6**, 743-747.

De Jong, K. A. 1982. Tectonics of the Persian Gulf, Gulf of Oman, and southern Pakistan region. In: *The Indian Ocean* (edited by Mairn, A. E. M. & Stehli, F. G.). Plenum Press, New York.

Delaloye, M. & Desmons, J. 1980. Ophiolites and Melanges in Iran. *Tectonophysics* **68**, 83-111.

Dimtrijevic, M. D. 1973. Geology of Kerman region. *Iran geol. Surv. Rep.* **52**.

Dunnington, H. V. 1958. Generation, migration, accumulation and dissipation of oil in northern Iraq. In: *Habitat of oil, a symposium* (edited by Weeks, L. G.). *Bull. Ass. Petrol. Geol.* 94-125.

Dziewonski, A. M. & Woodhouse, J. H. 1983. An experiment in systematic study of global seismicity; centroid-moment tensor solutions for 201 moderate and large earthquakes of 1981. *J. Geophys. Res.* **88**, 3247-3271.

Edgell, H. S. 1996. Salt tectonism in the Persian Gulf Basin. In: *Salt Tectonics* (edited by Alsop, G. I, Blundell, D. J. & Davison, I.). *Spec. Publs. geol. Soc. Lond.* **100**, 129-151.

Falcon, N. L. 1947. Raised beaches and terraces of Iranian Makran Coast. *Geographical J.* **109**, 149-151.

Falcon, N. L. 1950. Evidence for large-scale flexuring in the southwest Persian mountain zone. *Iran oil Expl. Prod. Co. Geol. Dept. Report.*

Falcon, N. L. 1961. Major earth flexuring of the Zagros Mountains of South-West Iran. *Q. J. geol. Soc. Lond.* **117**, 367-376.

Falcon, N. L. 1967. The geology of north-east margin of the Arabian basement shield. *Adv. Sci. Lond.* **24**, 31-42.

Falcon, N. L. 1969. Problems of the relationship between surface structure and deep displacements illustrated by the Zagros Range. In: *Time and Place in Orogen* (edited by Kent, P., Satterthwaite, G. & Spencer, A.). *Spec. Publs. geol. Soc. Lond.* **3**, 9-22.

Falcon, N. L. 1974. Southern Iran; Zagros mountains. In: *Mesozoic-Cenozoic orogenic belts* (edited by Spencer, A.). *Spec. Publs. geol. Soc. Lond.* **4**, 119-211.

Farhoudi, G. 1978. A comparison of Zagros geology to island arcs. *J. Geology* **86**, 323-334.

REFERENCES

Gansser, A. 1955. New aspects of the geology in central Iran. *4th World Petroleum Cong. Pro., Rome*, 279-300.

Gansser, A. 1960. Ausseralpine Ophioliteproble. *Eclog. geol. Helv.* **52**, 659-680.

Geological Survey of Iran (GSI) 1980. *The Geological Map of Minab.* Scale 1:100,000.

Gray, K. W. 1950. A tectonic window in SW Iran. *Q. J. geol, Soc. Lond.* **105**, 189-222.

Gussow, W. C. 1966. Salt temperature: a fundamental factor in salt dome intrusion. *Nature* **210**, 518-519.

Gussow, W. C. 1968. Salt diapirism: importance of temperature and energy source of emplacement. In: *Diapirism & Diapirs* (edited by Braunstein, J. & O'Brien, A.). *Mem. Am. Ass. Petrol. Geol.* **8**, 16-52.

Hallam, A. 1976. Geology and plate tectonics of the Neyriz region of southern Iran. *Bull. geol. Soc. Am.* **87**, 45-52.

Harrison, J. V. 1930. The geology of some salt plugs in Laristan (south Persia). *Q. J. geol. Soc. Lond.* **86**, 463-522.

Harrison, J. V. 1931. Salt domes in Persia. Symposium on Salt Domes, *J. Inst. Petrol. Tech.* **17**, 300-320.

Harrison, J. V. & Falcon, N. L. 1936. Gravity collapse structures and mountain ranges as examplified in South-West Iran. *Q. J. geol. Soc. Lond.* **62**, 91-102.

Harrison, J. V. 1941. Coastal Makran. *Geographical J.* **97**, 1-17.

Harrison, J. V. 1952. Topography as a factor in structural geology. *Int. Geol. Cong. 18th GB Rep.* **13**, 114-121.

Harrison, J. V. 1956. Comments on salt domes. *Verh. K. Ned. geol-mijnb. Genoot.* **14**, 1-8.

Haynes, S. J. & McQuillan, H. 1974. Evolution of Zagros suture zone. southeastern Iran. *Bull. geol. Soc. Am.* **85**, 739-744.

Heim, A. 1991/2. *Geologie der Schweiz*. Band **II**, Leipzig, Tauschnitz.

Hills, E. S. 1972. *Elements of Structural Geology* (2nd edn). Chapman & Hall, London.

Iranpanah, A. & Esfandiari, B. 1979. Structural evolution and correlation of tectonic events in the Alborz Mountains, the Zagros Range, and Central Iran. *Bull. Soc. belge de Géologie* **88**, 285-295.

Jackson, J. A. 1080a. Errors in focal depth determination and the depth of seismicity in Iran and Turkey. *Geophys. J. R. astr. Soc.* **61**, 285-301.

Jackson, J. A. 1980b. Reactivation of basement faults and crustal shortening in orogenic belts. *Nature* **283**, 343-346.

REFERENCES

Jackson, J. A. & Fitch, T. J. 1981. Basement faulting and the focal depths of larger earthquakes in the Zagros Mountains (Iran). *Geophys. J. R. astr. Soc.* **64**, 561-586.

Jackson, J. A., Fitch, T. J. & McKenzie, D. P. 1981. Active thrusting and the evolution of the Zagros fold belt. In: *Thrust and Nappe tectonics* (edited by McClay, K. & Prive, N.). *Spec. Publs. geol. Soc. Lond.* **9**, 371-379.

Jackson, J. A. & McKenzie, D. P. 1984. Active tectonics of the Alpine Himalayan Belt between western Turkey and Pakistan. *Geophys. J. R. astr. Soc.* **77**, 185-264.

Jackson, J. A. & McKenzie, D. P. 1988. The relationship between plate motions and seismic moment tensor, and the rates of active deformation in the Mediterranean and Middle East. *Geophys. J.* **93**, 45-73.

Jackson, J. A. 1992. Partitioning of strike-slip and Convergent Motion Between Eurasia and Arabia in Eastern Turkey and the Caucasus. *J. Geophys. Res.* **97**, 12,471- 12,479.

Jackson, J. A. & Vendeville, B. C. 1994. Regional extension as a geologic trigger for diapirism. *Bull. geol. Soc. Am.* **106**, 57-73.

Jackson, J. A., Haines, J. & Holt, W. 1995. The accommodation of Arabia-Eurasia plate convergence in Iran. *J. Geophys. Res.* **100**, 15205-15219.

James, G. A. & Wynd, J. G. 1965. Stratigraphic nomenclature of Iranian oil consortium agreement area. *Bull. Am. Ass. Petrol. Geol.* **49**, 2182-2245.

Jaros, J. 1981. The Zagros mountains, its development and analysis of tectonic styles. *Vestnik-Ustredniho-Ustravu-Geologickeho* or *Bull. Geol. Surv. Prague* **56**, 113-120.

Kadinisky-Cade, K. & Barazangi, M. 1982. Seismotectonics of southern Iran: The Oman line. *Tectonics* **1**, 389-412.

Kasahara, K. 1981. *Earthquake Mechanics*. Cambridge University Press, Cambridge.

Kashfi, M. S. 1976. Plate tectonics and Structural evolution of the Zagros Geosyncline, SW Iran. *Bull. geol. Soc. Am.* **87**, 1486-90.

Kashfi, M. S. 1984. Evidence for vertical movements in the southern part of the Zagros Geosyncline, Iran. *J. Petrol. Geol.* **1**, 87-95.

Kashfi, M. S. 1985. The pre-Zagros integrity of the Iranian platform. *J. Petrol. Geol.* **8**, 353-360.

Kassler, P. 1973. The structural and geomorphic evolution of the Persian Gulf. In: *The Persian Gulf* (edited by Purser, B.). Springer-Verlag, Berlin.

Kazmin, V. G., Sbortshikov, I. M., Ricou, L. E., Zonen-Shain, L. P., Boulin, J., & Knipper, A. L. 1986. Volcanic belts as markers of Mesozoic-Cenozoic active margin of Eurasia. In: *Evolution*

of the Tethys (edited by Aubouin, J., Le Pichon, X. & Monin, A. S.). *Tectonophysics* **123**, 123-152. Elsevier, Amsterdam.

Kent, P. E. 1958. Recent studies of south Persian salt plugs. *Bull. Am. Ass. Petrol. Geol.* **42**, 2951-2972.

Kent, P. E. 1970. The salt plugs of the Persian Gulf region. *Trans. Leicester Lit. & Phil. Soc.* **64**, 56-88.

Kent, P. E. 1979. The emergent Hormuz salt plugs of southern Iran. *J. Petrol. Geol.* **2**, 117-144.

Koyi, H. 1988. Experimental modeling of role of gravity and lateral shortening in Zagros Mountains belt. *Bull. Am. Ass. Petrol. Geol.* **72**, 1381-1394.

Lees, G. M. 1927. Salzgletscher in Persien. *Vien, Mitt. Geol. Gesell.* **20**, 29-34.

Lees, G. M. 1928. The geology and tectonic of Oman and parts of southeastern Arabia. *Q. J. geol. Soc. Lond.* **84**, 485-670.

Lees, G. M. 1931. Salt-dome depositional and formation problems. *J. Inst. Petrol. Technology* **17**, 259-280.

Lees, G. M. 1933. The reservoir rocks of Persian oilfields. *Bull. Am. Ass. Petrol. Geol.* **17**, 229-240.

Lees, G. M. & Richardson, F. D. S. 1940. The geology of the oil field belt of S.W. Iran and Iraq. *Geol. Mag.* **77**, 227-252.

Lees, G. M. 1952. Foreland folding. *Q. J. geol. Soc. Lond.* **108**, 1-34.

Lees, G. M. & Falcon, N. L. 1952. The geographical history of the Mesopotamian plains. *Geographical J.* **118**, 24-39.

Lees, G. M. 1955. Recent earth movement in the Middle East. *Geol. Rdsch.* **43**, 221-226.

Le Pichon, X. 1968. Sea floor spreading and continental drift. *J. Geophys. Res.* **73**, 3361-3697.

Little, R. D. 1970. Terraces of the Makran coast of Iran. In: Physical geography of the Makran coastal plain of Iran (edited by Snead, R. E.). *U.S. Office Naval Research Geol. Prog. Reconnaissance Phase, Final Rep.* Chapt. **8**, 318-372.

Little, R. D. 1972. Terraces of the Makran coast of Iran. In: *Physical Geography of the Makran Coastal Plain of Iran* (edited by Snead, R. E.). New Mexico University, Albuquerque.

Laughton, A. S. 1966. The Gulf of Aden. *Philos. Trans. R.. Soc. Lond.* **259**, 150-171.

Mann, C. D. & Vita-Finzi, C. 1989. Holocene serial folding in the Zagros. In: *Gondwana and Tethys, Spec. Publs. geol. Soc. Lond.* **37**, 51-59.

Makris, J. Dehghani, A. and stobbe, C. 1981. Zagros collision and its connection to the sea floor spreading process of the Red Sea. *Trans. Am. Geophys. Union* **62**, 214.

REFERENCES

McKenzie, D. 1972. Active tectonics of the Mediterranean region. *Geophys. J. R. astr. Soc.* **30**, 109-185.

McQuillan, H. 1974. Fracture pattern on Kuh-e Asmari Anticline, Southwest Iran. *Bull . Am. Ass. Petrol. geol.* **58** (2), 236-246.

Mina, P., Paran, Y. & Razaghnia, M. 1967. Geological and Geophysical studies and exploratory drilling of the Iranian continental shelf, Persian Gulf. *7th World Petroleum Cong. Proc. Mexico* **2**, 871-903.

Minster, J. B. & Jordan, T. H. 1978. Present-day plate motions. *J. Geophys. Res.* **83**, 5331-5354.

Moody, J. D. & Hill, M. J. 1956. Wrench fault tectonics. *Bull. geol. Soc. Am.* **67**, 1207-1246.

National Iranian Oil Company (NIOC) 1957. *The Geological Map of Iran.* Scale 1:2,500,000.

National Iranian Oil Company (NIOC) 1973. *The Tectonic Map of Iran.* Scale 1:2,500,000.

National Iranian Oil Company (NIOC) 1975. *The Geological Map of Iran.* Scale 1:1,000,000.

National Iranian Oil Company (NIOC) 1959. *Geological map of Iran with explanatory notes and stratigraphic tables.* Scale 1:2,500,000.

National Iranian Oil Company (NIOC) 1977. *The Tectonic Map of southeast Iran.* Scale 1:2,500,000.

Ni, J. & Barazangi, M. 1986. Seismotectonics of Zagros continental collision zone and a comparison with the Himalayans. *J. Geophys. Res.* **91**, 8205-8218.

Niazi, M., Asudeh, I., Ballard, G., King, G. & McKenzie, D. 1978. The depth of seismicity in the kermanshah region of the Zagros mountains (Iran). *Earth Planet. Sci. Lett.* **40**, 270-274.

North, R. G. 1974. Seismic slip rates in the Mediterranean and Middle East. *Nature* **252**, 560-563.

Nowroozi, A. A. 1971. Seismo-tectonics of the Persian plateau, eastern Turkey, Caucasus and Hindu Kush regions. *Bull. seism. Soc. Am.* **61**, 317-341.

Nowroozi, A. A. 1972. Focal Mechanism of earthquakes in Persia, Turkey, west-Pakistan and Afghanistan and plate tectonics of the Middle east. *Bull. seism. Soc. Am.* **62**, 823-850.

Nowroozi, A. A. 1976. Seismotectonic provinces of Iran. *Bull. seism. Soc. Am.* **966**, 1249.

Nowroozi, A. A. 1985. Empirical relations between magnitudes and fault parameters for earthquakes in Iran. *Bull. seism. Soc. Am.* **75**, 1327-1338.

Nowroozi, A. A. 1986. Analysis of earthquake risk in Iran based on seismotectonic provinces. *Tectonophysics* **122**, 89-114.

REFERENCES

Nowroozi, A. A. 1987. Tectonics and earthquake risk of Iran. In: *Ground motion and engineering seismology* (edited by Cakmak, A. S.). Elsevier, Amsterdam.

Oberlander, T. 1965. *The Zagros streams: a new interpretation of transverse drainage in an orogenic zone*. Syracuse geographical series **1**, Syracuse University press, Syracuse.

Oberlander, T. 1985. Origin of drainage transverse to structures in orogens. In: *Teconic geomorpholgy* (edited by Morisawa, M. & Hack, J.). Allen & Unwin, 155-182.

O' Brien, C. A. E. 1950. Tectonic problems of oil field belt of southern Iran. *18th Inter. Geol. Cong. Great Britain, Proc. Pt.* **6**, 45-58.

O' Brien, C. A. E. 1957. Salt Diapirism in south Persia. *Geol. Mijnbouw N. S.* **19**, 357-376.

Obruchev, V. A. 1948. Osnovnyje certy kinetiki i plastiki neotectoniki. *Izv. Akad. Nauk SSSR Ser. Geol.* **5**.

Oliver, D. 1987. *The development of structural patterns above reactivated basement faults*. Unpublished Ph.D. thesis, University of London.

Pamic, J., Sestini, G. & Adib, D. 1979. Alpine magmatic and metamorphic processes and plate tectonics in the Zagros Range, Iran. *Bull. geol. Soc. Am.* **90**, 569-576.

Pavlides, S. B. 1989. Looking for a definition of neotectonics. *Terra Nova* **1**, 233-235.

Payne, A. 1990. A structural interpretation of the Zagros fold belt, SW Iran-NE Iraq. *British Petroleum Company Limited internal report.*

Pilgrim, G. E. 1908. The Geology of the Persian Gulf and adjoining portions of Persia and Arabia. *India geol. Surv. Mem.* **34**, 1-77.

Pilgrim, G. E. 1922. The sulphur deposits of southern Persia. *India Geol. Surv. Recs.* **53**, 343-358.

Pilgrim, G. E. 1924. The geology of parts of the Persian provinces of Fars, Kirman and Laristan. *India Geol. Surv. Mem.* **48**, 111.

Player, R. A. 1965. The Salt plugs of southern Iran. *Bull. Am. Ass. Petrol. Geol.* **49**, 3.

Player, R. A. 1969. *The Hormuz salt plugs of southern Iran.* Unpublished Ph.D. thesis, Reading University.

Price, N. J. 1975. Fluids in the crust of the earth. *Science Progress* **62**, 59-87.

Price, N. J. & Cosgrove, J. W. 1990. *Analysis of Geological Structures*. Cambridge University Press. Cambridge.

Reddy, N. J., Stein, R. J. & Wickham, J. S. 1982. Finite-Element modeling of folding and faulting. *Int. J. Num. and Anal. Methods* **6**, 425-440.

REFERENCES

Ramsay, J. G. & Huber, M. I. 1987. *Techniques of Modern Structural Geology, (v. 2, Folds and Fractures.* Academic Press, London.

Richardson, R. K. 1928. Weitere Bemerkungen zu der Geologie und den Salzaufbruchen am Persischen Gulf, *Centralblatt Min. Geol. u. Pal., Abt. B*, 43-49.

Richter, C. F. 1935. An instrumental magnitude scale. *Bull. seism. Soc. Am.* **25**, 1-32.

Ricou, L. E. 1968. Sur la mise en place au Crétacé supérieur d'importantes nappes á radiolarites et ophiolites dans les Monts Zagros (Iran). *Acad. Sci. Comptes Rendus* **267**, 2272-2275.

Ricou, L. E. 1971. Le croissant ophiolitique Peri-Arabe. une ceintive de nappes mises en place au Crétace supérier. *Rev. Géographie Phys. et Géologie Dynam.* (2) **13** (4), 327-350.

Robertson Research Publication (RRP) 1987. *The Geological Map of Iraq and Southwestern Iran*. Scale, 1:1,000,000.

Sanford, A. R. 1959. Analytical and experimental study of simple geological structures. *Bull. geol. Soc. Am.* **70**, 19-52.

Savage, W. V., Alt, J. N., & Mohajer-Ashjai, A. 1977. Microearthquake investigations of the 1972 Qir, Iran, earthquake zone and adjacent areas (abstr.). *Geol. Soc. Am.. Abs. w. prog.* **9** (4), 496.

Schröder, J. W. 1944. Essari sur la structure de l' Iran. *Ecologae Geologicae Helveliae* **37**, 37-81.

Sherman, D. J. 1976. The Geological evolution of southern Iran : the report of Iranian Makran expedition. *Geographical. J.* **142**, 393-413.

Shoja-Taheri, J. & Niazi, M. 1981. Seismicity of the Iranian plateau and bordering regions. *Bull. Seism. Soc. Am.***71**, 477-489.

Slemmons, D. B. 1991. Introduction. In: *The Geology of North America, Decade Map vol. 1 Neotectonics of North America* (edited by Slemmons, D. B., Engdahl, E. R., Zoback, M. D. & Blackwell, D. D.). *Geol. Soc. Am. Boulder, Colorado,* 1-20.

Snyder, D. B., Barazangi, M. & Ni, J. 1986. Deep crustal structure and seismotectonic of the Zagros collisional mountain belt and a comparison with the Himalayas. *Anonymous, Pro. inter. sympo. on neotect. in S. Asia*, 180-182.

Snyder, D. B. & Barazangi, M. 1986. Deep crustal structure and flexure of the Arabian plate beneath the Zagros collisional mountain belt as inferred from gravity observations, *Tectonophysics* **5**, 361-373.

Sobouti, F. & Arkani-Hamed, J. 1996. Numerical modeling of the deformation of the Iranian plateau. *Geophys. J. Int.* **126**, 805-818.

REFERENCES

Stearns, D. W. 1978. Faulting and forced folding in the Rocky Mountains foreland. *Bull. geol. Soc. Am.* **151**, 1-37.

Stewart, I. S. & Hancock, P. L. 1994. Neotectonics. In: *Continental Deformation* (edited by Hancock, P. L.). Pergamon Press, Oxford.

Stöcklin, J. 1968. Structural history and tectonic of Iran. *Bull. Am. Ass. Petrol. Geol.* **52**, 1229-1258.

Stöcklin, J. & Nabavi, M. H. 1973. *Tectonic map of Iran*, scale 1:5,000,000. Iran. geol. Surv., Tehran.

Stöcklin, J. 1974. Possible ancient continental margins in Iran. In: *The geology of continental margins* (edited by Burk, C. A. & Drake, C. L.). Springer-Verlag, New York.

Summers, J. M. 1979. *An experimental and theorical investigation of multilayer fold development.* Unpublished Ph.D. thesis, University of London.

Suppe, J. 1983. Geometry and kinematics of fault-bend folding. *Am. J. Sci.* **283**, 648-721.

Suppe, J. 1985. *Principals of Structural Geology*. Prentice-Hall, New Jersey.

Sykes, L. R. 1967. Mechanism of earthquakes and nature of faulting on the mid-oceanic ridges, *J. Geophys. Res.* **72**, 2131-2153.

Szabo, F. & Kheradpir, P. 1978. Permian and Triassic stratigraphy, Zagros basin, south-west Iran. *J. Petrol. Geol.* **1**, 57-82.

Takin, M. 1972. Iranian geology and continental drift in the Middle East. *Nature* **235**, 147-150.

Talbot, C. J. & Alavi, M. 1996. The past of a future syntaxis across the Zagros. *Spec. Publs. geol. Soc. Lond.* **100**, 89-109.

Tchalenko, J. S. & Braud, J. 1974. Seismicity and structure of the Zagros (Iran), the main recent faults between 33° and 35° N. *Philos. Trans. R. Soc. Lond.* **277**, 1-25.

Tchalenko, J. I. 1975. Strain and deformation rates at the Arabian-Iranian plate boundary. *J. geol. Soc. Lond.* **131**, 585-586.

Tillman, J. E., Poosti, A., Rossello, S. & Eckert, A. 1981. Structural evolution of Sanandaj-Sirjan ranges near Esfahan Iran. *Bull. Am. Ass. Petrol. Geol.* **65**, 674-687.

Vita-Finzi, C. 1969a. Late Quaternary alluvial chronology of Iran. *Geol. Rdsch.* **58**, 951-73.

Vita-Finzi, C. 1975. Quaternary deposits in the Iranian Makran .*Geographical J.* **141**, 415-420.

Vita-Finzi, C. & Ghorashi, M. 1978. A recent faulting episode in the Iranian Makran. *Tectonophysics* **44**, 21-25.

Vita-Finzi, C. 1979a. Contribution to the Quaternary geology of southern Iran. *Iran geol. Surv. Rep.* **47**, 1-52.

REFERENCES

Vita-Finzi, C. 1979b. Rates of Holocene folding in the coastal Zagros near Bandar Abbas, Iran. *Nature* **278**, 632-634.

Vita-Finzi, C. 1981. Late Quaternary deformation on the Makran coast of Iran. *Z. Geomorph. Suppl.* **40**, 213-226.

Vita-Finzi, C. 1982. Recent coastal deformation near the strait of Hormuz. *Mathematical and Physical Sciences* **382**, 441-457.

Vita-Finzi, C. 1986. *Recent Earth Movements: an introduction to Neotectonics*. Academic Press, London.

Vita-Finzi, C. 1987. ^{14}C chronologies in coastal Iran, Greece and Jordon. *J. geol. Soc. Lond.* **144**, 553-560.

von Dollen, F. J., Alt, J. N., Tocher, D. & Nowroozi, A. 1977. Seismological and geological investigations near Bandar Abbas, Iran (Abstr.). *Geol. Soc. Am.* **9**, 521.

Wells, A. J. 1969. The crush zone of the Iranian Zagros Mountains and its implications. *Geol. Mag.* **166**, 385-394.

Westaway, R. 1990. Seismicity and tectonic deformation rate in Soviet Armenia: implications for local earthquake hazard and evolution of adjacent region. *Tectonics* **9**, 477-503.

White, R. S. & Ross, D. A. 1979. Tectonics of the western Gulf of Oman. *J. Geophys. Res.* **84**, 3479-3489.

Wilson, J. T. 1965. A new class of faults and their bearing on continental drift, *Nature* **207**, 343-347.